PREFACE

This thesis contains an account of the experimental work carried out by the author during the period October 1958 to October 1961 in the Department of Natural Philosophy, the Royal College of Science and Technology.

The problem of measuring diffusion coefficients in thin films as investigated in this thesis was suggested by my supervisor, Mr. C. Weaver. I should like to express my thanks for his constant advice and close guidance on all phases of this work.

Chapter 1 is a review of previous experimental methods for finding diffusion coefficients in thin films.

Chapter 2 is a survey of the relevant diffusion theory.

Chapter 3 describes the apparatus which I have constructed for producing thin film diffusion couples and for measuring their reflectivities during ageing. The work of designing this apparatus was shared with my supervisor.

Chapters 4 to 12 describe the experimental results obtained by myself. The electron diffraction photographs shown in chapter 11 were taken by myself on an EM3 electron microscope. I should like to express my thanks to Mr. J.W. Sharpe for the use of this instrument.

The discussion to each chapter and chapter 13 deal with the interpretation of the experimental results. These sections were written following discussion with my supervisor.

DIFFUSION IN THIN FILMS

by

Laurence C. Brown, A.R.C.S.T.

A Thesis

Submitted for the Degree of Doctor of Philosophy

in the Faculty of Science

University of Glasgow

July 1961

CONTENTS

CONTENTS (Cont'd)

CONTENTS (Cont'd)

CONTENTS (Cont'd)

CONTENTS (Cont'd)

CONTENTS (Cont'd)

ACKNOWLEDGEMENTS

The author would like to express his gratitude to Professor J. Irving, M.A., Ph.D., and to all the members of staff of the department of Natural Philosophy of the Royal College of Science and Technology, Glasgow. In particular, he would like to thank Mr. J.W. Sharpe, M.A., F.Inst.P., for the use of the electron microscope, and Mr. C. Weaver, B.Sc., M.I.R.E., A.R.T.C., F.Inst.P., A.M.I.E.E., for the use of the high vacuum equipment and laboratory, and particularly for his continued assistance and encouragement. Finally the author would like to acknowledge the receipt of a maintenance grant from the Department of Scientific and Industrial Research.

ABSTRACT

Diffusion coefficients and activation energies for diffusion in several successively evaporated two layer metal films have been determined by measurements of the reflectivity changes at the metal surfaces on annealing. The reflectivity changes were due to the motion of phase boundaries and it proved possible to identify the phases formed. Results indicated a vacancy diffusion mechanism rather than grain boundary diffusion and satisfactory agreement was obtained with results for the faster direction of diffusion in bulk specimens. A mechanism for the motion of the atoms was postulated in terms of a vacancy flow.

CHAPTER 1

INTRODUCTION

1.1 Diffusion Measurements in Thin Films

When two metal films are evaporated one on top of the other, diffusion will occur at the common interface to form layers of solid solution or intermetallic compounds. The presence of these diffusion layers can readily be detected by electron diffraction, X-ray diffraction, or by resistance and adhesion observations (Weaver and Hill 1959), but these methods cannot normally give the rate of growth of the diffusion layer and so the diffusion coefficient of the system.

Techniques used for determining diffusion coefficients in bulk metal diffusion couples are inapplicable to evaporated films since any method of sectioning is impossible and the quantity of material available is not sufficient for normal chemical analysis. The use of radioactive tracer methods is also precluded since the absorption of the films is negligible even for particles of low energy such as weak β rays. Consequently no changes in emission would be observed as the radioactive particles diffused through the films.

The only practicable technique in thin films is to allow the diffusion zone to extend to the surfaces and to make

observations of the change of concentration at the surface with time. This permits diffusion coefficients to be determined. Suitable quantities to observe are reflection electron diffraction, surface potential, and the optical properties of the surface. The last is the easiest quantity to measure, and the variation of reflectivity has been used by Schopper (1955) and by Coleman and Yeagley (1943) for determining diffusion coefficients in gold-lead and copper-zinc.

1.2 Previous Work

Schopper (1955) studied diffusion in thin films of gold-lead by measuring the change in reflectivity at the gold surface. The gold and lead films were evaporated successively on to a glass substrate at a pressure of 10^{-5}mm. of mercury and the thicknesses of the films were found by the three-slit method of Schopper and Fleischmann (1951), measuring the absolute change of phase of light reflected at the free metal surface. The slide was heated whilst still under vacuum, the temperature being measured by means of a thermocouple in contact with the slide. Reflectivity measurements were made at the glass surface and this eliminated any possibility of surface contamination or reflectivity changes due to causes other than diffusion. A typical curve obtained by Schopper is shown in fig. 1.1.

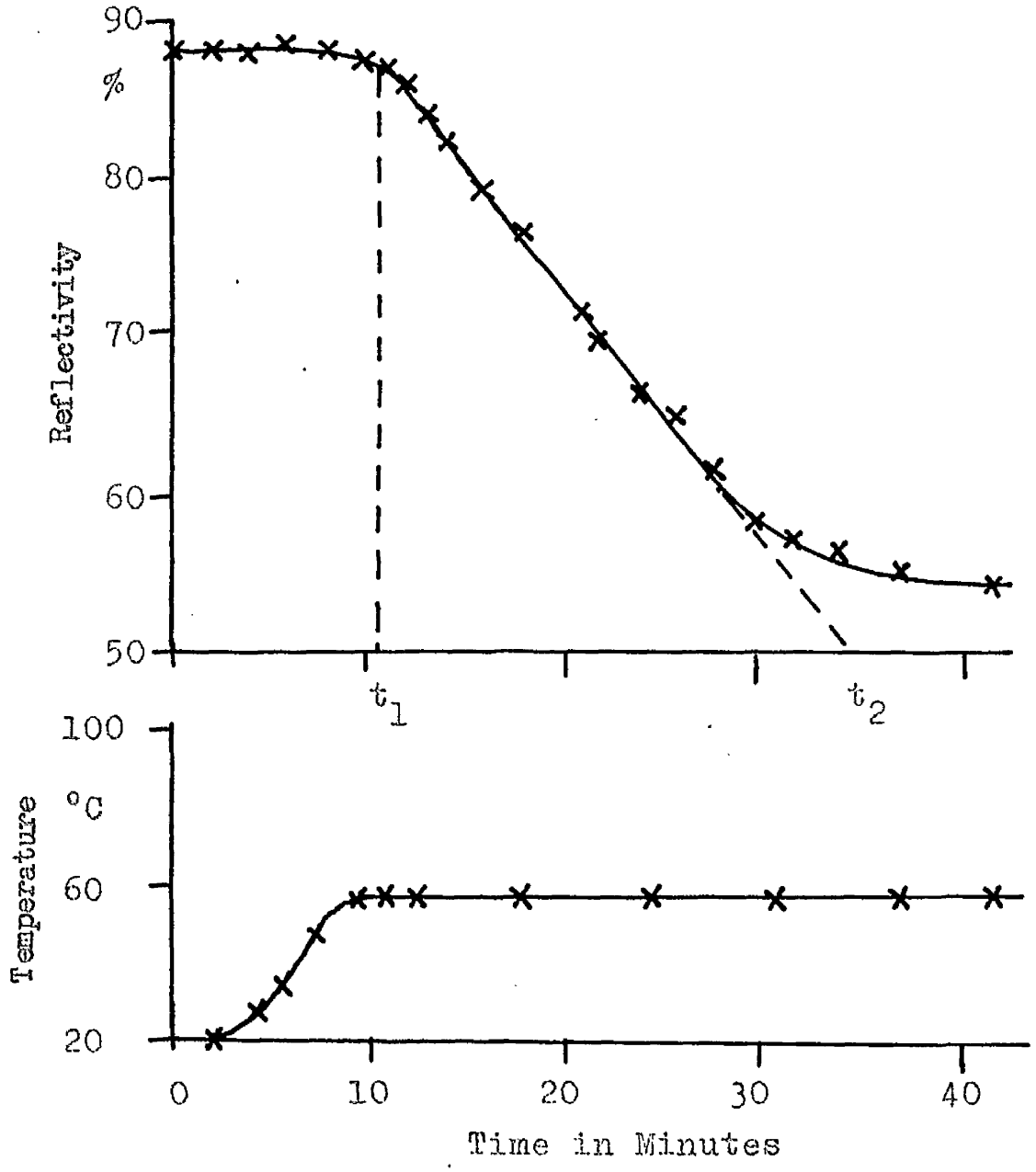

Fig. 1.1 The Reflectivity at the Gold Surface of a Gold-Lead Film and the Temperature as a Function of Time for a Gold Thickness of 1060Å and a Lead Thickness of 2930Å. t_1 and t_2 are the intercepts of the tangent with reflectivity values of 88% (pure gold) and 51% (pure lead). Light wavelength = 6430Å. Reproduced from Schopper (1955).

The reflectivity dropped from the value for pure gold to a figure of 51%, close to that of lead. The actual length of the initial plateau was not known with certainty because of the time taken for the slide to reach its steady temperature, but it was only a small fraction of the total ageing time. Gold films were prepared with different film thicknesses, and as far as could be seen the shapes of the curves were closely similar. If the reflectivity was plotted as a function of t/d^2, where d was the gold thickness, the curves coincided (fig. 1.2). On the basis of these results, Schopper developed a theory (given in 2.7) for determining the diffusion coefficient from the intercepts of the tangent drawn at the turning point of the curve with abscissae corresponding to concentration values of 1 and 0. The diffusion coefficient was found from

$$D = 1{\cdot}08\ d^2/(t_2-t_1)$$

where t_1 and t_2 are the time values corresponding to these intercepts. This formula depended only on the region of variation of concentration and consequently a knowledge of the exact length of the initial plateau was not required.

The activation energy of diffusion was found by measurements of the diffusion coefficient of different specimens over a range of temperature. $\mathrm{Log}_{10}D$ was plotted against $1/T$ and the gradient of the straight line obtained gave the activation energy (fig. 1.3) and the intercept

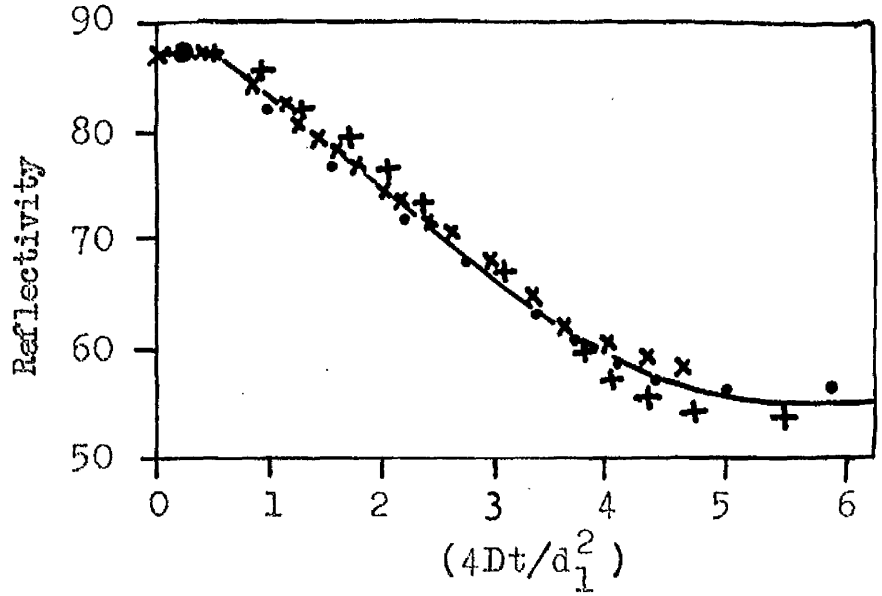

Fig. 1.2 Graph of Reflectivity against the Dimensionless Expression $4Dt/d_1^2$ for Three Different Film Thicknesses.
× for d_{Au}=1130Å, • for d_{Au}=480Å (T=52°C)
+ for d_{Au}=1220Å (T=70°C) (Schopper 1955).

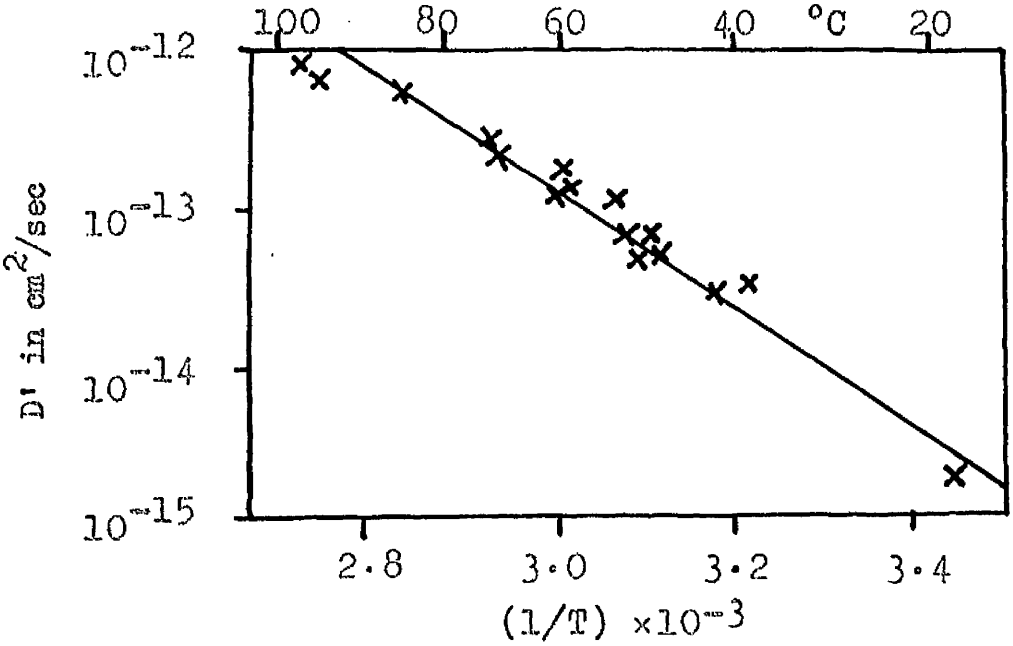

Fig. 1.3 Graph of Diffusion Coefficient against (1/T) for the Diffusion of Lead in Gold (Schopper 1955).

with the $\log_{10}D$ axis gave D_o. The results over the temperature range 20°C to 100°C were consistent and gave D_o = 0·016 cm^2/sec and activation energy, E, = 17·0 kcal/mole for the diffusion of lead through gold. The value of activation energy was rather higher than the values of 13·6 and 14·0 kcal/mole obtained for the diffusion of gold in lead (Jost 1952), but Schopper considered this difference to be reasonable since lattice changes in gold require greater energies than in lead, this being obvious from the great differences in melting point of the two metals. The same reason was advanced to account for the lower value of D_o as compared with D_o = 0·35 cm^2/sec for the diffusion of gold in to bulk lead.

The solid solubility of gold in lead is only 0·08 at.%, and Schopper considered that this small solubility would not cause much reflectivity change. Furthermore it was found that to obtain the full reflectivity drop to 51% the lead thickness had to be at least twice the gold thickness. These facts made Schopper conclude that the reflectivity changes were due to the formation of intermetallic compounds rather than to solid solubility effects. The compound $AuPb_2$ was identified in the diffusion zone by X-ray diffraction, and this led to the suggestion that a sharply defined layer of compound was formed between the gold and the lead. This hypothesis did not agree with the experimental observations

which indicated a gradual formation of compound at the surface, and the conclusion finally reached was that diffusion occurred by the movement of lead atoms into vacant sites in the gold lattice possibly helped by the movement of gold atoms into interstitial sites in the lead.

Much earlier, Coleman and Yeagley (1943) studied the diffusion of copper into thin films of zinc. The copper and zinc films were successively evaporated onto microscope slides, the film thicknesses being obtained by weighing. Films approximately 2000Å thick were used, and after deposition the specimens were placed in a reflectometer so that the variation in the reflectivity of the upper zinc surface could be measured. The slide was heated by means of a thermostatically controlled electric iron in contact with the back surface of the slide, and it was claimed that this held the slide temperature constant to $\pm 1^{\circ}C$ during the period of diffusion. The output current from a photocell in the reflectometer was recorded continuously and was taken as giving a measure of the reflectivity.

The theory developed by Coleman and Yeagley was purely empirical. A quantity t_{∞} was defined as the time at which dR/dt (i.e. the rate of change of reflectivity with time) was equal to a constant 'a', where 'a' was taken as 0·00291. This gave a point at which the alloy was almost

homogeneous. t_∞ was taken to be proportional to the thickness x of the zinc, and to the quantity m of metal which had to diffuse across the interface to produce homogeneity. i.e. $t_\infty \propto xm$

$$t_\infty = (1/K)xm$$

where K was taken to be a form of diffusion coefficient. Substituting values of x and m, an expression for K was found in terms of the copper thickness (d_{Cu}) and the zinc thickness (d_{Zn}), namely

$$K = d_{Zn}^2 W_{Cu}/(d_{Cu}+d_{Zn})t_\infty \qquad (1.1)$$

where W_{Cu} was the weight of the copper film per unit area. Experimentally it was found that

$$K = A \exp(-E/RT)$$

and so the activation energy was found by plotting log K against 1/T.

Only one curve was given for the diffusion of copper into zinc and no values for K or E were recorded. Results were, however, given for similar experiments with gold and lead where diffusion of the gold into the upper layer of the lead was measured. A value of 13·7 kcal/mole was obtained for the activation energy, rather different from Schopper's value of 17·0 kcal/mole, but in good agreement with the values of 13·6 to 14·0 kcal/mole obtained in bulk specimens for diffusion of gold into lead.

In a later paper, Coleman and Yeagley (1944) stated that their value of activation energy in copper-zinc was the same as the one found in earlier determinations in bulk specimens, but A was several orders of magnitude higher. This was attributed to anisotropy of diffusion and to the existence of preferred orientation in the deposited films (Burr Coleman and Davey 1944).

1.3 Scope of Present Work

The work presented in this thesis consists of a detailed investigation into reflectivity changes taking place in a number of two layer metal films, carried out in order to determine values for diffusion coefficients and activation energies.

A survey was made of 39 metal pairs to see which gave reflectivity changes on ageing. The fact that no miscible or partially miscible systems gave reflectivity changes was not surprising, because diffusion in these systems is known to take place very slowly. Reflectivity changes occurred in most metal systems where metal intermediate phases were formed, and 8 of these were studied in detail. Reflectivity changes usually took place at both sides and ageing was studied at both metal surfaces.

It was found in general that the reflectivity

changes were due to the motion of a reaction boundary rather than to the gradual change in concentration observed by Schopper. The variations with film thickness showed that reaction boundary was due to phase precipitation and it proved possible to identify the phase or phases formed. These results were confirmed by direct measurements of the reflectivity of the various intermediate phases, these alloy films being prepared either by evaporation of the alloy, or, more usually, by "flash" evaporating mixed grains of the pure metals.

In two of the systems studied, investigations had been carried out by other workers on similar bulk diffusion couples at much higher temperatures. The same compounds were found in thin film diffusion couples and the rates of diffusion were fairly similar. It appeared that the mechanism of diffusion was the same in both cases.

The phase boundary was frequently sharply defined, but in certain metal pairs a diffuse boundary was observed. This has been attributed either to penetration of the substrate metal during evaporation of the overlayer, or to the effects of an initial fast diffusion forming a supersaturated solid solution before precipitation of the compound. It was shown that Schopper's results on gold-lead were probably due to this effect.

Measurements of diffusion coefficients and activation energies in very thin films (under 200Å) indicated that the diffusion observed arose from a vacancy rather than a grain boundary mechanism. D_o and E in thin films were found to be similar to D_o and E for the faster direction of diffusion in bulk specimens. Hence in thin films, diffusion into the lower melting point component (i.e. the faster direction of diffusion) was the rate determining process, and the reflectivity changes at the other metal surface were due simply to the loss of metal in the formation of the intermetallic compound. On the basis of these results a mechanism for the motion of the atoms was postulated in terms of a vacancy flow.

An electron diffraction investigation was carried out on four of the metal systems, and it was conclusively shown that reflectivities changed due to diffusion and the formation of intermetallic compounds. Phases observed by electron diffraction were generally the same as those found from the reflectivity observations.

The variation of phase change of light reflected from a metal surface was used to observe diffusion in two of the systems. The shapes of the ageing curves were the same as those found by reflectivity observations, confirming that the reflectivity changes were true concentration effects.

Eleven non-miscible metal systems were investigated for reflectivity changes, and most surprisingly one of them (silver-lead) gave reflectivity changes. This was tentatively attributed to diffusion into a disordered structure to form supersaturated solid solution. The reflectivity changes were found to occur only in very thin films.

CHAPTER 2

THE THEORY OF DIFFUSION

2.1 Fick's Laws

The mathematical expressions for diffusion are due to Fick (1855). The quantity, J, of the diffusing substance transferred in unit time across unit area perpendicular to the concentration gradient is proportional to the concentration gradient $(\partial c/\partial x)$, i.e.

$$J = -D\,(\partial c/\partial x) \qquad (2.1)$$

where D is called the diffusion coefficient. In the case where the concentration in a fixed region changes with time, (2.1) becomes

$$\frac{\partial c}{\partial t} = \frac{\partial}{\partial x}\left(D\,\frac{\partial c}{\partial x}\right) \qquad (2.2)$$

if it is assumed that there is no net gain or loss of atoms. In the special case where D is independent of concentration we obtain the simplified form

$$\frac{\partial c}{\partial t} = D\,\frac{\partial^2 c}{\partial x^2} \qquad (2.3)$$

2.2 Thermodynamic Analysis of Diffusion

The thermodynamic treatment of diffusion starts by considering not the concentration but the Gibbs free energy (G) of a phase containing a number of components

whose molar concentrations are c_1, c_2, etc.. If the compositions change by amounts dc_1, dc_2, etc., then the change in free energy is

$$dG = (\partial G/\partial c_1)dc_1 + (\partial G/\partial c_2)dc_2 + \ldots$$

$$= \mu_1\, dc_1 + \mu_2\, dc_2 + \ldots.$$

where the μ_i are the chemical potentials. Thermodynamic equilibrium is attained when each of the μ_i is constant throughout the system regardless of phase. Otherwise diffusion will occur to equalise the potentials. A difference in μ_i at two sites does not necessarily signify a corresponding difference in c_i, and it can be associated with no concentration difference at all. To study the tendency for diffusion it is more fundamental to consider potentials than to consider concentrations.

In solid solution, μ_i is given in terms of the activity of the solution a_i by the expression

$$\mu_i = k_o + RT \log a_i \qquad (2.4)$$

where k_o is the free energy per mole of the pure substance i. The ratio a_i/c_i is called the activity coefficient, γ, and is equal to unity for ideal solid solution.

The decrease in free energy of the system due to the displacement of 1 mole of the i th. component over distance dx is

$$dG = d\mu_i = (\partial \mu_i / \partial x)dx + \text{second order terms}$$

and hence we may consider that there is an effective diffusion force F_i acting on one atom, given by

$$F_i = -\frac{1}{N}\frac{du}{dx}$$

where N is Avogadro's number. If the average velocity of the atoms under unit force is M_i (the mobility), and if the average diffusion drift velocity is v_i, then the number of atoms crossing unit area normal to x per second is

$$j_i = n_i v_i = -(n_i M_i / N)(du_i/dx) \qquad (2.5)$$

where n_i is the number of atoms of i per unit volume i.e. $n_i = c_i A$, A being the total number of atoms/unit volume. Substituting (2.4) in (2.5), we find

$$j_i = -M_i kT \left(1 + \frac{\partial \log \gamma_i}{\partial \log c_i}\right)\frac{dc_i}{dx} \qquad (2.6)$$

Comparing (2.1) and (2.6), we obtain the following expression for the diffusion coefficient:

$$D_i = M_i kT \left(1 + \frac{\partial \log \gamma_i}{\partial \log c_i}\right) \qquad (2.7)$$

In the case of an ideal solid solution ($\gamma = 1$), the diffusion coefficient is given simply by $D_i = M_i kT$, which is the well known Einstein equation relating diffusion and mobility.

2.3 Atomic Movements in Diffusion

Diffusion may occur in metals along external surfaces, along grain boundaries or through the bulk of the solid. The last process is generally referred to as volume diffusion and much attention has been devoted to suggesting a unique model for the elementary diffusion process.

A few suggested mechanisms are illustrated in fig. 2.1. Each will now be considered in turn:

(a) Interchange and Ring Mechanisms: In this model, the diffusing atom moves by interchanging its position with that of another lattice atom by a correlated rotation of two or more atoms about a common centre.

(b) Vacancy Mechanism: Diffusion results from the existence in the crystal lattice of vacancies which may move. The diffusing atom moves by jumping into a neighbouring vacant lattice site.

(c) Interstitial Mechanism: An atom may occupy an interstitial position in the lattice either because it belongs there (interstitial solid solution) or because it has left a normal lattice site. Such an atom will migrate from one interstitial position to another through the lattice, until it may or may not end by occupying again a normal lattice site.

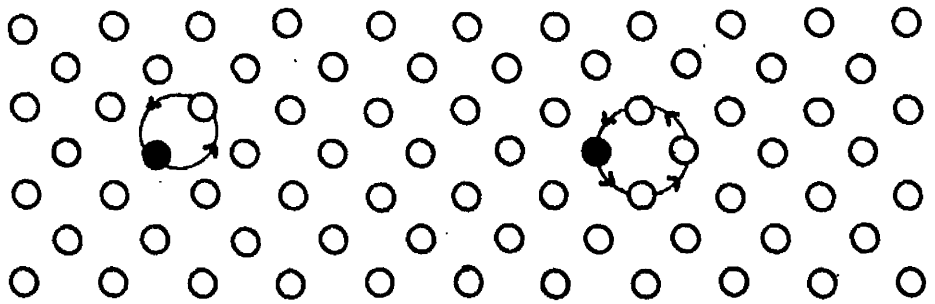

(a) Interchange and Ring-of-Four

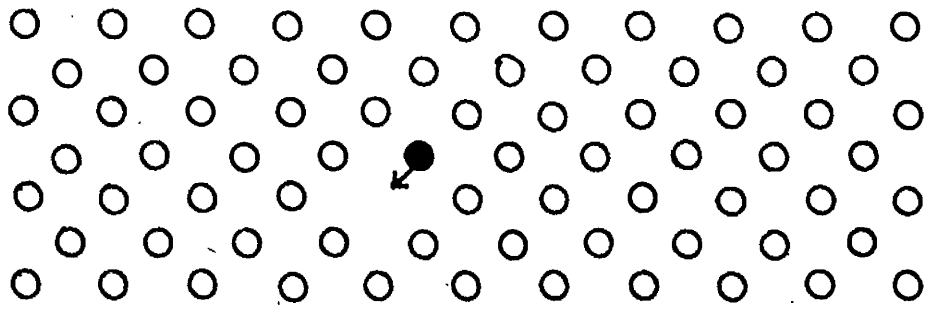

(b) Vacancy

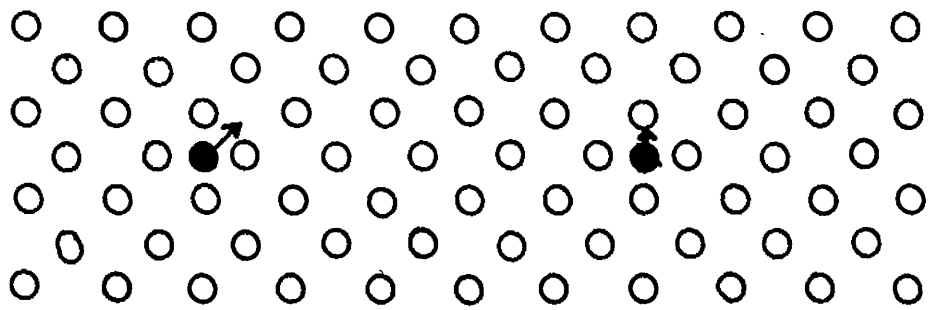

(c) Interstitial

Fig. 2.1 Mechanisms for Diffusion.

Detailed calculations have been carried out to estimate the activation energy of diffusion for the processes given above. Results have been calculated for self diffusion in copper and are shown in table 2.1. It can be seen that the vacancy model has the least activation energy of diffusion and is in good agreement with the experimental value. It has been generally accepted that this is the normal mechanism for diffusion, at least in close packed metal lattices. The detailed atomic theory for vacancy diffusion will be considered in the next section.

2.4 Vacancy Diffusion

An atom jumping from a lattice position into a neighbouring vacant site will leave behind a vacancy. Another atom (or the same one) can jump into this vacant site, and this jump in general shifts the vacancy to a third position. In the presence of a potential gradient, the net drift of a large number of vacancies will be such that after a sufficient time the required transport of atoms will have taken place to equalise the potentials.

The jumping probability of an atom depends on the vacancy concentration, on the diffusive force (potential gradient), and on the height of the free energy barrier between two neighbouring atom positions X and Y (fig. 2.2(a)).

TABLE 2.1

CALCULATED ACTIVATION ENERGIES FOR SELF DIFFUSION IN COPPER

Mechanism	Activation Energy (eV)	Reference
Pair Interchange	10·0	Huntington & Seitz (1949)
Ring-of-Four	4·0	Zener (1950)
Interstitial	5·2	Brooks (1955)
Vacancy	2·0	Brooks (1955)
Experimental	2·1	Kuper et al. (1955)

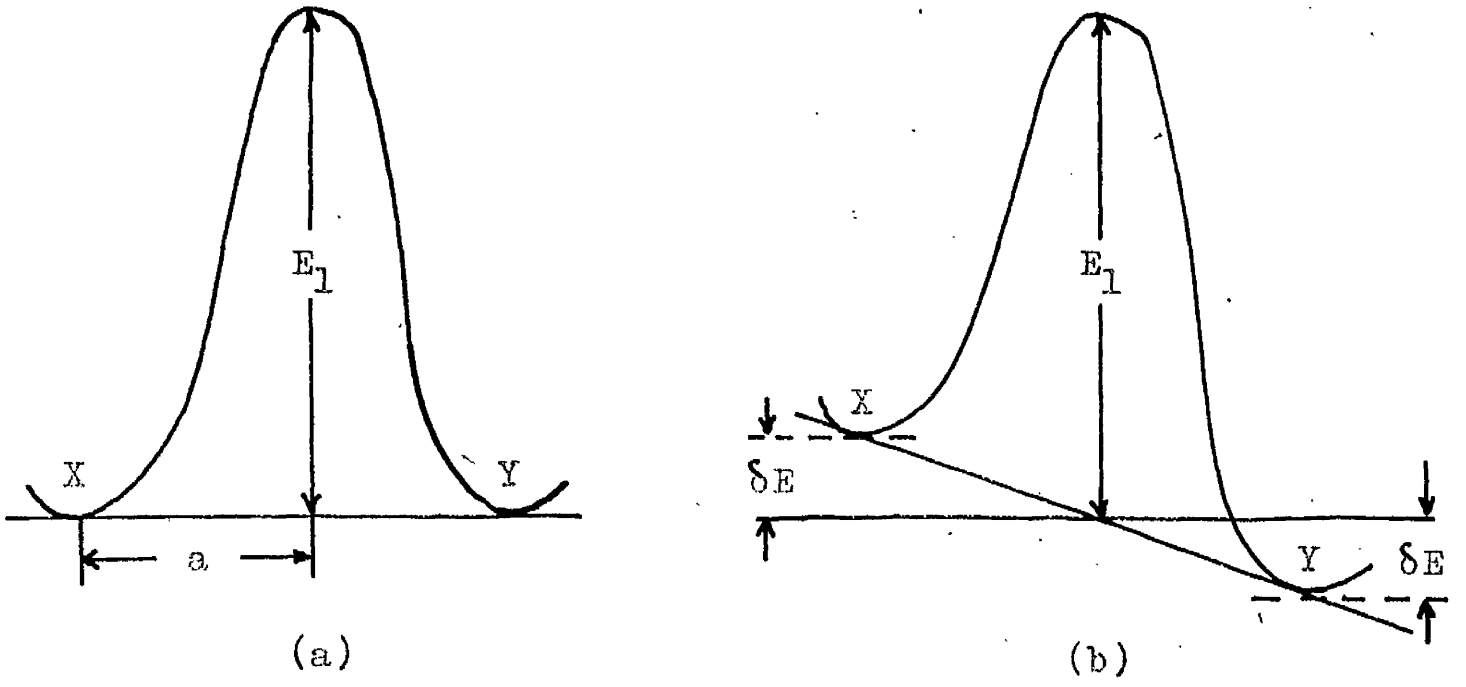

Fig. 2.2 Effect of Potential Gradient on the Free Energy Barrier between Two Atomic Sites.

If E_1 is the height of the free energy barrier, then it can be shown from simple reaction rate theory (Glasstone Laidler and Eyring 1941) that the average number of transitions per second from X to Y is

$$n = \alpha \nu_o \exp(-E_1/kT)$$

where α is a numerical factor depending on the diffusion geometry and ν_o is the atomic vibration frequency.

The transitional probability is altered when a potential gradient $d\mu/dx$ of the diffusing particles is present. The potential energies of positions X and Y are now different by an amount $2\delta E$ (fig. 2.2(b)) where

$$\delta E = \frac{1}{N} \frac{d\mu}{dx} \frac{a}{2}$$

The number of migrations per second from X to Y exceeds the number from Y to X by the amount

$$\Delta n = \alpha \nu_o \left\{ \exp(-(E_1-\delta E)/kT) - \exp(-(E_1+\delta E)/kT) \right\}$$

$$= \frac{\alpha \nu_o a}{NkT} \frac{d\mu}{dx} \exp(-E_1/kT) \qquad \text{provided } \delta E \ll kT$$

The drift velocity of the atoms is simply $v = a\Delta n$ and from (2.5) we obtain the atomic mobility

$$M_i = -\frac{Nv}{d\mu/dx}$$

$$= \frac{\alpha \nu_o a^2}{kT} \exp(-E_1/kT)$$

The diffusion coefficient can be found from equation (2.7)

which gives the general formula

$$D = \alpha \nu_0 a^2 \left(1 + \frac{\partial \log \gamma}{\partial \log c}\right) \exp\left(-E_1/kT\right) \qquad (2.8)$$

α takes into account two factors. The first allows for the atom jumping equally probably on m different directions (m = 6 in a F.C.C. lattice) in each of which the component in the direction X to Y of the distance the atom moves is different. Hence α contains a factor of the order of (1/m).

Furthermore, an atom at X can only jump to Y when the atomic site at Y is empty. The probability of this is c_v, the vacancy concentration in the material. In thermal equilibrium c_v is given by $c_v = \exp\left(-E_v/kT\right)$, where E_v is the energy required to form a vacancy. α therefore also contains the term A $\exp\left(-E_v/kT\right)$, where A is a constant taking into account the dependence of E_1 and E_v upon temperature and the difference in the vibration frequencies of atoms which have and have not a vacancy as neighbour (Mott and Gurney 1940). We finally obtain from (2.8) the diffusion coefficient

$$D = D_0 \exp\left(-E/RT\right) \qquad (2.9)$$

where

$$D_0 = A\nu_0 a^2/m \left(1 + \frac{d \log \gamma}{d \log c}\right) \qquad (2.10)$$

and

$$E = E_1 + E_v \qquad (2.11)$$

E is now expressed in calories per mole of the diffusing material.

2.5 The Kirkendall Effect

It can be seen from equation (2.7) that each atomic species in a system will have its own diffusion coefficient, and that each component will diffuse at a different rate. If we consider a diffusion couple AB in which vacancy diffusion takes place, then one species of atom, say A, will have a greater mobility than the other and will change places with a vacancy more readily. In this case the average drift velocity of A in a potential gradient will be greater than that of B, and so net transfer of mass will take place during diffusion.

The phenomenon of net mass flow is called the Kirkendall effect and was first observed by Smigelskas and Kirkendall (1947) in the copper-α brass system. The detection of a Kirkendall effect, say by observations on the displacement of inert markers in the diffusion zone, points unambiguously to a defect mechanism for diffusion. The Kirkendall effect has been observed in alloys of silver-gold, silver-cadmium, silver-palladium, gold-nickel, copper-nickel, and copper-zinc (Lazarus 1960).

Darken (1948) has shown that the chemical interdiffusion coefficient (D) defined in equations (2.1)

to (2.3) can be expressed in terms of the diffusion coefficients (D_a and D_b) of the two components A and B by the relation

$$D = f_a D_b + f_b D_a \qquad (2.12)$$

where f_a and f_b are the fractional concentrations of A and B. Many values are available for the diffusion coefficient of a dilute alloy of B in A into the pure metal A. In this case (2.12) reduces to

$$D = D_b \qquad (2.13)$$

Hence the diffusion coefficient will be characteristic of the mobility of atoms of B present only in small quantities. It is found experimentally (Jost 1952) that diffusion takes place more quickly in alloys with small concentrations of the higher melting point component than in alloys with small concentrations of the lower melting point component, indicating that diffusion of the higher melting point metal is faster than the lower melting point one.

2.6 Diffusion Couples

In a diffusion couple the metals may be completely miscible, completely non-miscible, partially miscible, or they may form one or more intermediate phases at the temperature at which diffusion is being studied. We are interested in the different types of concentration-penetration curves obtained in these cases and wish to obtain formulae for calculating the diffusion coefficients.

2.7 Miscible Systems

If the two metals were completely miscible we would expect a uniform gradation of concentration from one pure metal to the other in the diffusion zone, and after infinite time the concentrations everywhere would be uniform. Normally the diffusion coefficient will be a function of concentration and the concentration-penetration curve will be non-symmetrical (fig. 2.3(a)). To obtain a solution it is necessary to assume that the diffusion coefficient is independent of concentration (fig. 2.3(b)), so that equation (2.3) can be used for deriving formulae for the diffusion coefficient.

The concentration distribution in a semi-infinite diffusion couple has been given by Crank (1956). The boundary and initial conditions for such a system are

$$\begin{aligned} &\text{I.C.} && c = c_o \text{ at } 0 < x < d_1 \\ & && c = 0 \text{ at } d_1 < x < d_2 \qquad \text{with } d_1 \ll d_2 \\ &\text{B.C.} && J = 0 \text{ at } x = 0 \text{ and } x = d_1 + d_2 \end{aligned} \tag{2.14}$$

The concentration distribution is given by

$$c(x,t) = \frac{c_o}{2}\left\{ \operatorname{erf}\left(\frac{d_1 - x}{2\sqrt{Dt}} \right) + \operatorname{erf}\left(\frac{d_1 + x}{2\sqrt{Dt}} \right) \right\} \tag{2.15}$$

where $$\operatorname{erf} z = \frac{2}{\sqrt{\pi}} \int_0^z \exp(-\eta^2)\, d\eta$$

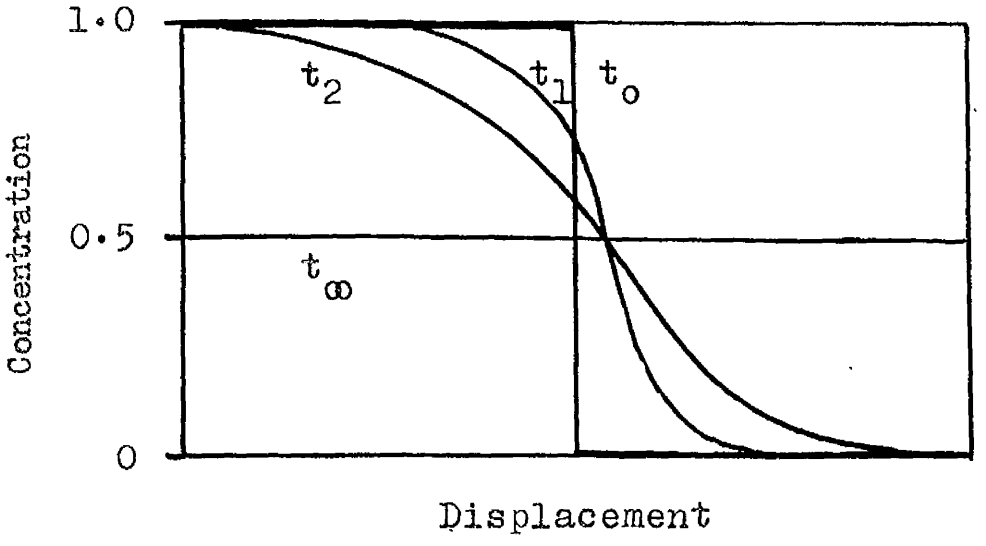

(a) D is a function of Concentration

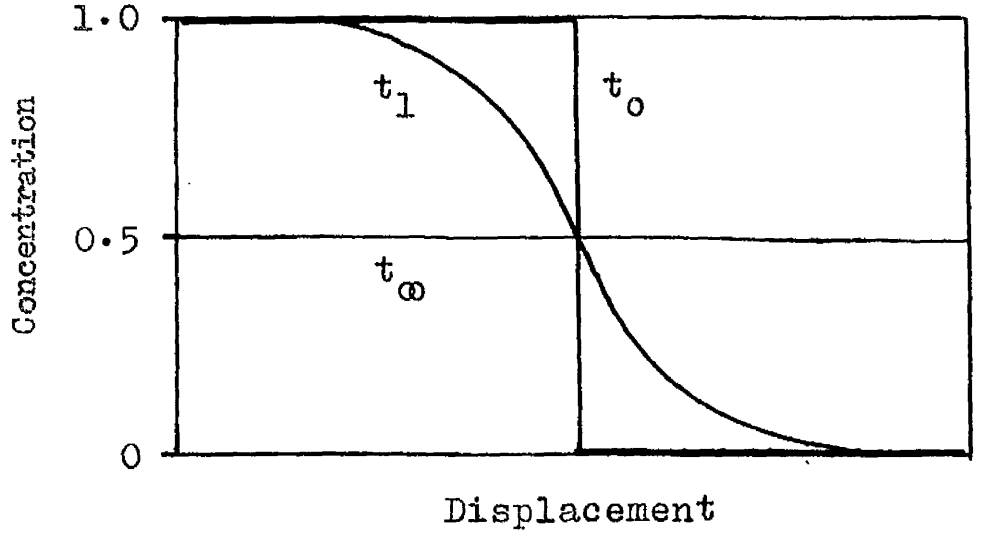

(b) D is independent of concentration

Fig. 2.3 Diffusion in Miscible Systems.

At $x = 0$, equation (2.15) reduces to

$$c/c_0 = \text{erf}\ (d_1/2\sqrt{Dt}) \qquad (2.16)$$

and hence the change in concentration at the metal surface ($x = 0$) is as shown in fig. 2.4.

The solution of the diffusion equation for the conditions (2.14) except that $d_1 \sim d_2$ is much more difficult, but has been derived by Carslaw and Jaeger (1959) for the corresponding case in heat conduction. The result is

$$c/c_0 = \frac{d_1}{d_1+d_2} + \frac{2}{\pi} \sum_{n=1}^{\infty} \frac{1}{n} \left\{ \exp\ \left(- \frac{n\pi}{d_1+d_2}\right)^2 Dt \right\} \sin \frac{n\pi d_1}{d_1+d_2}$$

and the solution is shown in fig. 2.4 for different ratios of d_1 to d_2. It can be seen that the curves coincide for different thickness ratios at the beginning of diffusion but diverge to separate final values of concentration.

Schopper (1955) has used these curves to derive the diffusion coefficient from graphs of concentration against time at the metal surface. The diffusion coefficient can be found from

$$D = (d_1/2\sqrt{t_p})^2 \qquad (2.17)$$

where t_p is the value of t at the point of inflection in the graph of concentration against time. If the tangent at the point of inflection is drawn, another formula can be used

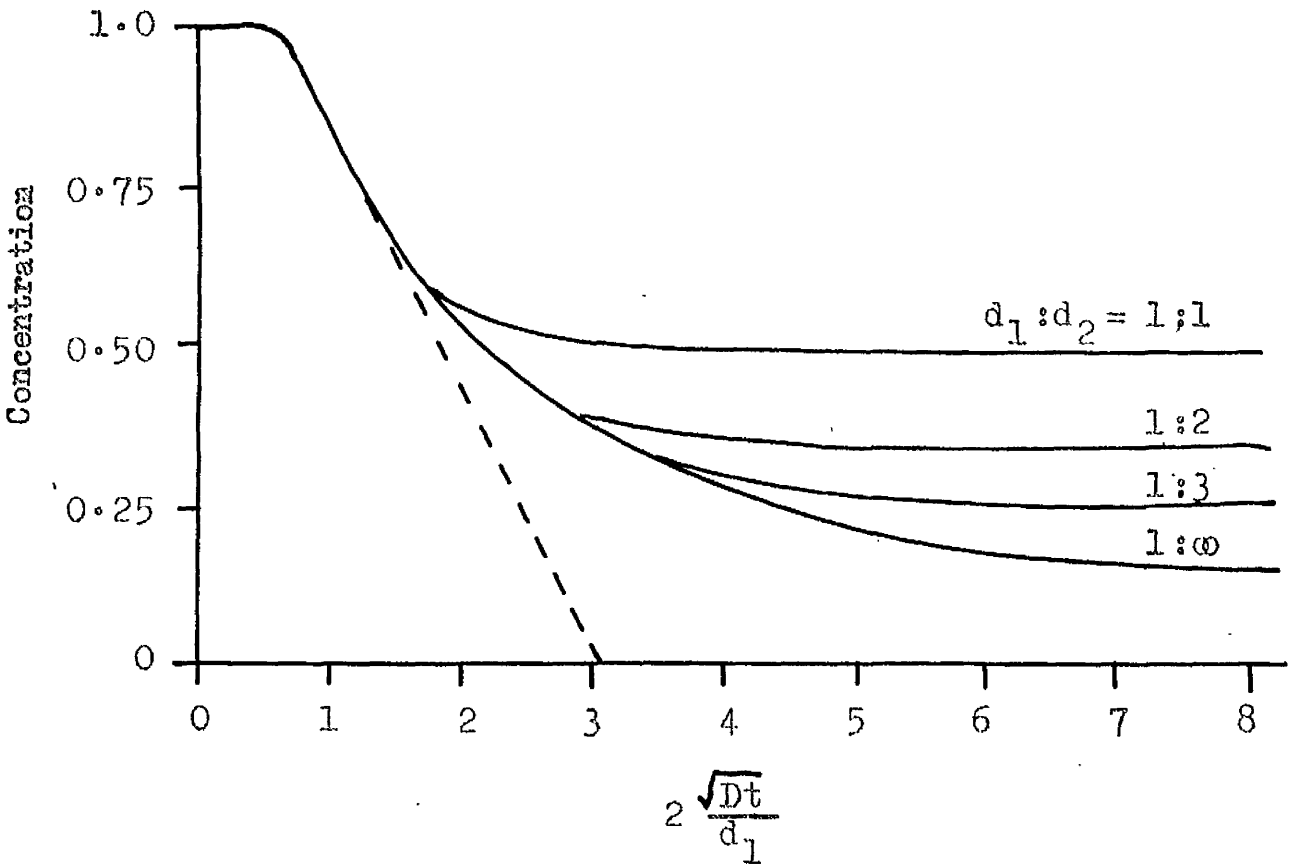

Fig. 2.4 The variation of Concentration of Metal 1 at the Boundary $x = 0$ as a function of the Dimensionless Expression $2\sqrt{Dt}/d_1$ for Different Thickness Ratios $d_1:d_2$.

$$D = 9{\cdot}18\ (d_1/2\sqrt{t_i})^2 \qquad (2.18)$$

where t_i is the intercept of the tangent on the time axis. A third formula used by Schopper was

$$D = 1{\cdot}08\ (d_1^2/(t_2-t_1)) \qquad (2.19)$$

where t_1 and t_2 correspond to the intercept of the tangent with concentration values of 1 and 0. This formula is particularly useful when the length of the initial constant concentration plateau in the graph of concentration against time is not known with accuracy, for it depends only on the region in which the concentration is varying.

2.8 Partially Miscible Systems

In a partially miscible system there are regions of solid solubility near the two pure metals but there is a miscibility gap at the centre. On heating a diffusion couple of the two pure metals at temperature T_o (fig. 2.5), diffusion occurs to form the solid solutions α and β, but there is a discontinuity in concentration from c_1 to c_2 at the $\alpha-\beta$ interface.

Jost (1952) has considered the development of the discontinuity assuming that it does not move from the original interface. He considered the diffusion coefficients D_a and D_b in the α and β phases to be constant, and so obtained the differential equations

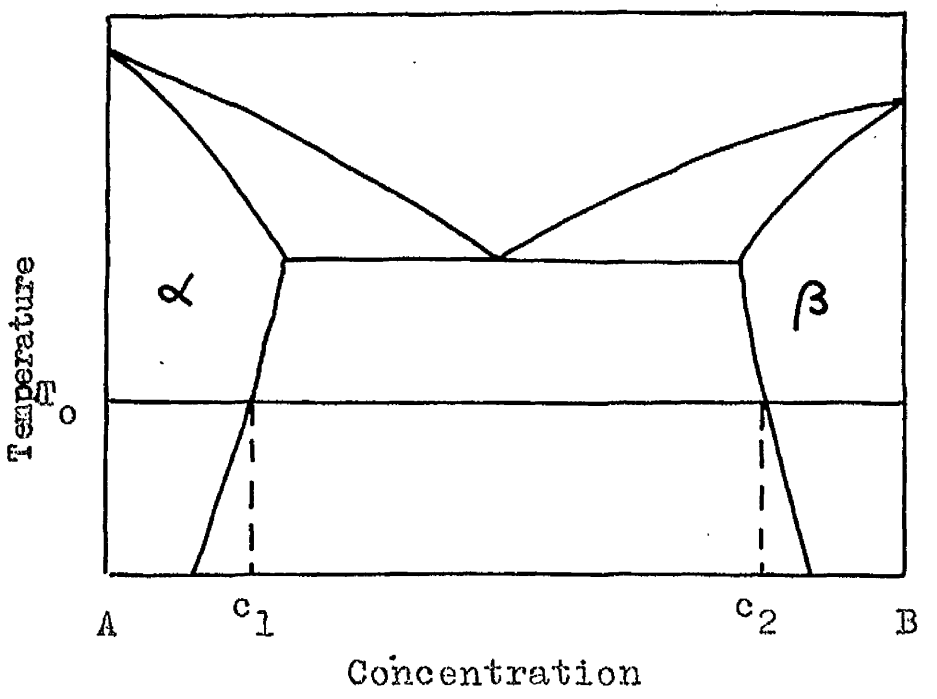

(a)

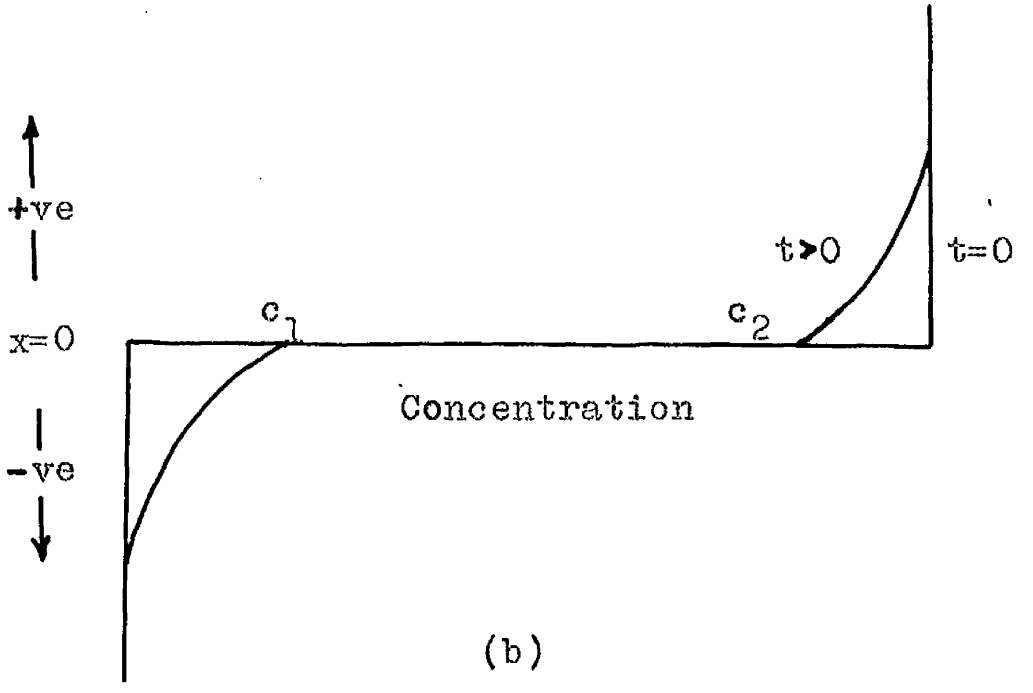

(b)

Fig. 2.5 Diffusion in a Partially Miscible System. (a) Phase Diagram (b) Concentration-penetration curve at T_o.

$$\frac{dc}{dt} = D_a \frac{d^2c}{dx^2} \quad \text{for } x<0, \quad \text{and} \quad \frac{dc}{dt} = D_b \frac{d^2c}{dx^2} \quad \text{for } x>0$$

The initial conditions are $c = 0$ for $x<0$, $c = 1$ for $x>0$, and $c_1/c_2 = k$, a constant. The boundary condition is

$$D_a \frac{dc_a}{dx} = D_b \frac{dc_b}{dx} \quad \text{at } x = 0.$$

This last equation expresses the continuity of flow across $x = 0$. The solutions of the equations are

$$c = c_o \left\{ 1 - \frac{k\sqrt{D_b}}{k\sqrt{D_b} + \sqrt{D_a}} \left(1 + \text{erf } (x/2\sqrt{D_a t})\right) \right\} \quad \text{for } x<0$$

$$c = c_o \left\{ \frac{k\sqrt{D_a}}{k\sqrt{D_b} + \sqrt{D_a}} \left(1 - \text{erf } (x/2\sqrt{D_b t})\right) \right\} \quad \text{for } x>0$$

Solutions of these equations are plotted in fig. 2.6. After infinite time the concentrations on either side of the interface are constant but the discontinuity from c_1 to c_2 remains indefinitely. This is the equilibrium condition for such a system. It is interesting to note that concentrations c_1 and c_2 are developed at the interface immediately after the beginning of diffusion and further ageing tends to equalise the concentrations in each phase. This effect has been considered in some detail by Kirkaldy (1958), who showed that the equilibrium conditions should be attained at the interface in the very early stages of diffusion.

The problem becomes more complicated when we consider motion of the plane of discontinuity (Buckle

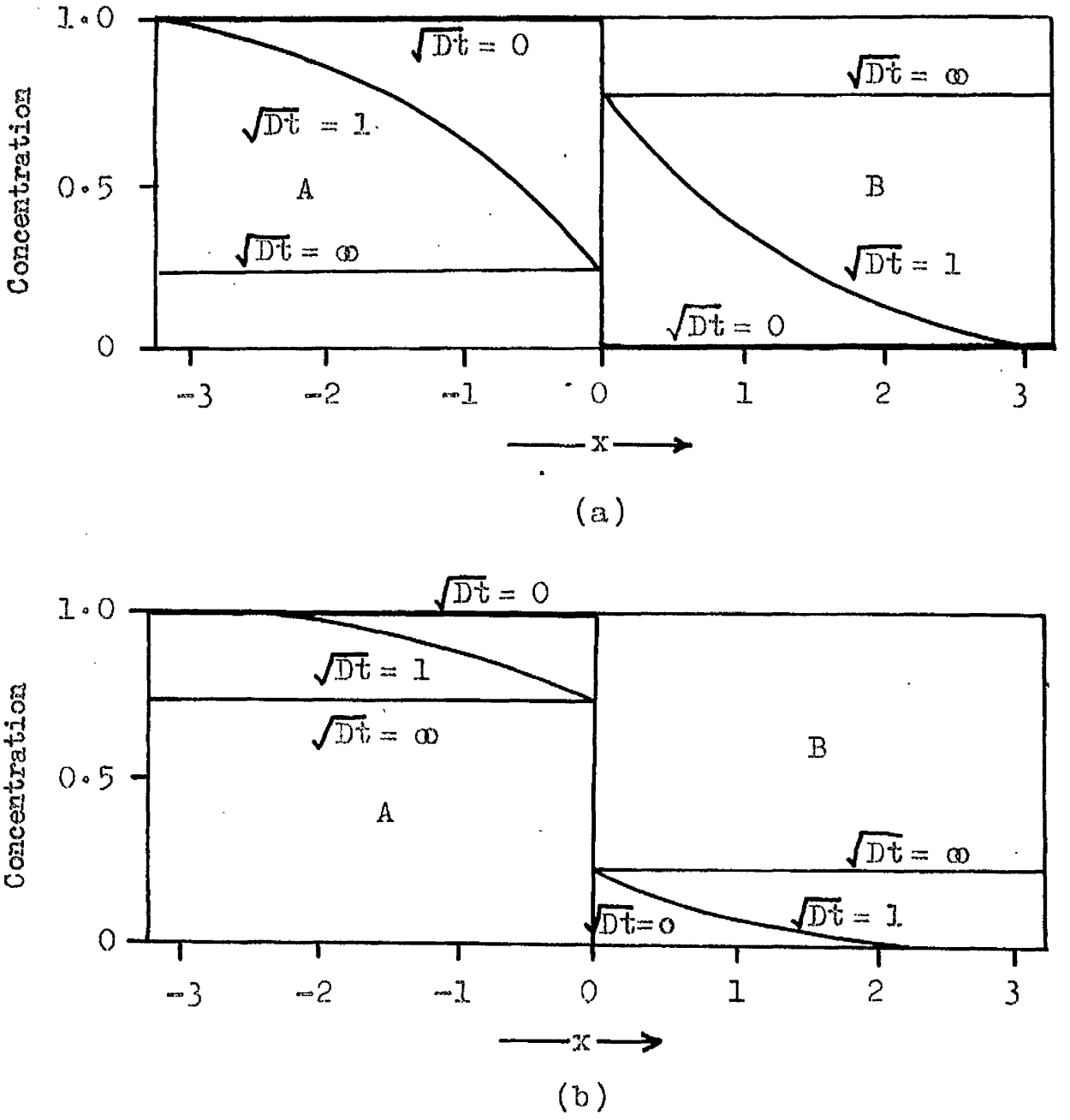

Fig. 2.6 Diffusion in a Partially Miscible System (Jost 1952). (a) k= 3 and $D_a = D_b$, (b) k= $\frac{1}{3}$ and $D_a = D_b$.

1946). It is found that the distance (ξ) moved by the interface in time t is given by

$$\xi = 2\gamma\sqrt{D_a t}$$

where γ is a constant.

2.9 Intermediate Phase Systems

The type of phase diagram where one or more intermetallic compounds are formed between the two pure metals is the most common. The compounds may be formed directly from the melt or they may be formed by a peritectic reaction. At the temperatures at which diffusion couples are studied, however, the mode of formation of the phase has no effect upon the results (fig. 2.7).

Consider first of all a couple composed of two pure metals A and B with no solid solubility in the parent phases but having an intermediate compound γ with a region of solubility from c_1 to c_2 (fig. 2.8) (Wagner 1952). After time t a homogeneous region of γ phase extends from ξ' to ξ'', diffusion in this phase obeying the differential equation

$$\frac{dc}{dt} = D_\gamma \frac{d^2c}{dx^2} \qquad (2.20)$$

The boundary conditions in the γ phase are

$$c_{\xi'} = c_2 \quad \text{and} \quad c_{\xi''} = c_1 \qquad (2.21)$$

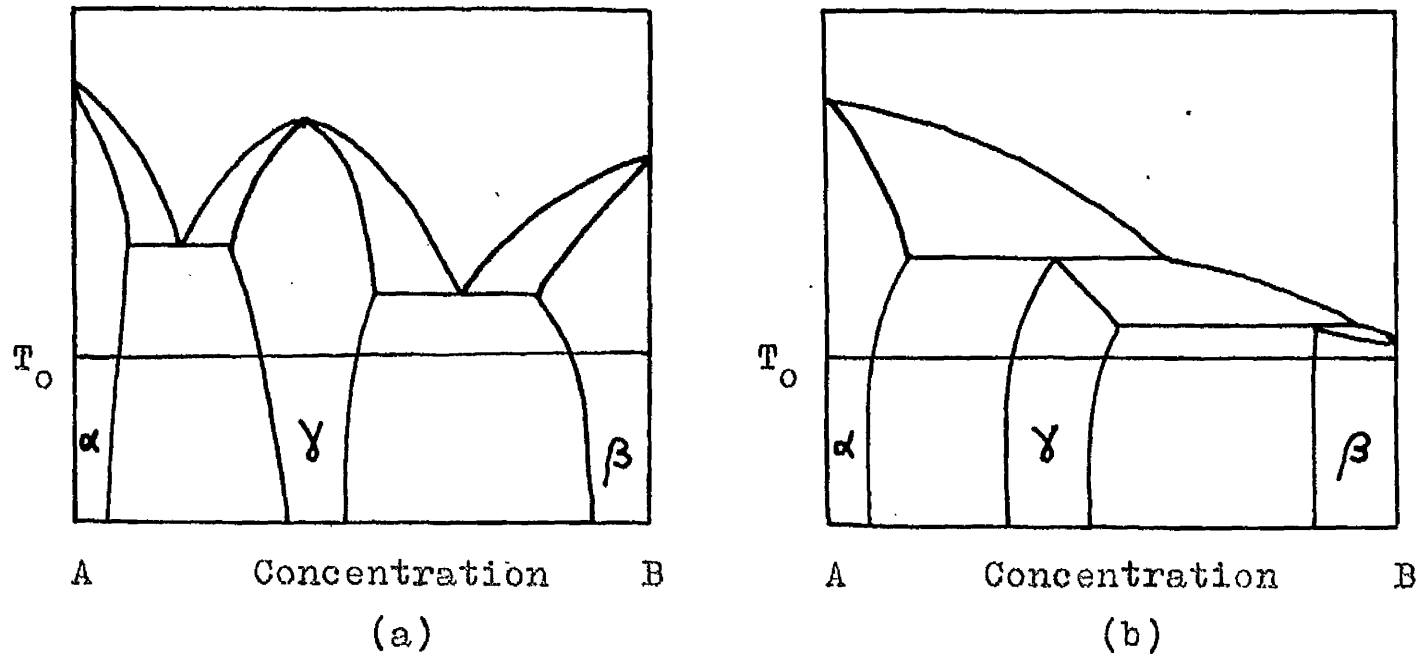

Fig. 2.7 Intermediate Phase Systems. (a) Intermediate phase formed directly from the melt, (b) Intermediate phase formed by peritectic reaction. At temperature T_o the phase diagram of the two systems is similar.

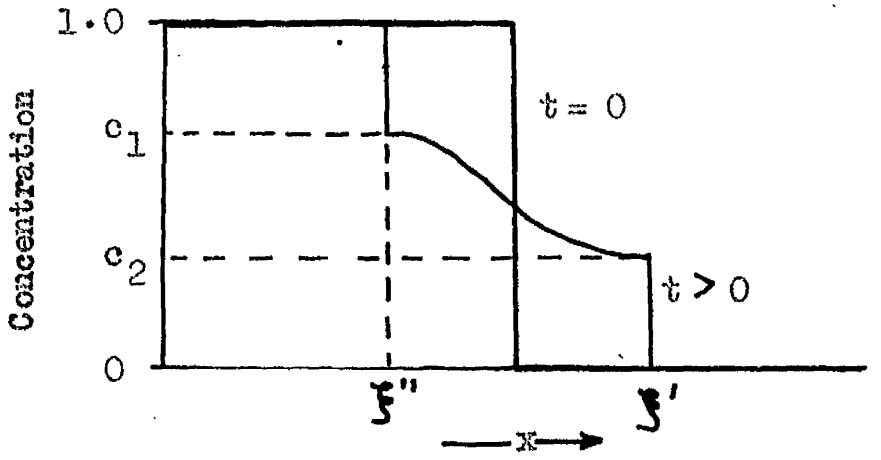

Fig. 2.8 A Diffusion Couple in an Intermediate Phase System with No Terminal Solid Solubility.

A particular solution of (2.20) is

$$c = A - B \operatorname{erf} (x/2\sqrt{D_\gamma t}) \quad \text{for } \xi'' < x < \xi' \qquad (2.22)$$

At $x = \xi'$ we obtain from (2.21)

$$c_2 = A - B \operatorname{erf} (\xi'/2\sqrt{D_\gamma t})$$

$$\arg (A - c_2/B) = \xi'/2\sqrt{D_\gamma t}$$

where arg u is the number whose error function is u.

$$\therefore \xi' = \arg (A - c_2/B)\, 2\sqrt{D_\gamma t}$$

$$= 2\gamma'\sqrt{D_\gamma t} \qquad \text{(say)} \qquad (2.23)$$

A similar relation is found at $x = \xi''$

$$\xi'' = 2\gamma''\sqrt{D_\gamma t} \qquad (2.24)$$

Expressions must now be derived for γ' and γ''.

From the dynamic equilibrium condition at $x = \xi'$ we obtain

$$c_2 d\xi' = -D_\gamma dt \, (dc/dx)_{\xi'} \qquad (2.25)$$

Substituting equations (2.23) and (2.24) in (2.25) gives

$$c_2 = \frac{B}{\sqrt{\pi}} \exp (-\gamma')^2 \qquad (2.26)$$

B can be found by substituting the boundary conditions (2.21) in (2.22) to give

$$B = \frac{c_1 - c_2}{2(\operatorname{erf}\gamma' + \operatorname{erf}\gamma'')}$$

Substituting this in (2.26) leads to the final expression

$$\frac{c_1 - c_2}{c_1} = \sqrt{\pi}\gamma' \exp (\gamma')^2 \, (\operatorname{erf}\gamma' + \operatorname{erf}\gamma'') \qquad (2.27)$$

A similar expression is found for γ'', viz:

$$\frac{c_1-c_2}{1-c_1} = \sqrt{\pi}\,\gamma''\exp(\gamma'')^2\,(\operatorname{erf}\gamma' + \operatorname{erf}\gamma'') \qquad (2.28)$$

From these expressions it may be seen that γ' and γ'' are true constants depending only on c_1 and c_2. Hence the motion of the phase boundaries obeys the parabolic law

$$\xi^2 = D' t \qquad (2.29)$$

where D' is nearly equal to D_γ, the diffusion coefficient in the phase, and is simply a constant times D_γ. D_γ obeys the Arrhenius equation (2.9), and consequently

$$D' = 4\gamma'^2 D_{0\gamma} \exp(-E/RT)$$

$$= D_0' \exp(-E/RT) \qquad \text{(say)}$$

Hence D' has the same activation energy as D_γ.

The case where there is solid solubility in both the terminal phases is rather more complicated (Buckle 1958) but solutions can be derived in a similar manner (fig. 2.9). The motion of the phase boundaries is again according to equations (2.23) and (2.24). γ' and γ'' can be calculated from the equilibrium conditions at the phase boundaries:

$$(c_1-c_2)\frac{d\xi''}{dt} = D_\gamma\left(\frac{dc}{dx}\right)_{\xi''} - D_\alpha\left(\frac{dc}{dx}\right)_{\xi''}$$

and

$$(c_3-c_4)\frac{d\xi'}{dt} = D_\beta\left(\frac{dc}{dx}\right)_{\xi'} - D_\gamma\left(\frac{dc}{dx}\right)_{\xi'},$$

where D_α, D_β and D_γ are the diffusion coefficients in the terminal solid solutions and in the intermediate phase.

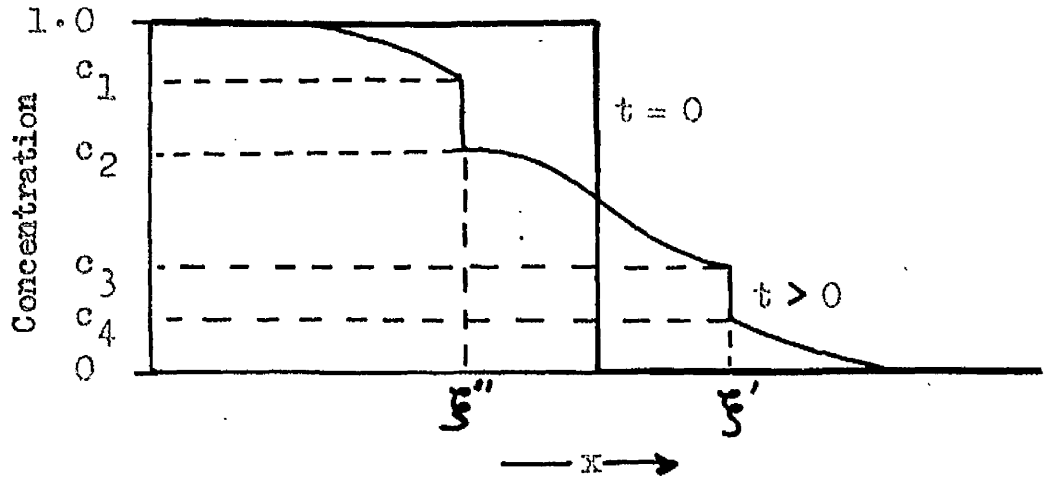

Fig. 2.9 A Diffusion Couple in an Intermediate Phase System with Solid Solubility in the Terminal Phases.

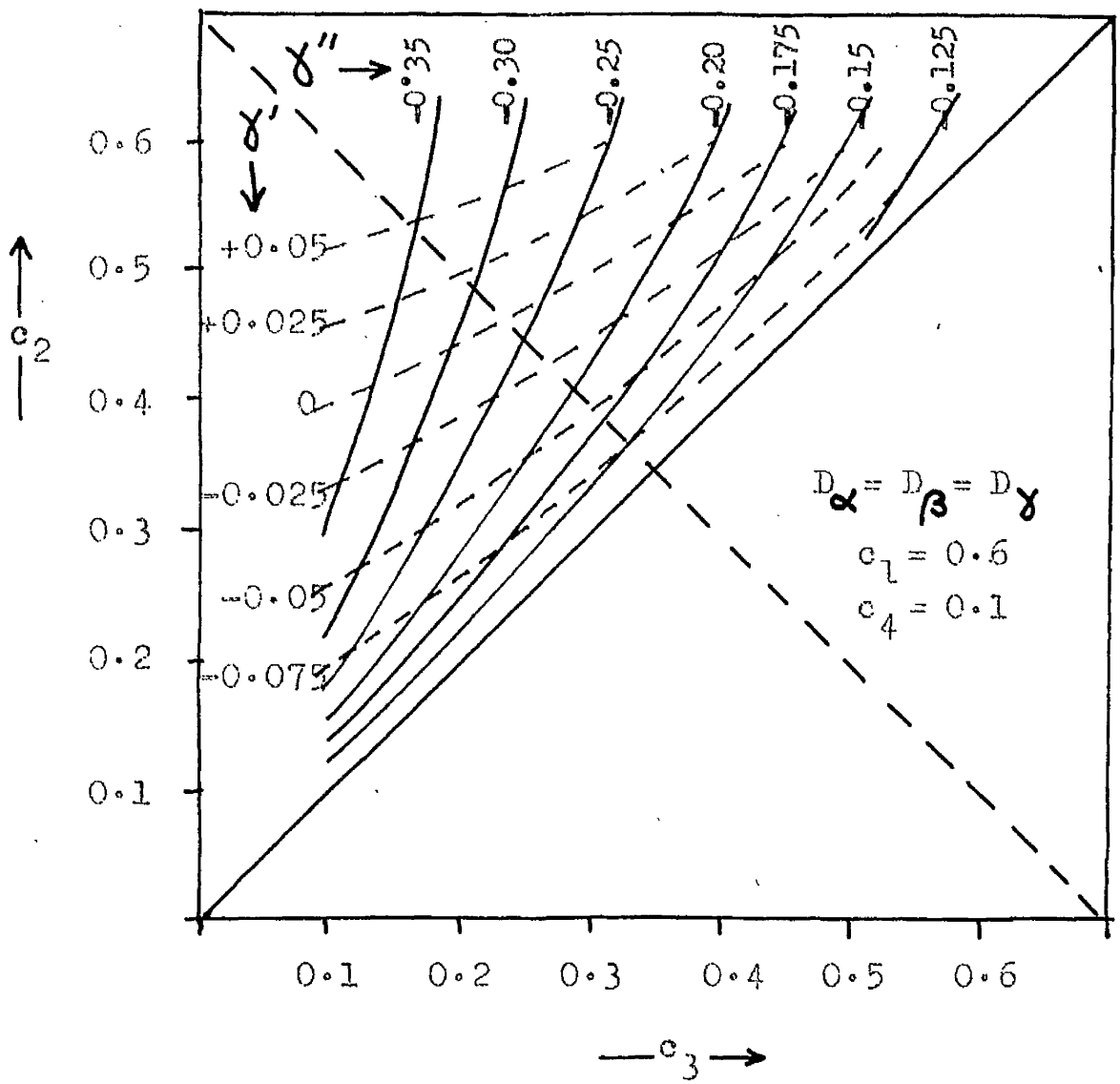

Fig. 2.10 Variation of the Constants γ' and γ'' as a Function of the Concentration Limits of the γ Phase.

The expressions for γ' and γ'' are complicated and are best shown graphically. Fig. 2.10 shows results for different values of c_2 and c_3 with $D_\alpha = D_\beta = D_\gamma$ and with c_1 and c_4 fixed. It can be seen that the values and the signs of γ can change considerably, and indeed in certain cases the intermediate phase may not appear at all.

The solutions for the case where more than one intermediate compound is formed have been considered by Kirkaldy (1958). He shows that the motion of all the boundaries will obey equation (2.29), even when the diffusion coefficients vary with concentration, provided equilibrium conditions obtain at each boundary.

Comparatively few experimental observations have been made of the motion of phase boundaries. Buckle (1946) examined diffusion couples of silver-aluminium, silver-zinc and silver-cadmium, and in every case he found that the motion of the phase boundary obeyed the parabolic law (2.29). Similar results were obtained with aluminium-zinc (Kirkaldy 1958), and with uranium-titanium (Adda and Philibert 1958), and it would appear that equation (2.29) holds in all metal systems.

2.10 Grain Boundary Diffusion

The rate of diffusion along grain boundaries is

generally greater than that through the lattice. Activation energies for grain boundary diffusion have usually been found to be 50% to 60% of the values for volume diffusion. Hence, in experiments carried out at low temperatures, grain boundary diffusion is particularly noticeable.

An approximate phenomenological theory for grain boundary diffusion has been developed by Fisher (1951). He considered a grain boundary in the form of a plane slab of width δ (fig. 2.11) filled with a material of diffusion coefficient D_g, much greater than the diffusion coefficient D_v of the bulk material in which it was imbedded. Diffusion of material was initially much greater along the grain boundary than through the lattice, but after a short time it was found that the material which had diffused along the grain boundary was distributed from there laterally into the bulk, and so the penetration along the grain boundary was not much greater than that in the bulk. Nevertheless, much of the material in the lattice had been transported along the grain boundary and the total amount of material which had diffused a certain distance was much greater than it would have been if only volume transport had been taking place.

Fisher showed that in a narrow section of width Δy distance y from the surface, the total quantity of

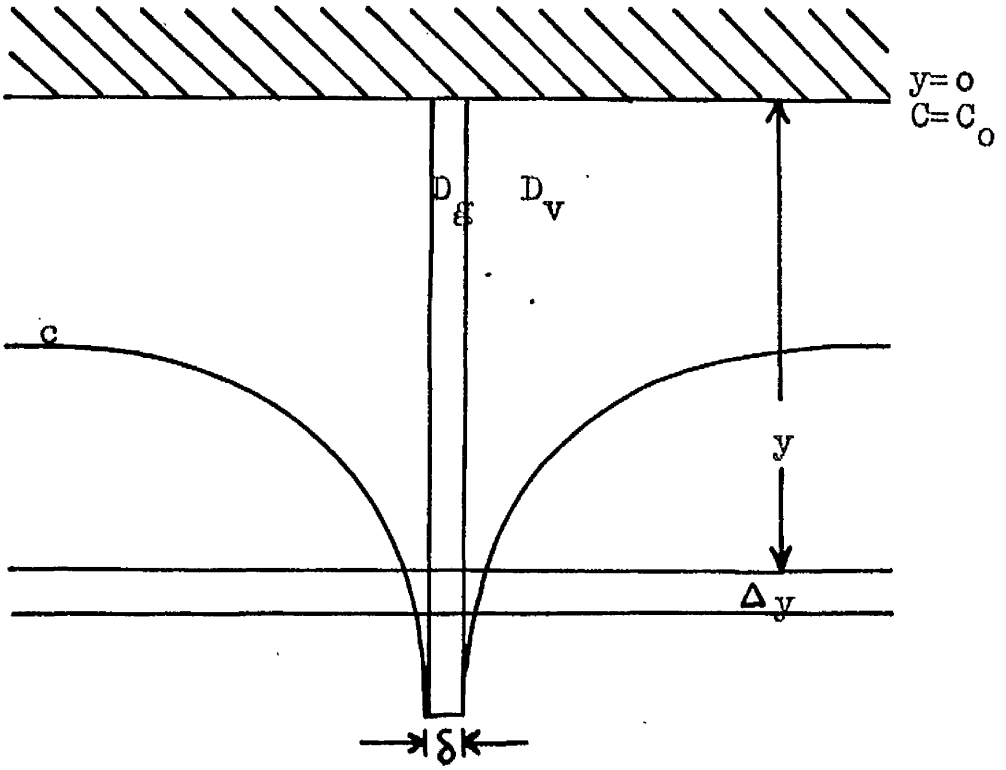

Fig. 2.11 Mathematical Model of Diffusion through a Grain Boundary (Fisher 1951). c is curve of constant concentration

diffusing material which had arrived after time t from y = 0 was given by

$$A_{v,g} = 4.5\ nR\Delta y\ c_o\ (D_v t)^{\frac{1}{2}}\ \exp\left\{-\left(\frac{4D_v}{\pi t}\right)^{\frac{1}{4}} \frac{y}{(D_g\delta)^{\frac{1}{2}}}\right\} \qquad (2.30)$$

where each cm^2 of the surface was divided into n regions of average area R^2 by the grain boundaries perpendicular to it. If only volume diffusion had occurred, the quantity of material in layer Δy would be only

$$A_{v,v} = nR^2\Delta y\ c_o\ (1 - \text{erf}\ (y/2\sqrt{D_v t})) \qquad (2.31)$$

Comparing (2.30) and (2.31), it was found that if R was taken to be 1 micron, D_g/D_v had to be greater than 10^5 for grain boundary diffusion to be detectable.

CHAPTER 3

EXPERIMENTAL

3.1 Film Deposition

Films were evaporated onto glass microscope slides, which were cleaned with Teepol and polished with lens tissue before insertion in the vacuum chamber. The slides were finally exposed to a glow discharge for 10 min. during the pumping cycle. The evaporations were carried out in a glass bell jar evacuated by an oil diffusion pump, using Apiezon oil, which produced pressures of $2 - 5 \times 10^{-5}$ mm. of mercury as measured by an ionization gauge. The slides were mounted on a jig (fig. 3.1) 20cm. above the evaporating heaters, and the jig could be rotated so that the slides lay directly above each heater in turn. It was calculated (Holland 1958) that the thickness of the evaporated film over different parts of the slide would not vary more than 4%.

The layout of the evaporated films on the slide was as shown in fig. 3.2. The substrate metal was evaporated over the whole surface of the slide except for a small area at one edge which provided a step for thickness measurements. The overlayer metal was then evaporated on

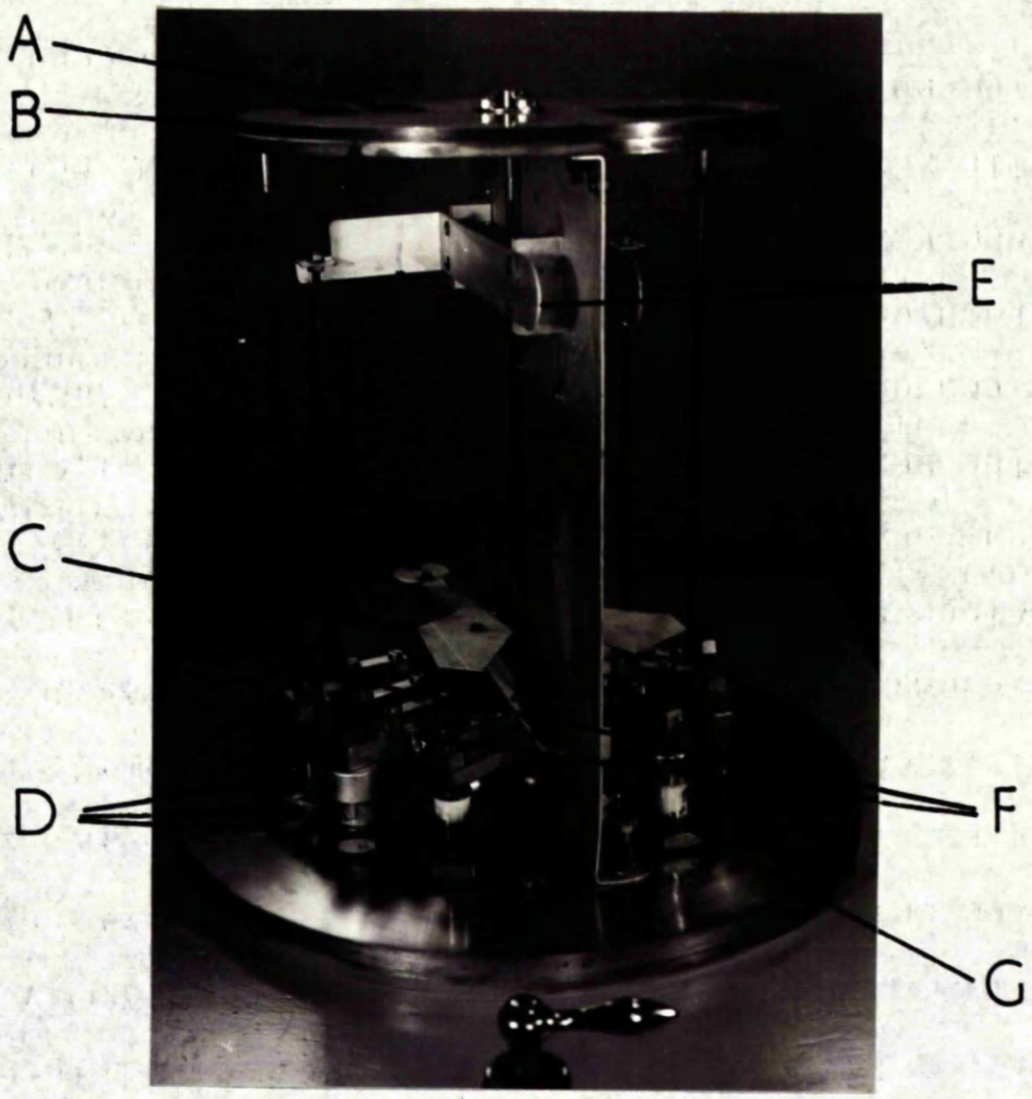

Fig. 3.1 The Evaporating Chamber.

A Glass Slide

B Slide Carrier

C Evaporating Shutter

D Heater Electrodes

E Glow Discharge Electrodes

F Evaporation Sources

G Gearing Mechanism

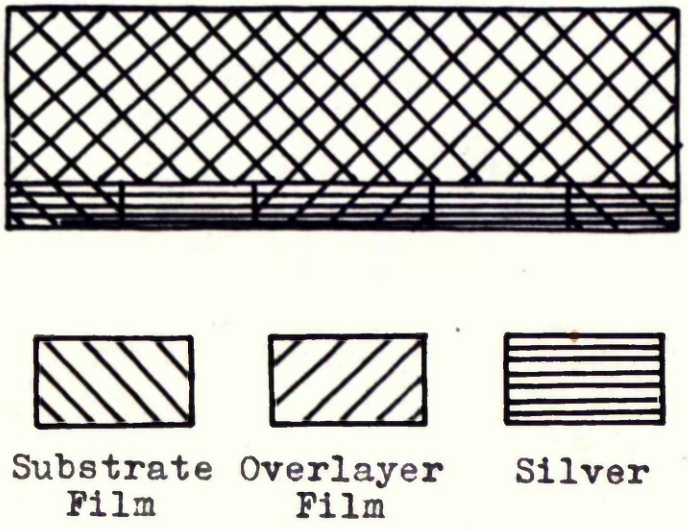

Fig. 3.2 Layout of Evaporated Metal Films on Glass Slide.

top, there being a delay of no more than 1½ min. between the two evaporations. A small area at one side was again left clear to give a step for thickness measurements. Finally, an opaque silver film was deposited over the steps at the edge of the slide.

Two basic types of evaporation sources were used - boats made from 0·010 in. molybdenum sheet and baskets wound from 1 mm. tungsten wire, single or stranded. In table 3.1 the types of heater used for each metal are listed. High purity metals were used and to remove any impurities introduced in handling, evaporation was allowed to proceed for the first few seconds with a shutter in position over the crucible.

The completed slide was removed from the vacuum chamber and the film thicknesses were found by multiple-beam interferometry using Fizeau fringes of equal thickness as described by Tolansky (1948). The slides were then stored at room temperature till required for annealing. Provided diffusion took place extremely slowly at room temperature, it was found that the length of time for which the slide was stored did not affect the ageing curve.

3.2 Reflectometers and Annealing Procedure

The reflectivities of the slides were determined

TABLE 3.1

Metal	Form of Metal	Type of Heater	Heater Material	Approx. Rate of Evaporn. (Å/sec)
Aluminium	1mm. Wire	Basket	Stranded Tungsten	90
Cadmium	Small Chips	Boat	Molybdenum	500
Copper	2mm. Wire	Boat	Molybdenum	40
Gold	0·013" Wire	Boat	Molybdenum	70
Indium	Small Chips	Boat	Molybdenum	350
Lead	Foil	Boat	Molybdenum	400
Magnesium	2mm. Wire	Basket	Tungsten	40
Manganese	Small Chips	Basket	Tungsten	20
Silver	0·5mm. Wire	Boat	Molybdenum	150
Tin	Small Chips	Boat	Molybdenum	150
Zinc	Small Chips	Boat	Molybdenum	300

by using the reflectometer shown in fig. 3.3, and comparing the light intensity reflected by the slide under measurement with the intensity of the undeviated light beam. Lens L_1 focussed an image of the source, an 80 watt high pressure mercury discharge tube, onto a screen, and a pin-hole (A_1) in the screen acted as a point source. Lens L_2 of long focal length gave a beam of almost parallel light and the diameter of this light beam was reduced to 4 mm. by the aperture A_2. The light was reflected by the slide as shown. It was found in preliminary experiments that the slides used were not perfectly plane and that they tended to act as concave or convex mirrors, thus affecting the intensity of the light beam striking the photomultiplier. This effect was eliminated by using lens L_3 to focus A_2 onto A_3. The light intensity was measured by an RCA 931A photo-multiplier cell contained in a light-tight box with a filter over the only aperture A_3. The accuracy of the reflectivity values obtained with this instrument was $\pm 1\%$. Over several separate evaporations, the reflectivity of a given metal was found generally to be constant to $\pm 2\%$.

This reflectometer was used for reflectivity changes taking 4 hr. or longer. The slide was annealed in a hot air oven thermostatically controlled to $\pm 1°C$, and was removed at regular intervals and its reflectivity measured. Allowance had to be made for the time taken by the slide

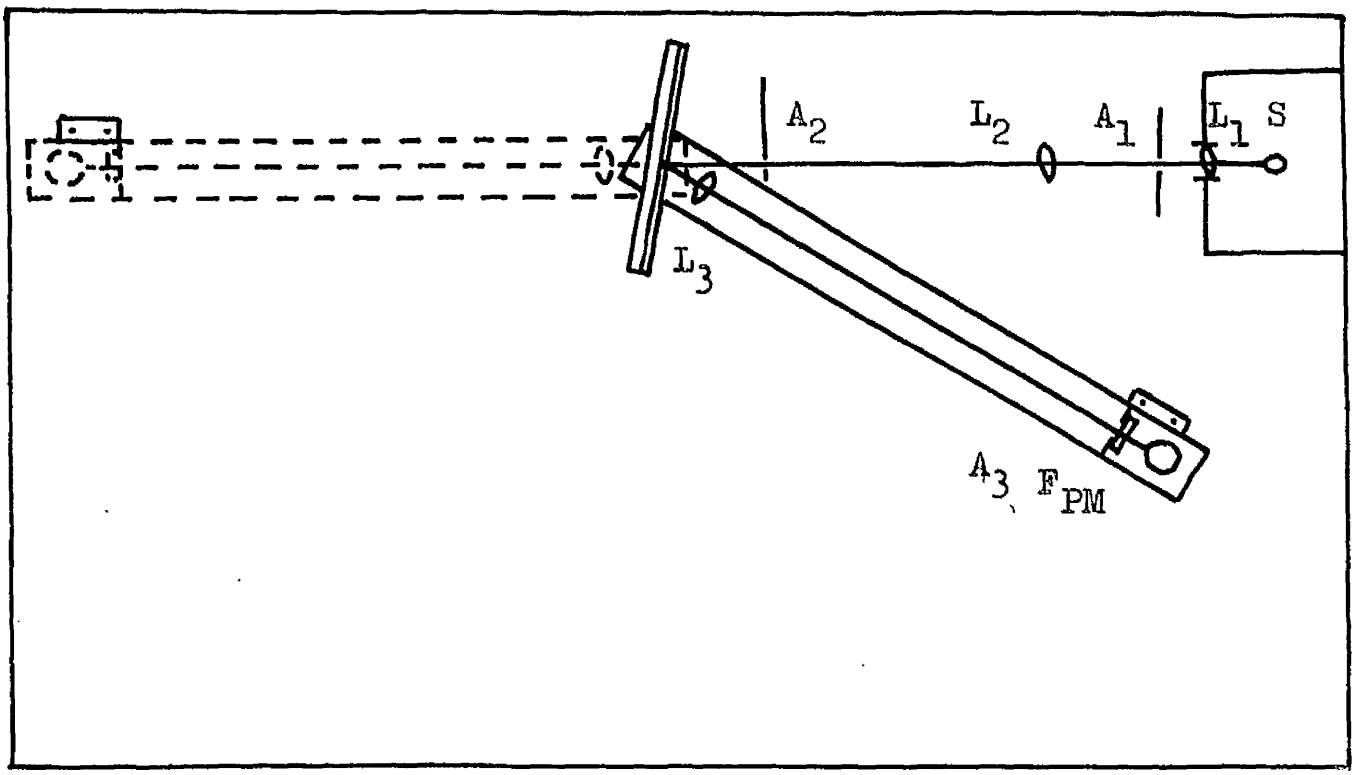

Fig.3.3 Diagram of Standard Reflectometer: S light source, L_1 L_2 L_3 lenses, A_1 A_2 A_3 apertures, F filter, PM photomultiplier.

to regain the temperature of the oven. For periods under 4 hr. this allowance led to considerable errors and it was necessary to devise a reflectometer in which the reflectivity could be measured while the slide was still being heated.

This "hot stage" reflectometer was based on the design of Coleman and Yeagley (1943) and a general view is shown in fig. 3.4.

The optical system is shown in fig. 3.5. Lens L_1 focussed an image of the source, an 80 watt mercury discharge tube, onto a screen and a pin-hole (A) in the screen acted as a point source. Lens L_2 gave a beam of near parallel light and this entered the light-tight box through a tube 5 in. long to exclude stray light. Part of the light was reflected upwards by the beam splitter (BS), struck the heated slide, and was reflected back along the same path. Part of this reflected light was transmitted through the beam splitter and struck the photomultiplier (PM), whose output was directly proportional to the reflectivity of the heated slide. The photomultiplier was found to age in use, and the output tended to decrease somewhat even while the reflectivity remained constant. It was accordingly found necessary to incorporate a reference surface of constant reflectivity in the apparatus. The portion of the incident light beam transmitted by the beam

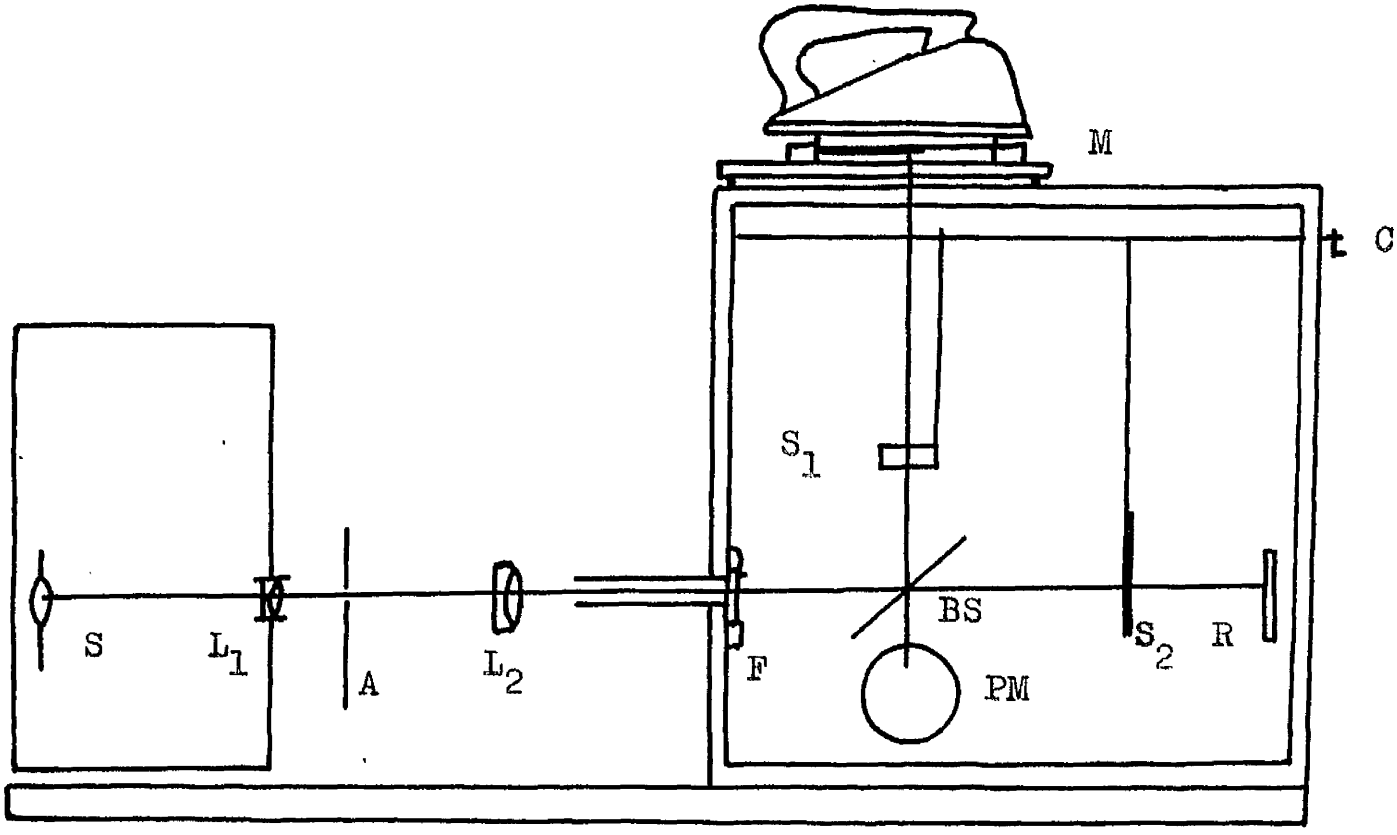

Fig. 3.5 Diagram of Hot Stage Reflectometer; S light source, L_1 L_2 lenses, A aperture, BS beam splitter, R reference surface, M slide under measurement, PM photomultiplier, S_1 S_2 Shutters, C Crank.

splitter was reflected by this reference surface (an evaporated aluminium film) and part of this light was reflected by the beam splitter downward into the photomultiplier. Light from either the heated slide or the reference surface was selected by moving shutters S_1 and S_2. The photomultiplier was adjusted to give a constant output from the reference surface before any reading was taken from the heated slide. These readings were checked against the other reflectometer to give values of reflectivity.

The slide under test was held in a groove milled into the top of a brass block. Two chromel-alumel thermocouples were let into the brass block and made direct contact with the lower surface of the glass slide so that the exact slide temperature was measured. A second brass block rested on the lower one and just touched the glass surface. Two thermocouples were let into this block directly above the point where the reflectivity of the slide was being measured. The two lower thermocouples were used for reflectivity measurements at the air surface, and the two upper ones for measurements at the glass surface. One thermocouple was used for measuring the slide temperature accurately, whilst the second was used for control purposes as described below.

It had been suggested by Coleman and Yeagley (1943) that a thermostatically controlled electric iron would keep the slide temperature constant to ±1°C. The temperature differential of the iron purchased by the author was ±15°C, and so was useless for control purposes. The iron was accordingly used simply as an electric hot-plate and operated in conjunction with a temperature controller.

The circuit diagram of the temperature controller is shown in fig. 3.6. The output from the thermocouple was connected to a spot galvanometer. The thermocouple current was opposed by a constant current of 40 μa from a bell battery. A variable proportion of this 40 μa could be sent through the galvanometer by means of the 300Ω variable resistance. This gave null readings in the temperature range 0 to 310°C. On one side of the galvanometer scale a photocell was fitted, and this, operating through an amplifier and relay, controlled the current to the hot-plate. If the temperature of the slide exceeded the balance temperature, the spot of light deflected onto the photocell, the power to the hot-plate was switched off, and the slide cooled until the spot moved off the photocell. Hence the slide temperature cycled round the control setting, the mean differential being ±1½°C.

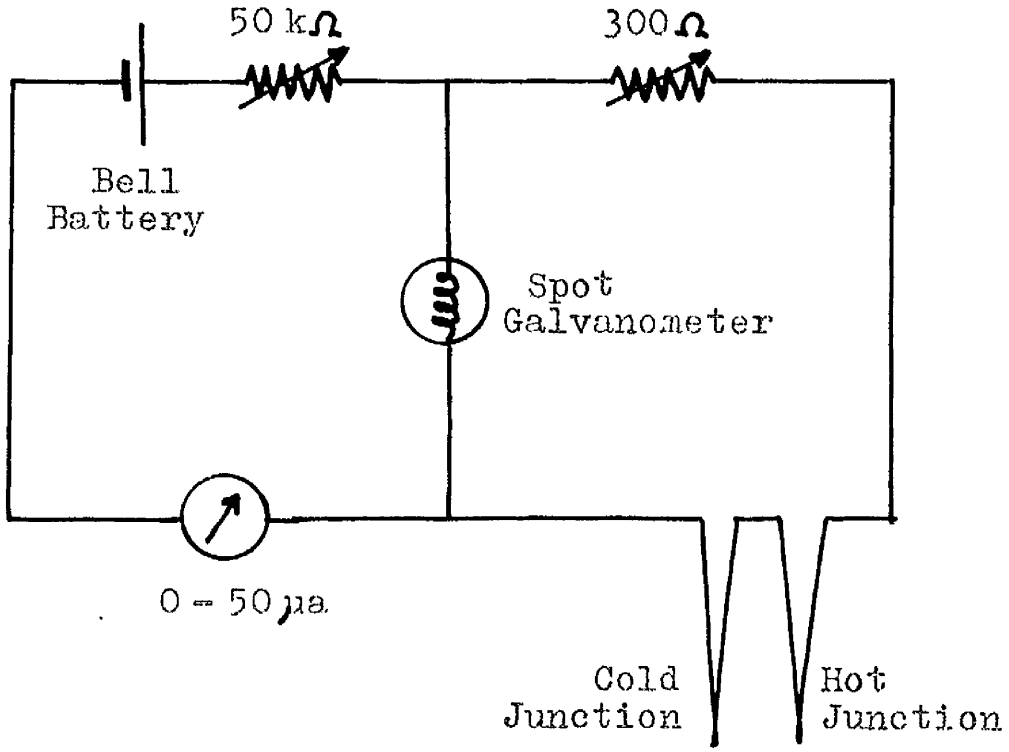

Fig. 3.6 Circuit Diagram of Temperature Controller.

The "hot stage" reflectometer allowed ageing processes of duration as short as 2 min. to be investigated. The hot air oven was used for ageing periods of from 4 hr. to 100 hr. or more. There was no critical temperature beneath which ageing phenomena were not observed. Indeed, some specimens in the gold-lead system gave perfectly normal ageing curves for 3 months ageing at room temperature.

3.3 The Evaporation of Alloys

Reflectivities were required for a large number of alloys, but a search of the literature revealed very few such values. Consequently, techniques were developed for evaporating opaque films of alloys.

It is not normally possible to evaporate an alloy in the same way as a pure metal, for the more volatile component will evaporate off more quickly to give an evaporated film different in composition from the original alloy.

A method of determining the rates of evaporation of the components of an alloy has been developed by Holland (1958). The mass of a metal evaporated in unit time is given by the Langmuir equation,

$$E = kP\,(M/T)^{\frac{1}{2}} \qquad (3.1)$$

where P is the vapour pressure at T°C, M the molecular

weight of the substance evaporated, and k is a constant.

Consider an alloy with composition W_a gm. of component A and W_b gm. of component B. To obtain an evaporated film with the same composition it is necessary that the ratio of the rates of evaporation E_a/E_b must be equal to W_a/W_b. From (3.1) we find

$$E_a/E_b = (P'_a/P'_b)(M_a/M_b)^{\frac{1}{2}} \qquad (3.2)$$

where P'_a and P'_b are the partial vapour pressures of the components.

Dushman (1949) has assumed that Raoult's law, applicable to dilute solutions, can be applied to both alloy components. It is found that

$$\frac{E_a}{E_b} = \frac{W_a P_a}{W_b P_b} \left(\frac{M_b}{M_a}\right)^{\frac{1}{2}} \qquad (3.3)$$

where P_a and P_b are the vapour pressures of the pure metals. Hence, for the evaporated alloy film to have the same composition as the original alloy we require

$$P_a/M_a^{\frac{1}{2}} = P_b/M_b^{\frac{1}{2}} \qquad (3.4)$$

Values of $P/M^{\frac{1}{2}}$ varied from 1.9×10^{4} for cadmium to 7.9×10^{-5} for gold (table 3.2), indicating that the rates of evaporation varied very considerably from metal to metal.

Normal evaporation techniques could be used only for copper-aluminium, which has been called a

TABLE 3.2

THE VAPOUR PRESSURES OF METALS

Metal	Vapour Pressure (P) at 1200°C (mm. of Hg)	M	$\sqrt{M}$	$P/\sqrt{M}$
Cadmium	2.0×10^{5}	112.4	10.6	1.9×10^{4}
Zinc	2.0×10^{4}	65.4	8.1	2.5×10^{3}
Lead	1.8×10^{1}	207.2	14.4	1.3
Indium	7.0×10^{-1}	114.8	10.7	6.5×10^{-2}
Silver	1.7×10^{-1}	107.9	10.4	1.6×10^{-2}
Aluminium	9.0×10^{-3}	27.0	5.2	1.7×10^{-3}
Tin	7.4×10^{-3}	118.7	10.9	6.8×10^{-4}
Copper	2.8×10^{-3}	63.5	8.0	3.5×10^{-4}
Gold	1.1×10^{-3}	197.2	14.0	7.9×10^{-5}

"constant evaporation rate " alloy (Holland 1954), and evaporates without undue fractionation.

It had been suggested (Holland 1958) that a stranded tungsten heater was most satisfactory for evaporating copper-aluminium alloys. Specimens of bulk alloys were prepared and were evaporated from stranded tungsten filaments. It was found that the molten copper-aluminium readily wet the tungsten and evaporated easily. No fractionation was found in any of the alloys vaporized, the films having the same tint at both the air and glass surfaces.

3.4 "Flash" Evaporation Technique

When one of the alloy components is more volatile than the other, films of uniform composition can be prepared by dropping the mixed metals, a few grains at a time, onto a molybdenum boat maintained at a high temperature. This means that the film is prepared by a series of discrete rapid evaporations. This "flash" evaporation technique was first used by Harris and Siegel (1948) to prepare alloy films of AuCd and of β brass. The technique was used very extensively in the present investigation to find the reflectivities of a large number of alloys.

The apparatus used for the flash evaporation is

shown in fig. 3.7. Finely granulated metal powders were carefully mixed together in the correct proportions and laid on a strip of thin paper resting on a perspex plate. The paper could be moved over the edge of the plate by means of a wire connected to a push-pull vacuum seal. As the paper moved over the edge, the powder fell onto the steeply inclined upper chute and dropped down to emerge from the lower chute immediately above the boat crucible. Preliminary experiments were carried out with several metal and alloy powders but it was always found that the finely divided grains were repelled from the hot source. The technique finally adopted was to carry out the evaporation in a series of about ten steps by dropping a few grains of powder onto the warm boat, heating the boat till the grains were evaporated, and then allowing the boat to cool down somewhat before dropping in further grains. This technique generally gave films uniform in appearance which did not normally require annealing to aid homogenization. The uniformity of the films was checked very simply by comparing the reflectivity values at the glass and air surfaces.

Graphs of reflectivity against concentration were obtained by "flash" evaporation for the systems: gold-aluminium, silver-aluminium, gold-cadmium, gold-indium, silver-indium, silver-cadmium, gold-lead, and silver-lead.

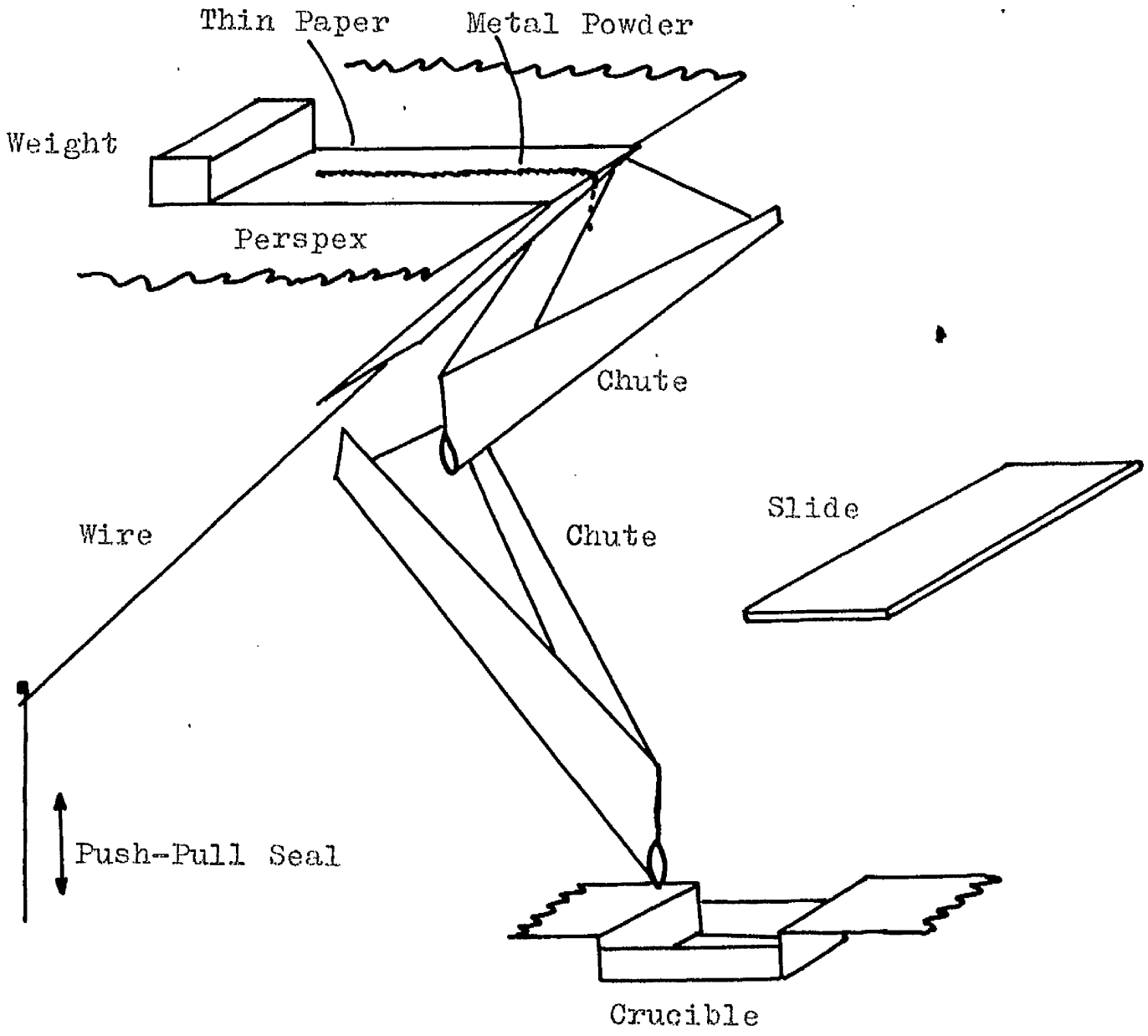

Fig. 3.7 Apparatus for the "Flash" Evaporation of Metal Alloys.

CHAPTER 4

PRELIMINARY SURVEY OF REFLECTIVITY CHANGES

4.1 Introduction

In order to determine which metal pairs gave reflectivity changes on heating, a survey was made of 39 different pairs. In each case two slides were prepared, the order of deposition being reversed for the second slide. The film thicknesses were not measured, but each film was deposited till it was just opaque i.e. until the thickness was roughly 1000Å. The slides were cut and the portions were aged at three different temperatures- room temperature for one week, 146°C for one day, and 260°C for 8 hr.

We shall discuss the results obtained by considering in turn the different types of metal systems.

4.2 Miscible Systems

Two miscible metal systems were investigated - silver-gold and copper-gold, but neither gave a reflectivity change on annealing. It was not possible to investigate any other miscible system (e.g. silver-palladium, gold-palladium and gold-platinum) because of the difficulty of

evaporating thick films of palladium and platinum.

It is unfortunate that no miscible metals could be investigated in detail, since these are the simplest alloy systems with no formation of intermetallic compounds. Diffusion is generally very slow in miscible systems, for the two metals have similar structures and melting points, and this appears to be the reason why no reflectivity changes were observed. Higher temperatures could not be used since these caused aggregation of the films.

4.3 Partially Miscible Systems

The metal pairs silver-manganese and copper-manganese were investigated. In these systems a solid solution of manganese in the other metal is formed, but otherwise the metals are immiscible. Neither of these systems showed reflectivity changes on ageing.

4.4 Non-Miscible Metals

Metals which are not miscible in one another would not normally be expected to give reflectivity changes. Eleven non-miscible metal pairs were prepared to check this - silver-copper, silver-lead, aluminium-indium, aluminium-lead, aluminium-zinc, cadmium-lead, copper-lead, indium-zinc, magnesium-manganese, manganese-lead and lead-zinc. Ten of these pairs showed no reflectivity change as expected.

In the silver-lead, however, a definite reduction in the silver reflectivity was observed on ageing. A detailed investigation was therefore carried out on this system (see chapter 10).

4.5 Intermediate Phase Systems

The most common type of phase diagram shows one or more intermetallic compounds between the two pure metals. These compounds may be formed directly from the melt or by a peritectic reaction, but as has been shown in fig. 2.7 this makes no difference to the form of the phase diagram at the temperature at which diffusion is being studied.

A total of 24 intermediate phase systems were studied for reflectivity changes. These are given in table 4.1. Most systems showed ageing effects, 18 out of the 24 giving definite reflectivity changes. Detailed investigations were carried out for eight of these systems (table 4.2), chosen for their ease of evaporation and to give groups of systems with, for example, a gold substrate. The results are given in chapters 5 to 9 where each system is considered in turn, and where, for clarity, the same order of presentation and discussion is followed for each system.

TABLE 4.1

LIST OF INTERMEDIATE PHASE SYSTEMS INVESTIGATED

Silver-Aluminium*	Silver-Cadmium*	Silver-Indium*
Silver-Magnesium	Silver-Zinc*	Aluminium-Gold*
Aluminium-Copper*	Aluminium-Magnesium*	Gold-Cadmium*
Gold-Indium*	Gold-Magnesium*	Gold-Manganese*
Gold-Lead*	Gold-Tin*	Gold-Zinc*
Copper-Indium*	Copper-Magnesium	Copper-Zinc*
Indium-Magnesium	Indium-Manganese	Indium-Lead
Magnesium-Lead	Magnesium-Zinc*	Manganese-Zinc*

(* indicates reflectivity changes take place)

TABLE 4.2

INTERMEDIATE PHASE SYSTEMS STUDIED IN DETAIL

System	Results Given in Chapter No.
Gold-Aluminium	5
Silver-Aluminium	6
Gold-Cadmium	7
Silver-Cadmium	7
Gold-Indium	7
Silver-Indium	7
Copper-Aluminium	8
Gold-Lead	9

4.6 The Rate of Diffusion

Results for the series of metals with gold are given in table 4.3. The order in which the metals are given is the decreasing order of the rate of disappearance of the gold colour (i.e. cadmium diffuses most readily and silver and copper do not diffuse).

It can be seen that the order is not closely related to the evaporating temperature of the second metal. There is a moderate correlation, however, with the temperature difference between the melting point of the metal and that of gold. This is in agreement with results for bulk specimens which show that diffusion is slower the closer are the melting points of the two metals (Le Claire 1949).

TABLE 4.3

Metal	Cadmium	Lead	Tin	Indium	Aluminium	Magnesium	Zinc	Manganese	Silver	Copper
Evaporating Temperature	264°C	718°C	1189°C	952°C	1100°C	443°C	343°C	980°C	1047°C	1273°C
Melting Point	324°C	328°C	232°C	157°C	660°C	651°C	419°C	1244°C	961°C	1083°C
Difference in Melting Points Compared with Gold	739°C	735°C	831°C	906°C	403°C	412°C	644°C	181°C	102°C	20°C

CHAPTER 5

REFLECTIVITY CHANGES IN GOLD-ALUMINIUM

5.1 Introduction

Very pronounced reflectivity changes were observed in thin film diffusion couples of gold-aluminium. Changes took place at both surfaces and measurements of diffusion in both directions were made. The gold was usually deposited before the aluminium to prevent possible formation of an oxide layer which might hinder diffusion.

The phase diagram of gold-aluminium is shown in fig. 5.1. Five phases appear to be thermally stable at low temperatures - $AuAl_2$, AuAl, Au_2Al, Au_5Al_2 and Au_4Al. We would expect all these phases to be precipitated at the gold-aluminium interface at the beginning of diffusion.

5.2 Reflectivity Changes at the Gold Surface

84°C was selected as a convenient ageing temperature since it allowed most of the films to be aged in the hot air oven. Fig. 5.2 shows the effect of light wavelength on a typical ageing curve. The curve was of the same basic form for all three wavelengths. Mercury yellow light, since it gave a greater reflectivity change (34%)

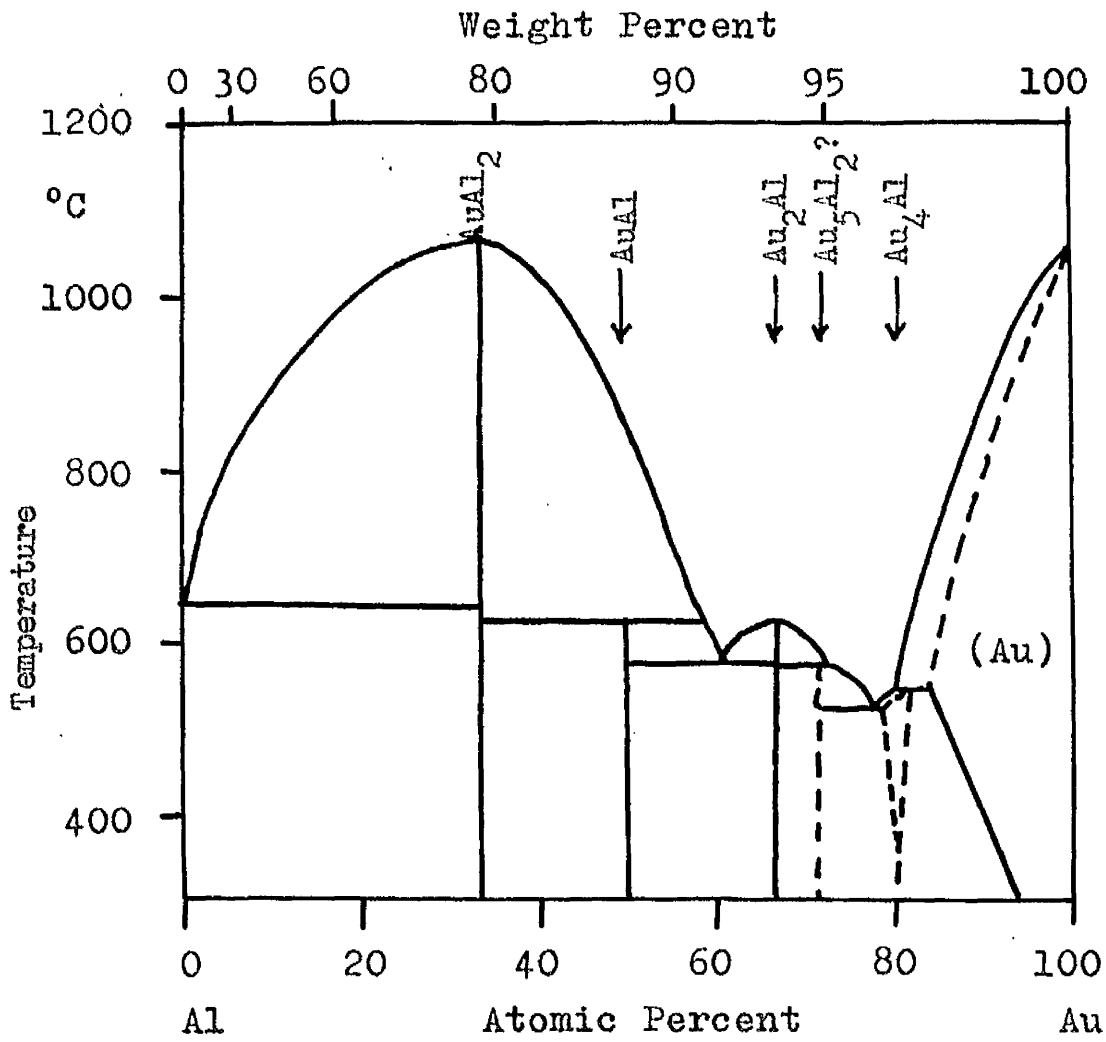

Fig. 5.1 Equilibrium Phase Diagram for Gold-Aluminium (Hansen 1958)

than mercury green light (25%) or mercury blue light (20%), was used for all subsequent measurements.

A set of slides was prepared with gold films of different thicknesses in the range 400Å to 3000Å. The gold was overlaid with a thick film of aluminium so that all reflectivity changes at the gold surface were complete before any change took place at the surface of the aluminium. Typical ageing curves are shown in fig. 5.2 to 5.4. As can be seen, the shapes of the curves differed, the length of the initial plateau increasing with film thickness.

The end of the initial plateau obviously corresponds to the stage at which the advancing atoms were first detected. We can either follow Schopper (see chapter 1.2) and assume that the subsequent changes in reflectivity were due to progressive changes in the surface composition, or, since it is well known that light waves can penetrate a small but finite distance into a metal, we may assume that the advancing atoms were detected before they actually reached the surface, and that the change in reflectivity took place while the advancing front was covering the remaining distance to the surface proper.

According to Schopper's theory the results should coincide when the results are plotted against t/d^2, but as shown in fig. 5.5 the curves coincide only at the

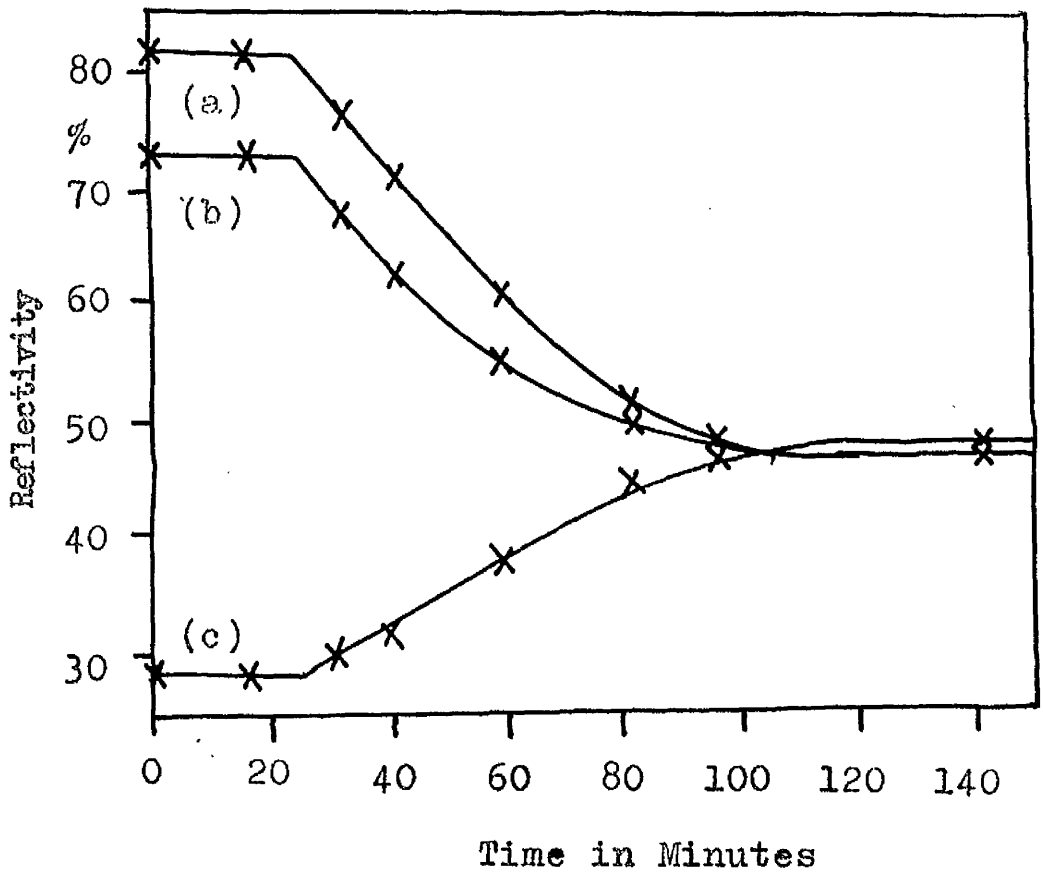

Fig. 5.2 Ageing of Gold-Aluminium Film at 84°C. Reflectivity changes at gold surface for gold thickness of 790A.
(a) Curve for mercury yellow light (λ = 5790A)
(b) Curve for mercury green light (λ = 5461A)
(c) Curve for mercury blue light (λ = 4358A)

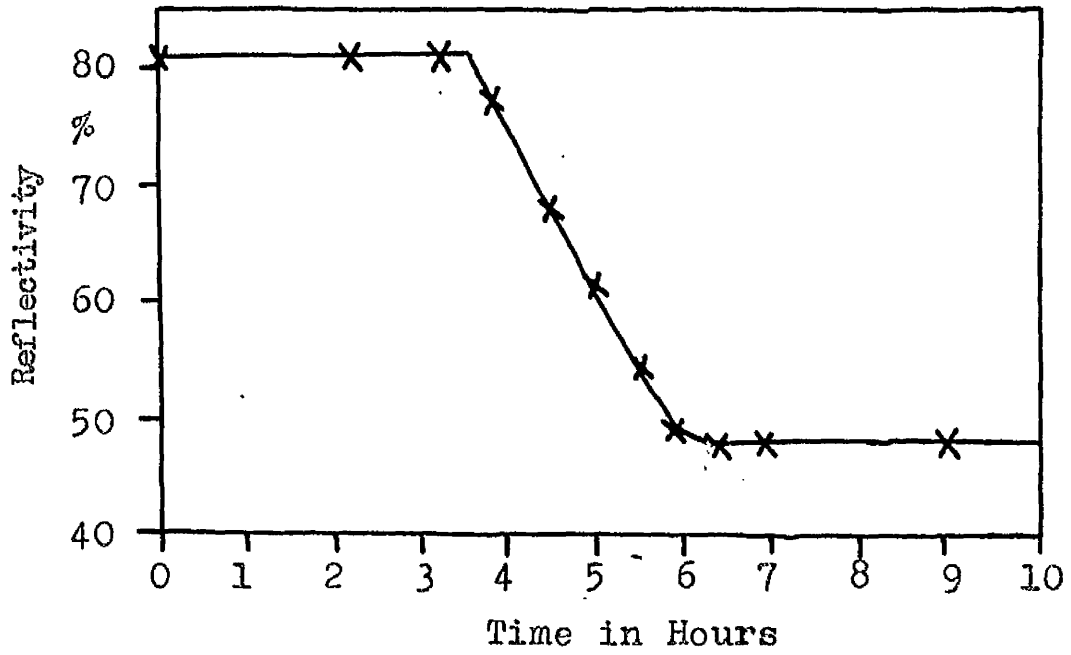

Fig. 5.3. Ageing of Gold-Aluminium Film at 84°C. Reflectivity change at gold surface for gold thickness of 1530A.

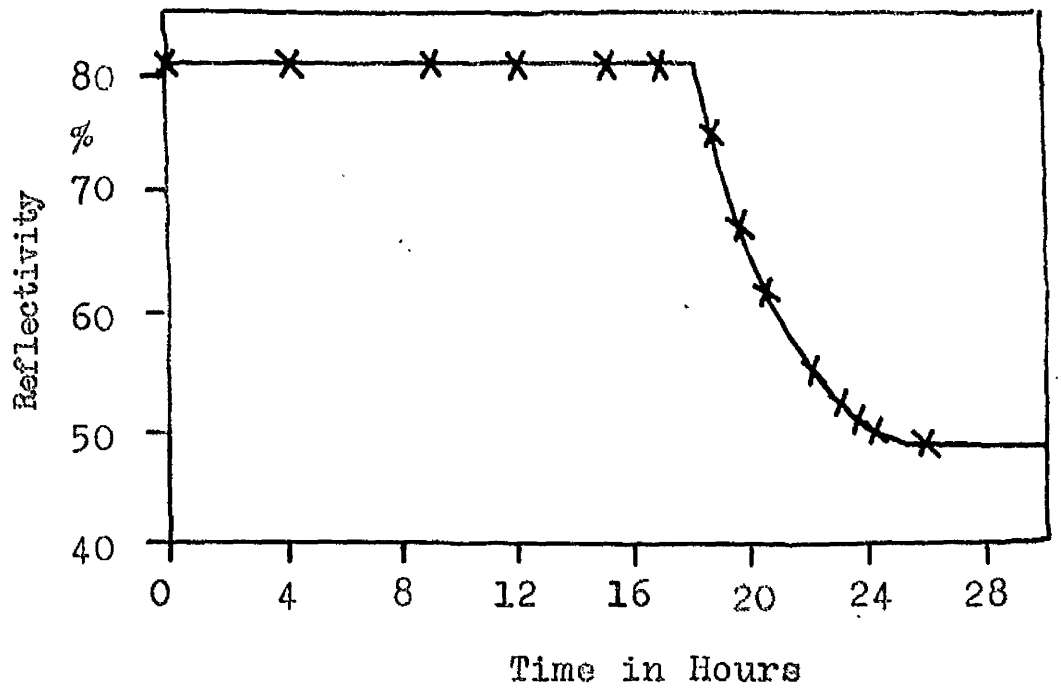

Fig. 5.4 Ageing of Gold-Aluminium Film at 84°C. Reflectivity change at gold surfaces for gold thickness of 3120A.

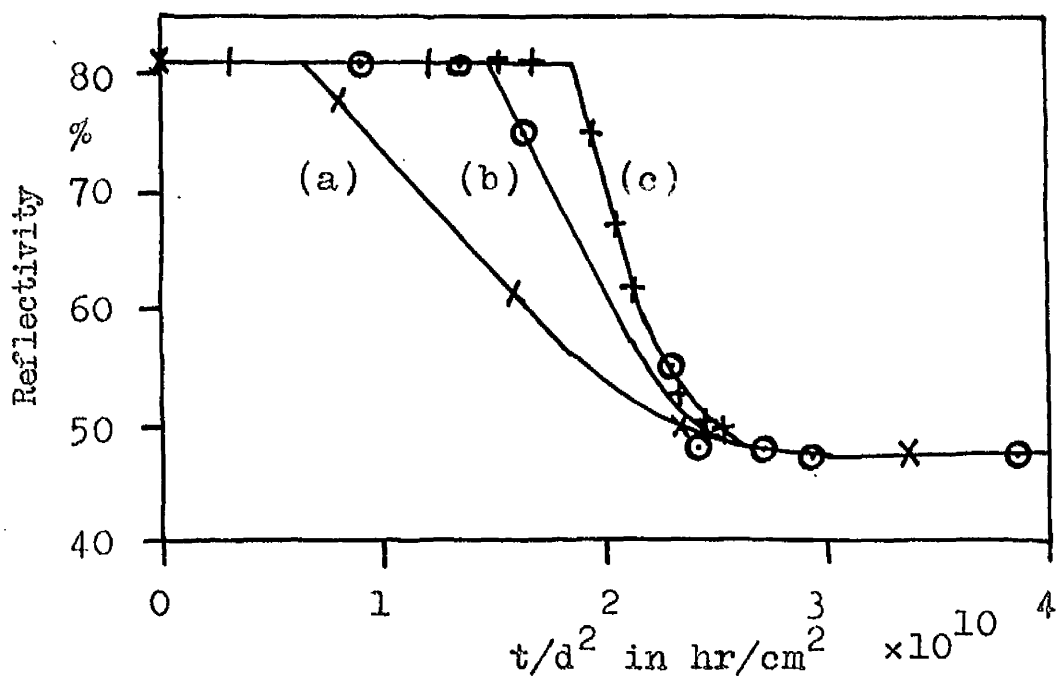

Fig. 5.5 Graph of reflectivity against t/d^2 for specimens shown in fig. 5.2 to 5.4. (a) Gold thickness = 790A, (b) gold thickness = 1530A, (c) gold thickness = 3120A.

beginning and end. The position of the break in the curves varies with film thickness. Assuming then that the advancing atoms are detected before they reach the surface, the abruptness of the change in reflectivity suggests that the advancing front is fairly sharply defined. It is unreasonable to expect a small concentration of aluminium atoms some distance from the surface to produce a marked change in reflectivity. Furthermore, the pronounced fall in reflectivity is somewhat surprising in view of the relatively high reflectivity of aluminium. We would expect only a slight change in reflectivity for small additions of aluminium to gold. These considerations, together with the low solubility of aluminium in gold, suggest that the reflectivity changes are produced by a sharply defined phase boundary.

It has been shown in chapter 2.9 that the motion of a phase boundary should follow the law $x^2 = D't$, where x is the distance the boundary moves from the initial interface in time t, and D' is the diffusion coefficient for the boundary. Assuming this relation in the case of a gold film 1000Å thick, the time required for the phase boundary to reach the glass surface, i.e. for the reflectivity to stop changing, is $t_2 = 10^{-10}/D'$ sec.. If it is assumed that light can penetrate 400Å into a gold film, then the time for the reflectivity to start changing

will be the time taken for the phase boundary to penetrate (1000 - 400) Å, i.e. $t_1 = 3{\cdot}6\times10^{-11}/D'$ sec.. Hence the ratio of the time taken for the reflectivity to begin changing to the time taken for the reflectivity to cease changing (i.e. ratio t_1/t_2) is

$$\frac{t_1}{t_2} = \left(\frac{3{\cdot}6\times10^{-11}}{D'}\right)\left(\frac{D'}{10^{-10}}\right) = 0{\cdot}36$$

This ratio was found for different values of film thickness, and in fig. 5.6 graphs of the ratio against gold thickness have been plotted for light penetrations of 300Å, 400Å and 500Å. The experimental values of ratio have also been plotted on this graph, and it can be seen that the points all lie close to the line for 400Å penetration. This is a reasonable value for the thickness of a near opaque gold film, and the close agreement of the experimental values with the theoretical curve suggests that this theory is correct and that the reflectivity changes are due to the motion of a sharply defined boundary rather than to a gradual change in concentration such as would occur if atoms in the gold lattice were being gradually replaced by aluminium atoms. The low solubility of aluminium in gold suggests that only a small amount of aluminium can exist in equilibrium with gold, and hence that the advancing aluminium atoms must be followed closely by a phase boundary. The low concentration of aluminium atoms preceding the

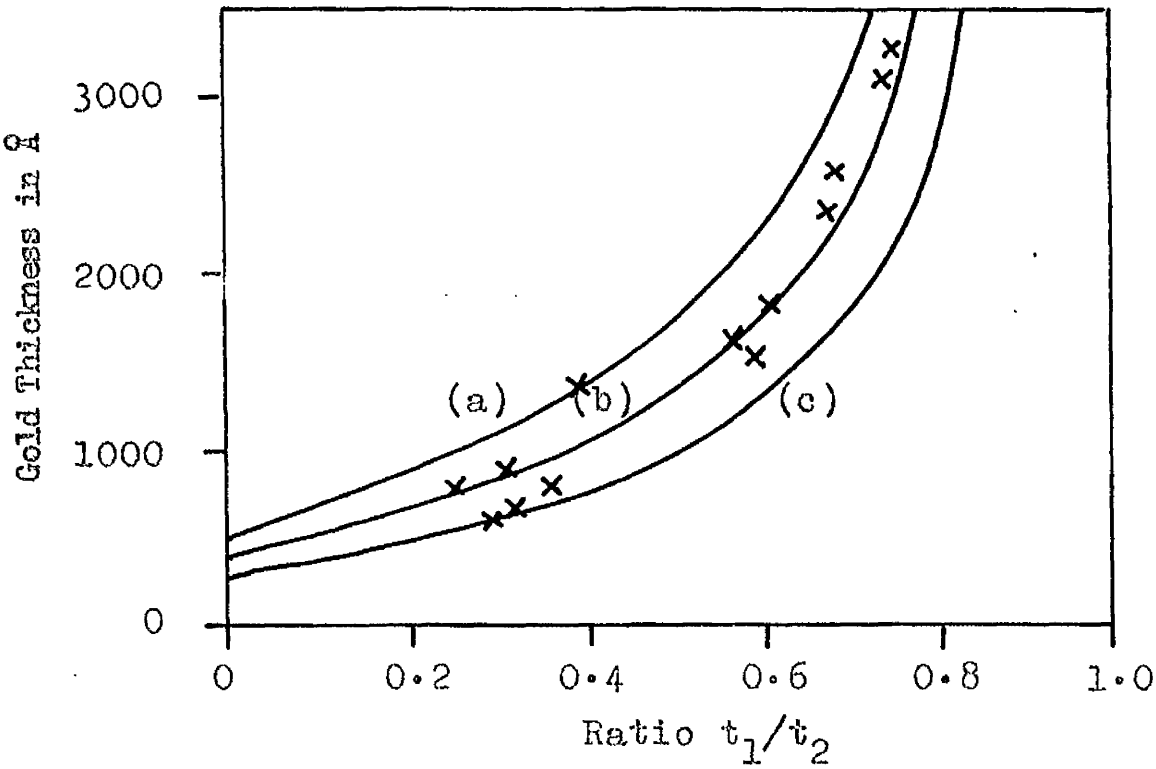

Fig. 5.6 Graph of Gold Thickness against Ratio t_1/t_2. Theoretical curves are plotted for light penetrations of (a) 500Å (b) 400Å (c) 300Å.

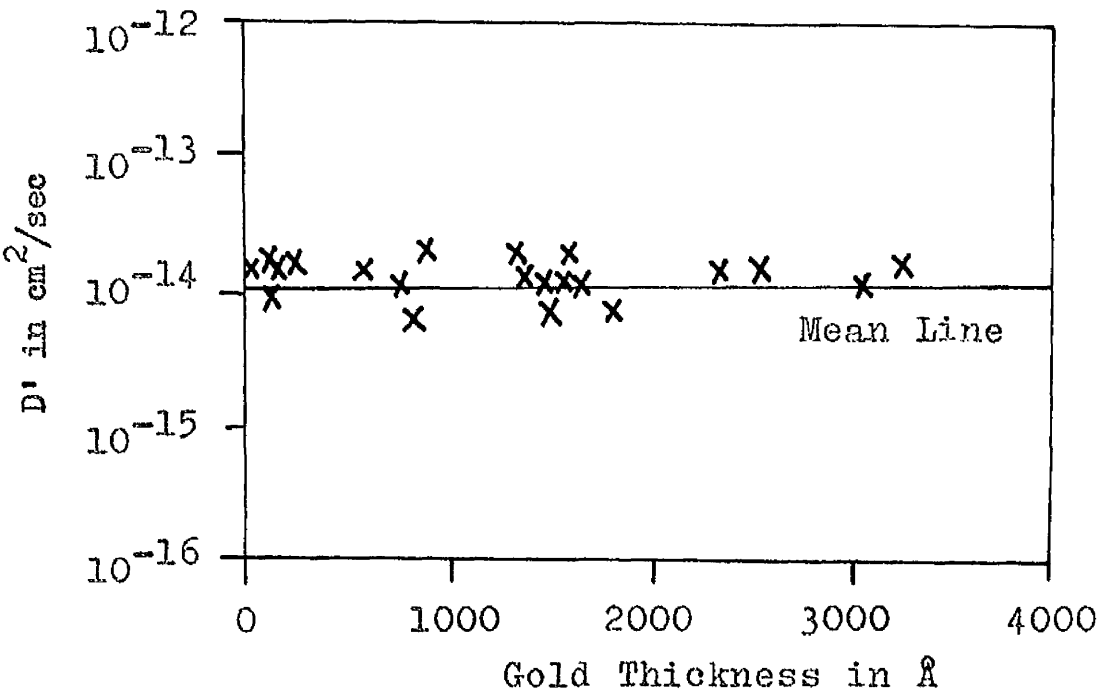

Fig. 5.7 Graph of Diffusion Coefficient (D') at 84°C against Gold Thickness.

phase boundary and forming a solid solution in the gold would not affect the reflectivity significantly and the reflectivity changes will be due to the advancing phase boundary. The results given later for very thin gold films (< 400Å) agree with these conclusions. These films showed no trace of an initial plateau and the reflectivity changes for these films resembled the tail end of the changes in thicker films.

Values of the diffusion coefficient (D') were calculated from the time taken for the reflectivity to stop changing. These results are plotted in fig. 5.7, which shows that there is no tendency for D' to vary with gold thickness. The mean value of D' at 84°C was found to be $1{\cdot}01 \times 10^{-14}$ cm^2/sec.

Different portions of the same slides were aged over a range of temperature from 70°C to 164°C. Typical results are shown in fig. 5.8 to 5.10 for a film thickness of 2620Å. The time of diffusion varied from 15 hr. at 84°C to 4 min. at 164°C, and yet the shape of the curve did not vary despite this vast difference in time. It has been shown in chapter 2.9 that the diffusion coefficient (D') will vary with temperature according to the Arrhenius equation (2.9), viz.

$$D' = D'_0 \exp(+E/RT)$$

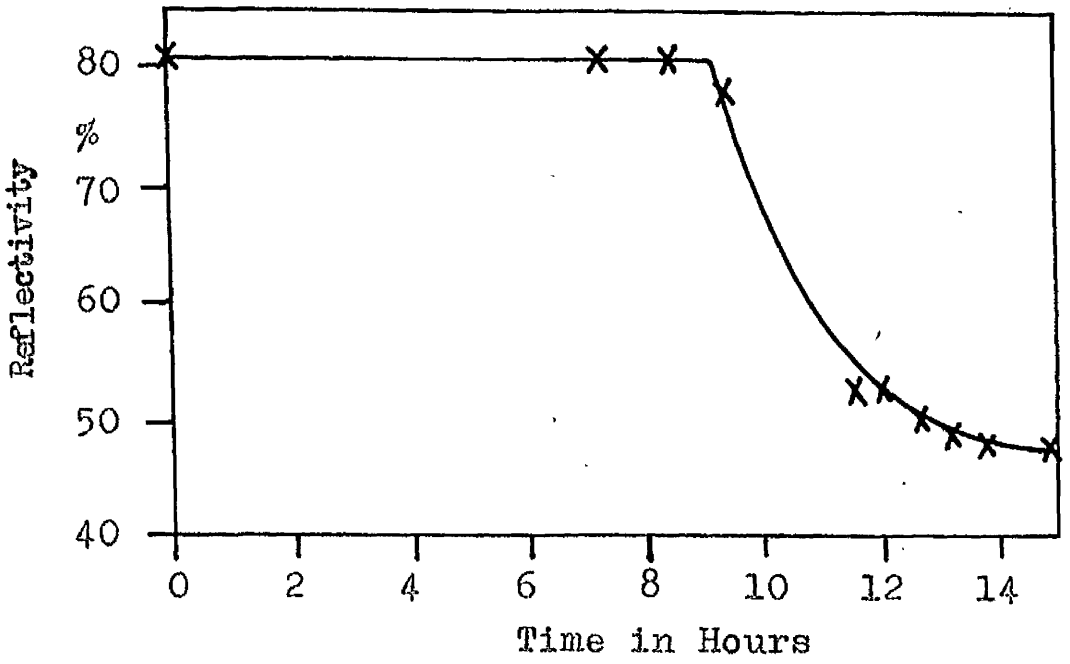

Fig. 5.8 Ageing of Gold Surface at 84°C for Gold Thickness of 2620Å.

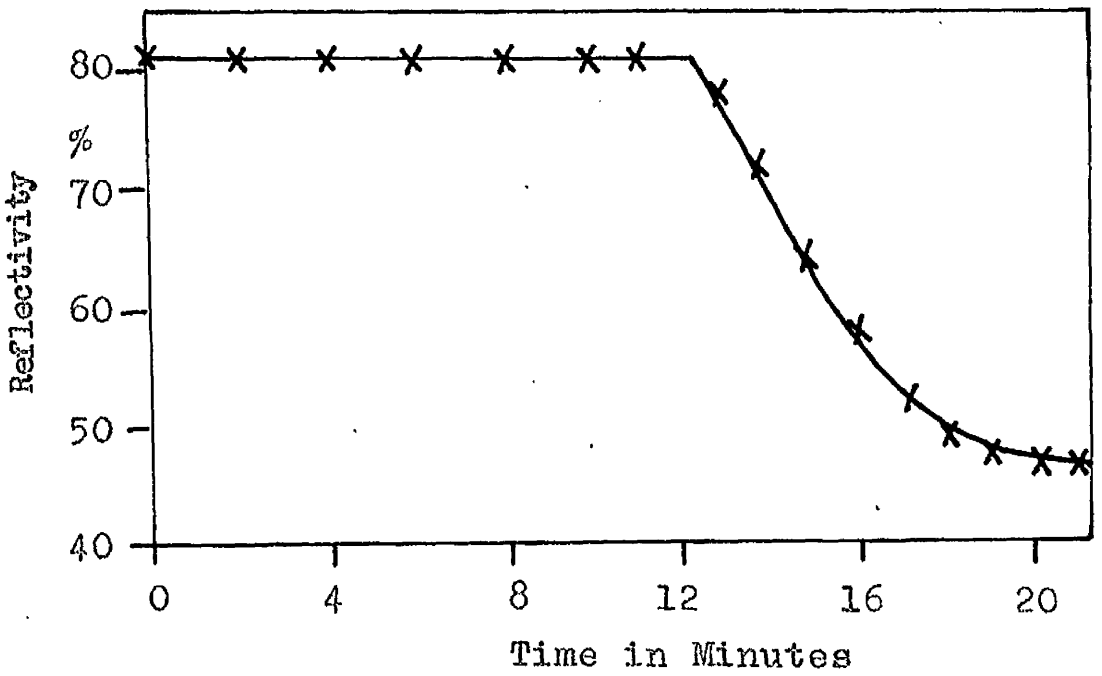

Fig. 5.9 Ageing of Gold Surface at 130°C for Gold Thickness of 2620Å.

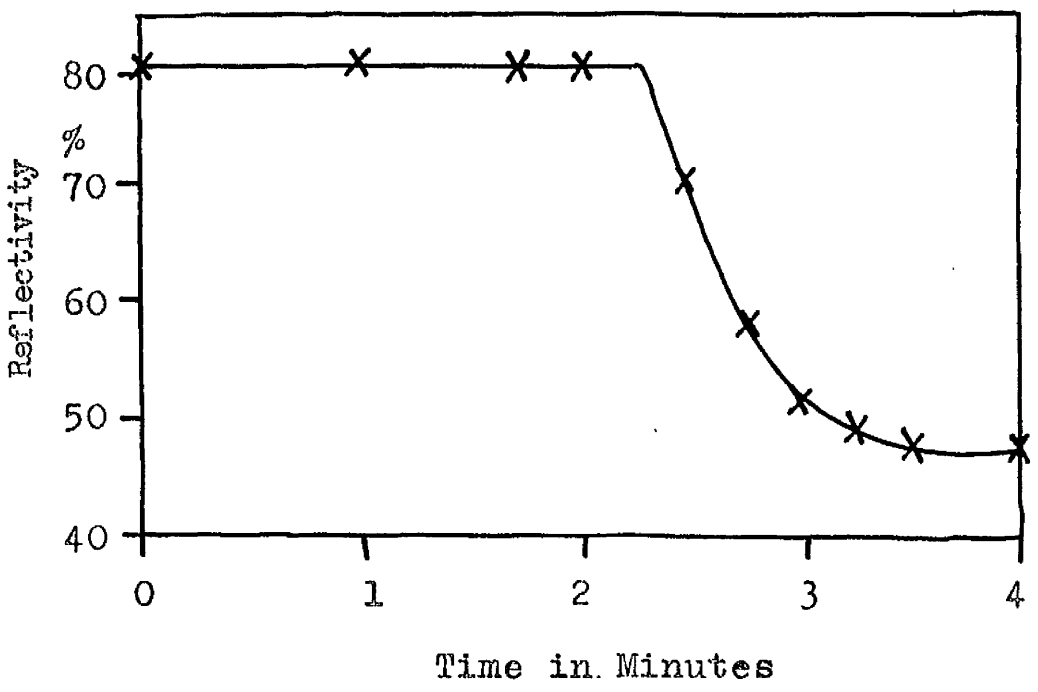

Fig. 5.10 Ageing of Gold Surface at 163½°C for gold thickness of 2620A.

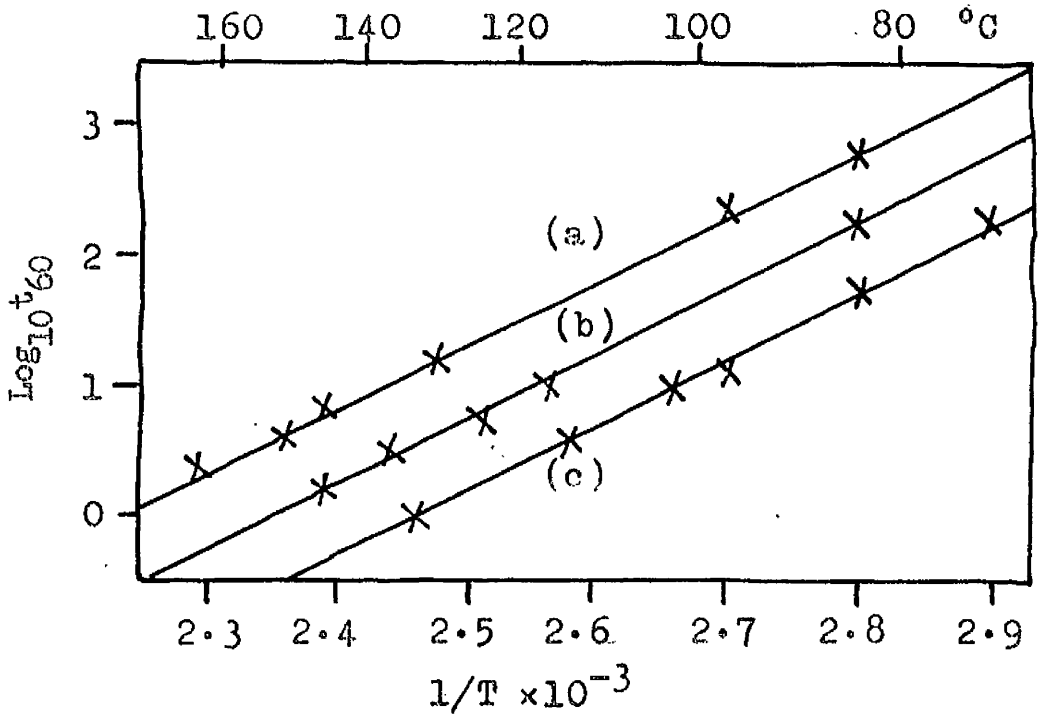

Fig. 5.11 Graph of $\log_{10} t_{60}$ against 1/T, where t_{60} is the time in minutes for the reflectivity to fall to 60% and T is the temperature in °K. (a) Gold thickness = 2620A, (b) gold thickness = 1630A, (c) gold thickness = 790A.

Hence $$1/D' = 1/D'_0 \exp (E/RT)$$

$$\log_{10}(1/D') = \log_{10}(1/D'_0) + E/2{\cdot}3RT$$

But $$D' = (d^2/t_2)$$

where d is the gold thickness. It is found experimentally that the shape of the ageing curve does not vary with temperature. Hence

$$t_2 = k\, t_{60}$$

where t_{60} is the time for the reflectivity to drop to 60% and k is a constant.

$$\log_{10}(kt_{60}/d^2) = \log_{10}(1/D'_0) + E/2{\cdot}3RT$$

$$\log_{10} t_{60} = \log_{10}(d^2/D'_0 k) + E/2{\cdot}3RT$$

$$\log_{10} t_{60} = K + E/2{\cdot}3RT$$

where K is a constant.

A plot of $\log_{10} t_{60}$ against (1/T) will give a straight line with gradient E/2·3R. This has been carried out in fig. 5.11 for the specimen shown in fig. 5.8 to 5.10. Similar lines are plotted on the same graph for slides with gold thicknesses of 1630Å and 680Å. The gradients, which depend only on E, are all equal, but they are shifted relatively to one another. E was calculated to be 22·6 kcal/mole, and knowing D' at 84°C, D'_0 was calculated to be 0.85 cm^2/sec.

Several slides were prepared with very thin gold films in the range 70Å to 350Å. These film thicknesses

were determined by measuring the reflectivity and transmission of the films and using the results of Rouard Malé and Trompette (1953) to obtain the thickness. Typical ageing curves are shown in fig. 5.12 and 5.13. No initial plateau was found in any of the ageing curves since the gold was not opaque and as soon as any diffusion occurred at the interface with the aluminium the reflectivity began to fall. The very thinnest film (70Å) gave only a very small reflectivity change (4%) as the diffusion zone in this case was very thin. Slides were aged over a temperature range from 21°C to 95°C and a graph of $\log_{10} t_{55}$ against (1/T) was plotted for film thicknesses of 155Å and 230Å (fig. 5.14). The activation energy was found to be 23·3 kcal/mole, in excellent agreement with the value for thicker films (22·6 kcal/mole). Values of D' were calculated from the time the reflectivity took to stop changing. These values were converted to 84°C using the value already obtained for the activation energy, and have been plotted with the previous results in fig. 5.7. We can see from this graph that there is no significant difference in D' for these very thin films compared with thicknesses greater than 400Å. Furthermore, the activation energy is the same, and so we can say that the same diffusion mechanism holds in films from 70Å to 3000Å thick.

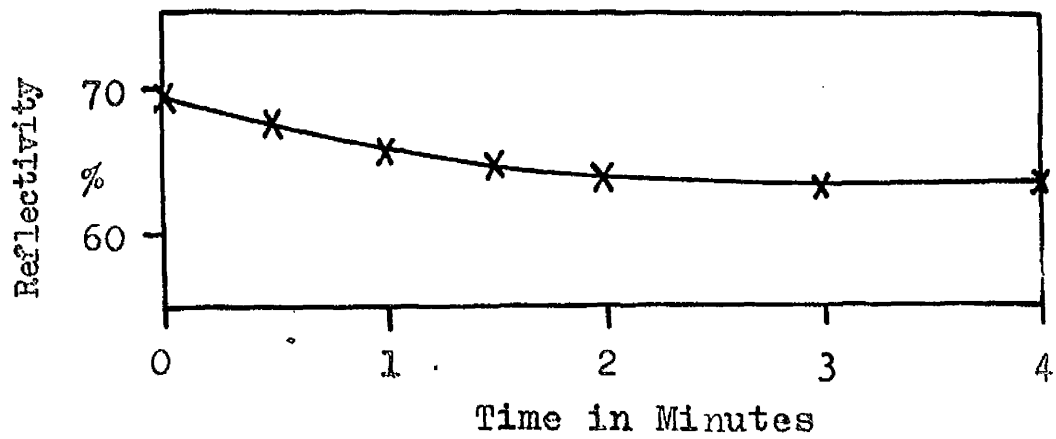

Fig. 5.12 Ageing of gold surface at 70°C for gold thickness of 70A.

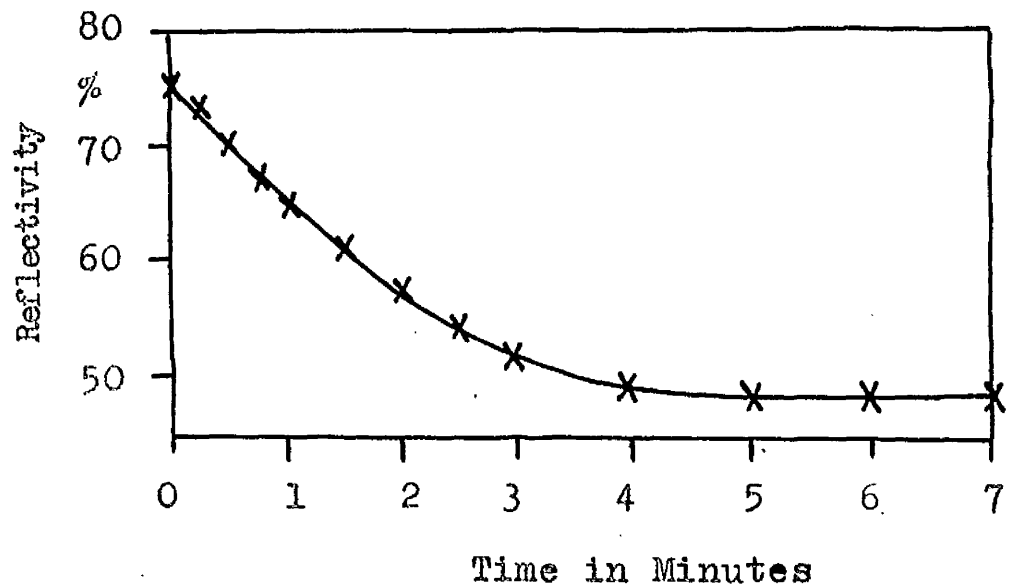

Fig. 5 13 Ageing of gold surface at 79°C for gold thickness of 155A.

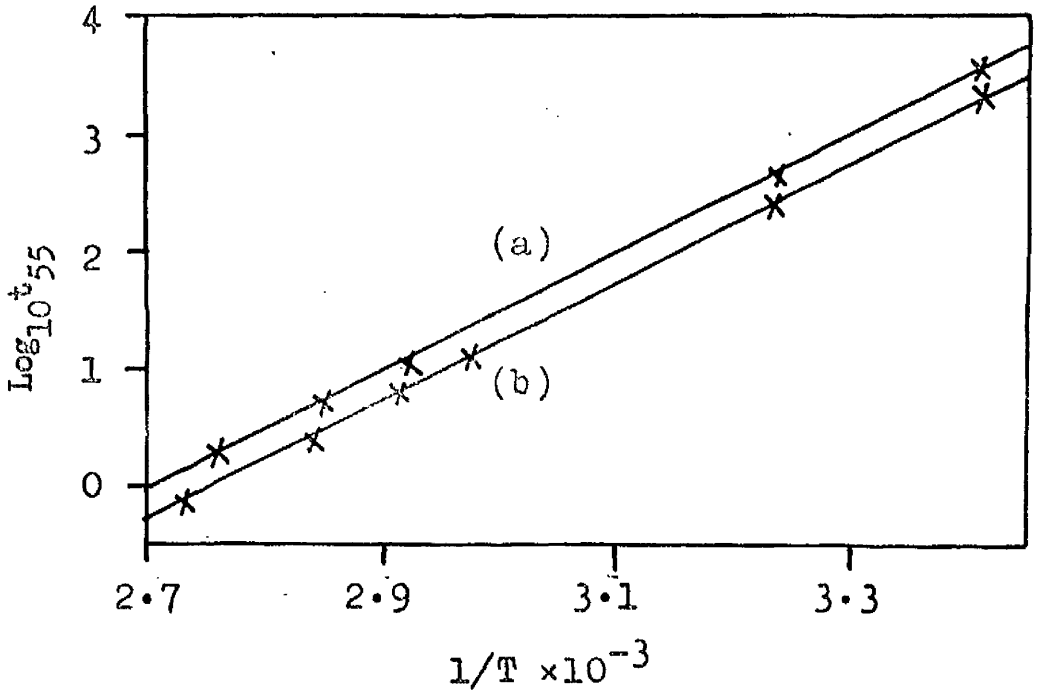

Fig. 5.14 Graph of $\log_{10}t_{55}$ against 1/T for very thin gold films. (a) Gold thickness = 230A, (b) gold thickness = 155A.

5.3 Reflectivity Changes at the Aluminium Surface

Reflectivity changes were also studied at the aluminium surface. This time the gold underlayer was made sufficiently thick for all reflectivity changes to be completed at the aluminium surface before any change took place in the reflectivity of the gold. A suitable ageing temperature was found to be 102°C, and slides were prepared with aluminium thicknesses varying in the range 500Å to 1600Å. Typical ageing curves are shown in fig. 5.15 to 5.17. On plotting against t/d^2 (fig. 5.18), it can be seen that the curves again coincided at the beginning and end of diffusion but the length of the initial plateau varies. The results in general resemble those for diffusion in the opposite direction.

Values of the ratio of the time for the reflectivity to start changing (t_1) to the time for it to cease changing (t_2) were calculated for all the specimens prepared, and are plotted against the aluminium thickness in fig. 5.19. The points all lie close to the theoretical curve for a light penetration of 300Å. It is less than the corresponding light penetration into gold (400Å) which was found for diffusion of aluminium into gold, but this is not surprising since the absorption coefficient (k) is greater for aluminium films (5·32) than for gold films (2·83)

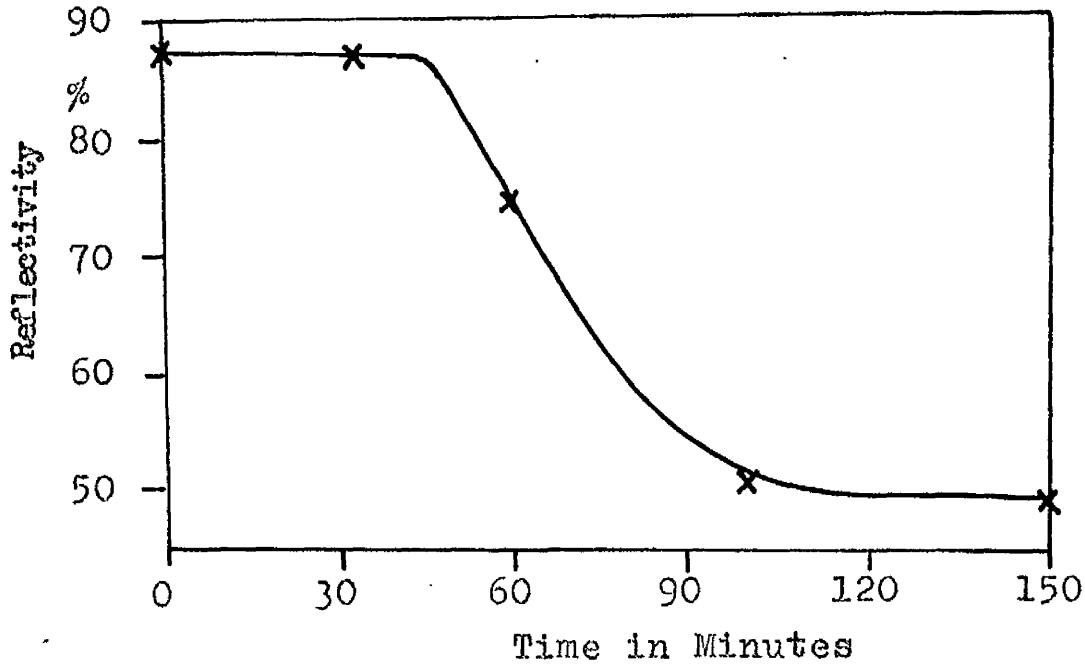

Fig. 5.15 Ageing of Aluminium Surface at 102°C for Aluminium Thickness of 720Å.

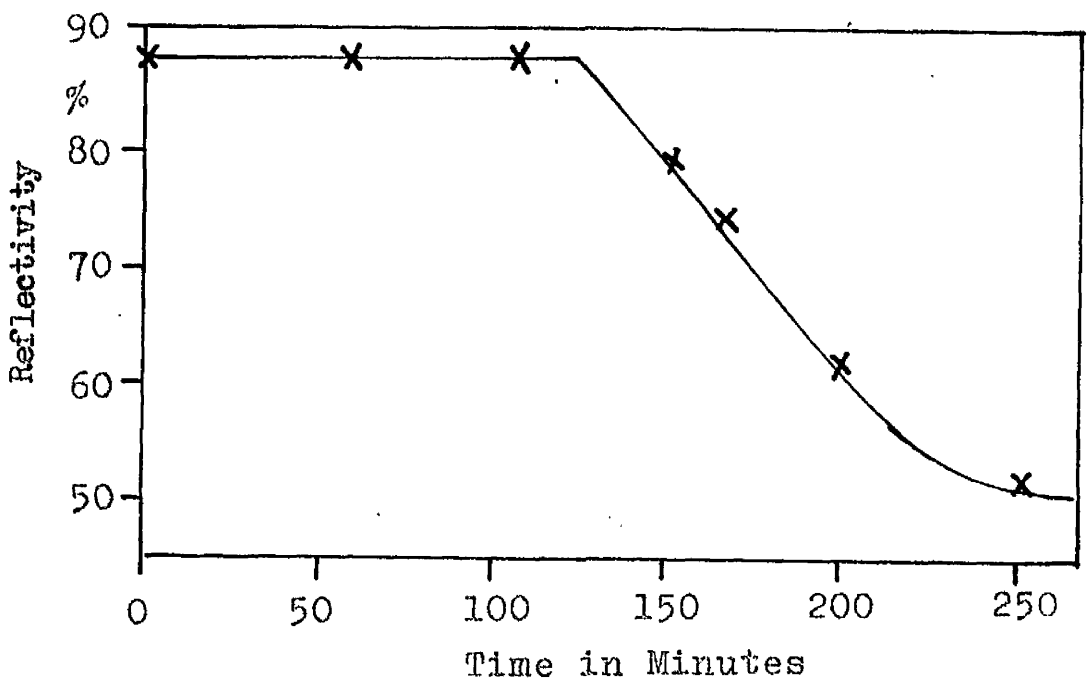

Fig. 5.16 Ageing of Aluminium Surface at 102°C for Aluminium Thickness of 1050Å.

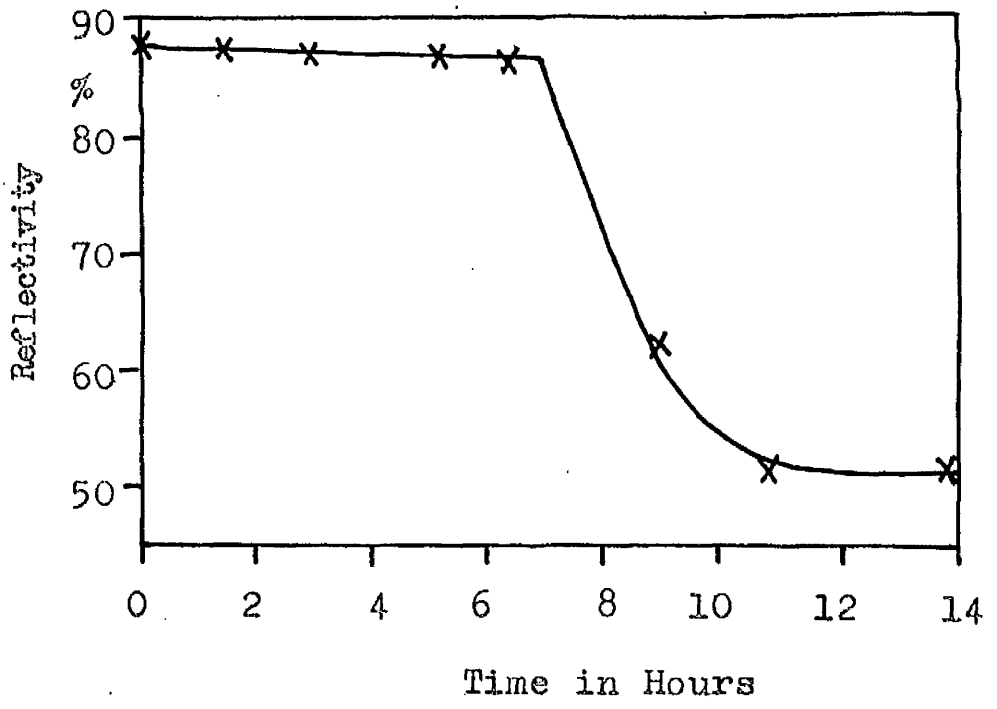

Fig. 5.17 Ageing of aluminium surface at 102°C for aluminium thickness of 1730A.

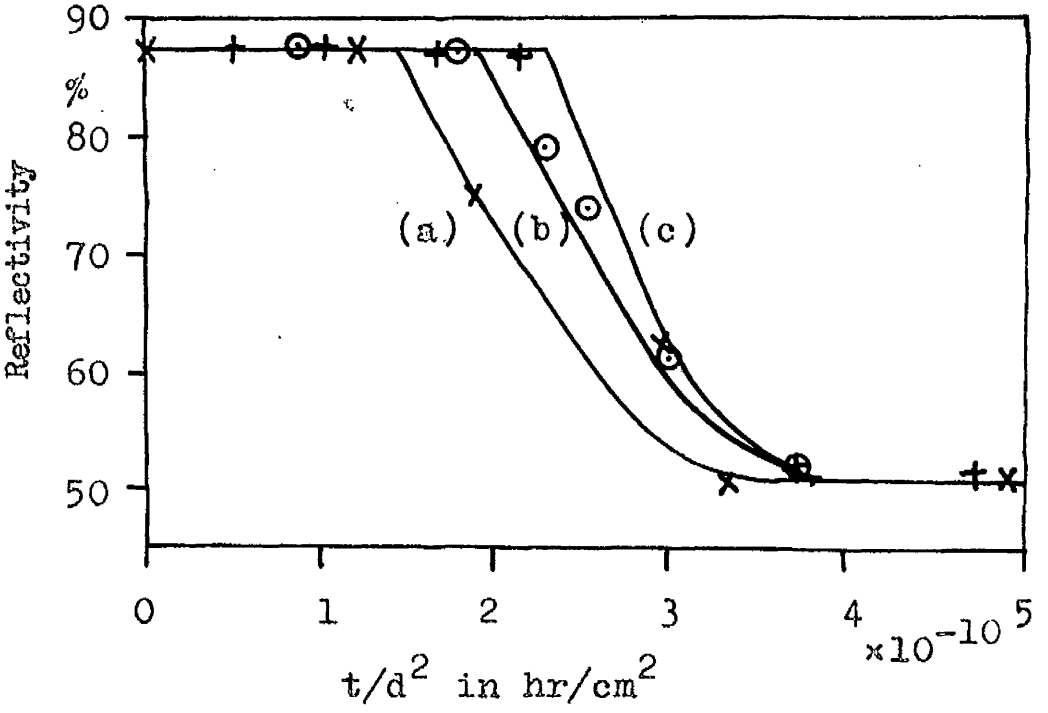

Fig. 5.18. Graph of reflectivity against t/d^2 for specimens shown in fig. 5.15 to 5.17. (a) Aluminium thickness = 720A, (b) aluminium thickness = 1050A, (c) aluminium thickness = 1730A.

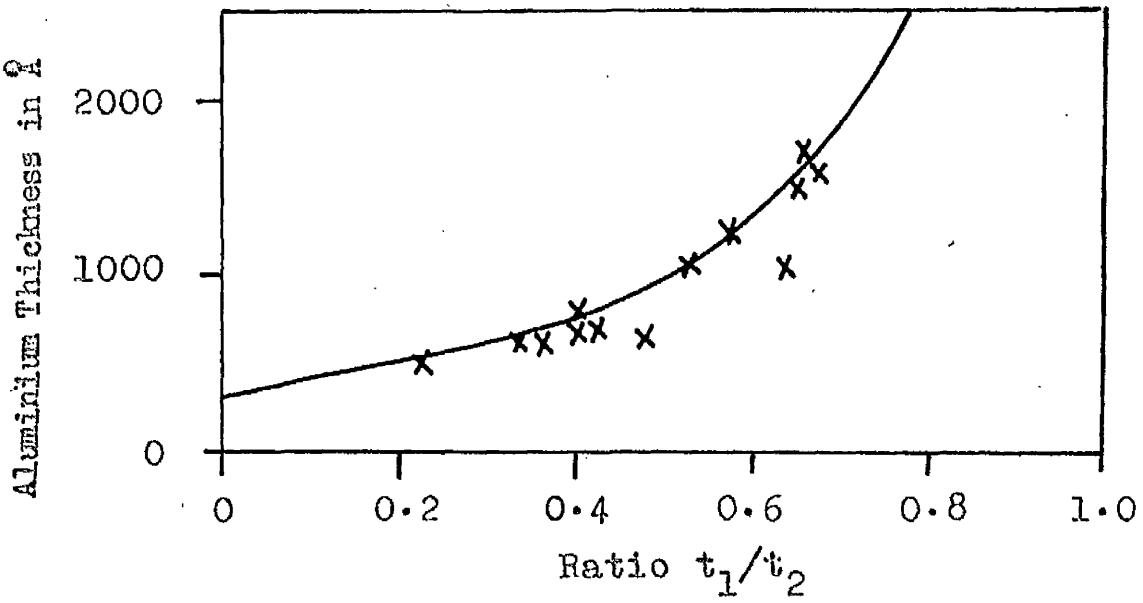

Fig. 5.19 Graph of Aluminium Thickness against Ratio t_1/t_2. The theoretical curve is plotted for a light penetration of 300Å.

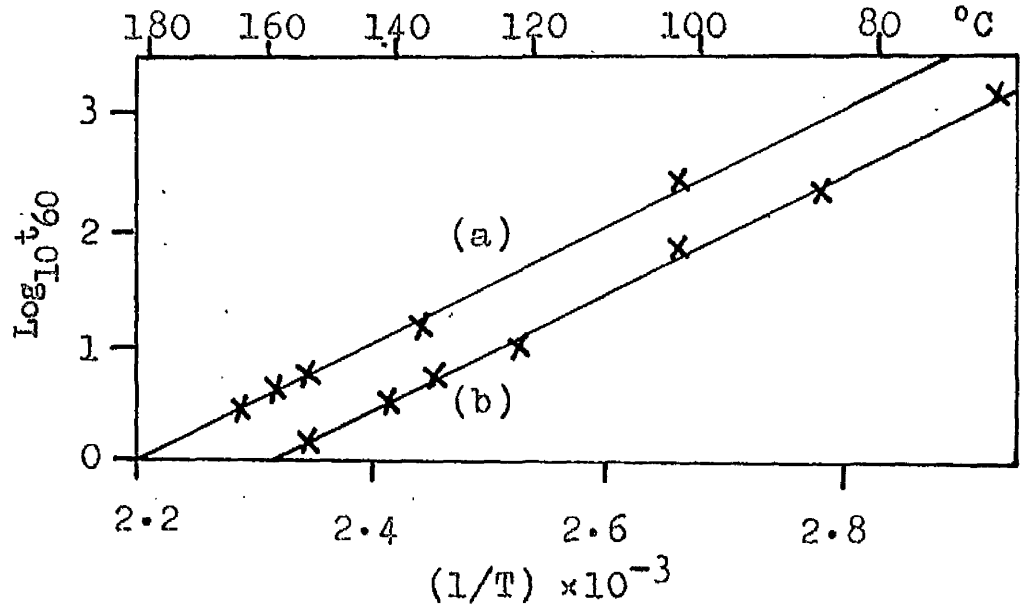

Fig. 5.20 Graph of $Log_{10}t_{60}$ against (1/T) for Diffusion at Aluminium Surface. (a) Aluminium thickness = 1290Å, (b) aluminium thickness = 720Å.

This tends to confirm that the reflectivity changes are due to the motion of a phase boundary rather than to a gradual change in concentration which would occur if atoms in the aluminium lattice could be gradually replaced by gold atoms. The solid solubility of gold in aluminium is almost negligable, and so the gold atoms diffusing into the aluminium would be closely followed by a phase boundary.

Values of D' at 102°C were calculated for all the specimens prepared from the time taken for the reflectivity to stop changing. The mean value of D' was found to be 8.2×10^{-15} cm^2/sec and the results showed no tendency for D' to change with increasing aluminium thickness.

Different portions of the same slides were aged over a temperature range. Portions of a slide with an aluminium thickness of 720Å, whose ageing curve at 102°C is shown in fig. 5.15, were aged at temperatures between 70°C and 152°C. The time of diffusion varied from 40 hr. to $2\frac{1}{5}$ min. but it was found that the shape of the ageing curve did not change. This enabled the activation energy to be calculated as before by plotting $\log_{10} t_{60}$ against (1/T). The results are shown in fig. 5.20 and give a value of 23.5 kcal/mole for the activation energy. From the known value of D' at 102°C, D'_0 was calculated to be 0.51 cm^2/sec.

5.4 Effect of Thickness Ratio

In all the results discussed so far, the thickness of the solute metal was sufficient for all reflectivity changes to be completed at the solvent metal surface before any changes took place at the surface of the solute metal. To investigate the effects of the thickness of the solute metal, the thickness of the solute metal was varied.

Several slides were prepared with a single layer of gold but with four separate aluminium films of different thicknesses. This was carried out by moving a shutter over the slide to expose successively all, $\frac{3}{4}$, $\frac{1}{2}$ and $\frac{1}{4}$ of the slide to the aluminium vapour. The thickness of each film was found by interferometry. The complete slides were aged at 84°C and typical ageing curves are shown in fig. 5.21 and 5.22 for gold thicknesses of 1450Å and 925Å respectively. In fig. 5.21 we can see that an aluminium thickness of 0·61 or more times the gold thickness gave the full reflectivity change, but if the aluminium thickness was only 0·19 times the gold thickness no reflectivity change took place. This suggested a critical thickness ratio of gold to aluminium lying between 0·61 and 0·19. Fig. 5.22 similarly suggests a critical thickness ratio between 0·71 and 0·43. From these and from three other slides prepared, it was verified that the effect depends

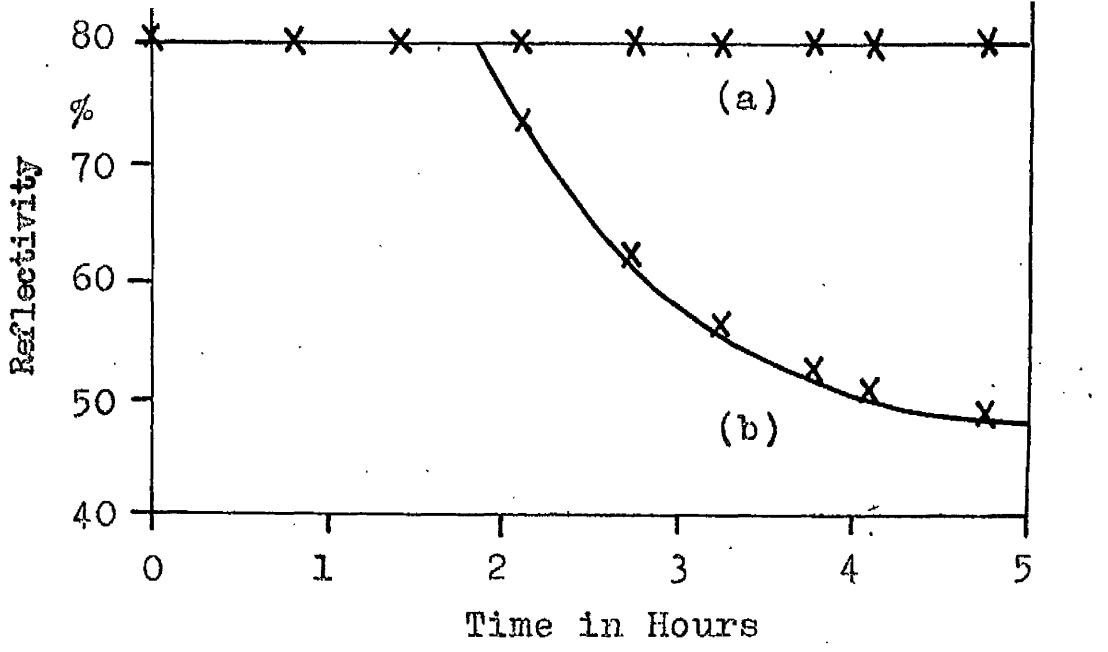

Fig. 5.21 Ageing of Gold Surface at 84°C for Gold Thickness of 1450Å

(a) Aluminium thickness = 275Å (Al:Au = 0·19)

(b) Aluminium thickness = 880Å, 1300Å and 5300Å (Al:Au = 0·61, 0·90, and 3·7)

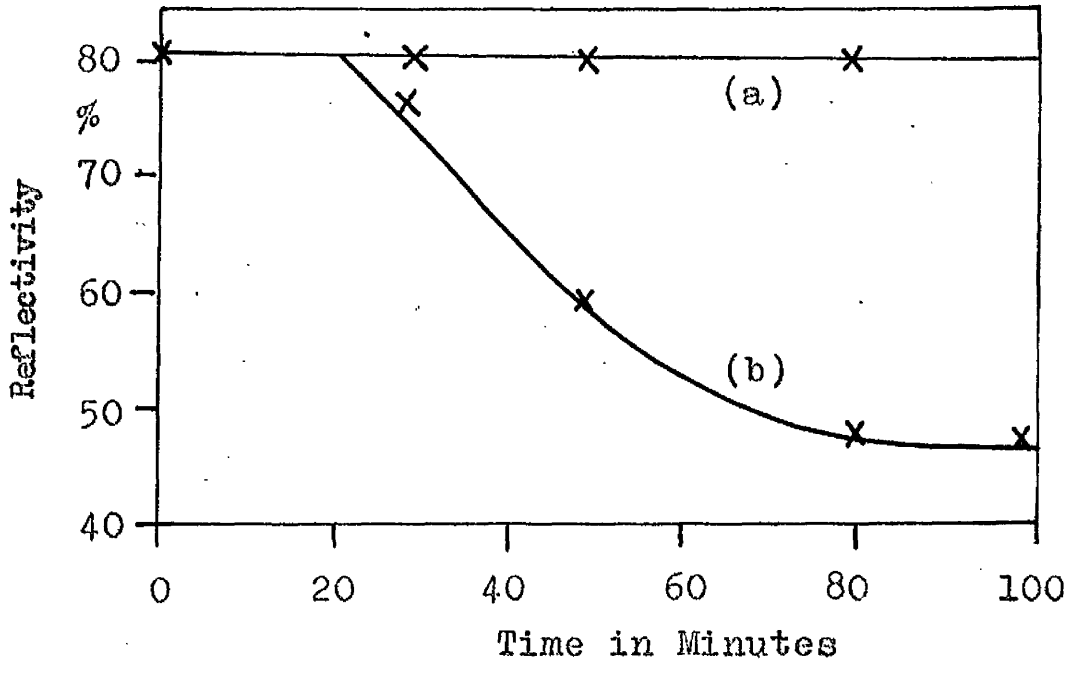

Fig. 5.22 Ageing of Gold Surface at 84°C for Gold Thickness of 925Å.

(a) Aluminium thickness = 400Å (Al:Au = 0·43)

(b) Aluminium thickness = 650Å, 1900Å and 3600Å (Al:Au = 0·71, 2·1 and 3·9)

depends on the thickness ratio rather than on the absolute thicknesses of the films, and the value of the critical thickness ratio was found to be 0·5. If the aluminium was more than half the gold thickness the full reflectivity change took place. If the aluminium was less than half the gold thickness no reflectivity change took place, and it would appear that the diffusing boundary did not reach the glass surface. Since the lattice spacings of gold and aluminium are nearly identical, the value of critical thickness ratio seems to imply that behind the boundary there must be at least one aluminium atom for every two gold atoms.

Reflectivity changes at the aluminium surface were studied with slides having a single aluminium layer but with three separate gold films of different thicknesses. The completed slides were aged at 84°C and typical curves are shown in fig. 5.23 and 5.24 for aluminium thicknesses of 635Å and 1060Å. From fig. 5.23 it can be seen that a critical thickness ratio of gold to aluminium would have to lie between 2·4 and 0·55. In fig. 5.24 it can be seen that the critical ratio would have to lie between 2·8 and 1·8. The portion with a gold thickness of 1900Å (ratio 1·8) gave some reflectivity change and so we can say that this figure would lie close to the critical thickness ratio but would be slightly less than it. From these and from four

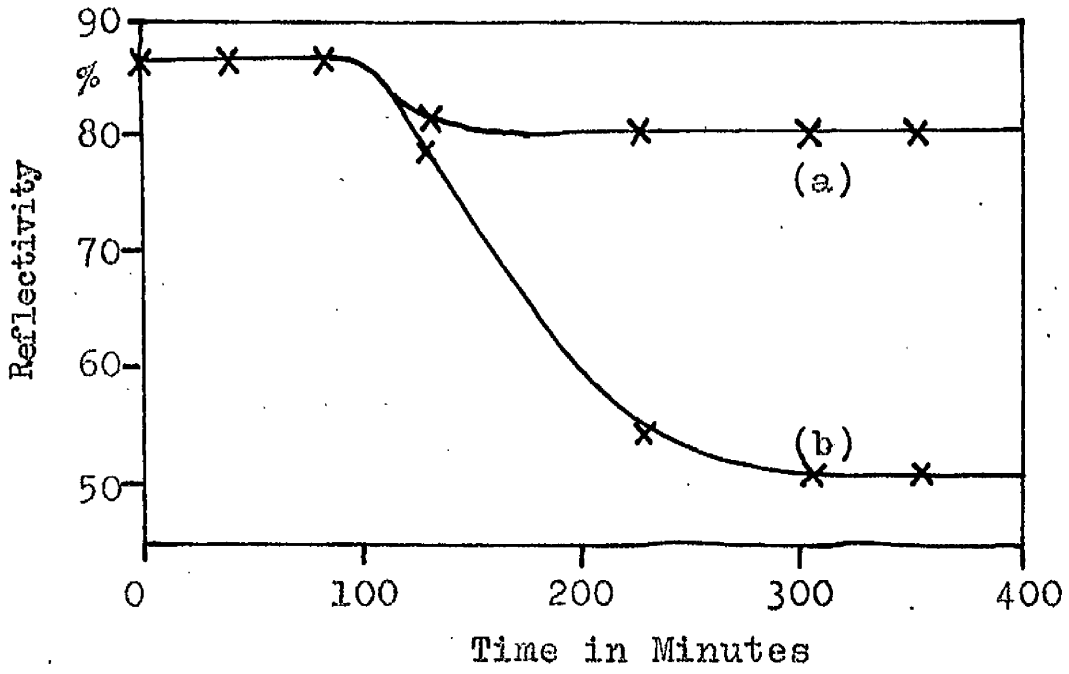

Fig. 5.23 Ageing of Aluminium Surface at 84 °C for Aluminium Thickness of 635Å.
(a) Gold Thickness = 350Å (Au:Al = 0·55)
(b) Gold Thickness = 1500Å and 2730Å (Au:Al = 2·4 and 4·3)

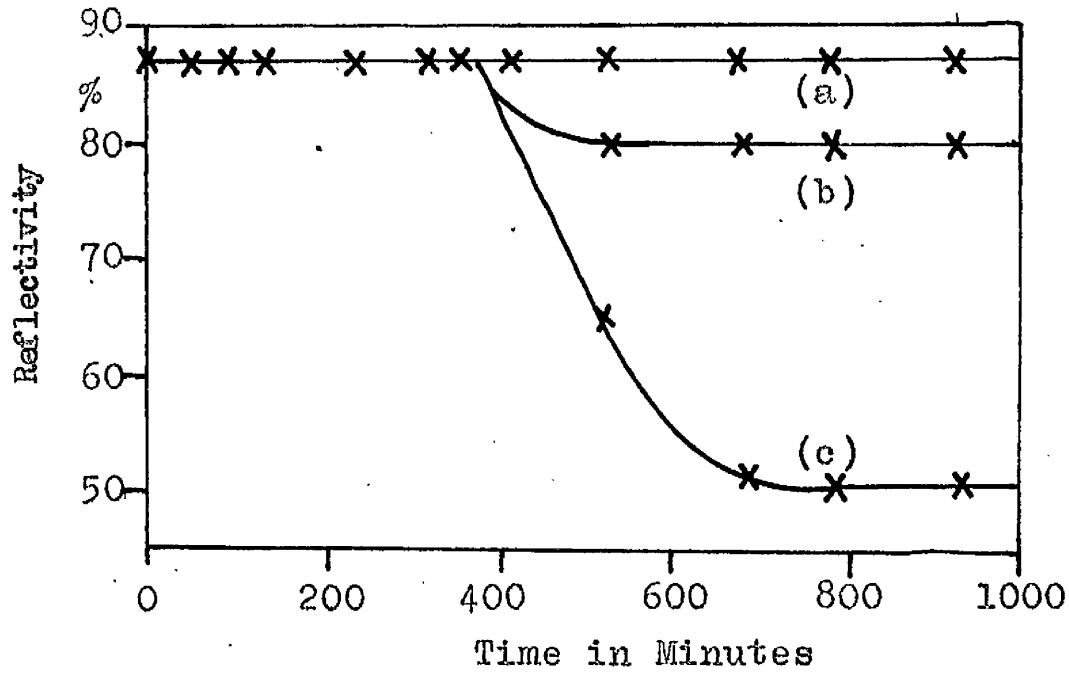

Fig. 5.24 Ageing of Aluminium Surface at 84 °C for Aluminium Thickness of 1060Å
(a) Gold thickness = 635Å (Au:Al = 0·60)
(b) Gold thickness = 1900Å (Au:Al = 1·8)
(c) Gold thickness = 3000Å (Au:Al = 2·8)

other slides prepared it was verified that the effect depends on the thickness ratio rather than on the absolute thickness of the films, and the critical thickness ratio was found to be 2·0.

This result indicates that behind the boundary there must be at least two gold atoms for every one aluminium atom. From measurements at the gold surface we have already concluded that there must be at most two gold atoms for every one aluminium atom. This seems to suggest that there is preferential formation of a compound with one aluminium atom associated with two gold atoms i.e. with composition Au_2Al.

Values of critical thickness ratio have been observed at 84°C. The value will vary with temperature, however, unless the activation energy in both directions is identical. The activation energy at the gold surface was found to be 22·6 kcal/mole, whilst that at the aluminium surface was found to be 23·5 kcal/mole. The figures are close to one another, and it seemed likely that the difference between them was due to experimental error. To check this possibility a specimen was prepared with a gold thickness of 2260Å and an aluminium thickness of 1110Å. This gave a thickness ratio of gold to aluminium of 2·04 and so was very close to the critical ratio. This meant that reflectivity

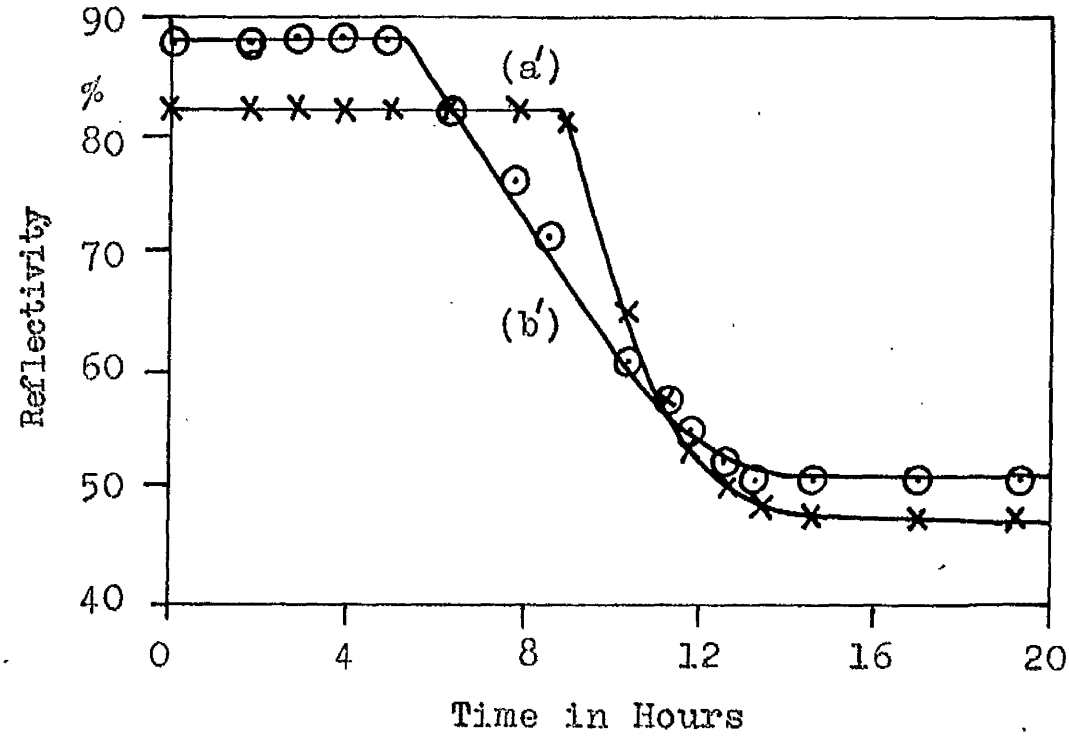

(a) Ageing at 84°C

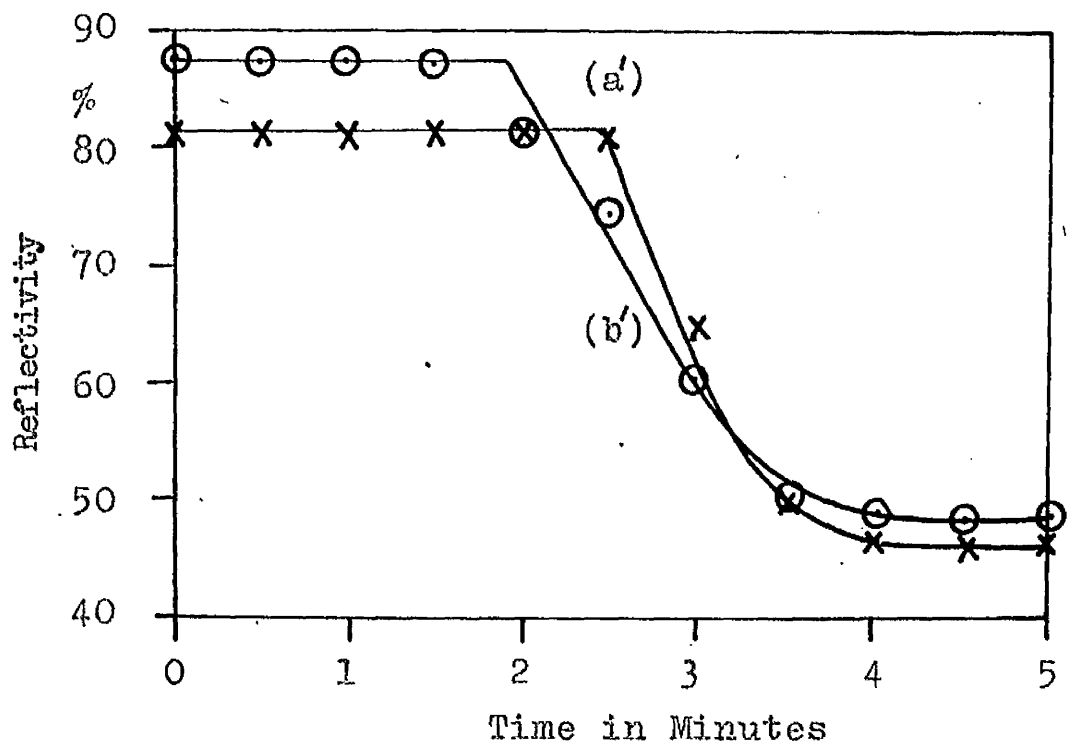

(b) Ageing at 160°C

Fig. 5.25 Ageing Gold-Aluminium Film with Gold Thickness of 2260Å and Aluminium Thickness of 1110Å (Au:Al = 2·04). Graph of reflectivity against time at (a') the glass and (b') the air surfaces.

changes could be observed both at the gold and at the aluminium surfaces. Portions of this specimen were aged at two widely different temperatures (84°C and 160°C) and the reflectivity changes were observed at both surfaces. The results are shown in fig. 5.25, and it can be seen that the ratio of the ageing periods at the two surfaces is the same at both temperatures. If the activation energy were slightly different, we would expect one of the curves to show a longer ageing period than the other at the same temperature. We would also expect a different value of critical ratio at 160°C, and so one of the curves would show less change in reflectivity than at 84°C. Since the curves remained the same shape at both temperatures, and since the reflectivity at each surface dropped to the same value at both temperatures, it appears that the activation energies are equal in the two directions, and hence that the value of the critical thickness ratio must be the same for all temperatures.

5.5 Results with Aluminium Substrating the Gold

Several specimens were prepared with the aluminium substrating the gold. It is well known that an aluminium surface oxidises very readily and it seemed possible that some oxide would form on the aluminium between the aluminium and gold evaporations and that this oxide might hinder

diffusion. It was decided to study this oxidation before obtaining any ageing curves.

Several slides were prepared with four separate thick aluminium films and a fairly thin gold film overlayering all four. The delay before evaporating the gold overlayer was different for the four aluminium films and varied from 20 min. to $\frac{3}{4}$ min. The complete slides were placed on an electric hot-plate which heated up slowly from room temperature at a rate of 7°C/min.. The temperature at which the colour of the gold surface changed was noted for each part of the slide. Results are shown in tabular form in table 5.1 for different residual gas pressures. The pressure in the vacuum chamber was kept constant for the duration of the evaporating period by continually adjusting the leak valve.

Very little oxidation took place at pressures under 10^{-5} mm. of mercury, and even for a delay of 10 min. between the evaporations, very little oxide was formed. At 10^{-4} mm., oxide forms more readily, but even here a delay of 2 min. would permit very little oxide to form. With the higher pressure of 10^{-3} mm., oxide begins to form very quickly, and even after $\frac{3}{4}$ min. some oxide is definitely present. The last result given is for a residual atmosphere of hydrogen and shows considerably reduced oxidation compared with an air atmosphere at the same pressure.

TABLE 5.1

THE FORMATION OF OXIDE ON ALUMINIUM AT LOW PRESSURES

(Temperature at which diffusion takes place in thin film couples of aluminium + gold)

Pressure in mm. of mercury	Delay between Al and Au Evaporations			
	20 min.	10 min.	2-3 min.	$\frac{3}{4}$-1 min.
under 10^{-5}	148°C	140°C	138°C	138°C
10^{-4}	170°C	156°C	148°C	145°C
10^{-3} *	200°C	180°C	165°C	149°C
10^{-3} * (hydrogen)	161°C	161°C	149°C	142°C
Belser (1960)	20 min.	6 min.	$2\frac{3}{4}$ min.	1 min.
	440°C	230°C	150°C	70°C

* Pressure measured by a Penning gauge. Evaporations were carried out at pressures of 5×10^{-5} mm., and results are for ageing only at 10^{-3} mm. between evaporations.

Belser (1960) has studied the same effect in aluminium-gold films by measuring the temperature above which diffusion caused a measureable increase in resistance. He does not give the pressure at which the evaporations were carried out, but it was probably under 10^{-4} mm., and certainly under 10^{-3} mm.. The resistance technique is very sensitive to the first stages of diffusion and changes were observed at 70°C for a delay of 1 min. where very little oxide was present. On ageing for longer periods between evaporations, however, the thickness of the oxide layer appeared to increase considerably, until for a delay of 20 min. a temperature of 440°C was required for diffusion. The rate of oxidation appears to have been very much higher than that found in the present investigation, although the resistance technique is very sensitive to diffusion and should give temperatures under those found from observations of colour change. Even at a pressure of 10^{-3} mm., a delay of 20 min. required a temperature of 200°C for diffusion in the present investigation, and 440°C according to Belser's results. This is a major discrepancy between the two sets of results, but is not due to errors in the present investgation in which results obtained at different pressures agree well.

In the preparation of diffusion couples evaporations were carried out at pressures of 2-5 $\times 10^{-5}$ mm.. From table 5.1

it can be seen that provided the delay between the aluminium and gold evaporations is 3 min. or less, no difficulties will arise from formation of oxide.

Reflectivity changes were studied first at the aluminium surface. The gold was made more than twice the aluminium thickness to prevent changes taking place at the gold surface before they took place at the aluminium surface. Ageing was carried out on the hot-stage reflectometer for convenience, and approximately equal ageing times were used for different film thicknesses rather than a standard ageing temperature. A typical ageing curve is shown in fig. 5.26. The ratio t_1/t_2 was calculated for the 6 specimens prepared and plotted against aluminium thickness (fig. 5.27). The points all lie near the theoretical curve for a light penetration of 300Å, the value found for aluminium overlayering the gold.

The activation energy of diffusion was found by ageing the specimen shown in fig. 5.26 over a temperature range from 99°C to 171°C. From a graph of $\log_{10} t_{60}$ against (1/T) the activation energy was found to be 23·3 kcal/mole. This gave a mean value for D_0' of 0·63 cm^2/sec. These figures agree satisfactorily with the values E = 23·5 kcal/mole and D_0' = 0·51 cm^2/sec obtained with a gold substrate and aluminium overlayer. Hence the order of

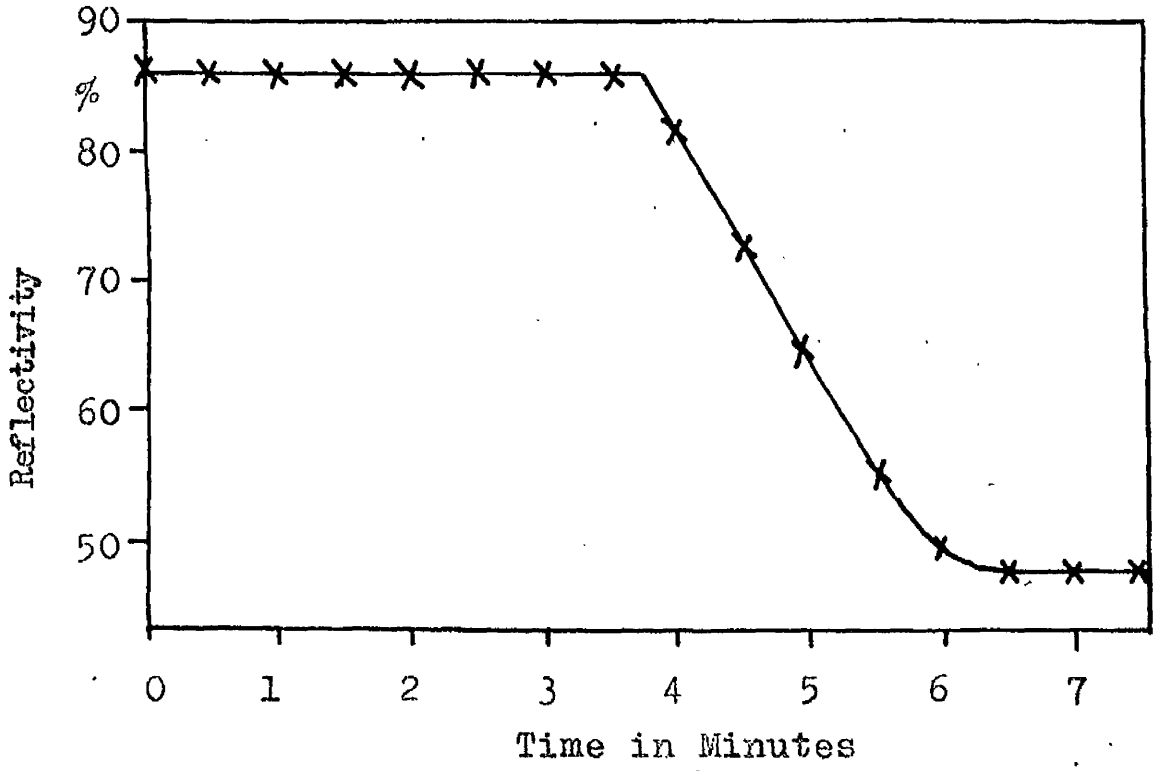

Fig. 5.26 Ageing at Aluminium Surface at 164°C with Gold Overlayering the Aluminium. Aluminium thickness = 1470Å

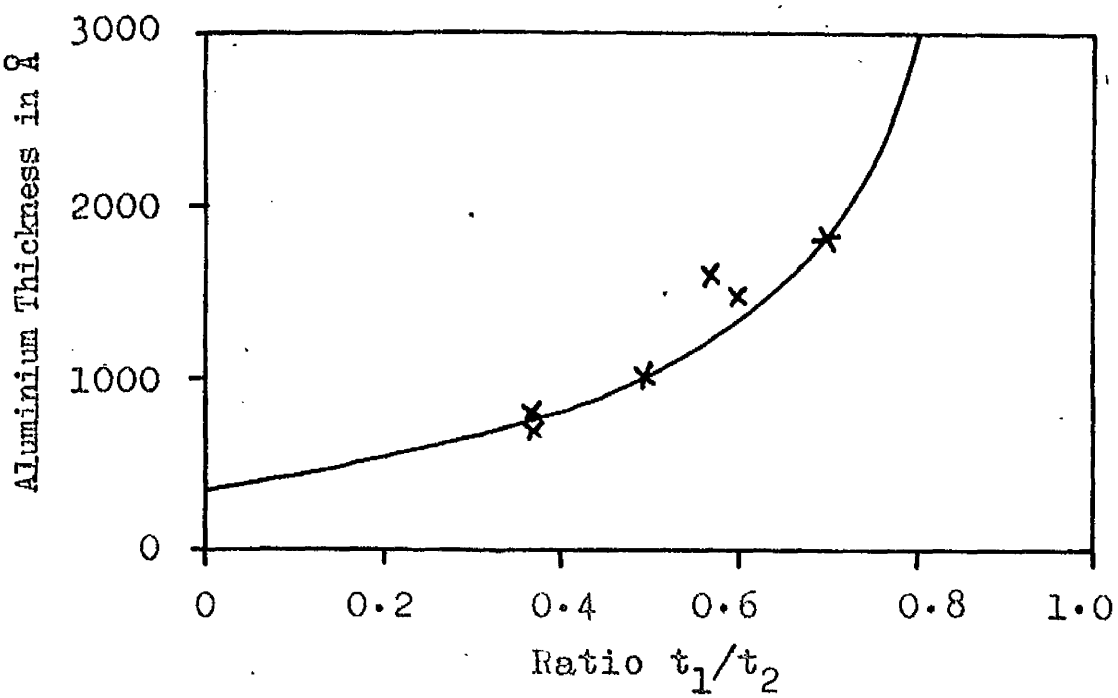

Fig. 5.27 Graph of Aluminium Thickness against Ratio t_1/t_2. The theoretical curve for a sharply defined boundary is plotted for a light penetration of 300Å.

evaporating the metal films makes no significant difference to the value of diffusion coefficient obtained.

Reflectivity changes were also studied at the gold surface with aluminium films at least half the thickness of the gold to prevent thickness ratio difficulties. Slides were prepared with the gold thickness varying in the range 500Å to 2050Å, and a typical ageing curve is shown in fig. 5.28. The ratio t_1/t_2 was calculated for the five specimens prepared and plotted against the gold thickness (fig. 5.29). The points all lie near the theoretical curve for a light penetration of 400Å, the same value as that found for gold substrating the aluminium.

D_o' was calculated assuming the activation energy of 22.6 kcal/mole found for observations with aluminium overlayering the gold. The mean value obtained for D_o' was 1.3 cm^2/sec, in good agreement with the value of 0.85 cm^2/sec obtained with gold acting as the substrate. Again the order of evaporating the metal films makes little difference to the value of diffusion coefficient obtained.

5.6 The Reflectivity of Gold-Aluminium Alloys

The graph of reflectivity against concentration for a series of gold-aluminium alloy films prepared by 'flash'

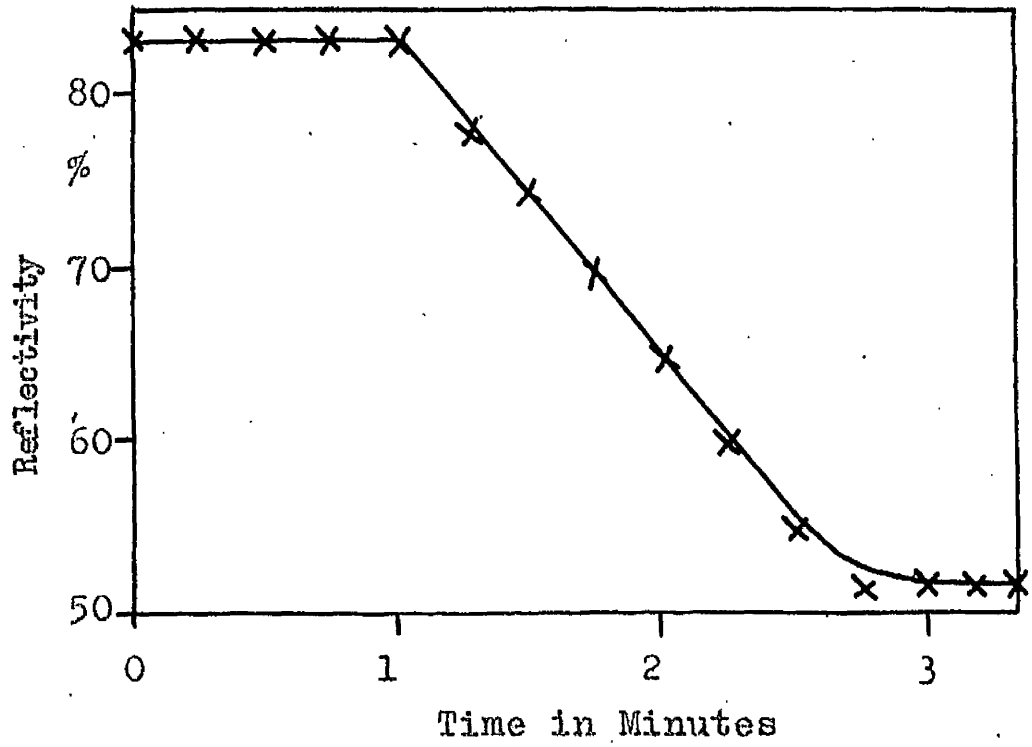

Fig. 5.28 Ageing at Gold Surface at 146°C with Gold Overlayering the Aluminium. Aluminium thickness = 955Å.

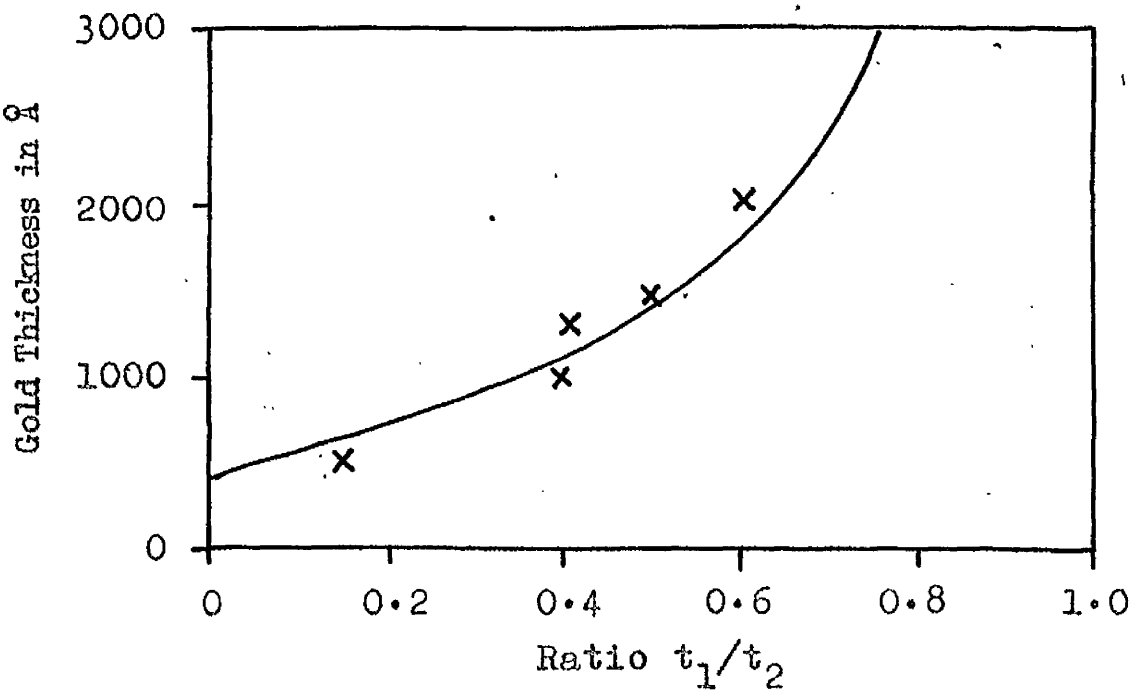

Fig. 5.29 Graph of Gold Thickness against Ratio t_1/t_2. The theoretical curve for a sharply defined boundary is plotted for a light penetration of 400Å.

evaporation are shown in fig. 5.30. Annealed films of the intermetallic compound $AuAl_2$ had a very pronounced purple colour in agreement with observations on bulk alloys (Coffinberry and Hultgren 1938). This alloy is called "purple gold" because of its unusual appearance. The very low reflectivity of this phase, together with its brittleness and high melting point, indicate ionic or covalent bonding rather than metallic.

In ageing observations with a gold substrate and aluminium overlayer, the reflectivities of the phases formed at the glass and air surfaces were 47½% and 52% respectively for mercury yellow light. Results with an aluminium substrate and gold overlayer gave final reflectivities of 48% and 53% at the glass and air surfaces. In one case we would expect a compound rich in gold at the glass surface. In the other case we would expect a compound rich in aluminium at the glass surface. Since the reflectivities of the phases formed are the same, we must conclude that the same compound is being formed in both cases. The difference in reflectivities at the glass and air surfaces is due to the presence of the glass with its refractive index of 1·5. This will normally tend to reduce the reflectivity somewhat.

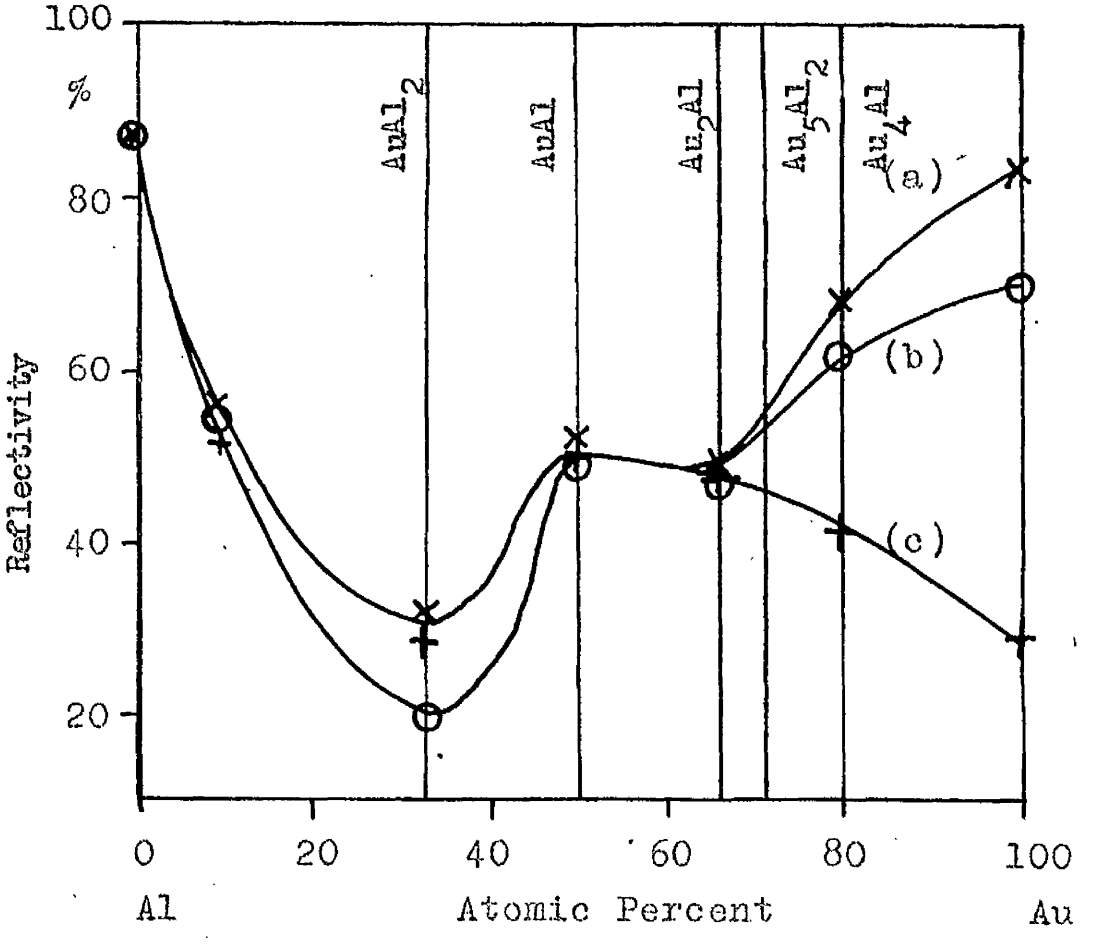

Fig. 5.30 Graph of Reflectivity against Concentration for "Flash" Evaporated Gold-Aluminium Films. Reflectivities measured at glass surface with mercury light of wavelengths (a) 5790Å (b) 5461Å and (c) 4358Å.

Values of 47½%, 47½% and 48½% have been found for ageing observations at the glass surface with mercury yellow, green and blue light respectively (fig. 5.2). These figures for reflectivity certainly do not fit the reflectivities found for flash evaporated alloys of $AuAl_2$ or Au_4Al (fig. 5.30), and it appears that only small amounts of these phases are present. The reflectivities of flash evaporated AuAl (52% 51% 50%) and Au_2Al (49% 48% 47½%) fit the observed results satisfactorily, and hence it seems that the reflectivity changes are due to the formation of these phases. Observations of critical thickness ratio indicate that the reflectivity changes are due to Au_2Al rather than to AuAl.

5.7 Discussion

We must expect all thermally stable phases to be precipitated at the gold-aluminium interface at the beginning of diffusion. Reflectivity measurements both at the gold and at the aluminium surfaces seem to indicate the motion of a particular phase boundary, and in view of the critical thickness ratios which have been found, it would appear that a layer of Au_2Al is being formed. This has been confirmed by measurements of the reflectivities of the gold-aluminium alloys.

For diffusion into the aluminium, D_0' has been found to

be 0·51 cm^2/sec and E to be 23·5 kcal/mole. D' at 84°C can be calculated from these and is found to be 2·0 $\times 10^{-15}$ cm^2/sec. D' at 84°C for diffusion into the gold has already been found to be 10·1 $\times 10^{-15}$ cm^2/sec. In a given time, the penetration of the reaction boundary layer is proportional to $\sqrt{D'}$. Hence the penetration of the diffusion layer into the gold is 2·3 times greater than its penetration into the aluminium. If the diffusion layer is homogeneous, then we would expect 2·3 gold atoms to be associated with every aluminium atom. This is close to the composition of the compound Au_2Al, the difference being due probably to errors in the determination of D'.

The values of critical thickness ratio and the relative rates of diffusion are both in agreement with the formation of the compound Au_2Al. It is difficult to see why preferential formation of this phase should occur, since we would expect all thermally stable phases to be formed. It would appear that there are only two reasonable explanations for the observed results, either that the light measurements are peculiarly sensitive to this phase and not to other phases, or that the layers of other compounds formed are extremely thin and have little effect upon the measurements. The first explanation seems unlikely as $AuAl_2$ has a pronounced purple coloration and any significant amount of it should have affected the reflectivity measurements. A specimen

with gold and aluminium layers in the ratio of approximately 1 to 2 was aged in a furnace at 300°C for 6 hr.. On removal the film had a definite red colour but unfortunately was badly aggregated and its reflectivity could not be measured. The second of the two explanations implies that the diffusion rate is higher into the Au_2Al than into the other compounds, and consequently the zone is much wider than the other zones formed. The theory given in chapter 2.9 indicates that this is quite likely.

It has been shown that D' and E are the same for very thin gold films as for thicker ones. This means that the mechanism of diffusion in very thin films is the same as in thicker ones. Films less than 150Å thick have very wide grain boundaries (Sennett and Scott 1950), and we would expect E to be less and D' to be higher for these films if grain boundary diffusion were occurring. Hence we can say that the diffusion observed is a true volume diffusion, most probably a vacancy mechanism. It would be expected that the values of diffusion coefficient and activation energy lie fairly close to values for bulk specimens, but unfortunately these figures are not available for this system.

CHAPTER 6

REFLECTIVITY CHANGES IN SILVER-ALUMINIUM

6.1 Introduction

Thin film diffusion couples of silver-aluminium gave pronounced reflectivity changes despite the similarity in reflectivities of silver and aluminium (94% and 87½% respectively).

The phase diagram of silver-aluminium is shown in fig. 6.1. Two phases (μ and ζ) should be precipitated at the silver-aluminium interface at the beginning of diffusion.

Both silver and aluminium have a bright colorless appearance. The appearance after annealing is darker but still colorless. For this reason, the wavelength of the light used makes little difference to the values of reflectivity obtained. Mercury green light (λ = 5461Å) was used throughout this investigation for convenience.

6.2 Reflectivity Changes at the Silver Surface

136°C was selected as a convenient ageing temperature as this allowed most of the films to be aged in the hot air oven. Slides were prepared with silver films of different thicknesses in the range 700Å to 4700Å, overlayered with a

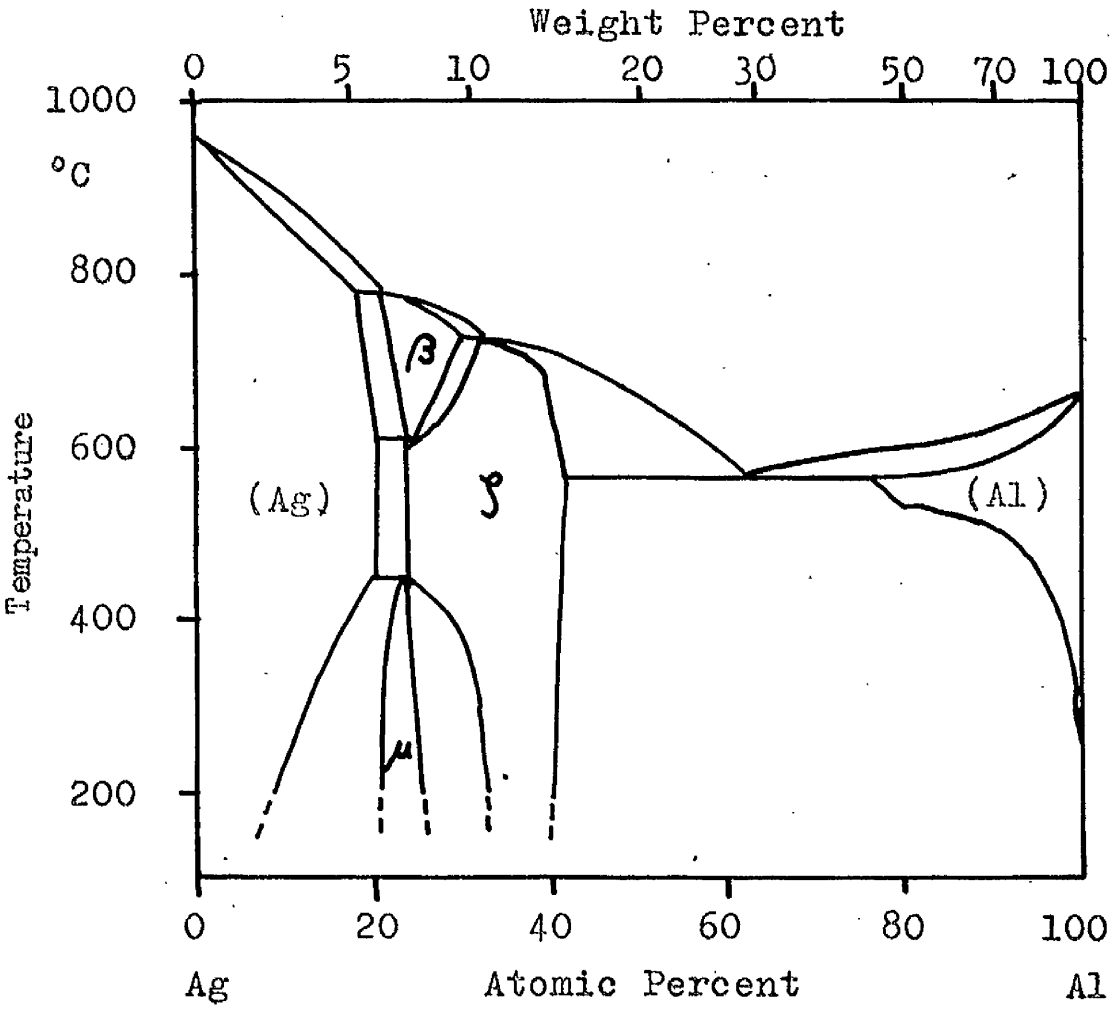

Fig. 6.1 Equilibrium Phase Diagram for Silver-Aluminium (Hansen 1958)

thick film of aluminium to avoid thickness ratio difficulties. Typical ageing curves are shown in fig. 6.2 to 6.4. The shapes of the curves differed, the length of the initial plateau increasing with thickness as in gold-aluminium. It difficult to explain the marked change in reflectivity from 94% to 55% on any basis other than the formation of an intermetallic compound in view of the similar reflectivities of silver and aluminium and the low solubility of aluminium in silver. In order to check this explanation, the ratio t_1/t_2 was calculated for all the specimens prepared and plotted against film thickness (fig. 6.5). The values obtained were consistent but lay well away from the curve for a light penetration of 400Å, the expected value for light penetration into silver, and close to the curve for a light penetration of 1100Å, much higher than the thickness of a near opaque silver film.

The results in this system are not explicable simply on the basis of a sharply defined phase boundary. In view of the large change in reflectivity, we are obviously observing a phase boundary, but in this case it appears to be diffuse. Since the length of the initial plateau was considerably less than expected, it appears that compound was being formed near the silver surface almost instantaneously. The aluminium for the formation of this of this compound must have been introduced into the silver

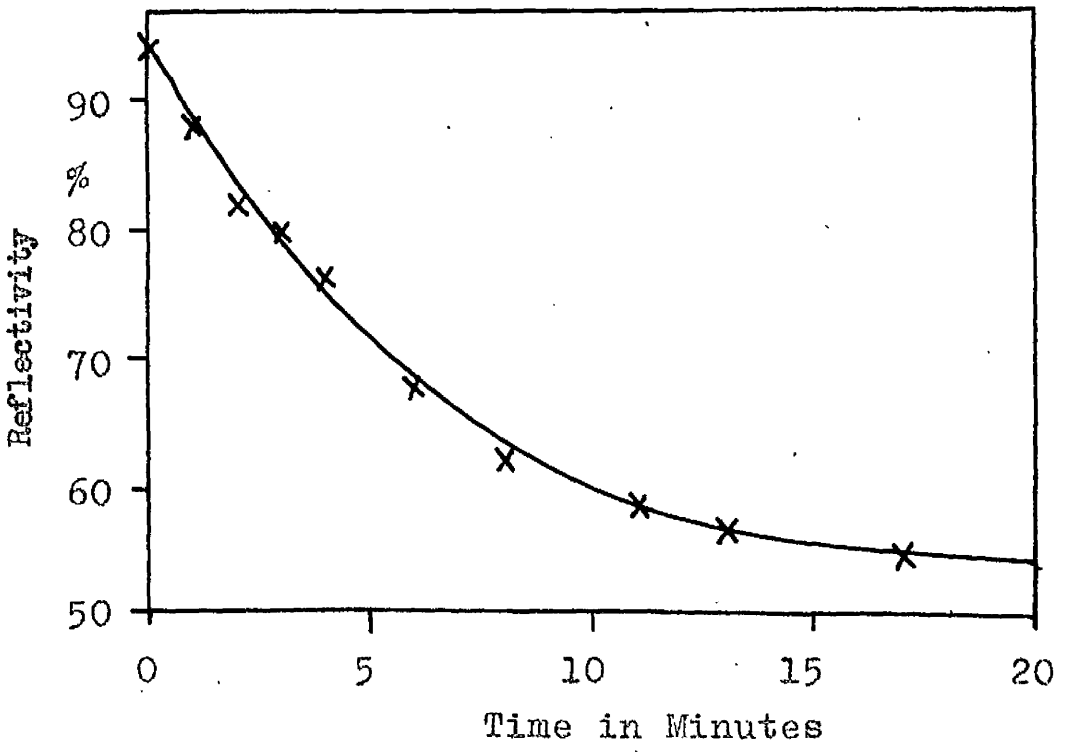

Fig. 6.2 Ageing of Silver-Aluminium at 136°C. Reflectivity change at silver surface for silver thickness of 780Å.

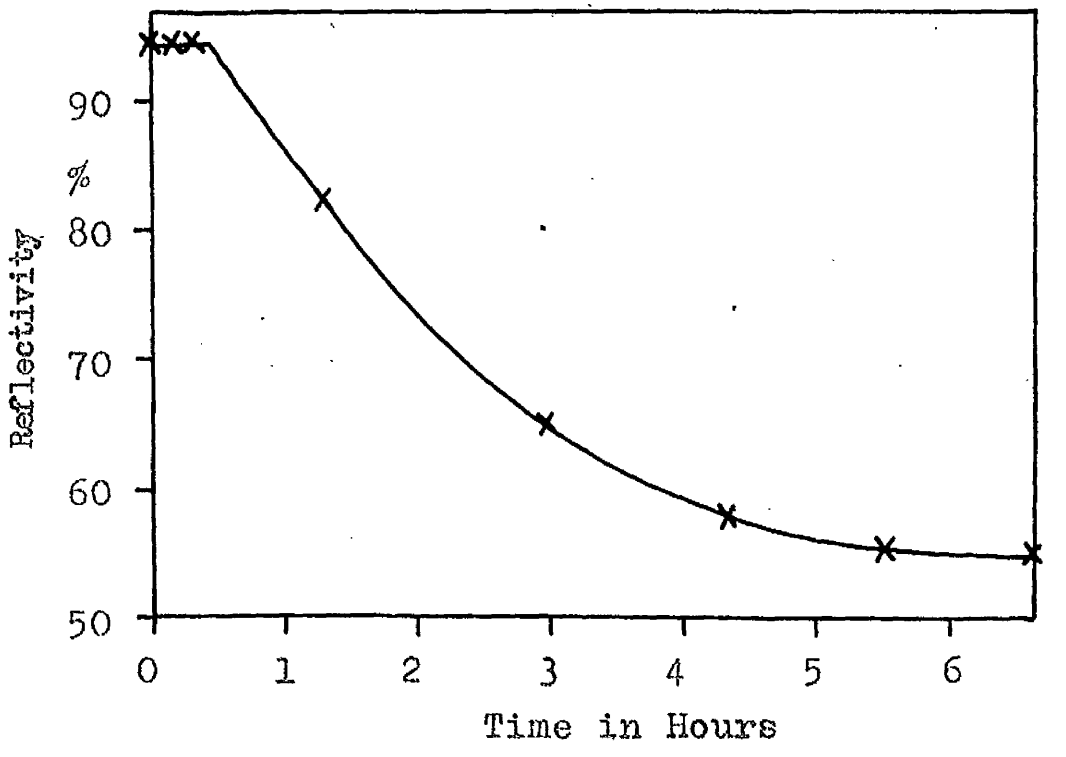

Fig. 6.3 Ageing of Silver-Aluminium at 136°C. Reflectivity change at silver surface for silver thickness of 1930Å.

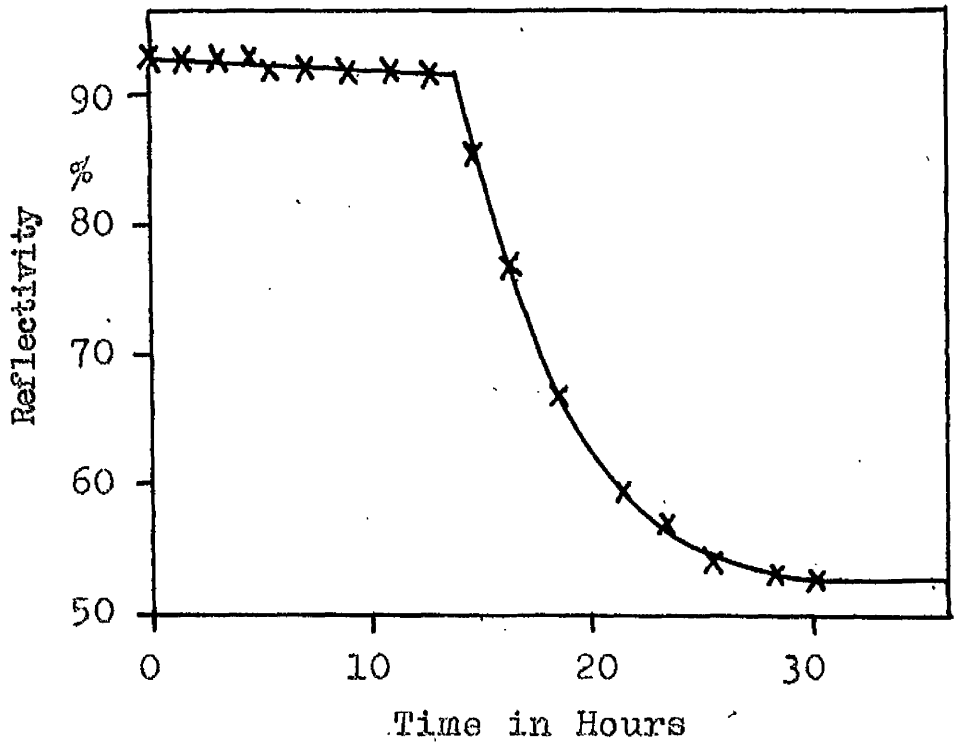

Fig. 6.4 Ageing of Silver-Aluminium at 136°C. Reflectivity change at silver surface for silver thickness of 4610Å.

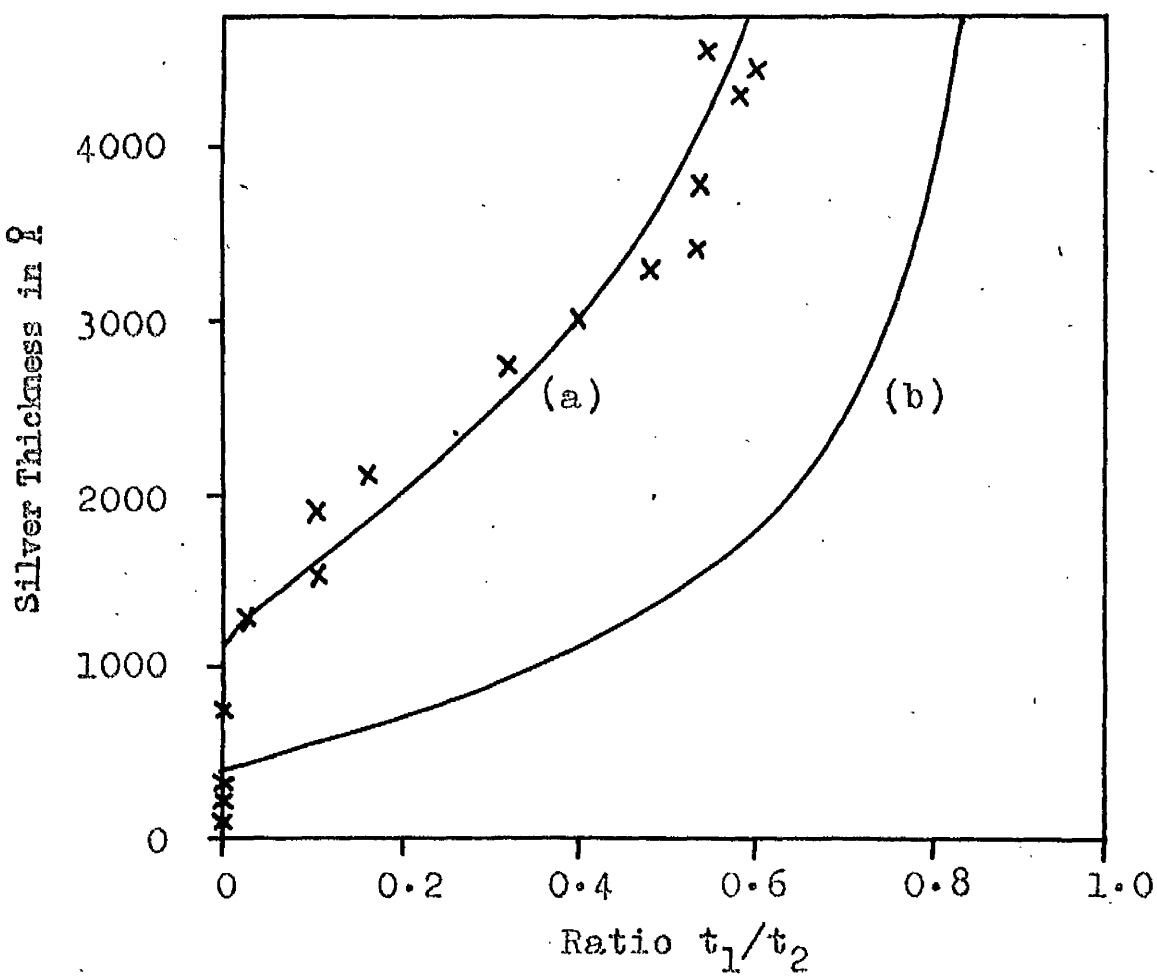

Fig. 6.5 Graph of Silver Thickness against Ratio t_1/t_2. Theoretical curves are plotted for light penetrations of (a) 1100Å (b) 400Å.

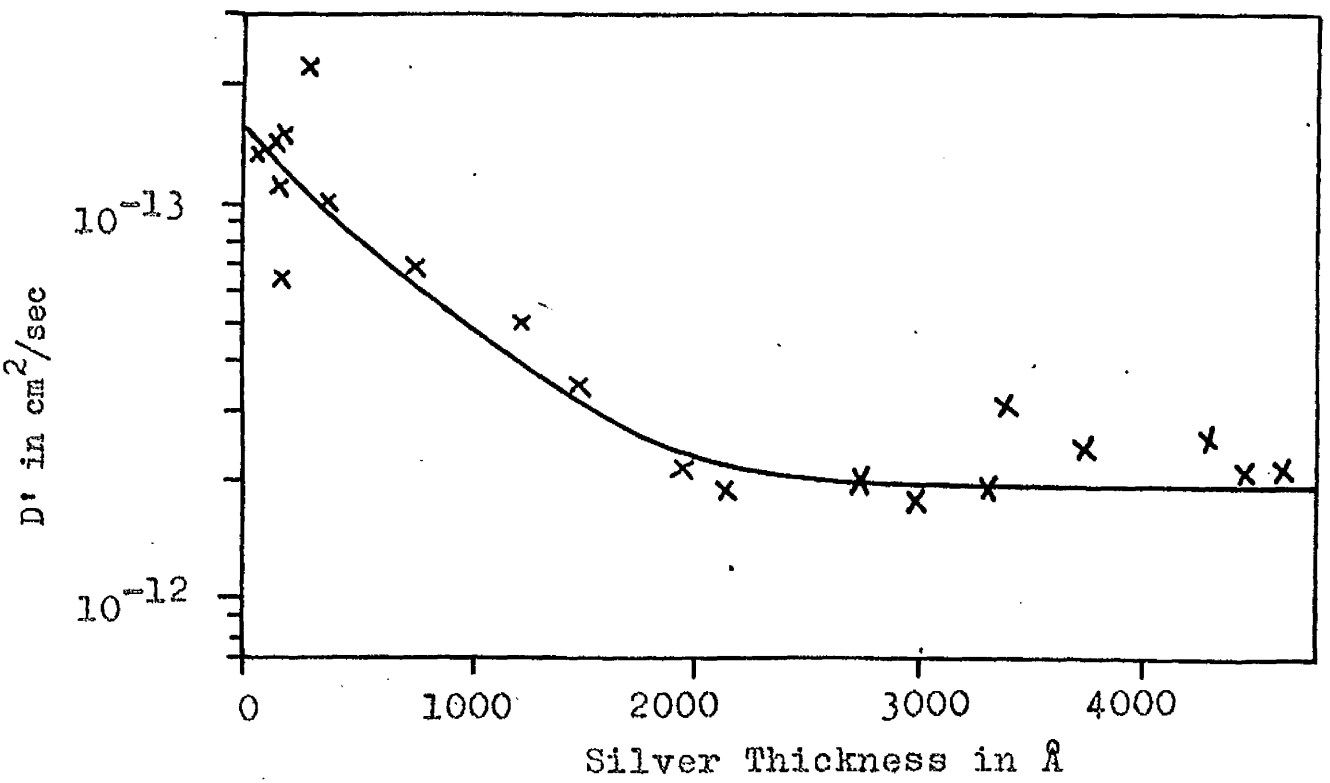

Fig. 6.6 Graph of Diffusion Coefficient (D') at 136°C against Silver Thickness.

either whilst it was being evaporated or during the very first stages of diffusion. We must assume that some aluminium penetrated 700Å into the silver lattice. These aluminium atoms would not be visible in the silver in view of the similarity in reflectivity of the two metals. As soon as intermetallic compound began to be precipitated the reflectivity would begin to drop. This would happen earlier than expected because of the presence of aluminium atoms in the silver lattice, and would give the short initial plateau observed. The reflectivity would cease changing when the original interface arrived at the metal surface, giving an apparant light penetration of (700 + 400) Å = 1100 Å.

Values of D' at 136°C were calculated from the time taken for the reflectivity to stop changing (fig. 6.6). D' was constant above a film thickness of 1900Å, but below this figure D' increased steadily, till with a film thickness of only 60Å, it was 7 times higher than the constant value. This variation indicates that the results are not characteristic merely of interpenetration, as this would not affect the motion of the original phase boundary, and D' calculated from the time taken for the reflectivity to stop changing should be constant. The steady value of D' at 136°C was 2.7×10^{-14} cm^2/sec.

Different portions of the same slides were aged over a temperature range from 117°C to 240°C to find the activation energy. Typical results are shown in fig. 6.7, 6.4 and 6.8 for a silver thickness of 4610Å. From a plot of $\log_{10} t_{70}$ against (1/T), the activation energy was found to be 27·5 kcal/mole. From the known value of D' at 136°C, D_0' was calculated to be 19·0 cm^2/sec.

Several slides were prepared with very thin silver films in the range 70Å to 350Å. These film thicknesses were determined by measuring the reflectivity and transmission of the films, and using the results of Sennett and Scott (1950). Typical ageing curves are shown in fig. 6.10 and 6.11. Even with a film thickness of only 70Å the initial reflectivity was high (85%), and this indicates that no intermetallic compound is present prior to annealing. The reflectivity began to drop immediately on heating, and with the thinnest film (70Å) fell only 14% since the diffusion zone in this case was very thin. Slides were aged over a temperature range from 84°C to 142°C, and from the graph of $\log_{10} t_{70}$ against (1/T) the activation energy was found to be 27·6 kcal/mole, in excellent agreement with the value of 27·5 kcal/mole found for thicker films, and this indicates as before that grain boundary diffusion is not occurring. Values of D' were calculated from the time taken for the reflectivity to stop changing. These values

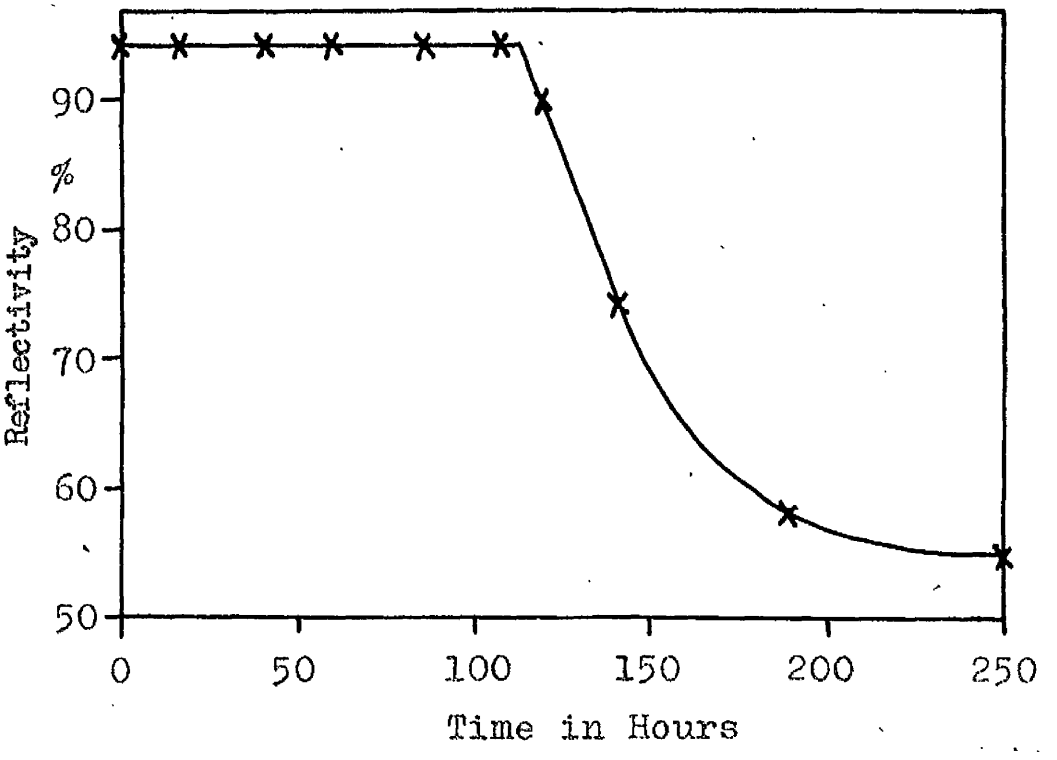

Fig. 6.7 Graph of Reflectivity against Time at Silver Surface at 117°C with Silver Film 4610Å Thick.

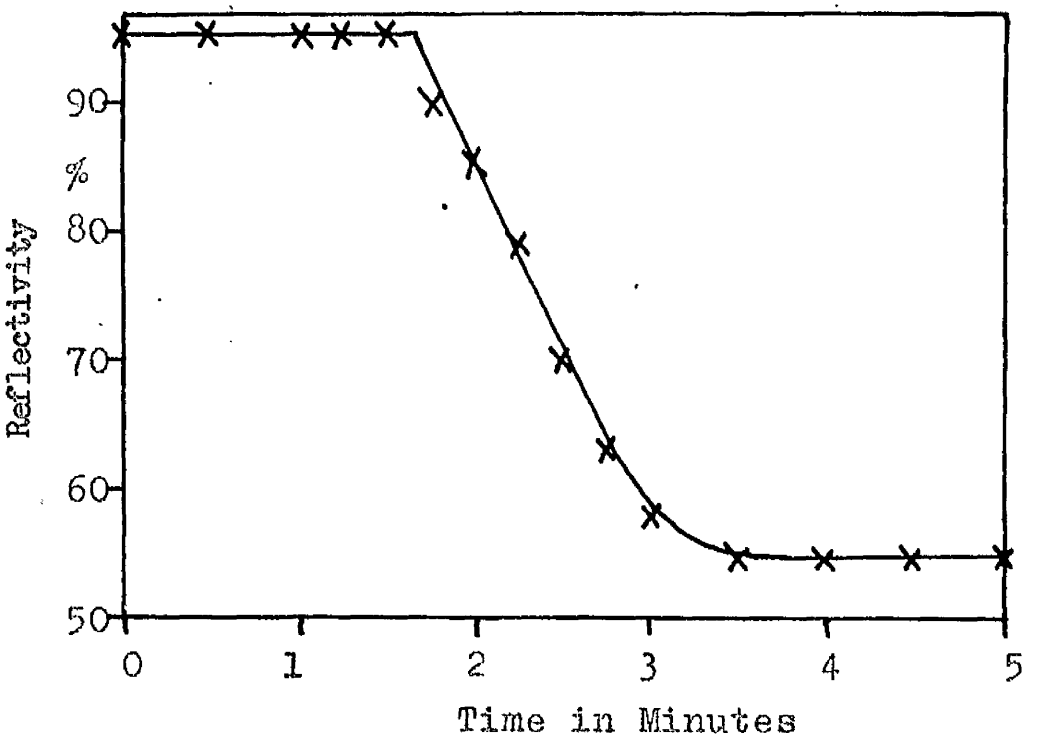

Fig. 6.8 Graph of Reflectivity against Time at Silver Surface at 240°C with Silver Film 4610Å Thick.

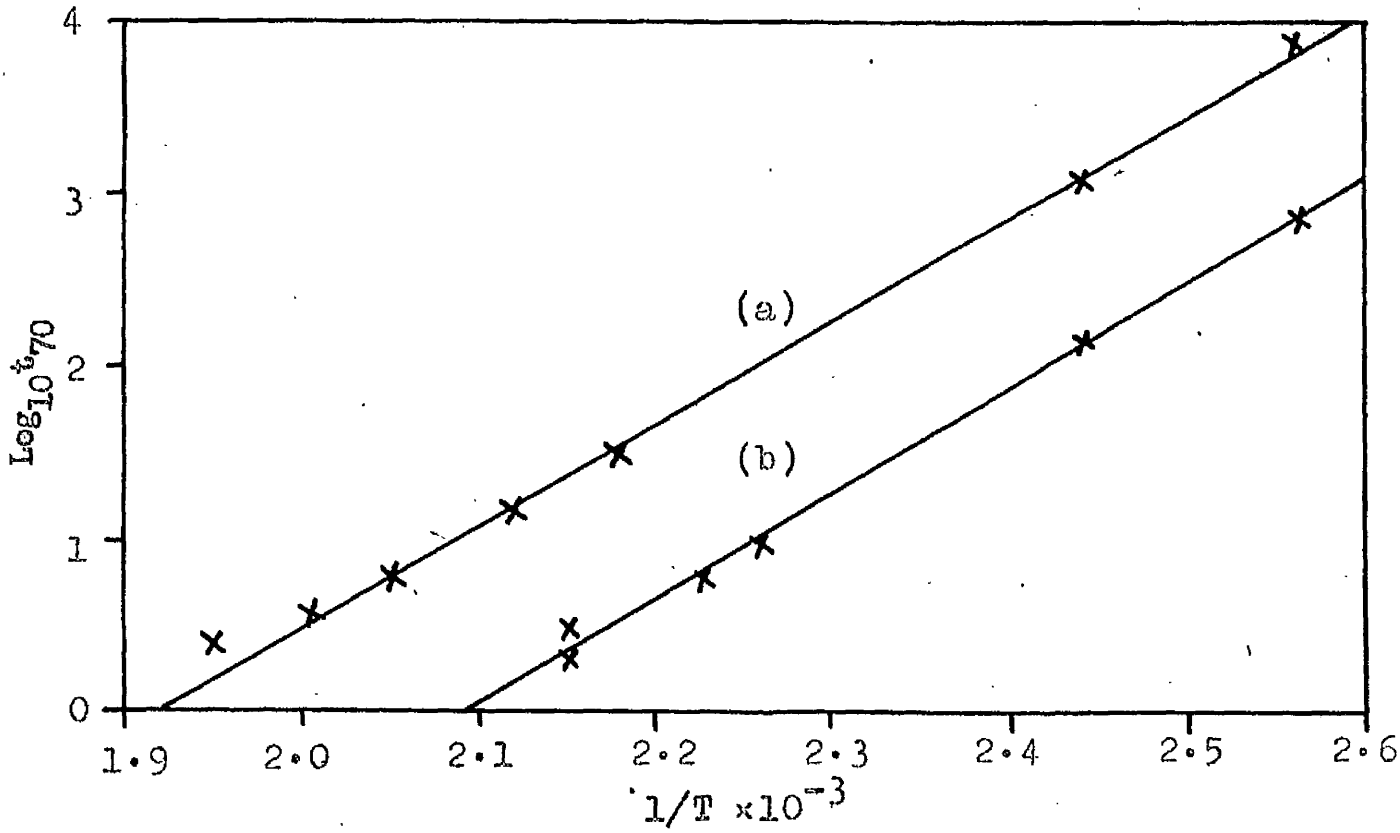

Fig. 6.9 Graph of $Log_{10}t_{70}$ against (1/T) for Silver Thicknesses of (a) 4610Å and (b) 1930Å.

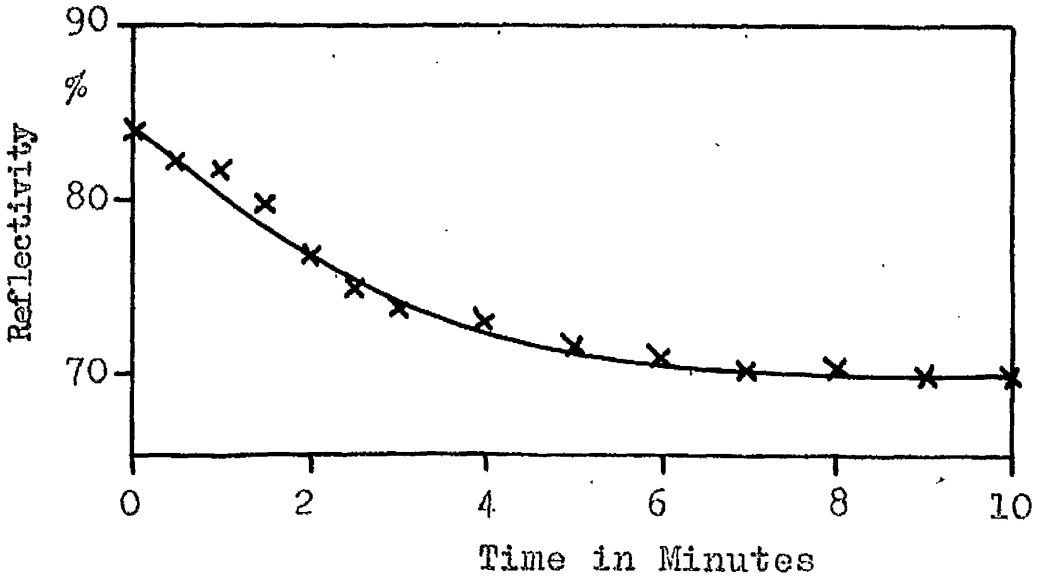

Fig. 6.10 Ageing at Silver Surface at 89½°C for Silver Thickness of 70Å.

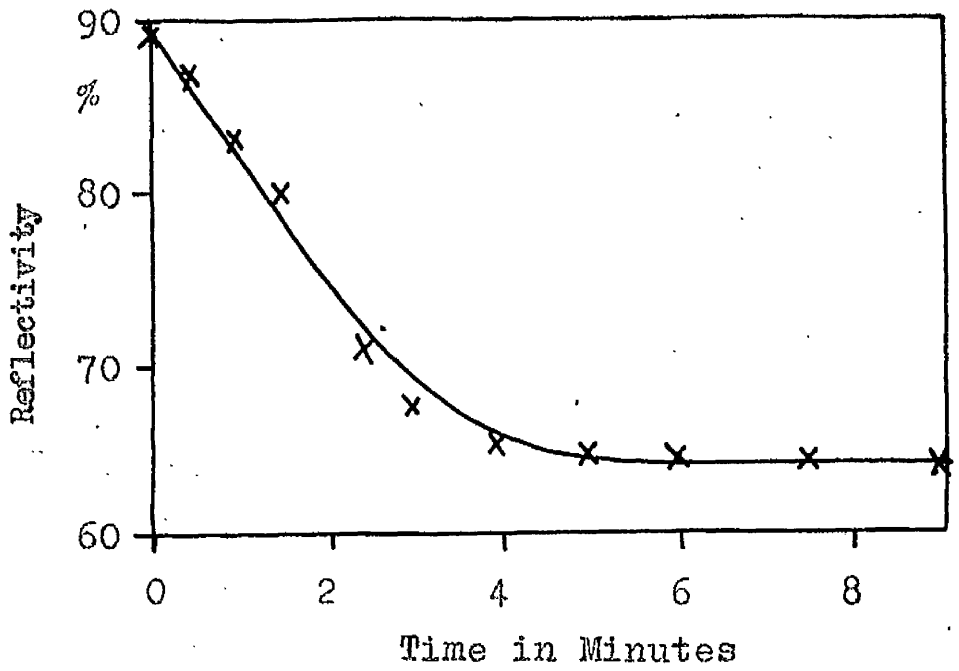

Fig. 6.11 Ageing at Silver Surface at 102½°C for Silver Thickness of 120Å.

were converted to 136°C using the value found for the activation energy, and have been plotted with the results for thicker films in fig. 6.6.

6.3 Reflectivity Changes at the Aluminium Surface

Reflectivity changes were also studied at the aluminium surface. Slides were prepared with the aluminium thickness varying in the range 500Å to 1400Å, and with very thick silver substrate films to prevent thickness ratio difficulties. The slides were aged at 140°C and typical ageing curves are shown in fig. 6.12 to 6.14.

The aluminium was found to age considerably in the initial part of the ageing curve, and allowance had to be made for this before analysing the results in detail. It was found that the effect was independent of the silver substrate thickness and substantially independent of the aluminium thickness. The ageing curve of a thick aluminium film with a comparatively thin silver substrate is shown in fig. 6.15. The corresponding reflectivity drop for a single aluminium film is shown in the same figure. This drop is very small (1% in 40 hr.) compared with the ageing of the substrated aluminium film (7% in 40 hr.). There must therefore be a difference in structure between the two films. The true diffusion reflectivity changes in fig. 6.12 to 6.14 were found by increasing the experimental

readings by an amount corresponding to the aluminium ageing in fig. 6.15. This gave the final reflectivity to be 61½% ±1% in every case. The large initial ageing was probably caused by the aluminium having a different structure when deposited on a silver substrate compared with when deposited on a glass substrate. It may possibly be associated with the penetration of silver into the aluminium as discussed below.

The shapes of the curves were again characteristic of the motion of a phase boundary. Values of the ratio t_1/t_2 were calculated for all the specimens prepared and are plotted in fig. 6.16 against the aluminium thickness. The points lie nowhere near the expected curve for 300Å light penetration, and it was found that the best fit was for a light penetration of 700Å. This effect was ascribed to the presence of silver atoms in the aluminium lattice, the penetration taking place either during evaporation or in the very first stages of ageing.

From the time taken for the reflectivity to stop changing, values of D' at 140°C were calculated for all the slides prepared. D' was constant for aluminium thicknesses above 800Å, and the mean value was found to be 1.22×10^{-14} cm^2/sec.

Different portions of the same slides were aged over

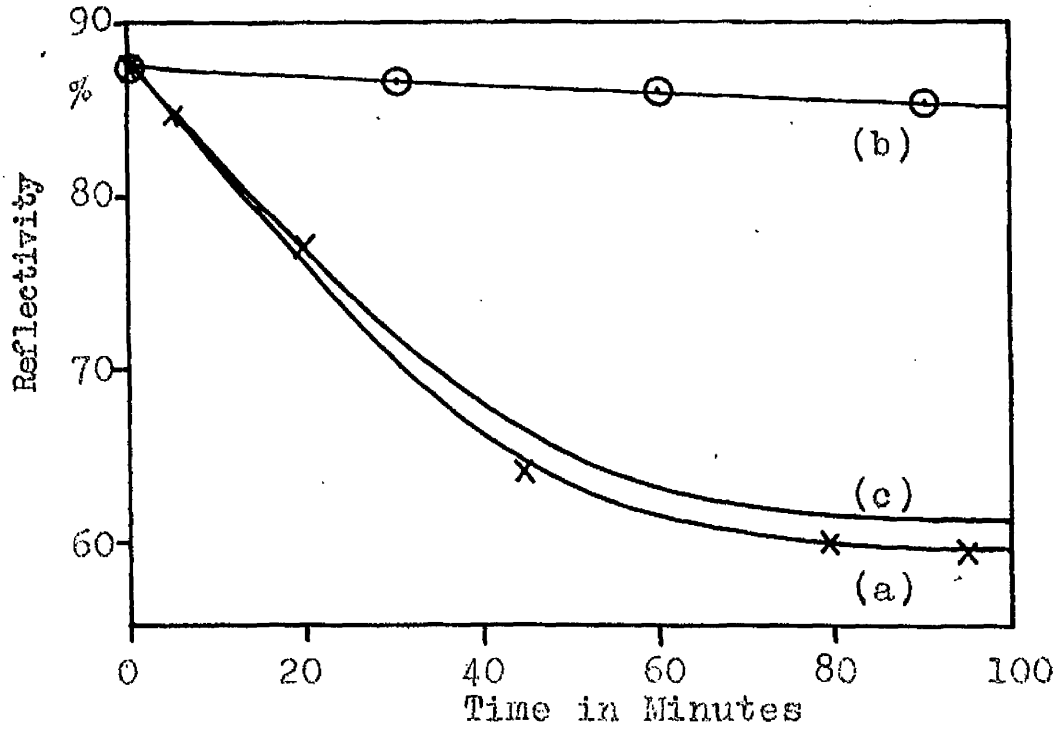

Fig. 6.12 Graph of Reflectivity against Time at Aluminium Surface at 140°C for Aluminium Thickness of 695Å. (a) Experimental curve, (b) Ageing curve for Aluminium, (c) Experimental curve corrected for ageing

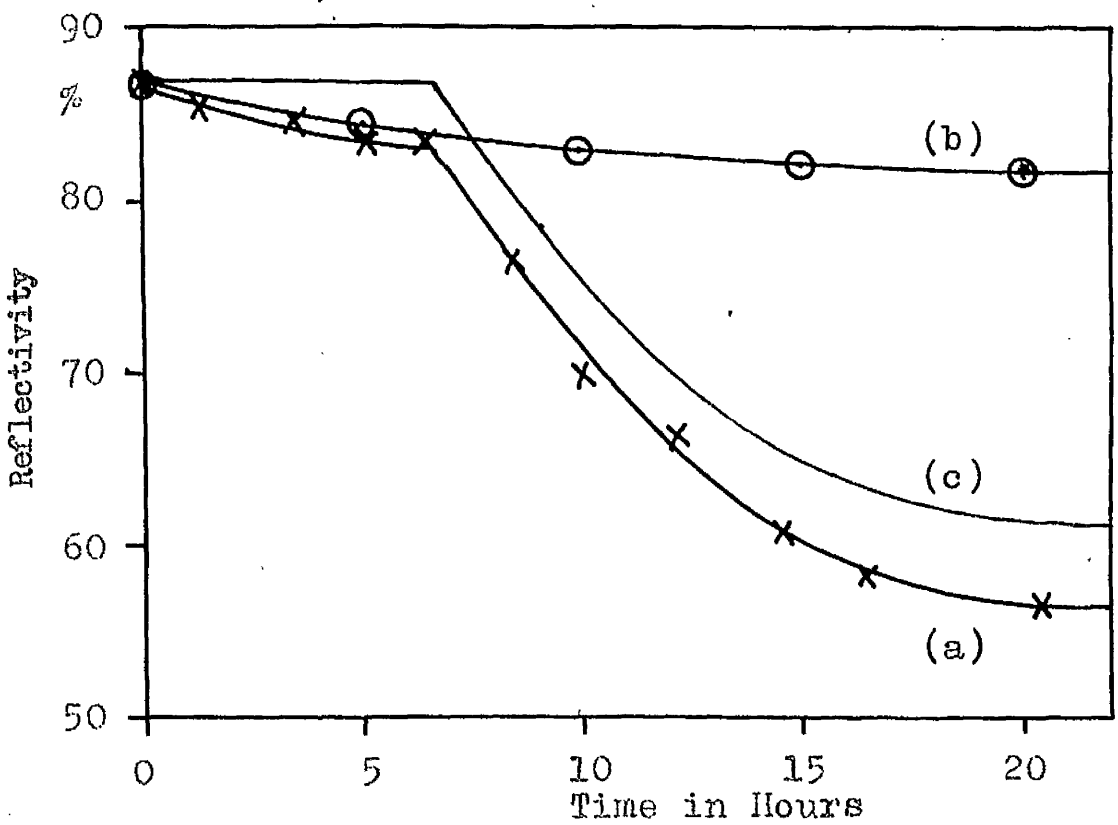

Fig. 6.13 Graph of Reflectivity against Time at 140°C for Aluminium Thickness of 2050Å. (a) Experimental curve, (b) Ageing curve for aluminium, (c) Experimental curve corrected for aluminium ageing.

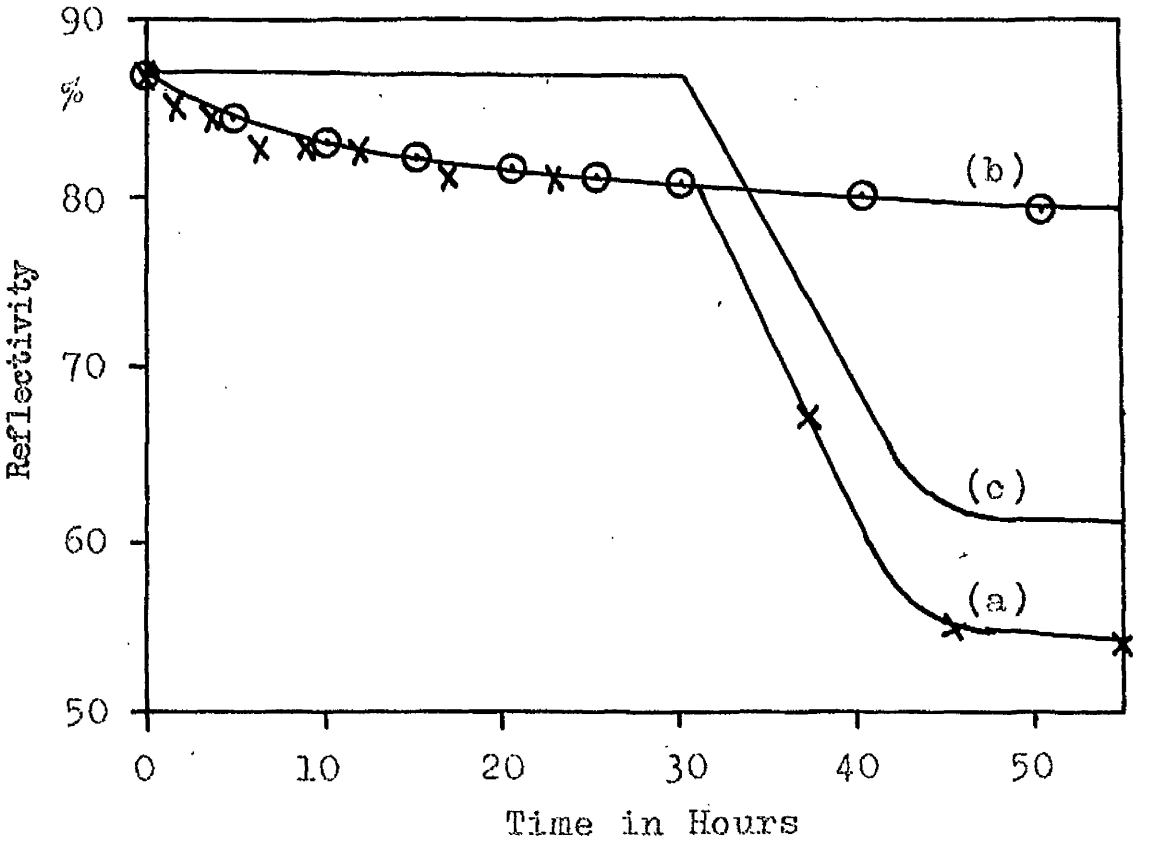

Fig. 6.14 Graph of Reflectivity against Time at 140°C for Aluminium Thickness of 4400Å. (a) Experimental curve, (b) ageing curve for aluminium, (c) experimental curve corrected for aluminium ageing.

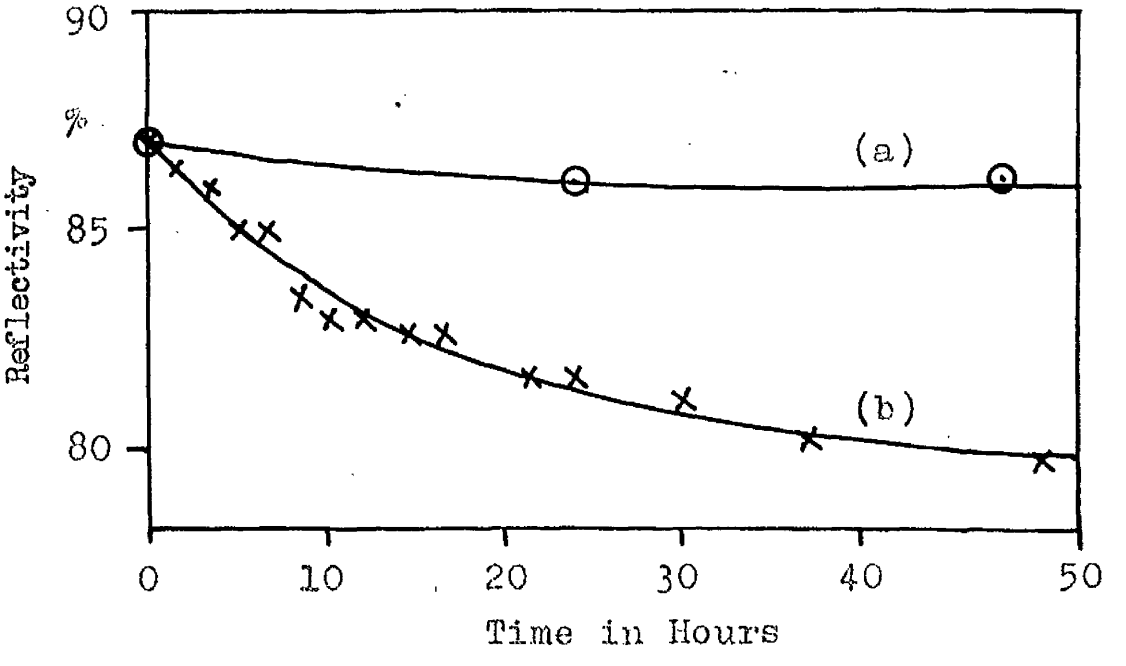

Fig. 6.15 Ageing of Thick Aluminium Film at 140°C. (a) Single Film (b) Aluminium substrated with a thin silver film.

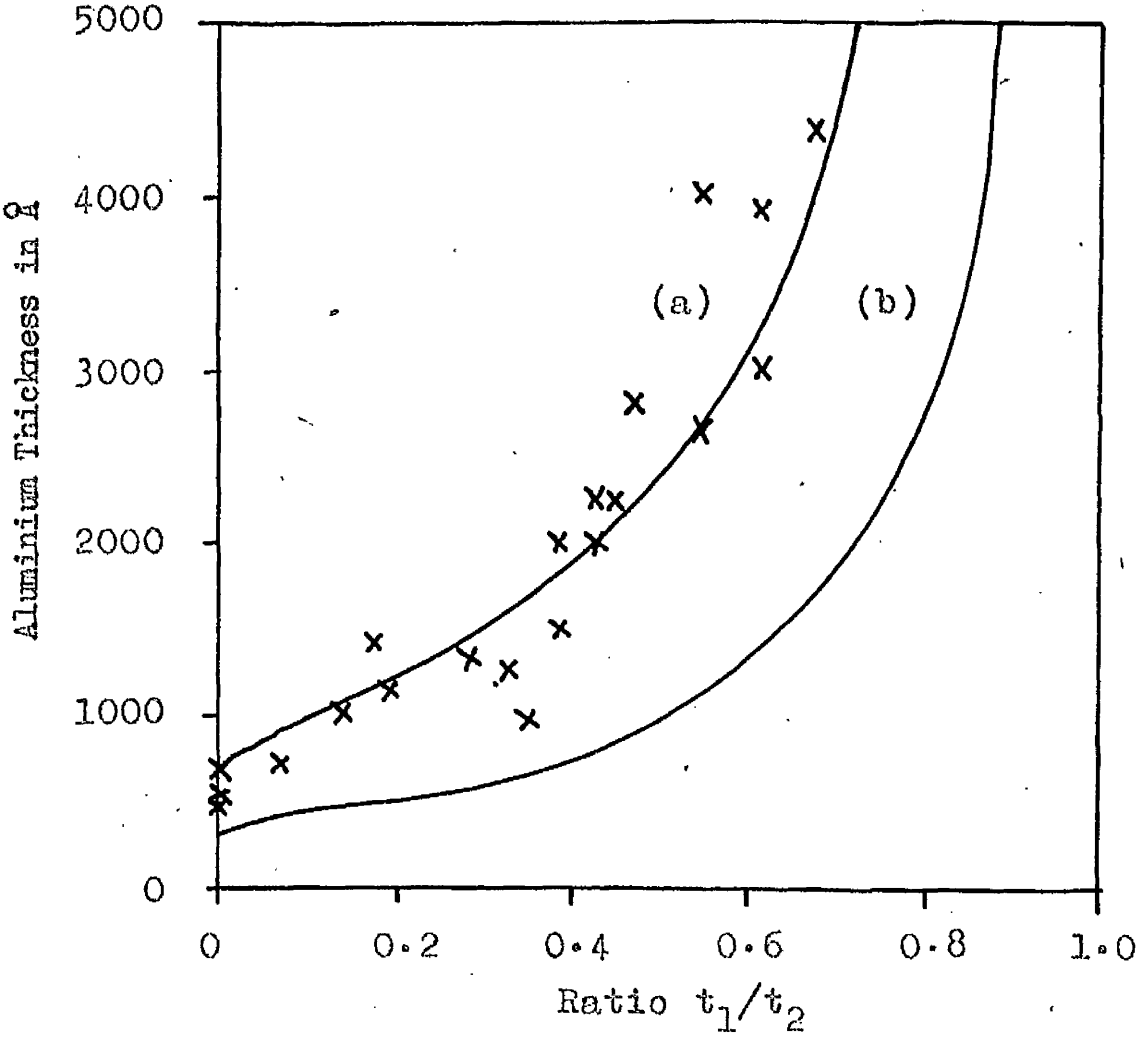

Fig. 6.16 Graph of Aluminium Thickness against Ratio t_1/t_2. Theoretical curves are plotted for light penetrations of (a) 700Å (b) 300Å.

a temperature range to find the activation energy. From a plot of $\log_{10} t_{65}$ against (1/T), the activation energy was found to be 27·7 kcal/mole, and, from the known value of D' at 140°C, D'_o was calculated to be 6·4 cm^2/sec.

6.4 Effect of Thickness Ratio

To study the effect of the thickness ratio, several slides were prepared with a single layer of silver and with four separate aluminium films of different thicknesses. Reflectivity measurements were made at the silver surface, and a typical ageing curve is shown in fig. 6.17. From the 6 slides prepared, the critical thickness ratio of aluminium to silver was found to be 0·5. Since the lattice spacings of silver and aluminium are nearly identical, this seems to imply that behind the phase boundary there must be at least one aluminium atom for every two silver atoms.

Reflectivity changes at the aluminium surface were studied with slides having a single aluminium layer and three separate silver films of different thicknesses. The slides were aged at 140°C, and a typical ageing curve is shown in fig. 6.18. The portion with a silver thickness of 3700Å (ratio of silver to aluminium = 1·9) gave almost the full reflectivity change, and so we can say that this ratio lies close to the critical ratio but is slightly less

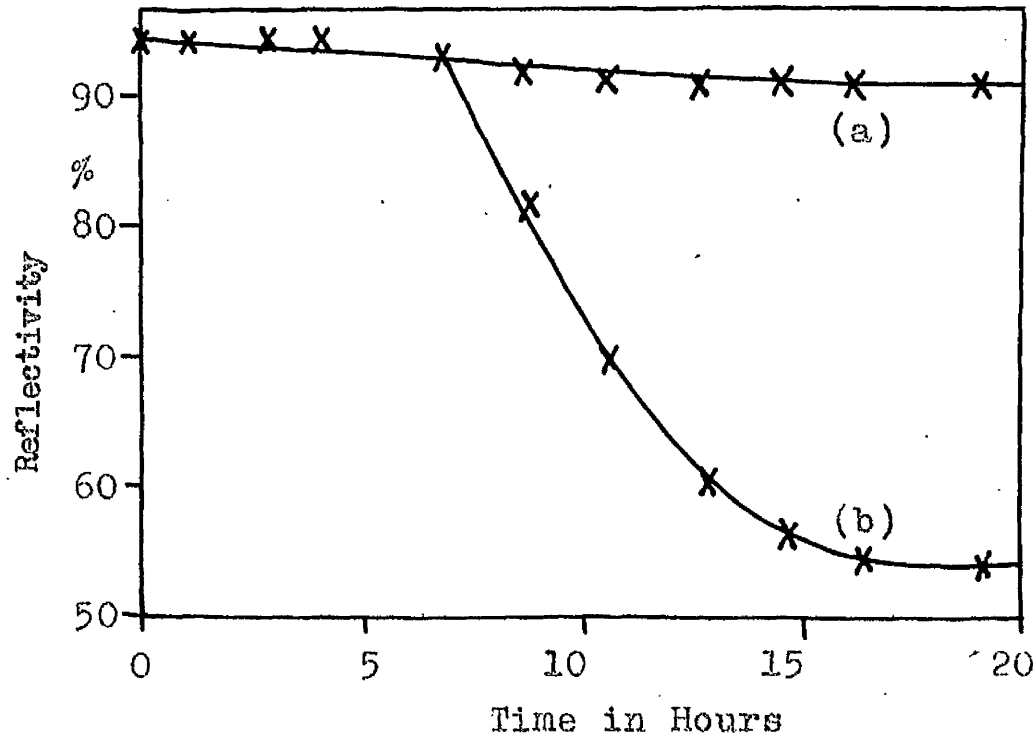

Fig. 6.17 Ageing of Silver Surface at 136°C for Silver Thickness of 3310Å.
(a) Aluminium Thickness = 1300Å & 500Å (Al:Ag=0·39&0·15)
(b) Aluminium Thickness = 3700Å & 2100Å (Al:Ag=1·1 & 0·63)

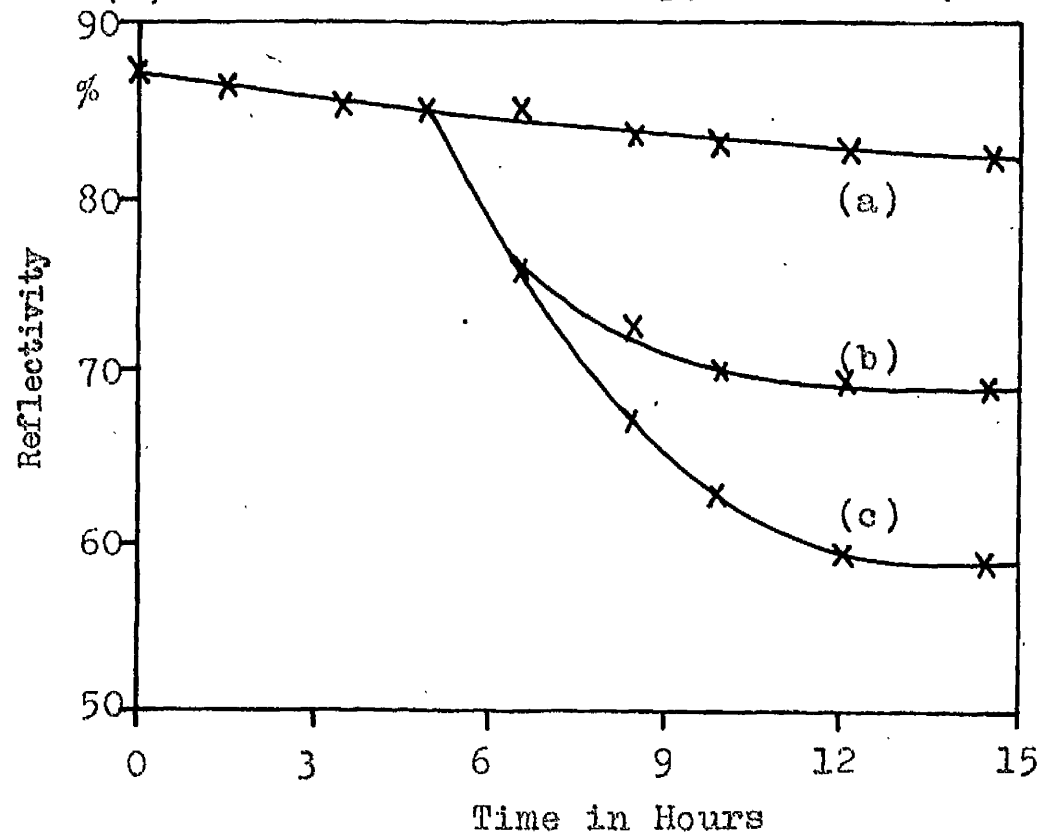

Fig. 6.18 Ageing of Aluminium Surface at 140°C for Aluminium Thickness of 2000Å.
(a) Silver Thickness = 2100Å (Al:Ag = 0·95)
(b) Silver Thickness = 3700Å (Al:Ag = 0·54)
(c) Silver Thickness = 5100Å (Al:Ag = 0·39)

than it. From the 7 slides prepared, the critical thickness ratio of silver to aluminium was found to be 2·0. The results indicate that behind the phase boundary there must be at least two silver atoms for every one aluminium atom.

From measurements at the silver surface we have concluded that behind the phase boundary there must be at least one aluminium atom for every two silver atoms. From observations at the aluminium surface we have found that there must be at most one aluminium atom for every two silver atoms. This seems to suggest that there is preferential formation of the compound Ag_2Al (ζ phase).

Values of critical thickness ratio have been observed at the two nearly equal temperatures of 136°C and 140°C. The activation energy at the silver surface was found to be 27·5 kcal/mole, whilst that at the aluminium surface was found to be 27·7 kcal/mole. These figures are nearly identical, and this means that the value of the critical thickness ratio will be the same for all temperatures.

6.5 Reflectivity Results with Aluminium Substrating the Silver

In all observations with aluminium substrating the silver, precautions similar to those observed in gold-

aluminium were taken to prevent formation of an oxide layer on the aluminium between the evaporations.

Reflectivity changes were studied first at the aluminium surface, using a thick silver overlayer to prevent thickness ratio difficulties. A typical ageing curve is shown in fig. 6.19. The ratio t_1/t_2 was calculated for the 10 specimens prepared, and is plotted against aluminium thickness in fig. 6.20. The points lie nowhere near the theoretical curve for a light penetration of 300Å. The fit for the previous value of 700Å is also poor, and the best fit was obtained on assuming a light penetration of 900Å. It would therefore appear that the value of light penetration which is obtained in this system is not a fundamental quantity but depends on the order in which the metals are evaporated.

The activation energy of diffusion was found as before. The value obtained was 27·4 kcal/mole, and this gave a mean value for D_0' of 1·8 cm^2/sec. These figures agree satisfactorily with values of E = 27·7 kcal/mole and $D_0' = 5·6$ cm^2/sec obtained with a silver substrate and aluminium overlayer. Hence the order of evaporating the metal films makes no significant difference to the value of diffusion coefficient obtained.

Reflectivity changes were also studied at the silver

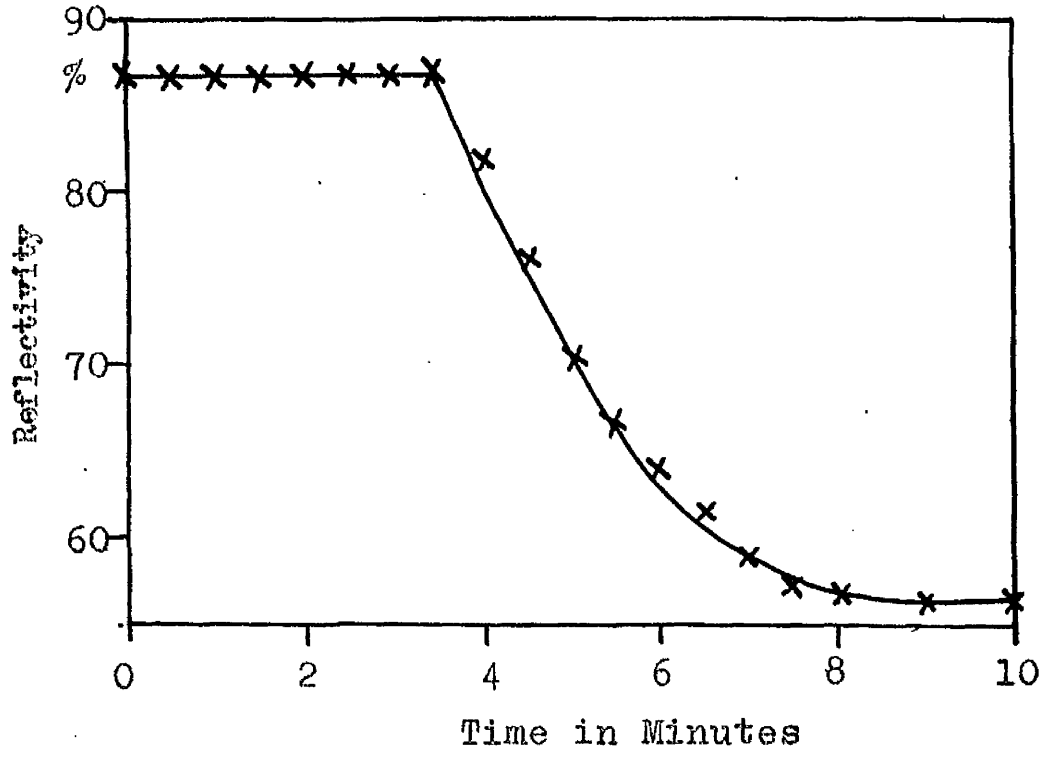

Fig. 6.19 Ageing at Aluminium Surface at 222°C with Silver Overlayering the Aluminium. Aluminium thickness = 2700Å.

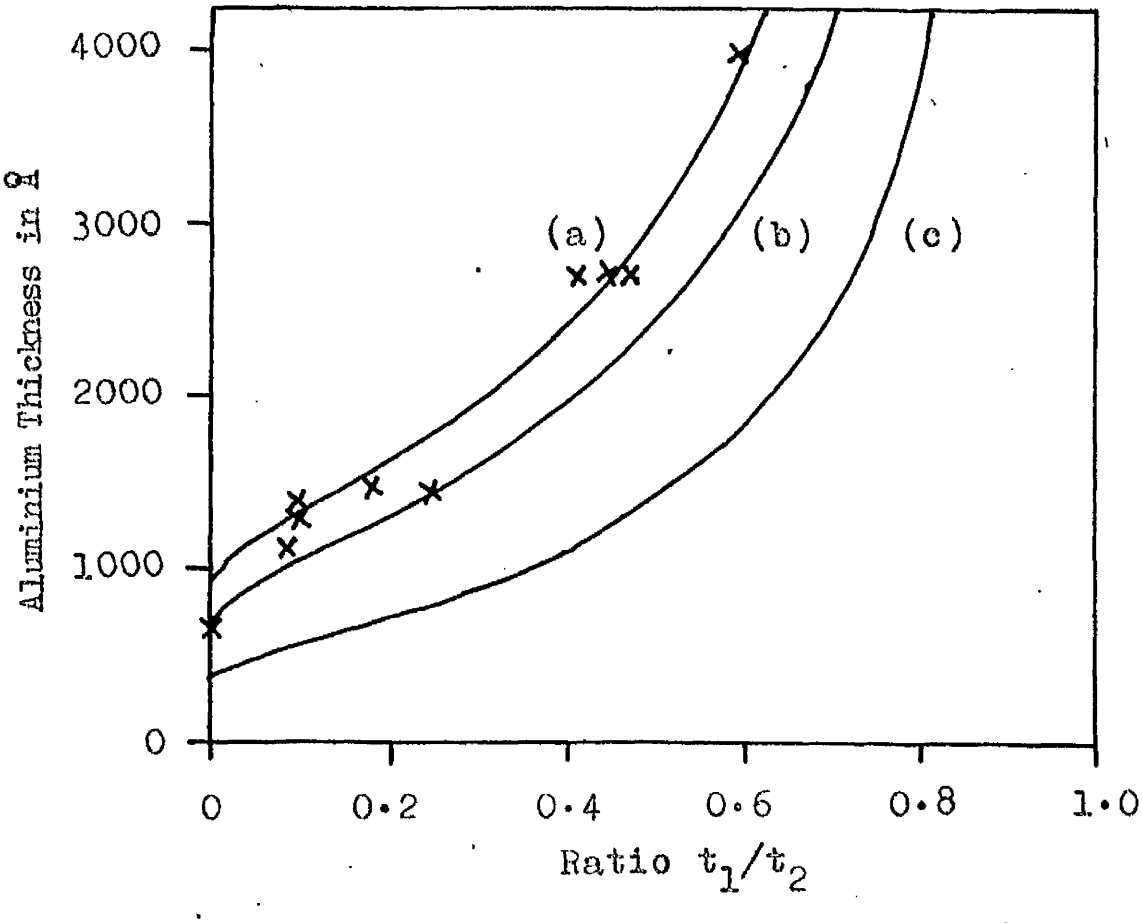

Fig. 6.20 Graph of Aluminium Thickness against Ratio t_1/t_2. Theoretical curves are plotted for light penetrations of (a) 900Å (b) 700Å (c) 300Å

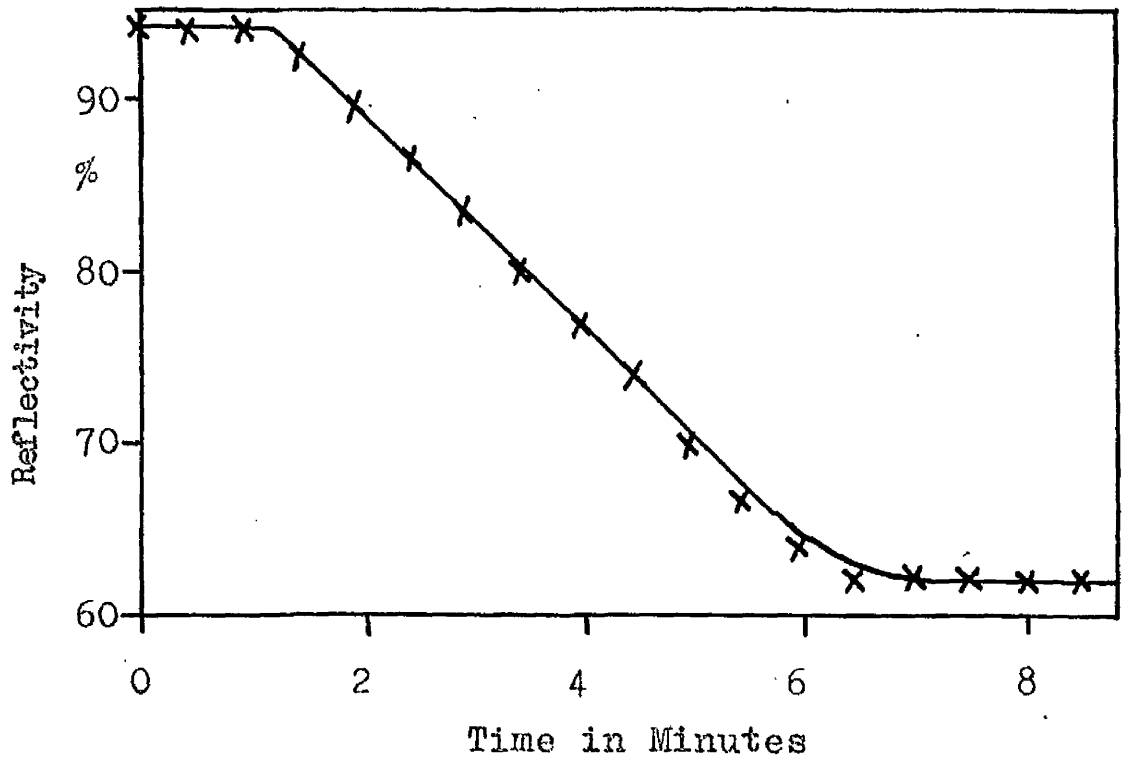

Fig. 6.21 Ageing at Silver Surface at 184°C with Silver Overlayering the Aluminium. Silver Thickness = 1300Å.

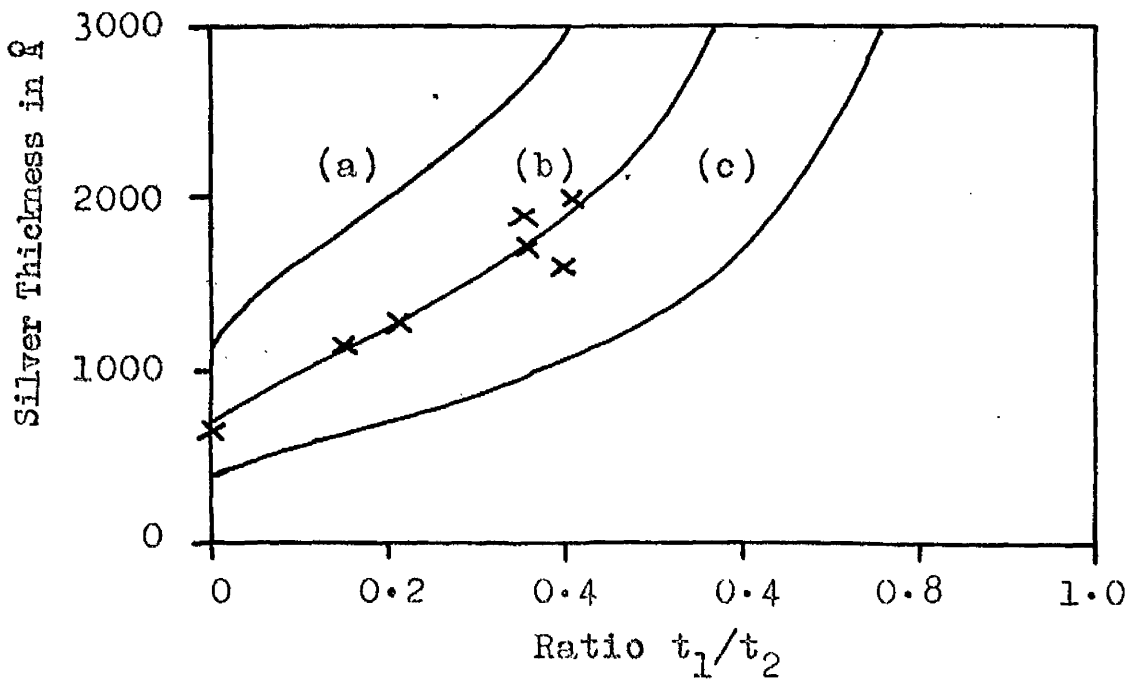

Fig. 6.22 Graph of Silver Thickness against Ratio t_1/t_2. Theoretical curves are plotted for light penetrations of (a) 1100Å (b) 700Å (c) 400Å.

surface. The silver tarnished rather readily at the high temperatures used on the hot-stage reflectometer, and consequently it proved impossible to obtain ageing curves for silver thicknesses above 2000Å. A typical ageing curve is shown in fig. 6.21, and the values of the ratio t_1/t_2 for the 7 specimens prepared are plotted against the silver thickness in fig. 6.22. The points on this graph lie between the theoretical penetration of 400Å and the experimentally found value of 1100Å for silver overlayered with aluminium. The best fit was obtained for a light penetration of 700Å. This again confirms that the value of light penetration is not a fundamental quantity in this system but depends on the order in which the metals are evaporated.

D_0' was calculated assuming the activation energy of 27·5 kcal/mole found for observations with aluminium overlayering the silver. The mean value obtained for D_0' was 6·1 cm^2/sec, in moderate agreement with the value of 19·0 cm^2/sec obtained with the silver acting as substrate.

6.6 The Reflectivity of Silver-Aluminium Alloys

The reflectivities of a series of silver-aluminium alloys prepared by "flash" evaporation are shown in fig. 6.23. The results of Wulff (1934) for the reflectivities

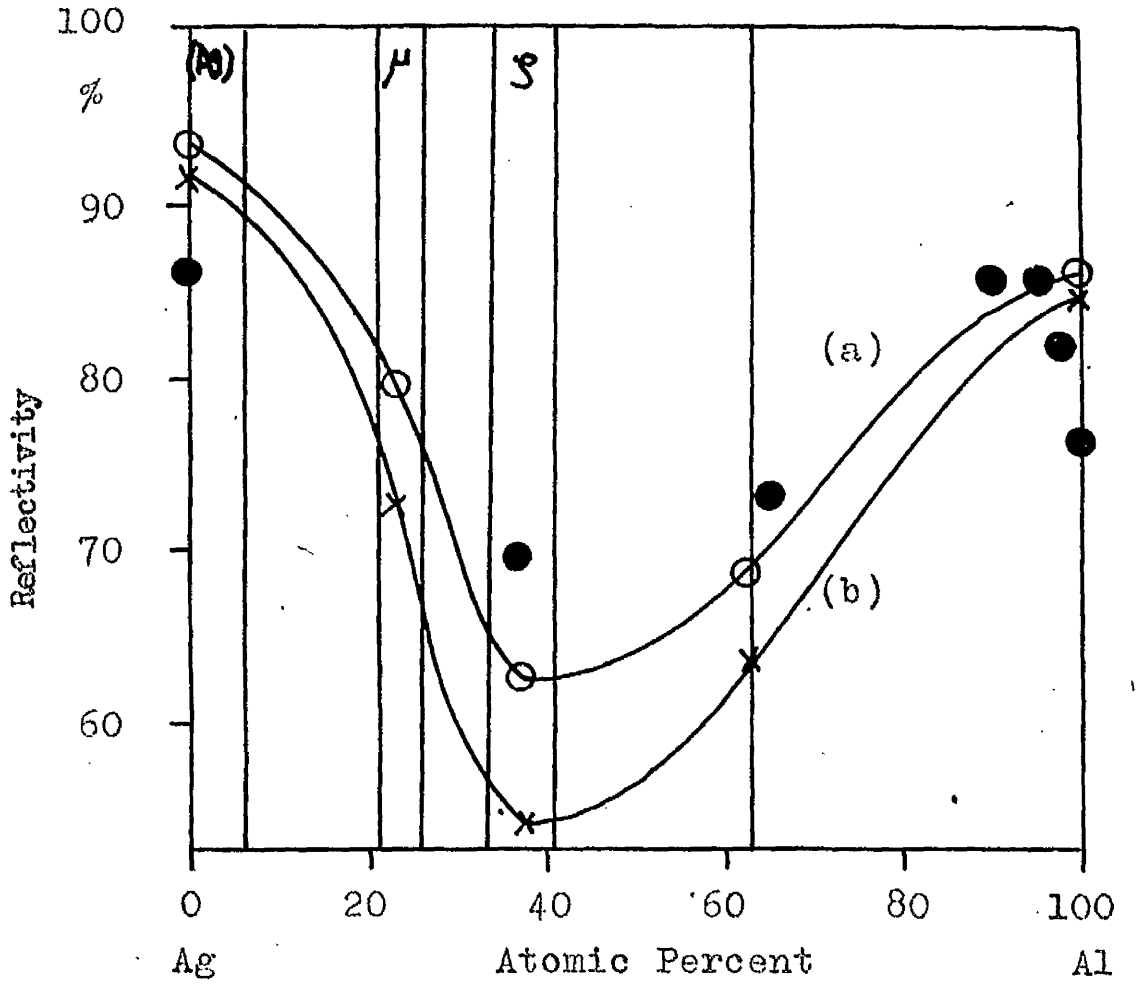

Fig. 6.23 Graph of Reflectivity against Concentration for "Flash" Evaporated Silver-Aluminium Films. (a) Measurements at air surface, (b) measurements at glass surface. ● indicate results of Wulff (1934).

of several bulk alloys are shown in the same diagram. The two sets of results have the same general trend, except that Wulff found that the reflectivity of aluminium increased with small additions of silver. This is an unexpected result since alloys in this concentration range should consist of aluminium grains imbedded in a matrix of the γ-Al eutectic. The eutectic has a reflectivity less than that of aluminium, and we would expect a mixture of it with aluminium to have a reflectivity intermediate between the two. Wulff's results may have been caused by working with a supersaturated solid solution of silver in aluminium in which the γ phase had not precipitated out. It would not be surprising if a solid solution of silver in aluminium had a higher reflectivity than pure aluminium. The reflectivities of pure aluminium and pure silver (78% and 88% respectively) found by Wulff are considerably less than the values normally found for these metals. This illustrates the difficulties caused in bulk specimens by surface films. Lowry and Moon (1932) have found that the reflectivity of a specimen can vary as much as 16% for different degrees of surface polish. Wulff has found the reflectivity of the γ phase (Ag_2Al) to be definitely less than that of either of the pure metals. This is certainly in agreement with the results for flash evaporated films, although the actual value of 72% is rather above the value of 65% found with

evaporated films.

In the ageing observations with a silver substrate and aluminium overlayer, the reflectivities of the phases formed at the glass and air surfaces were 55% and 61⅓% respectively. Results with an aluminium substrate and silver overlayer gave final reflectivities of 55% and 61⅓% at the glass and air surfaces. In the one case we would expect a compound rich in silver at the glass surface. In the other case we would expect a compound rich in aluminium at the glass surface. Since the reflectivities of the two are the same, we must conclude that the same compound is being formed in both cases.

This conclusion is confirmed by the values of 57% and 65% found at the glass and air surfaces for a flash evaporated specimen of the ζ phase (Ag_2Al). This result also shows that Ag_2Al is the main phase present in the diffusion zone, and is in agreement with observations of the thickness ratio. The only other stable phase, the μ phase, has reflectivities of 76% and 82% and so can be present only in very small quantities.

6.7 Discussion

Reflectivity measurements both at the silver and at the aluminium surfaces indicate the motion of a particular

phase boundary, and in view of the critical thickness ratios which have been found, it would appear that a layer of Ag_2Al is being formed. This has been confirmed by measurements of the reflectivities of the μ and ζ phases.

For diffusion in the aluminium, D_0' has been found to be 6·4 cm^2/sec and E to be 27·7 kcal/mole. D' at 136°C can be calculated from these values and is found to be $8·7 \times 10^{-15}$ cm^2/sec. D' at 136°C for diffusion into the silver has already been found to be 27×10^{-15} cm^2/sec. Hence the penetration of the diffusion layer into the silver is 1·8 times greater than its penetration into the aluminium. If the diffusion layer is homogeneous we would expect 1·8 silver atoms to be associated with every aluminium atom. This is close to the composition of the compound Ag_2Al, the difference being due probably to errors in the determination of D'.

The values of critical thickness ratio and the relative rates of diffusion are both in agreement with the formation of the compound Ag_2Al (ζ phase). Only two phases (μ and ζ) can exist in diffusion couples of silver-aluminium, and it is not surprising that only the ζ phase is observed. Presumably a thin layer of the μ phase is formed, but its presence is masked by the large amount of ζ phase.

Buckle (1946) has studied bulk diffusion couples of silver-aluminium. He aged specimens between 300°C and 500°C and in every case observed a broad band of the compound Ag_2Al with sharply defined edges. A small amount of the μ phase was also present in the diffusion zone, but its thickness was only around 1% of the thickness of the Ag_2Al zone. These results are in excellent agreement with those found in thin films where only the Ag_2Al was observed.

Very large values for apparent light penetration have been found in this system, far greater than can be explained by actual light penetration. The results were ascribed to interpenetration during evaporation or at the very beginning beginning of the diffusion anneal, and it was shown that this could certainly account for the very large values of light penetration observed.

It might be thought that interpenetration took place into grain boundaries and dislocations in the substrate metal. A large apparent light penetration would be observed at the substrate surface and an analagous effect would be seen at the overlayer metal surface as some parts of this would be thicker than others. It would certainly be possible to explain the apparent penetration into the silver by the aggregated structure of silver, but it would not be possible to explain the similar effect observed with an

aluminium substrate and silver overlayer. Aluminium is known to have a very continuous structure (Benjamin and Weaver 1961) and penetration into it would be difficult.

Silver-aluminium is well known as an age-hardening alloy system, and aluminium can take up to 24% silver in solid solution at high temperatures. It seems quite possible that aluminium can accept a considerable amount of silver in metastable solid solution at low temperatures. We must consider this diffusion to take place quickly either during evaporation or during the first stages of the diffusion anneal or both. This would give rise to a region of supersaturated solid solution at the interface between the two metals, but such a region would not be visible in view of the similarity in reflectivity of the two metals. Precipitation of the compound would then take place and reflectivity changes would be observed. In the initial stages, the silver atoms would require to move only small distances to react with aluminium atoms to form Ag_2Al. The value of activation energy would be characteristic of compound formation, but D' would be considerably higher by virtue of the short distances the atoms require to move. This argument therefore explains satisfactorily the large values of D' obtained in thin films despite the constant value for activation energy.

As precipitation proceeds, the effect of the initial fast diffusion will diminish and the phase edge will tend to follow the motion of a normal phase boundary. By virtue of the initial fast diffusion, however, the phase boundary will be rather diffuse, and this diffuseness will tend to give an anomolous light penetration for all film thicknesses. The value of D' will, however, tend to a constant value for thick films and beyond a certain thickness (at the silver surface, 1900Å) will show no change. The effect which has been observed in thin films is characteristic of the initial stages of diffusion only. In bulk diffusion couples where the diffusion couples are many microns thick the effect would not be observable, and this explains why Buckle obtained sharp boundaries to the phase.

The explanation given above can account for the fact that interpenetration takes place in silver-aluminium but not in gold-aluminium. Aluminium can accept considerable amounts of silver in solid solution at high temperatures and might well be expected to form metastable solid solution at low temperatures. Gold would not be accepted in solid solution in the aluminium lattice, on the other hand, because the high energy compound $AuAl_2$ would prevent this happening. Silver and gold have similar melting points, atomic size and lattice structures, and it is difficult to

see any explanation other than the difference in the phase diagrams which can explain the results.

Values for activation energy have been found to be the same in very thin films (< 400Å) as in thicker ones. Since such thin films have very large grain boundaries, we would expect the activation energy in them to be lower if grain boundary diffusion were occurring. We can therefore say that the diffusion observed in silver-aluminium, as in gold-aluminium, is a true volume diffusion, most probably a vacancy mechanism. We would expect the values of diffusion coefficient and activation energy to lie fairly close to the values for bulk specimens, and in table 6.1 the corresponding results are compared. Diffusion is generally slower into the higher melting point component (LeClaire 1949), and so we would expect D' to be considerably lower for diffusion of aluminium into silver than for diffusion of silver into aluminium. Good agreement is obtained between bulk specimens and thin film specimens for diffusion of silver into aluminium. The agreement for diffusion of aluminium into silver would be expected to be poor. We must therefore accept that diffusion of silver into aluminium is the rate determining process in thin films, and that the apparent diffusion observations at the silver surface are due simply to the loss of silver in the formation of the compound Ag_2Al.

TABLE 6.1

VALUES FOR DIFFUSION COEFFICIENT IN SILVER-ALUMINIUM

System	D_o cm^2/sec	E kcal/mole
Silver into Aluminium (Thin Films)	6·4	27·7
Aluminium into Silver (Thin Films)	19·0	27·5
Silver into Aluminium (Bulk Specimens)	1·1*	32·6*
Aluminium into Silver (Bulk Specimens)	not available	

* Results of Beerwald (1939)

CHAPTER 7

REFLECTIVITY CHANGES IN GOLD-CADMIUM, SILVER-CADMIUM, GOLD-INDIUM AND SILVER-INDIUM

7.1 Introduction

Reflectivity changes have been studied in thin film diffusion couples of gold-cadmium, silver-cadmium, gold-indium and silver-indium with the cadmium and the indium overlayering the gold and silver. Reflectivity changes took place at both surfaces, but because of the aggregated nature of evaporated cadmium and indium films, measurements were only possible at the glass surface.

The phase diagrams of the four systems are shown in fig. 7.1 to 7.4. All the systems form several intermediate phases apparently stable at low temperatures, and all show considerable solid solubility of the lower melting point metal in the gold and silver.

The four systems showed diffusion at a measurable rate at room temperature. This was used as the standard ageing temperature in gold-cadmium and in silver-indium, whilst in silver-cadmium and gold-indium, ageing measurements were made on the hot-stage reflectometer and no standard ageing temperature was used.

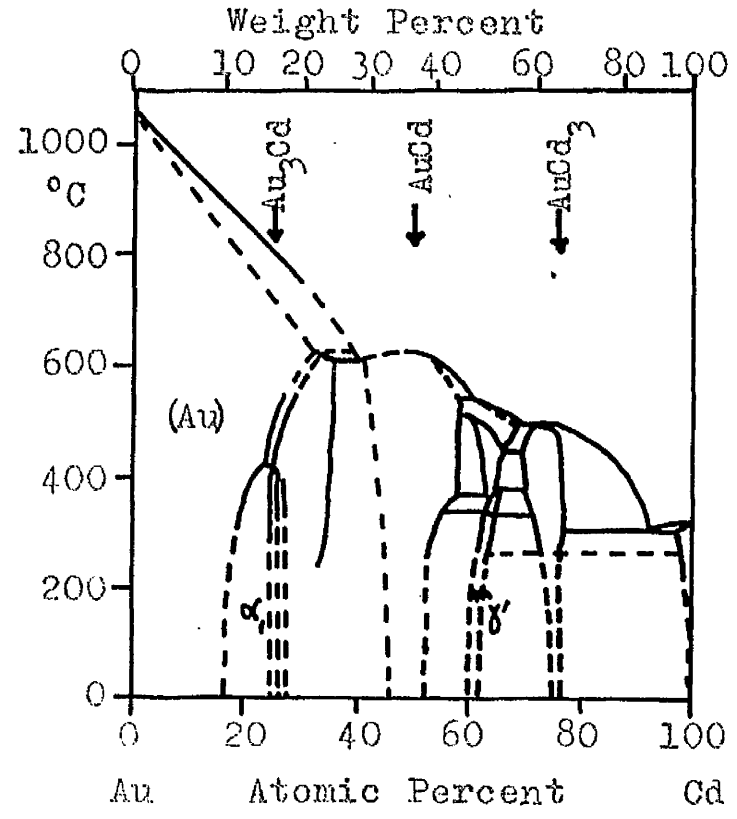

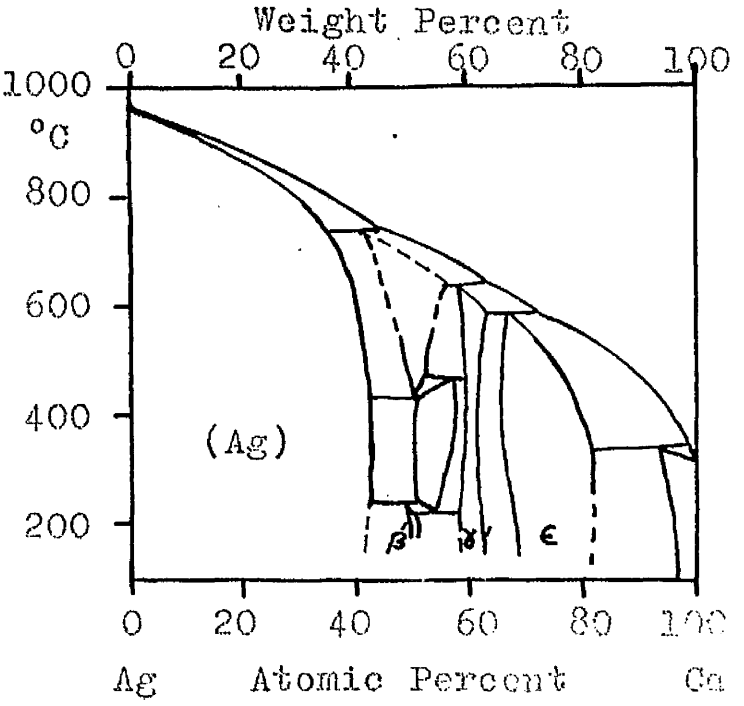

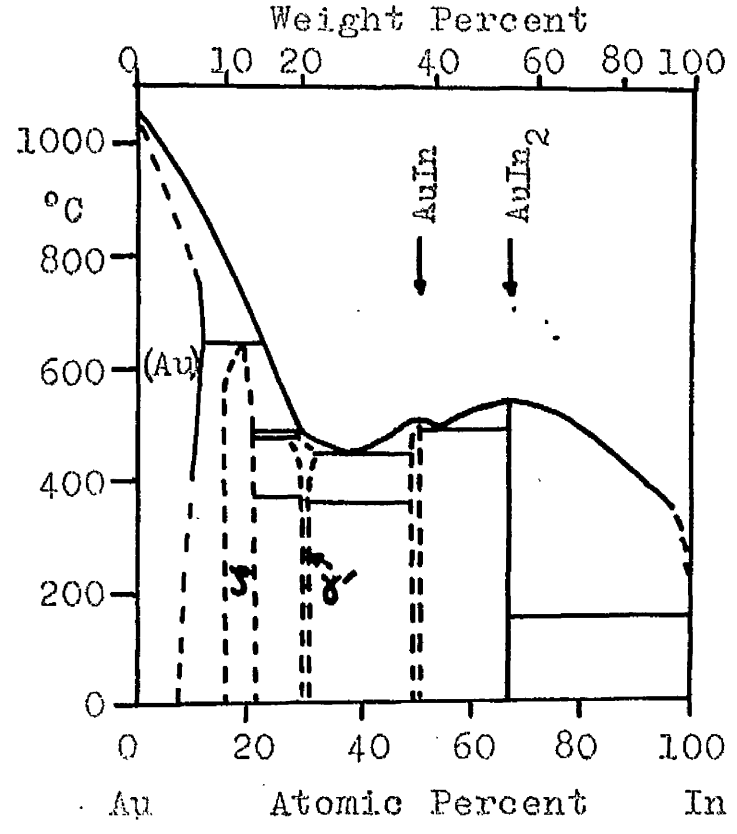

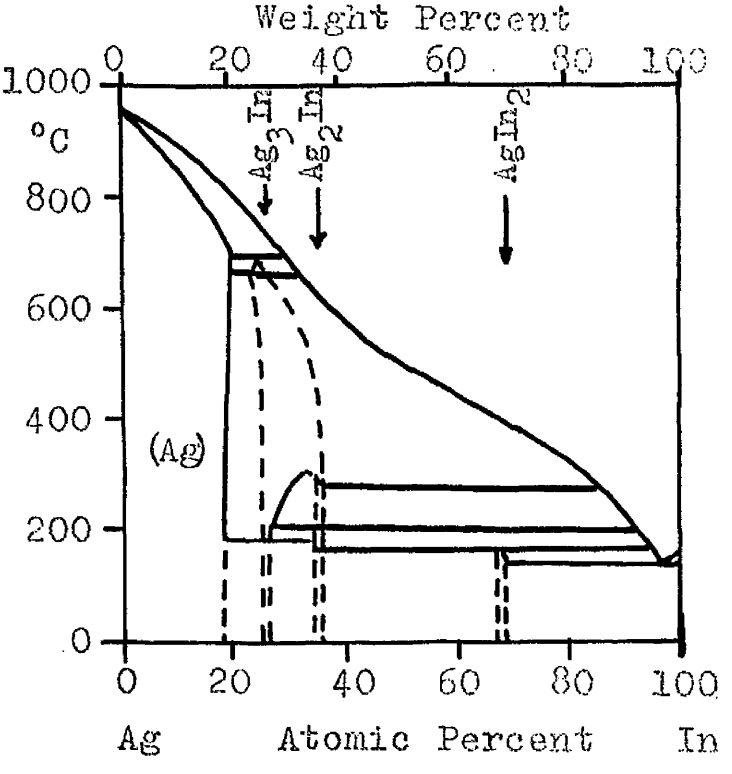

Fig. 7.1 to 7.4 Equilibrium Phase Diagrams for Gold-Cadmium, Silver-Cadmium, Gold-Indium and Silver-Indium.

7.2 Reflectivity Changes in Gold-Cadmium

The effect of light wavelength on the ageing curve of gold-cadmium is shown in fig. 7.5. Mercury yellow light was used for all subsequent measurements for convenience.

The variation in the ageing curves with different gold film thicknesses, overlaid with very thick cadmium films to prevent thickness ratio difficulties, is shown in fig. 7.5 to 7.7. The curves all gave the sudden reflectivity change characteristic of a sharply defined phase boundary. In fig. 7.8 the film thickness has been plotted against the ratio t_1/t_2. The experimental points lie near the theoretical curve for a light penetration of 400Å, which is the expected value for light penetration into gold. No anomolous effects were caused by the considerable solid solubility of cadmium in gold, and we must accept either that the zone of solid solubility is very narrow or that the reflectivity does not change much with small additions of cadmium in solid solution. Values of the diffusion coefficient (D') were found from the time taken for the reflectivity to cease changing, and the mean value of D' at 21°C was found to be 1.05×10^{-14} cm^2/sec, independent of thickness.

Different portions of the same slides were aged

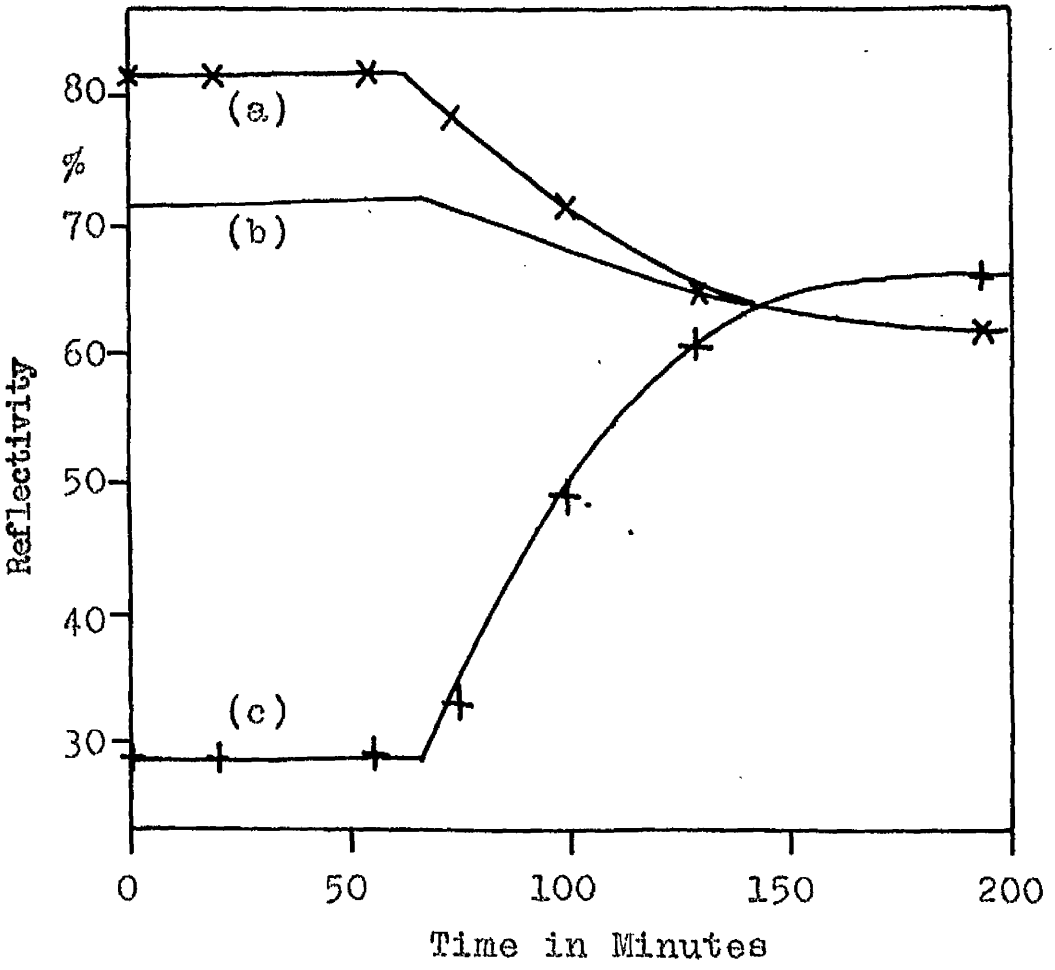

Fig. 7.5 Ageing of Gold-Cadmium Film at 21°C with Cadmium Thickness of 700Å. Reflectivity change at gold surface with mercury light of wavelength (a) 5790Å, (b) 5461Å, and (c) 4358Å.

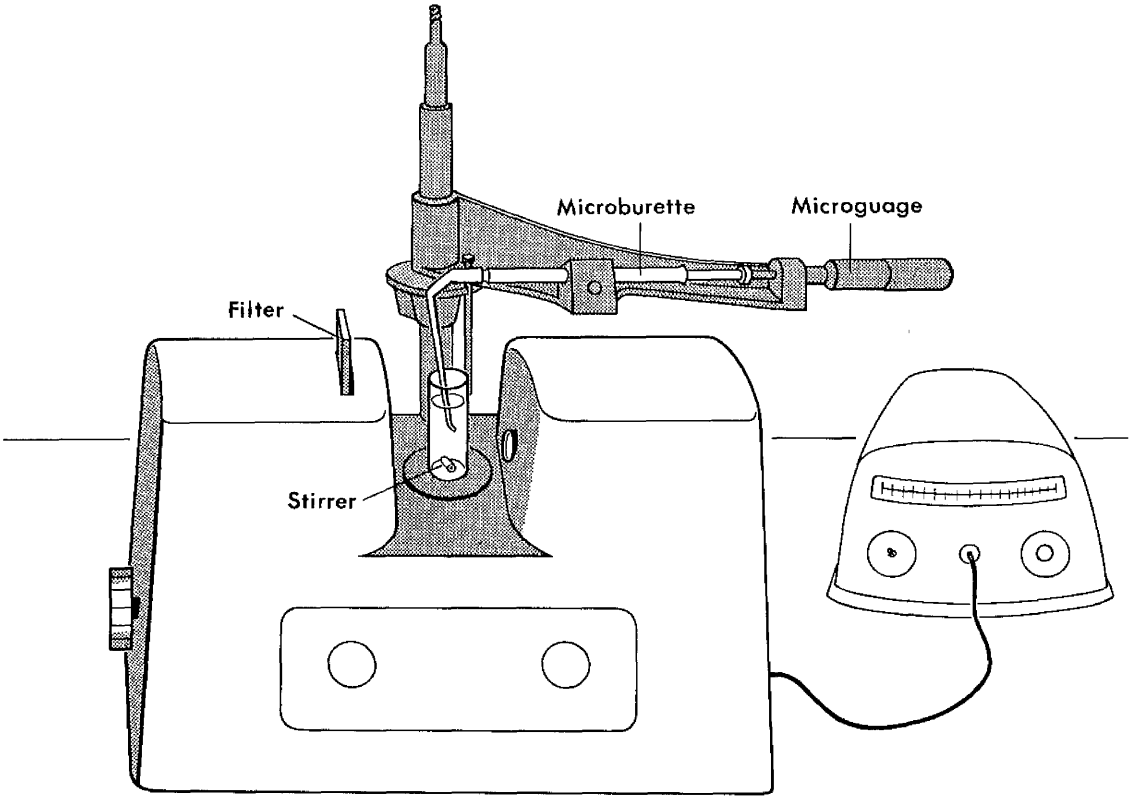

FIGURE 3. DIAGRAM OF E.E.L. PHOTOELECTRIC TITRATOR

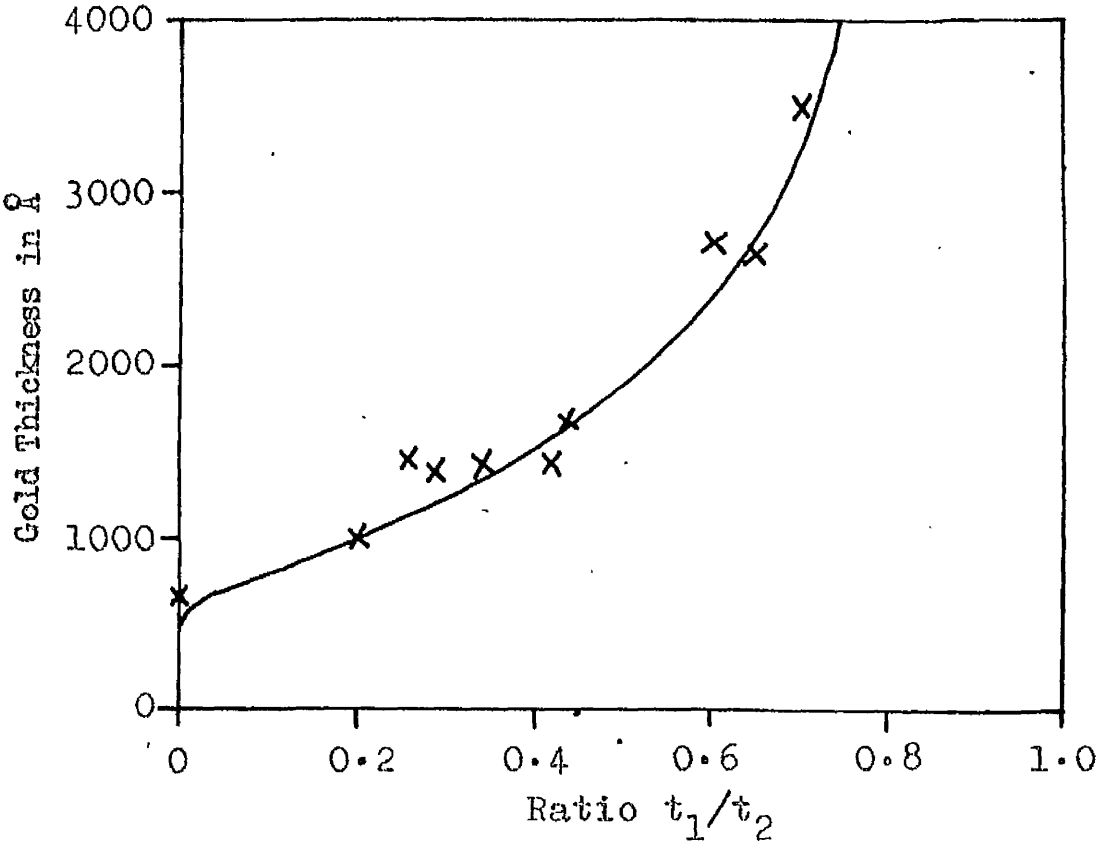

Fig. 7.8 Graph of Gold Thickness against Ratio t_1/t_2. The theoretical curve is plotted for a light penetration of 400Å.

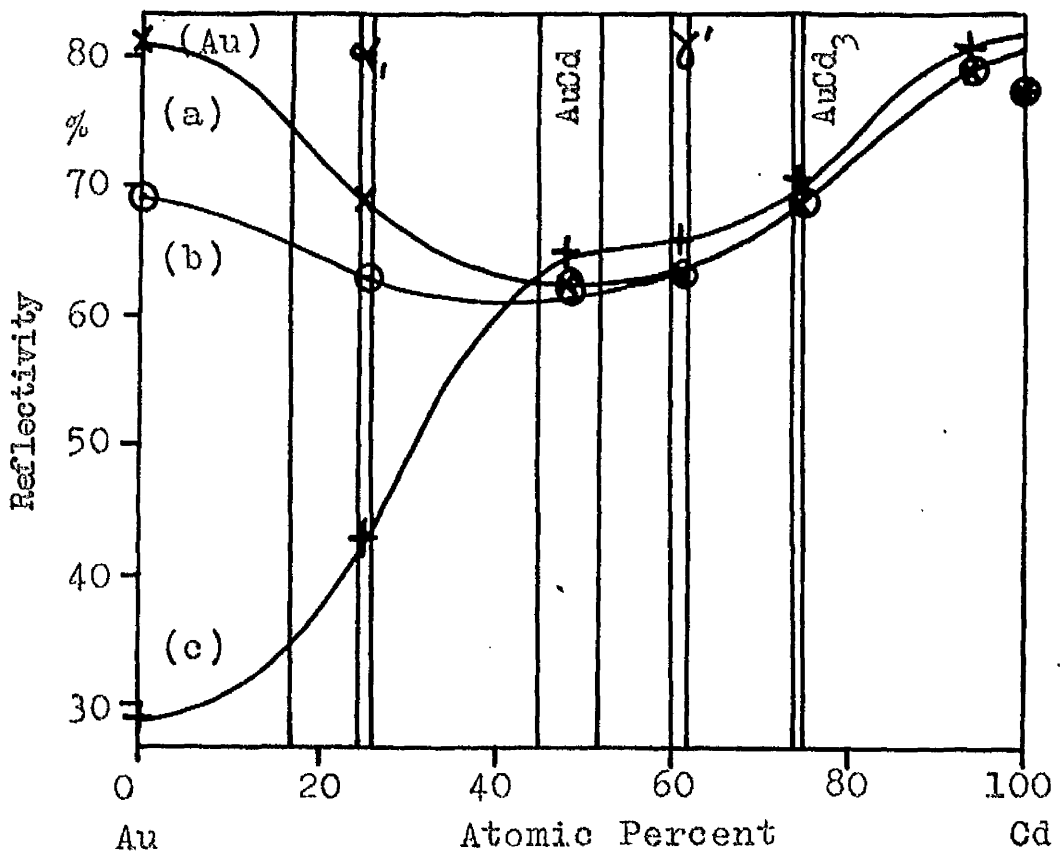

Fig. 7.9 Graph of Reflectivity against Concentration for Mercury Light of Wavelength (a) 5790Å (b) 5461Å (c) 4358Å.

over a temperature range to find the activation energy. From a graph of $\log_{10} t_{65}$ against (1/T), this was found to be 18.6 kcal/mole, and this gave D'_o equal to 0.83 cm^2/sec.

Five slides were prepared with one gold film and four separate cadmium films of different thicknesses, and these gave the critical thickness ratio of cadmium to gold to be 1.4. This corresponds to a cadmium concentration of 38⅓% by weight, and reference to fig. 7.1 shows that this is close to the composition of the compound AuCd. We can therefore conclude that the reflectivity changes observed were due to the formation of this compound.

The reflectivities of a series of gold-cadmium alloys prepared by "flash" evaporation are shown in fig. 7.9. Cadmium was deposited in a highly aggregated form and its reflectivity varied from 52% to 70% on the one slide. These figures were somewhat below the value of 78% found for a bulk specimen (Handbook of Physics and Chemistry 1957). A "flash" evaporated film with the addition of 5 at. % of gold to the cadmium condensed in a non-aggregated form, probably because the condensed gold atoms acted as nuclei for the alloy film. The reflectivity of this alloy was approximately 80%, indicating the reflectivity of cadmium to be slightly higher. The reflectivities of the phase formed by diffusion (fig. 7.5)

were 61%, 62% and 67% for mercury yellow, green and blue light respectively. These figures are in satisfactory agreement with the values found for the AuCd and γ' phases in "flash" evaporated alloys, indicating that the compound formed by diffusion was one of these two phases. Measurements of thickness ratio indicate the compound AuCd rather than the γ' phase.

7.3 Reflectivity Changes in Silver-Cadmium

Since both silver and the compound formed by diffusion in this system were colourless, the wavelength of the light used in measuring the reflectivities made little difference to the actual values of reflectivity obtained. Mercury green was used throughout the measurements.

The change in the shape of the ageing curves for different silver film thicknesses overlayered with very thick cadmium films is shown in fig. 7.10 and 7.11. The curves all showed the sudden reflectivity change associated with the motion of a phase boundary, and plotting the ratio t_1/t_2 in fig. 7.12 showed that the experimental points lay fairly near the theoretical curve for a light penetration of 550Å. The expected light penetration for a silver film has been shown to be 400Å, and so we must accept that the phase boundary was slightly diffuse, the

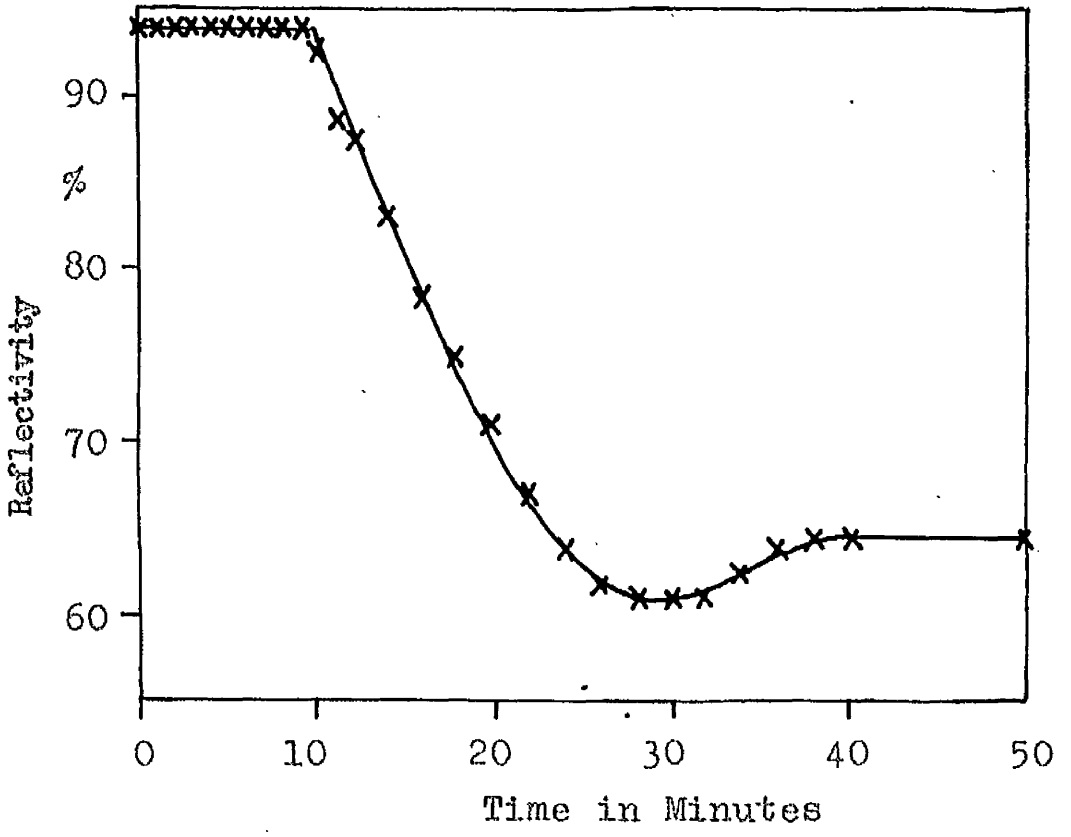

Fig. 7.10 Ageing of Silver-Cadmium at 86½°C. Reflectivity change at silver surface with silver 1440Å thick.

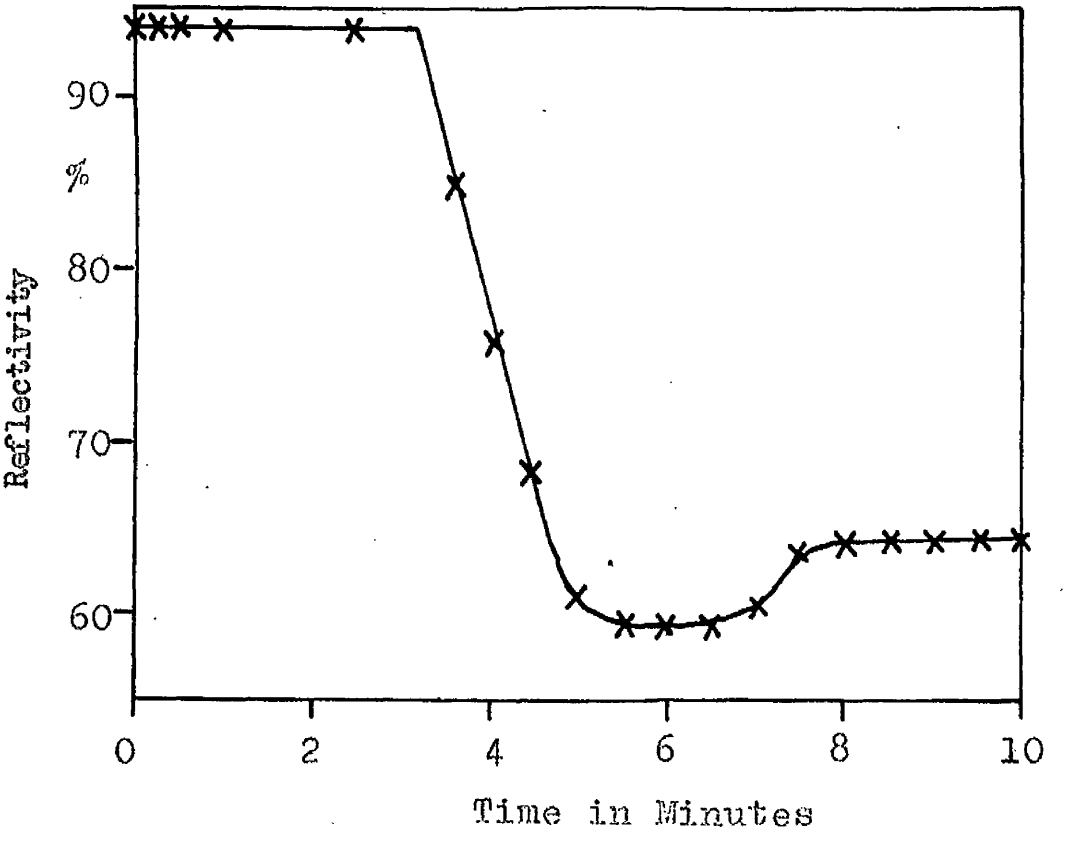

Fig. 7.11 Ageing of Silver-Cadmium at 143°C. Reflectivity change at silver surface with silver 3500Å thick.

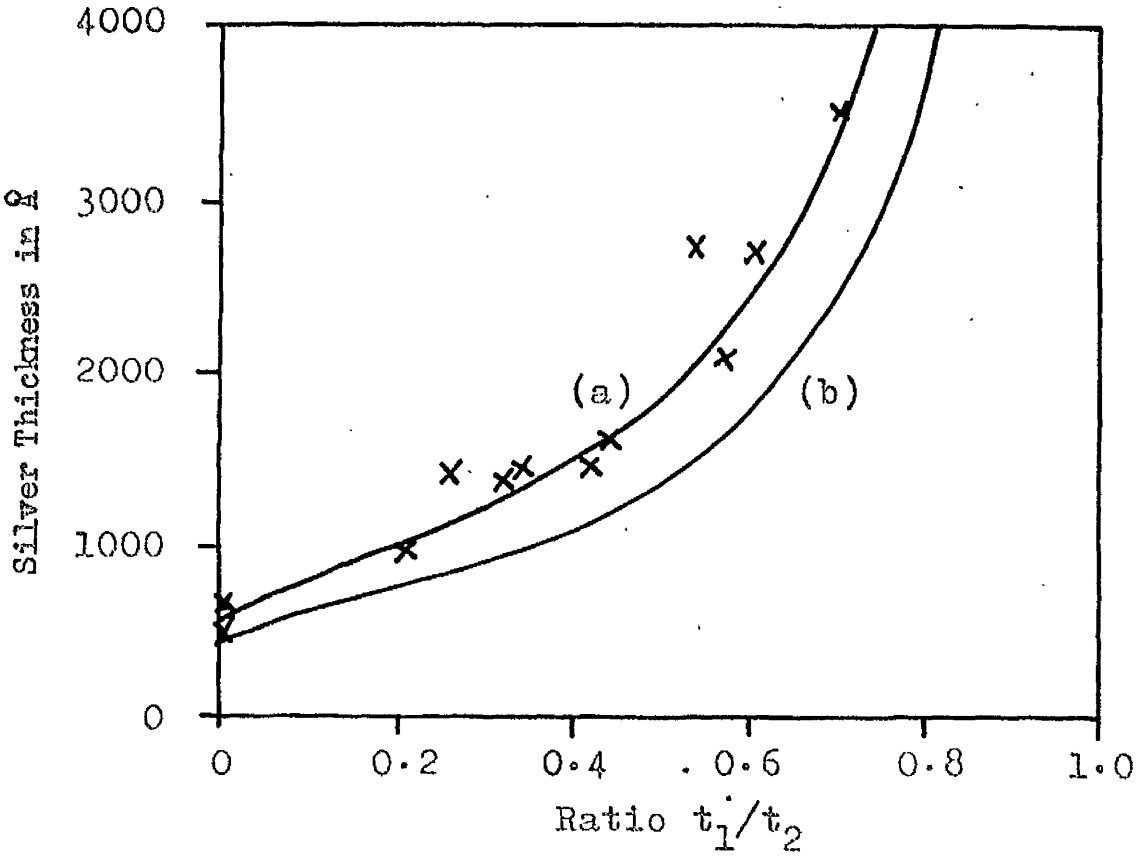

Fig. 7.12 Graph of Silver Thickness against Ratio t_1/t_2. Theoretical curves are plotted for light penetrations of (a) 550Å (b) 400Å.

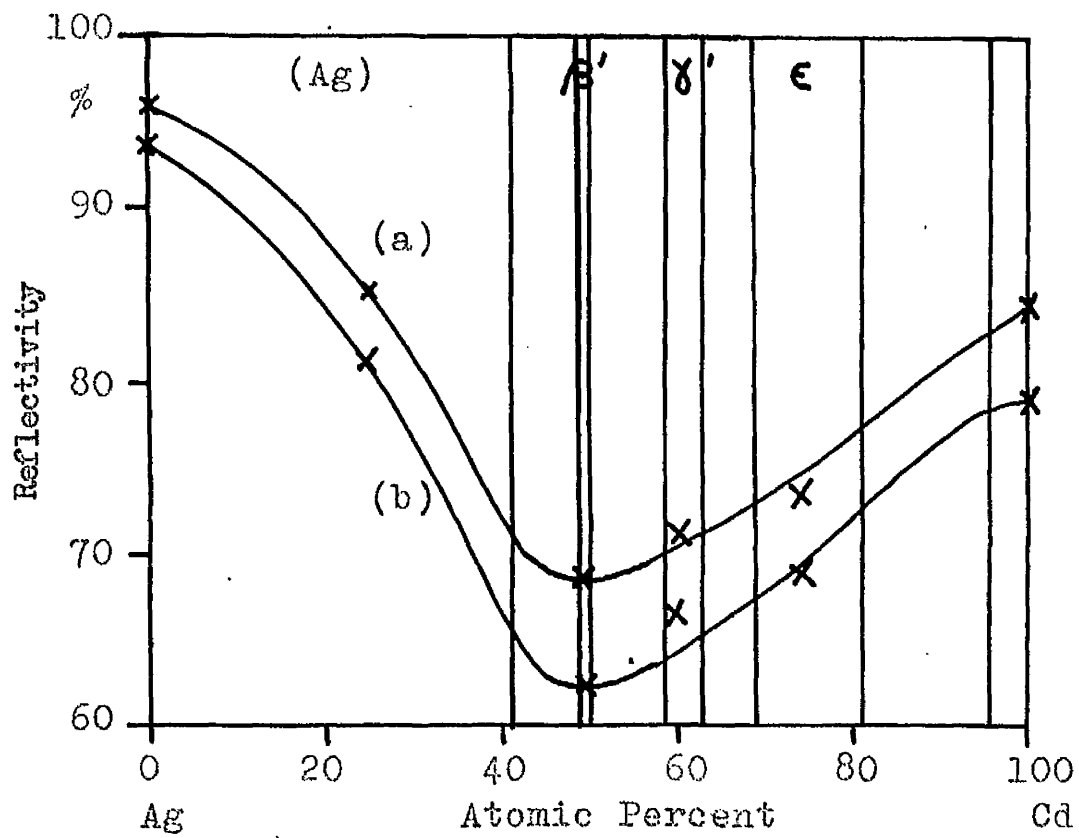

Fig. 7.13 Graph of Reflectivity against Concentration (a) at air surface (b) at glass surface.

extra 150Å light penetration being caused presumably by penetration of the cadmium into the silver.

At the end of the reflectivity changes just discussed, the reflectivity increased again by about 4%. This effect was small but was observed in all the specimens prepared. It appears that it may have been due to a change in concentration in the phase which diffused up to the silver surface, but in view of the small concentration ranges of the intermediate phases in silver-cadmium, it appears that this explanation is unlikely. A more probable explanation is that the effect was due to the presence in the diffusion zone of a second phase, which, following shortly behind the first phase, itself came up to the glass surface. This would mean that the second phase visible was much the wider of the two and had a higher cadmium concentration than the first phase.

Different portions of the same slides were aged over a temperature range to find the activation energy of diffusion. From a graph of $\log_{10} t_{72\frac{1}{2}}$ against (1/T), this was found to be 14.9 kcal/mole. The shape of the ageing curve did not vary with temperature, and, in particular, the final reflectivity increase did not change relative to the rest of the curve. Hence the activation energy associated with the first part of the reflectivity

change was the same as the activation energy associated with the second part of ageing - the reflectivity increase.

No special ageing temperature had been used in this system. To find D_o' it was necessary to determine D' for each specimen, plot log D' against (1/T), and draw in the mean line corresponding to an activation energy of 14·9 kcal/mole. The values of D' were all consistent and the best value obtained for D_o' was $3{\cdot}0 \times 10^{-4}$ cm^2/sec.

Six slides were prepared each with one silver film and four different thicknesses of cadmium overlayer. The critical thickness ratio of cadmium to silver was found to be 1·6, giving a cadmium concentration of 58% by weight. This thickness corresponded to the minimum cadmium thickness which caused the reflectivity to drop below 65%, and so did not distinguish between the portion of the curve with 61% reflectance and 65% reflectance. If, in fact, the reflectivity changes were due to a change in concentration only in one phase, then this phase was the γ' phase. If the reflectivity changes were due to the presence of two phases in the diffusion zone, then the second compound formed would be the γ' phase as this was much the wider of the two. The first (lower reflectivity) compound was probably the β' phase, for this was the only compound which had a higher silver concentration than the γ' phase.

The reflectivities of a series of silver-cadmium alloys prepared by "flash" evaporation are shown in fig. 7.13. The reflectivity of pure cadmium has been taken to be 80% for the reasons already given. The reflectivity of the γ' phase is 66%, and this is in good agreement with the final reflectivity of 65% obtained in the diffusion couple. The β' phase has a reflectivity definitely less than that of the γ' phase, and the value of 62⅓% is in good agreement with the 61% found as the minimum in the ageing curve. These changes tend to confirm that the reflectivity changes are caused by two separate phases in the diffusion zone, the first being the low reflectivity β' phase and the second the higher reflectivity γ' phase.

7.4 Reflectivity Changes in Gold-Indium

The effect of light wavelength on a typical ageing curve in this system is shown in fig. 7.14. Mercury yellow light has been used for all subsequent measurements.

The change in the shape of ageing curves for different gold thicknesses overlaid with very thick indium films is shown in fig. 7.14 to 7.16. The curves all showed the sudden reflectivity change associated with a phase boundary, and plotting the ratio t_1/t_2 (fig.7.17) showed that the experimental points lay fairly near the

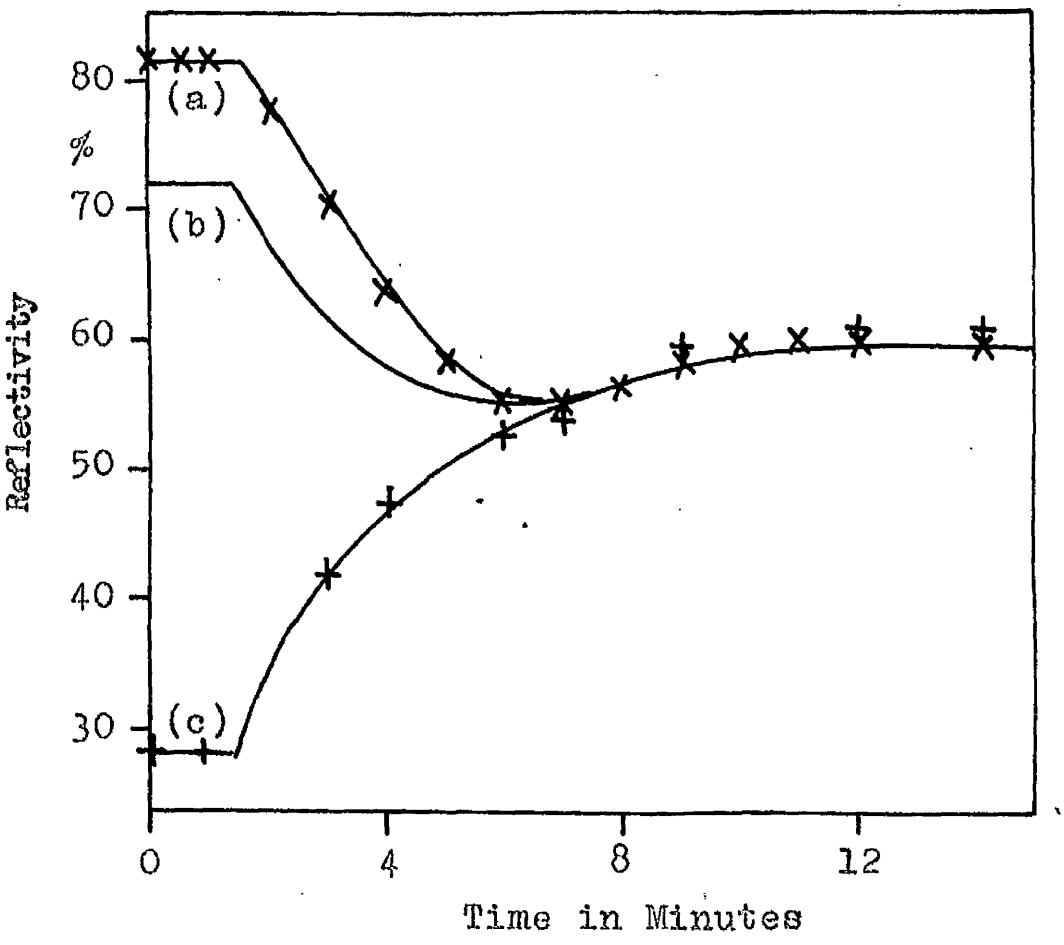

Fig. 7.14 Ageing of Gold-Indium at 97°C with Gold Thickness of 1270Å. Reflectivity change measured with mercury light of wavelength (a) 5790Å, (b) 5461Å and (c) 4358Å.

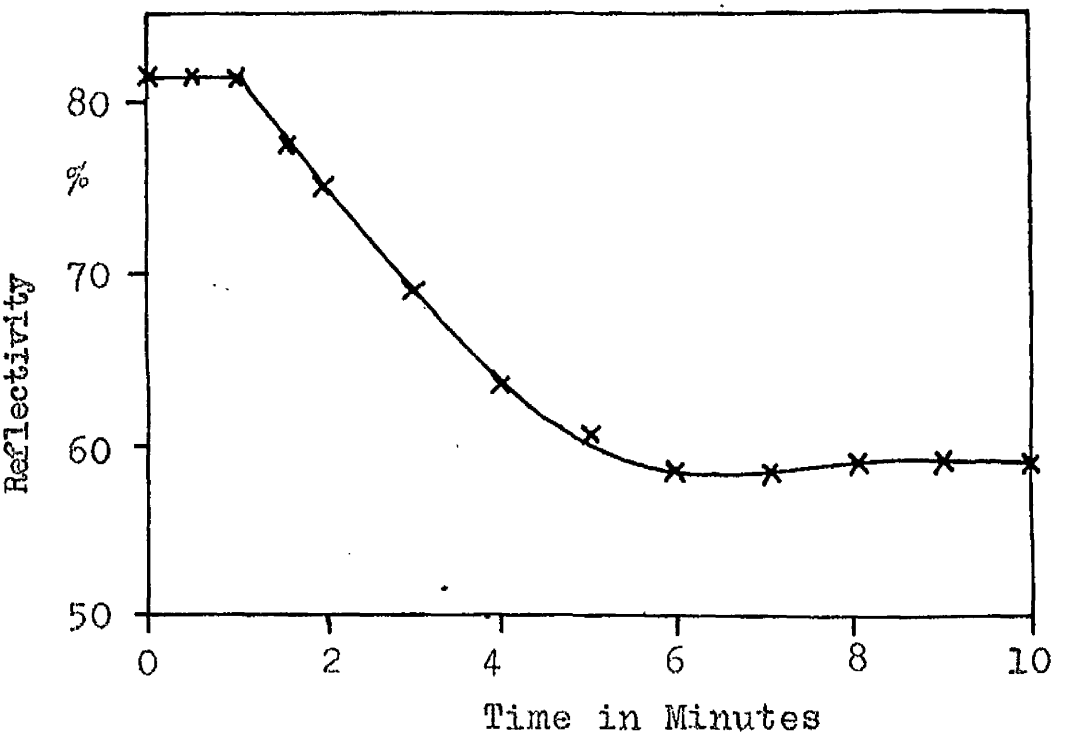

Fig. 7.15 Ageing of Gold-Indium at 95°C. Reflectivity change at gold surface for gold thickness of 680Å

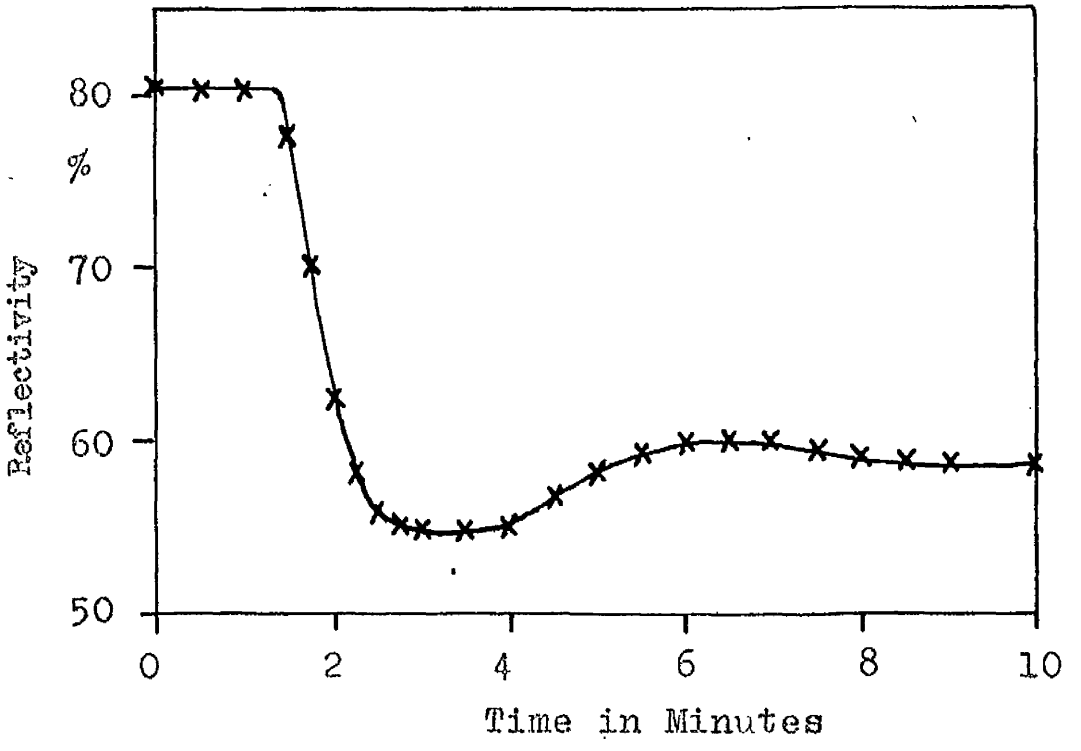

Fig. 7.16 Ageing of Gold-Indium at 139°C. Reflectivity change at gold surface for gold thickness of 2730Å.

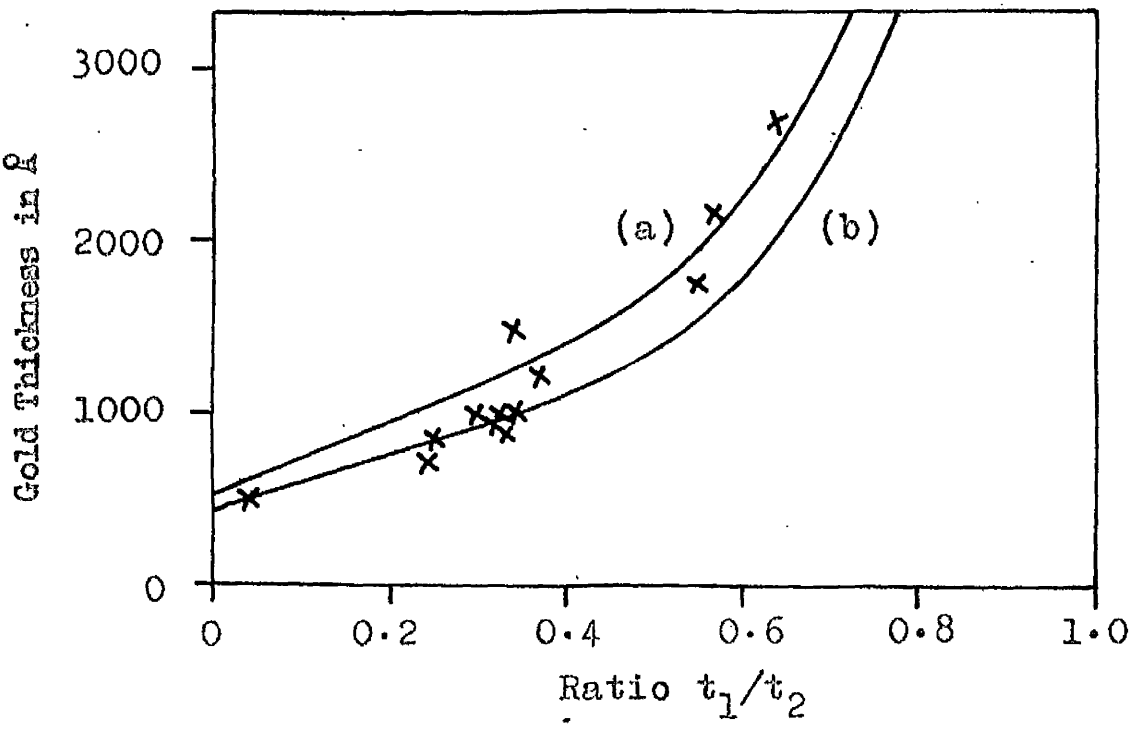

Fig. 7.17 Graph of Gold Thickness against Ratio t_1/t_2. Theoretical curves are plotted for light penetrations of (a) 500Å (b) 400Å.

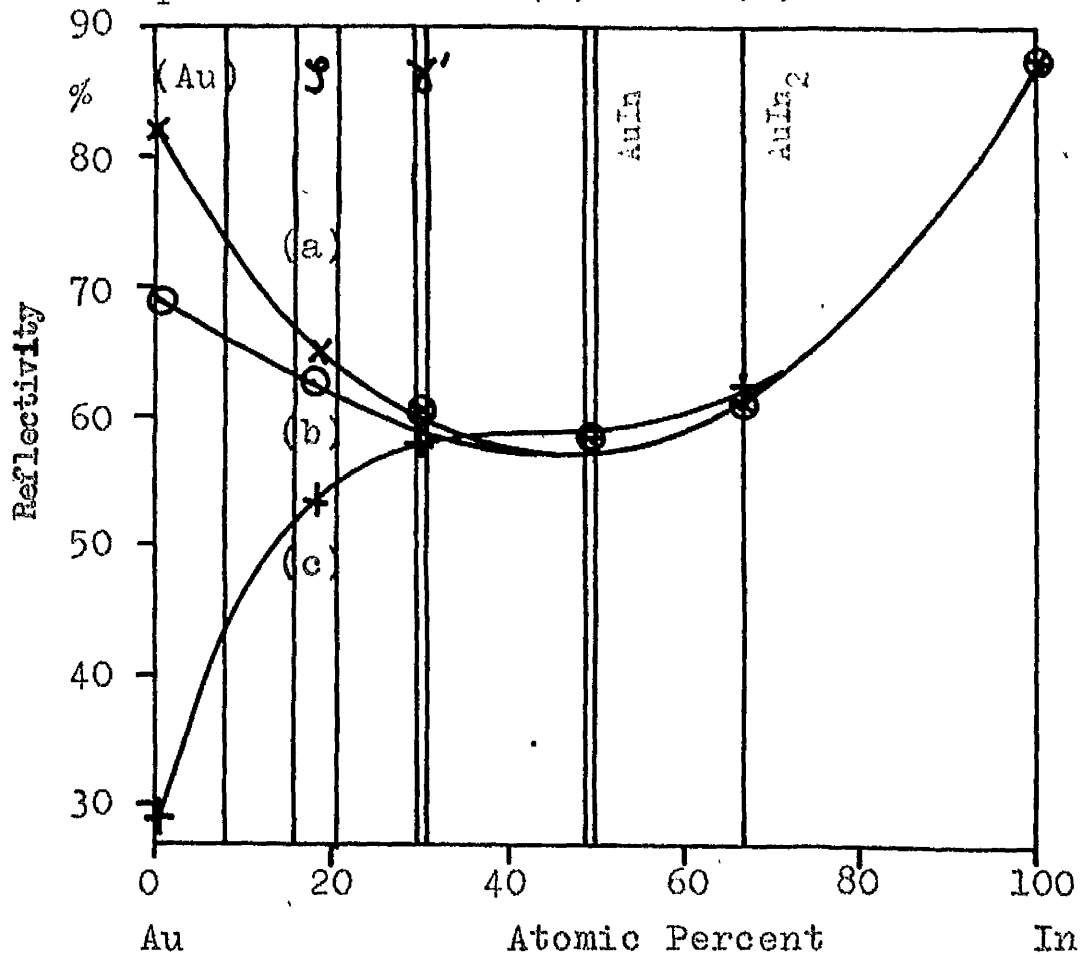

Fig. 7.18 Graph of Reflectivity against Concentration for Mercury Light of Wavelength (a) 5790Å (b) 5461Å (c) 4358Å.

theoretical curve for a light penetration of 500Å. The expected light penetration for a gold film is 400Å, and so we must accept that the phase boundary was slightly diffuse, the extra 100Å light penetration being caused by penetration of indium into the gold. The effect appeared greater for thick gold films than for thinner ones, and indeed for gold thicknesses less than 1000Å the effect appeared negligable.

At the end of the first reflectivity change the reflectivity increased again by about 5% to 60%. The effect was small but was observed in all the specimens aged. None of the intermediate phases in the gold-indium system can exist over a wide range of concentration, and, as in silver-cadmium, it seemed that the effect was most probably due to the presence of a second phase, which, following shortly behind the first phase, itself came up to the glass surface. This would mean that the second phase visible was much the wider of the two and had a higher indium concentration.

The activation energy of diffusion was found by ageing different portions of the same slides over a temperature range. For a specimen 2730Å thick, whose ageing curve at 139°C is shown in fig. 7.16, the overall time of diffusion varied from 43 days at 21°C to 3 min. at 145°C.

The shape of the ageing curve did not vary significantly with temperature, indicating that the two compounds had similar activation energies. From a plot of $\log_{10} t_{65}$ against (1/T), this activation energy was found to be 19·9 kcal/mole, and this gave the mean value of D_0' to be 0·38 cm^2/sec.

The critical thickness ratio of indium to gold was found to be 1·5. This thickness corresponded to the minimium indium thickness giving a reflectivity drop to under 60%, and did not distinguish between the compound with 55% reflectance and that with 60% reflectance. The compound with 55% reflectance was found only in small proportions, however, and indeed in the specimen shown in fig. 7.15 with 680Å gold thickness, the compound was hardly seen at all. The critical ratio therefore corresponds to the second compound formed. A ratio of indium to gold of 1·5 corresponds to an indium concentration of 36·8% by weight. This lies on the composition of the phase AuIn. The first compound observed must have had an indium concentration less than this and therefore probably corresponded to the γ' phase.

The reflectivities of a series of gold-indium alloys prepared by "flash" evaporation are shown in fig. 7.18. Indium was aggregated at the air surface, but not,

apparently, at the glass surface, which had a reflectivity of 88%. The reflectivity of the AuIn phase was 58½%, and this was in good agreement with the final reflectivity of 60% obtained in the diffusion couple. From ageing measuremnants, the reflectivity of the γ' phase was found to be 55%. The reflectivity of the γ' phase prepared by "flash" evaporation was fairly close to that of the AuIn phase, and certainly did not appear to have a lower reflectivity than it. This is not in good agreement with ageing results and is probably explained by the "flash" results only being approximately correct.

7.5 Reflectivity Changes in Silver-Indium

The wavelength of the light used for studying diffusion in this system makes little difference to the reflectivities obtained. Mercury green light was used for observations on this system.

The change in the shape of the ageing curves for different silver thicknesses overlaid with very thick indium films is shown in fig. 7.19. The curves all showed the sudden reflectivity change associated with the motion of a phase boundary, and plotting the ratio t_1/t_2 in fig. 7.20 against the silver film thickness showed that the experimental points lay fairly near the theoretical curve

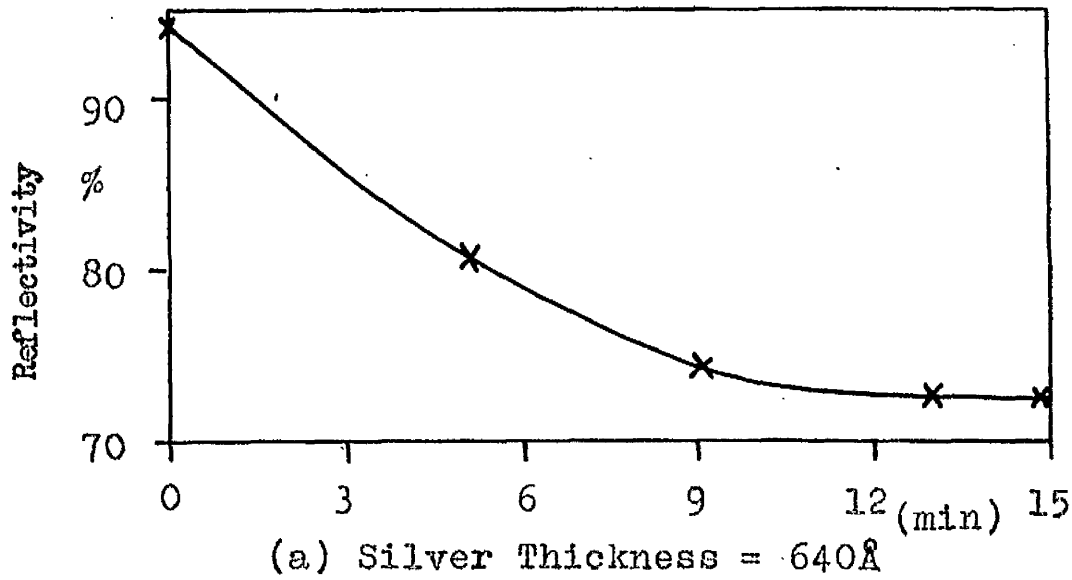

(a) Silver Thickness = 640Å

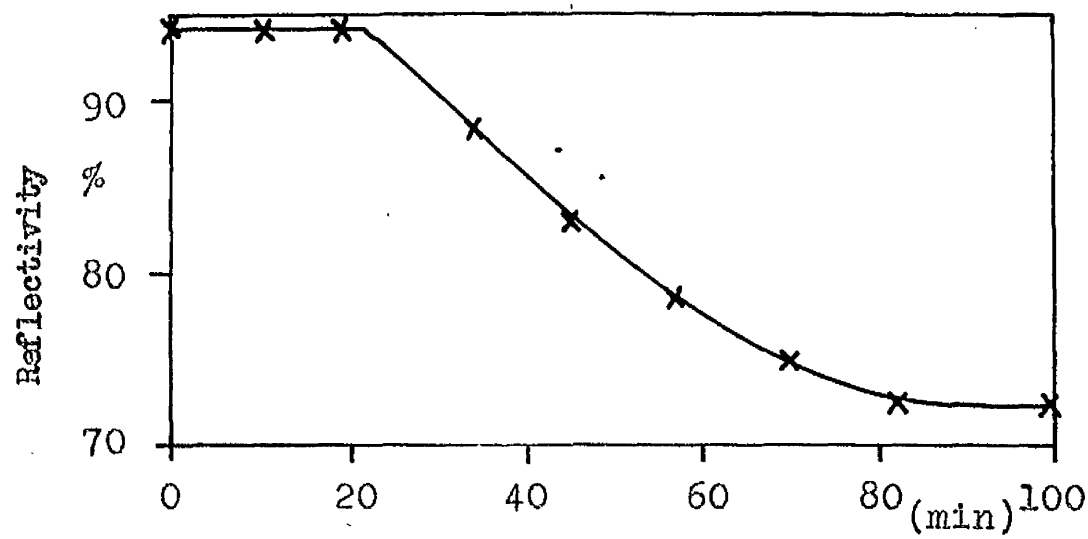

(b) Silver Thickness = 1460Å

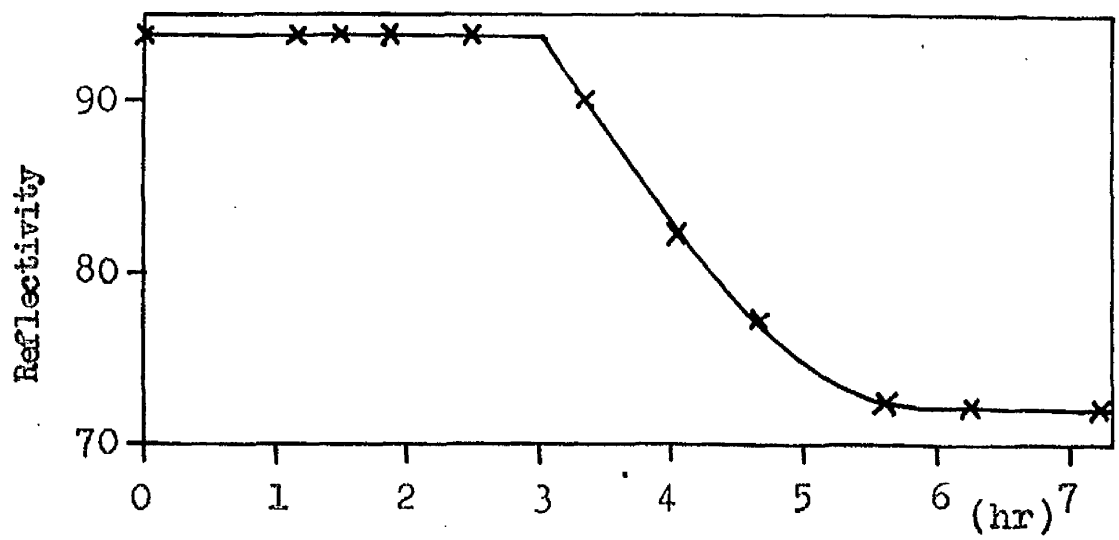

(c) Silver Thickness = 2730Å

Fig. 7.19 Ageing of Silver-Indium at 21°C. Reflectivity change at silver surface for various silver thicknesses.

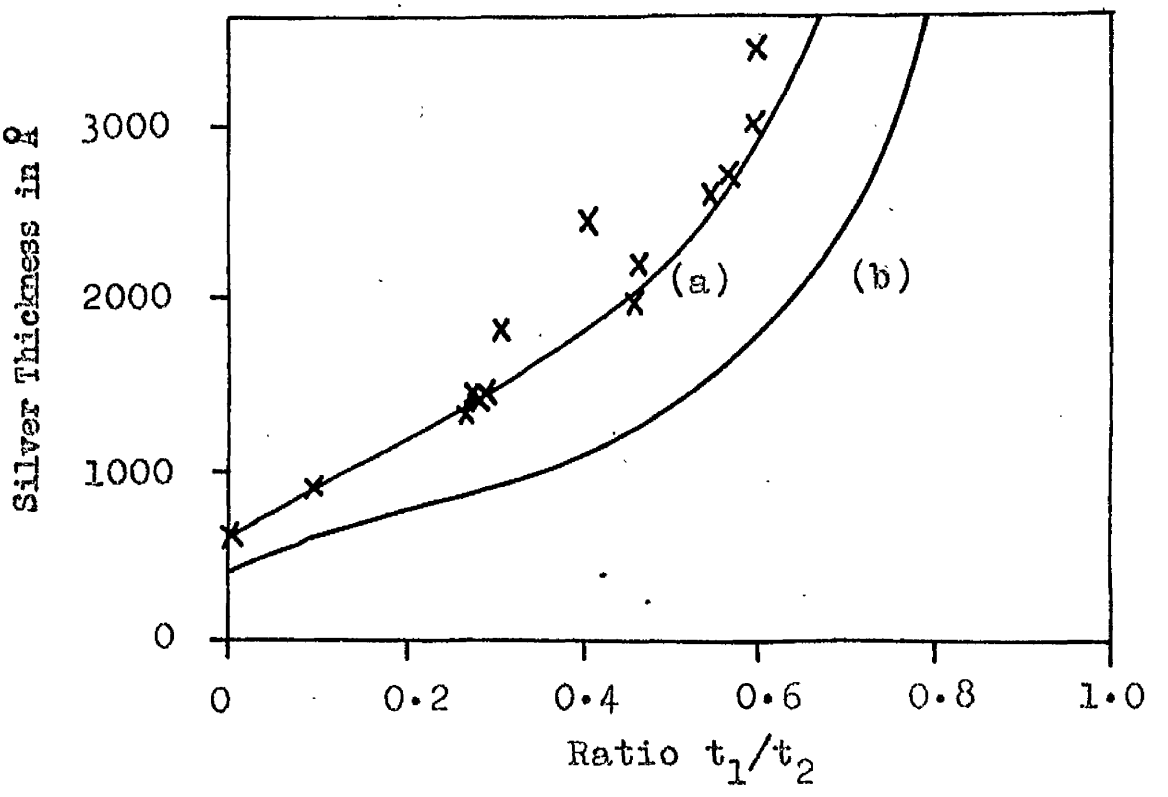

Fig. 7.20 Graph of Silver Thickness against Ratio t_1/t_2. Theoretical curves are plotted for light penetrations of (a) 650Å (b) 400Å.

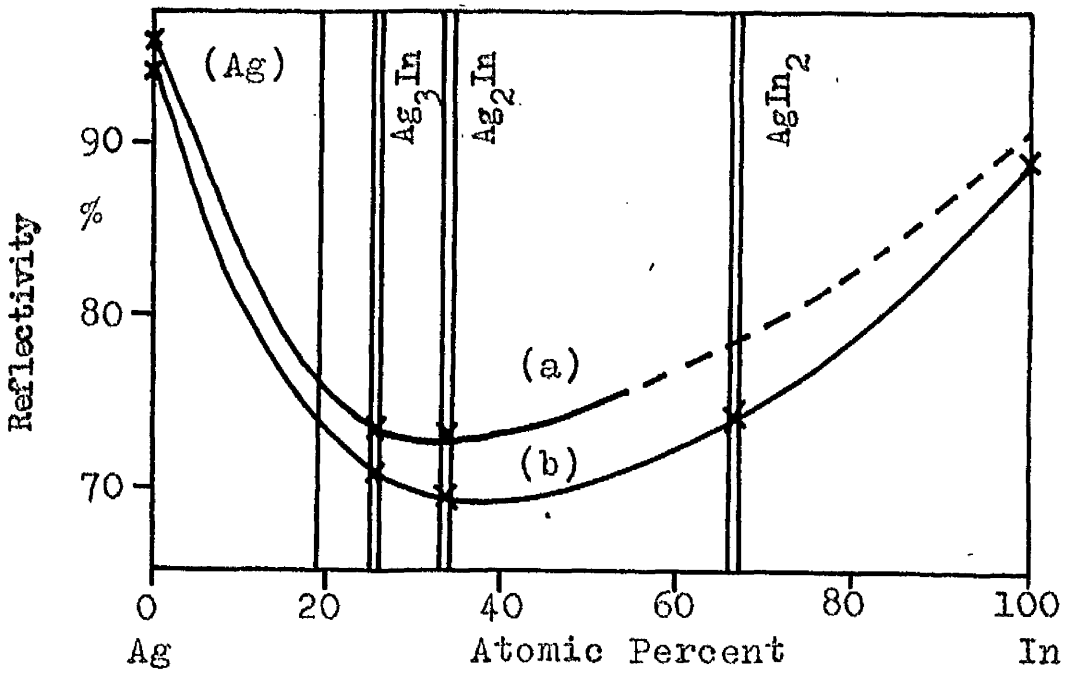

Fig. 7.21 Graph of Reflectivity against Concentration (a) at Air Surface (b) at Glass Surface.

for a light penetration of 650Å. The expected light penetration in a silver film is only 400Å, and so we can say that the phase boundary was rather diffuse, the extra 250Å light penetration being caused by penetration of indium into the silver. Values of diffusion coefficient were constant with increasing film thickness, and the mean value of D' at 21°C was found to be 5.04×10^{-14} cm^2/sec.

By ageing separate portions of the same slides over a temperature range, the activation energy of diffusion was found to be 14.1 kcal/mole. Substituting the value for D' at 21°C, D_o' was found to be 1.4×10^{-3} cm^2/sec.

The critical thickness ratio of indium to silver was found to be 3.0, corresponding to an indium concentration of 67% by weight. This lies fairly close to the composition of the compound $AgIn_2$ which we can accept as being the main phase present in the diffusion zone.

The reflectivities of a series of silver-indium alloys prepared by 'flash' evaporation are shown in fig. 7.21. The reflectivities of the three intermediate phases were approximately the same, varying from 69% for Ag_2In to 74% 74% for $AgIn_2$. The reflectivity of the compound formed by diffusion was 72½% and so we are unable to say from these results which phase was formed. Thickness ratio

measurements indicate the formation of the compound $AgIn_2$ and the "flash" evaporation results are in agreement with this conclusion.

7.6 Discussion

The reflectivity changes in the four systems described in this chapter were all characteristic of the motion of a phase boundary. This phase boundary was sharply defined in gold-cadmium, but in the other systems it was slightly diffuse and gave anomolous values for light penetration. In gold-indium the effect was small, the maximum extra penetration being approximately 100Å, and for gold thicknesses less than 100Å no interpenetration at all was observed. This comparatively slight effect can probably be explained quite simply by interpenetration into grain boundaries, dislocations or other defects in the gold, caused by the high temperature of the condensing indium atoms and by radient heating from the hot crucible. The effect will be greater in thick gold films than in thin ones because of the correspondingly greater indium film thicknesses used. No similar effect would be expected in gold-cadmium as the evaporating temperature of cadmium (264°C) is low compared with that of indium (952°C).

The light penetrations were rather greater in silver-cadmium (550Å) and silver-indium (650Å) than in

gold-cadmium and gold-indium, but still very much less than than in silver-aluminium (1100Å). It appears probable that penetration of cadmium and indium into grain boundaries, dislocations or other defects in the silver could probably account for the observed results in this case also. Silver has a more highly aggregated structure than gold (Sennett and Scott 1950), and penetration of it would be somewhat easier. The effect will be greater with indium than with cadmium because of the higher evaporation temperature of indium. Values of D' were quite consistent in these systems and no complications arise from an initial fast diffusion, as in silver-aluminium. Gold and silver have similar atomic sizes, structures and melting points, and it would be difficult to find any other reason for results with silver to be different from results with gold. The phase diagrams of gold-cadmium and silver-cadmium, and of gold-indium and silver-indium are very similar to one another. Hence it would be difficult to explain differences in light penetration by differencies in the phase diagrams.

Values for diffusion coefficient and activation energy for the four systems are shown in table 7.1. No results for bulk specimens of gold-cadmium and gold-indium are available, but values have been given for silver-cadmium and silver-indium (Jost 1952). The thin film values of activation energy are very much less than bulk values, and

TABLE 7.1

VALUES OF DIFFUSION COEFFICIENT AND ACTIVATION ENERGY IN GOLD-CADMIUM, SILVER-CADMIUM, GOLD-INDIUM AND SILVER-INDIUM

System	D' at 21°C cm^2/sec	D_o cm^2/sec	E kcal/mole
(a) Thin Film Results			
Cadmium into Gold	1.05×10^{-14}	0.83	18.6
Cadmium into Silver	2.4×10^{-15}	3.0×10^{-4}	14.9
Indium into Gold	4.8×10^{-16}	0.38	19.9
Indium into Silver	5.04×10^{-14}	1.4×10^{-3}	14.1
(b) Bulk Specimens			
Cadmium into Silver	7.8×10^{-22}	4.9×10^{-5}	22.4
Indium into Silver	4.2×10^{-23}	7.3×10^{-5}	24.4

it might be thought that this discrepancy was proof of a different mechanism of diffusion in thin films compared with bulk specimens. We have, however, shown in silver-aluminium that the faster diffusing metal determines the rate of diffusion, and a similar effect would be expected to occur in silver-indium. Silver has a higher melting point than indium, and consequently diffusion of silver into indium will be the faster direction. Hence, ~~diffusion~~ diffusion of silver into indium will be the rate determining process, and the reflectivity changes at the silver surface will be due simply to the loss of silver in the formation of the intermetallic compound. This will have a much lower activation energy than diffusion of indium into silver, in agreement with the experimental results. A value of activation energy of 14·1 kcal/mole for diffusion of silver into indium appears a very reasonable figure. For diffusion of silver into lead, a value of activation energy of 15·1 kcal/mole has been found, and a fairly similar value would be expected for diffusion of indium into silver. An explanation exactly similar to the above holds in silver-cadmium.

Buckle (1946) has studied bulk diffusion couples of silver-cadmium. He observed two phases in the diffusion zone but did not identify the actual phases. In the

present investigation, the probable presence of two phases has been shown and it has proved possible to identify these phases. From the results given by Buckle we can calculate D' at 300°C to be 9.3×10^{-10} cm^2/sec. On extrapolating the results obtained in the present investigation to 300°C, D' is found to be 5.8×10^{-10} cm^2/sec, in good agreement with Buckle's value. Buckle only gives results at 300°C, and so it is not possible to compare values for activation energy. It would appear, however, that the mechanism of diffusion in bulk couples and thin film couples of silver-cadmium is the same.

In none of the four systems described in this chapter was there any trace of the formation of a solid solution in the silver and gold before the phase boundary was observed. This is rather surprising, for the solid solubilities are fairly large, and in the case of silver-cadmium it is 42 at.%. Two possible explanations of the results can be given: either that the reflectivities of the solid solutions are little different from the pure metals, or that very little solid solution is actually formed. The first explanation seems unlikely in view of the different appearances of, say, gold and cadmium, and, indeed, in silver-cadmium, a flash evaporated alloy with 25 at.% cadmium had a reflectivity 11% less than that of pure silver. We must therefore conclude that only a very

little solid solution is formed.

It has been shown that the diffusion of, for example, silver into cadmium is the rate determining process, and that the reflectivity change at the silver surface is due to the loss of silver in the formation of intermetallic compound at the cadmium side. Very little diffusion of cadmium into silver can occur, and so very little solid solution would be formed in the silver.

CHAPTER 8

REFLECTIVITY CHANGES IN COPPER-ALUMINIUM

8.1 Introduction

Reflectivity changes in thin film couples of copper-aluminium proved very interesting, because a two stage ageing curve was obtained at the aluminum surface. Changes took place at both metal surfaces and measurements were made of diffusion in both directions. The copper was invariably deposited before the aluminium, since the copper oxidised readily in air without the protection of the aluminium film. The phase diagram for copper-aluminium is shown in fig. 8.1.

179°C was selected as the standard ageing temperature for diffusion in both directions, since this allowed most films to be aged in the hot air oven.

8.2 Reflectivity Changes at the Copper Surface

The effect of light wavelength on a typical ageing curve is shown in fig. 8.2. Mercury yellow was selected for all further measurements on this system, since the reflectivity change (25%) was greater with it than with mercury green (11%) or mercury blue (7%).

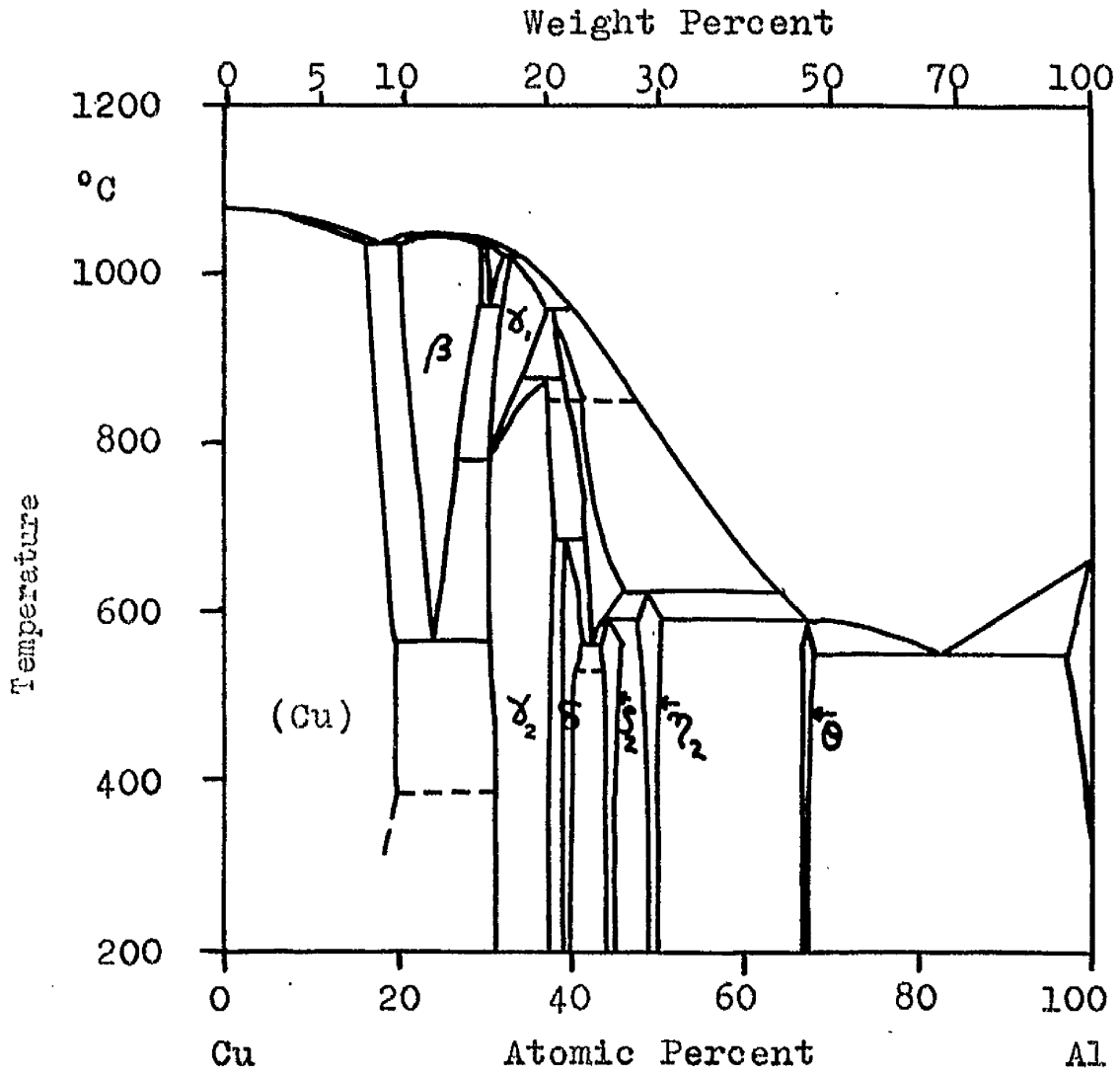

Fig. 8.1 Equilibrium Phase Diagram for Copper-Aluminium (Hansen 1958)

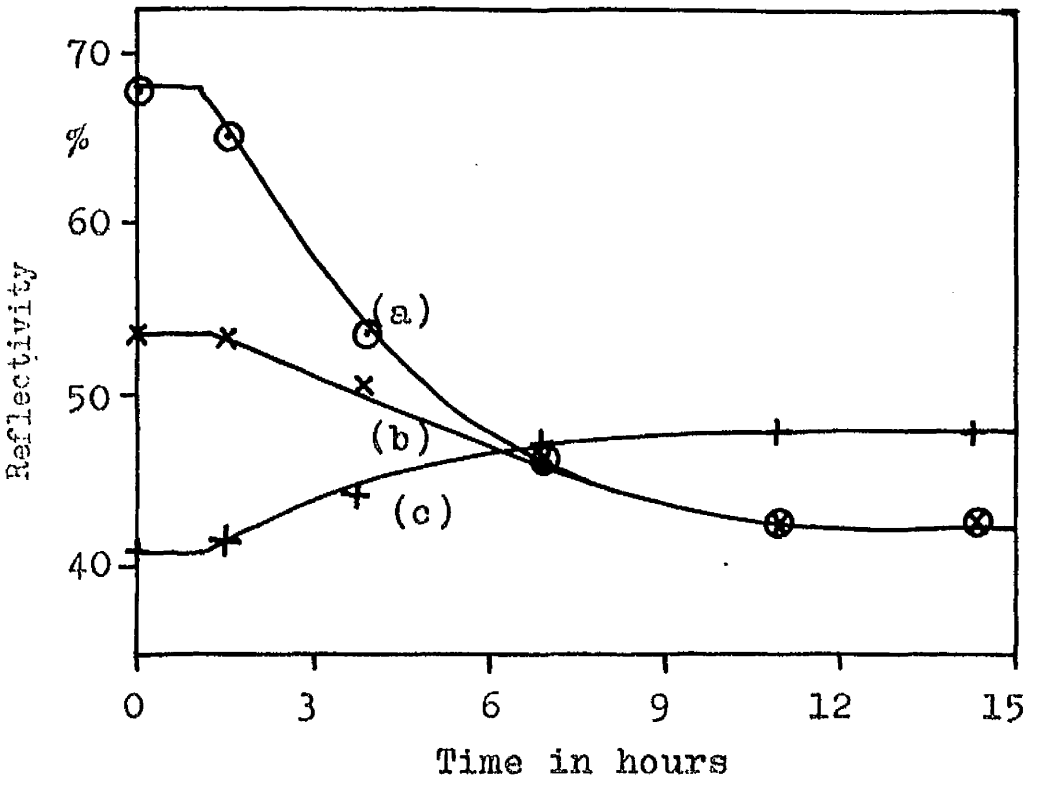

Fig. 8.2 Ageing of Copper-Aluminium Film at 179°C. Reflectivity change at copper surface for copper thickness of 770Å. (a) mercury yellow light, (b) mercury green light, (c) mercury blue light.

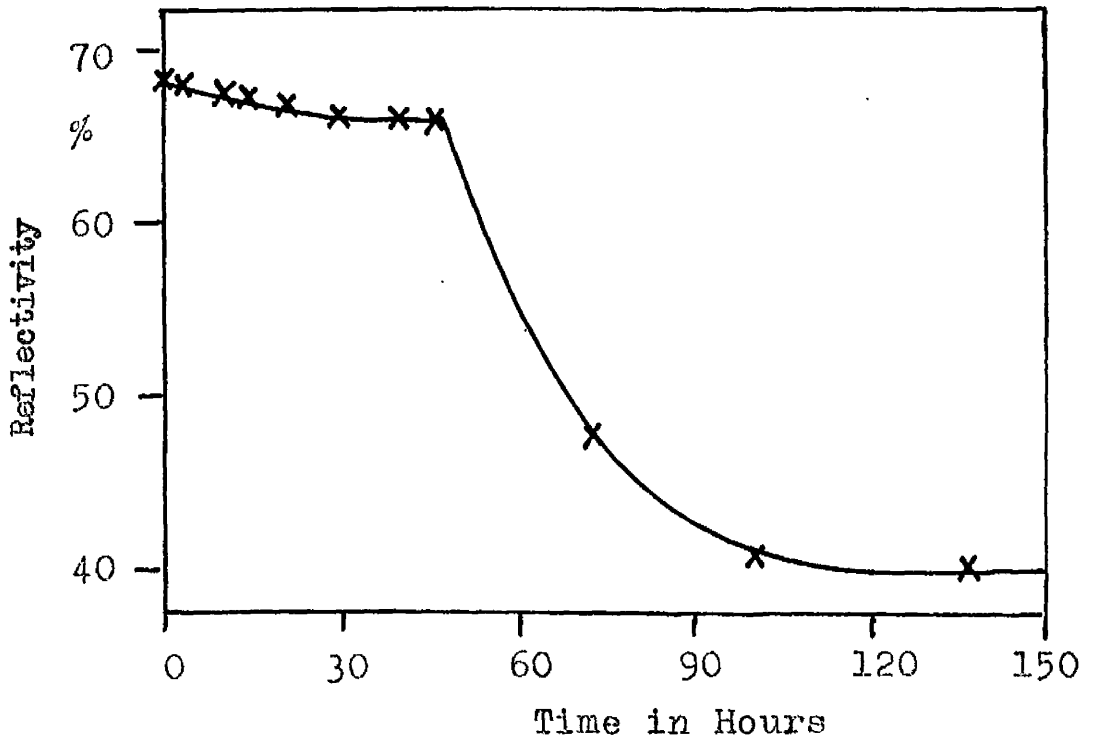

Fig. 8.3 Ageing of Copper-Aluminium Film at 179°C. Reflectivity change at copper surface for copper thickness of 1770Å.

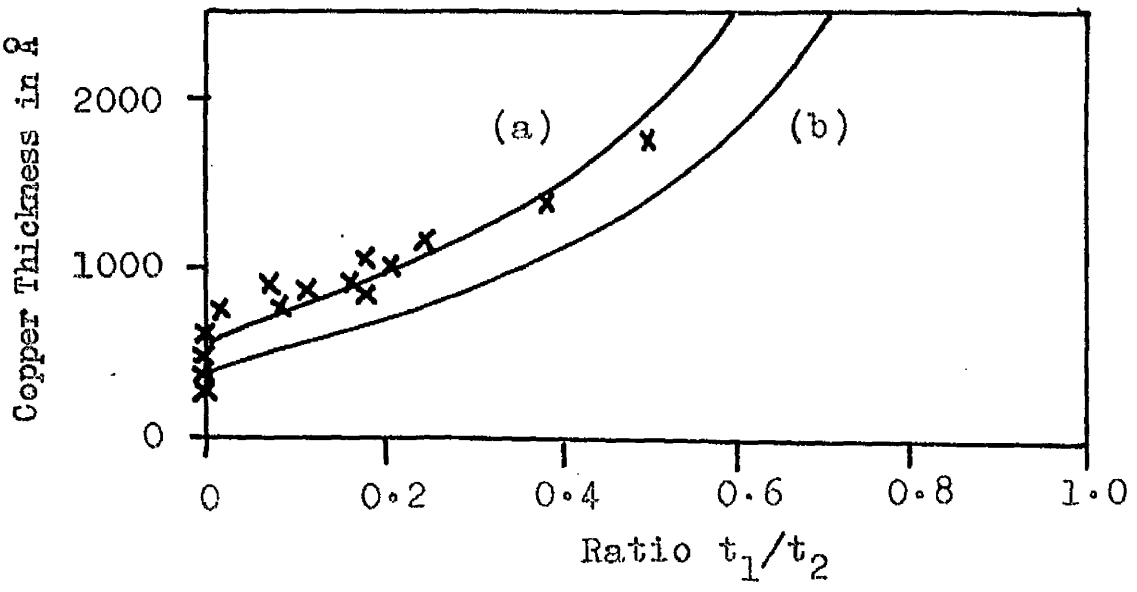

Fig. 8.4 Graph of Copper Thickness against the Ratio t_1/t_2. Theoretical curves are plotted for light penetrations of (a) 550Å (b) 400Å.

Slides were prepared with copper films of different thicknesses in the range 300Å to 1800Å, overlaid with thick films of aluminium to avoid thickness ratio difficulties. Typical ageing curves are shown in fig. 8.2 and 8.3. The curves all showed the sudden reflectivity change characteristic of a phase boundary. In fig. 8.5 the ratio t_1/t_2 has been plotted against film thickness for all the specimens prepared. The points lie close to the theoretical curve for a light penetration of 550Å. The expected light penetration for a copper film is 400Å, and we must therefore conclude that the phase boundary was slightly diffuse.

Values of diffusion coefficient were calculated from the time taken for the reflectivity to cease changing. The values were consistent, and the mean value of D' at 179°C was $1{\cdot}25 \times 10^{-15}$ cm^2/sec.

Different portions of the one slide were aged over a temperature range and the activation energy was found to be 31·9 kcal/mole. This gave D'_0 equal to 4·0 cm^2/sec.

8.3 Reflectivity Changes at the Aluminium Surface

Reflectivity changes were also studied at the aluminium surface. Slides were prepared with aluminium thicknesses varying in the range 180Å to 2730Å with very thick copper substrate films. In the very thin films

(< 300Å), thicknesses were found by measuring the reflectivity and transmission of the slides and using the results of Walkenhorst (1941) to find the film thickness. Typical ageing curves are shown in fig. 8.5 to 8.8. The curves are characteristic of the motion of two separate phase boundaries, the first with a reflectivity of 53%. We will analyse the two parts separately.

The aluminium was found to age somewhat in the initial part of curve, but this effect was small compared with subsequent reflectivity changes. The ageing was greater for thick films than for thin ones because of the longer ageing times involved, and consequently the reflectivity of the second plateau varied from 72% with an aluminium thickness of 535Å (fig. 8.6) to 68½% with an aluminium thickness of 2730Å (fig. 8.8).

The curves all showed the sudden reflectivity change associated with the motion of a phase boundary. In fig. 8.9 the ratio t_1/t_2 has been plotted against aluminium thickness for all the specimens prepared, taking t_2 as the time for the first part of the ageing curve to be completed. The points lie near the theoretical curve for a light penetration of 750Å, and we must therefore conclude that the phase boundary was diffuse, the extra 450Å light penetration being caused by the presence of copper atoms in the

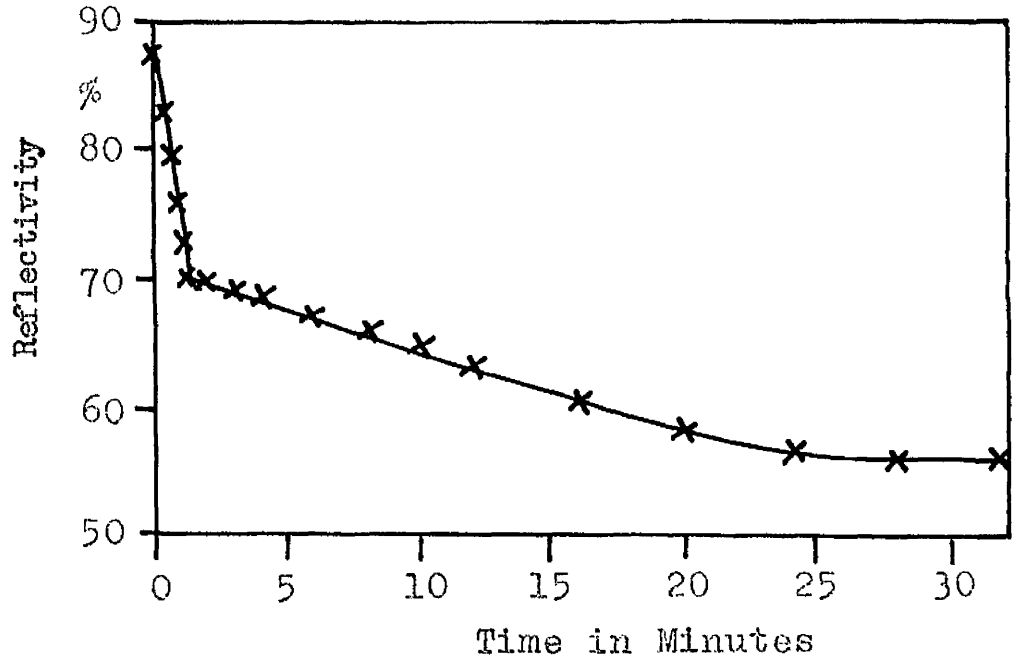

Fig. 8.5 Ageing of Copper-Aluminium Film at 179°C. Reflectivity chnnge at aluminium surface for aluminium thickness of 180Å.

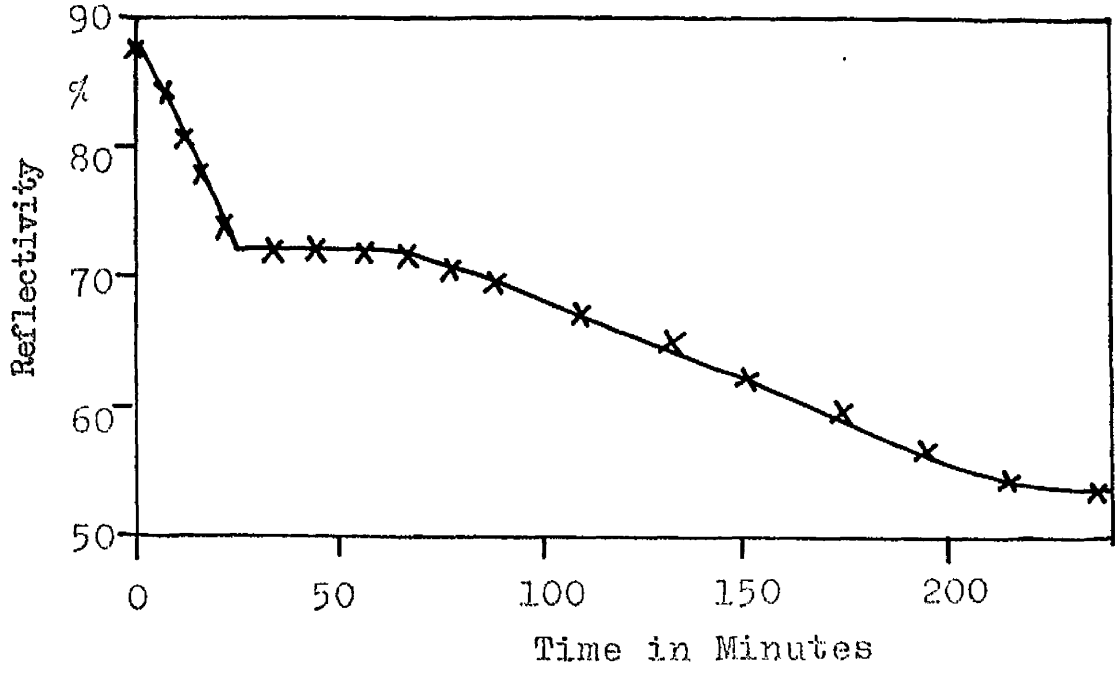

Fig. 8.6 Ageing of Copper-Aluminium Film at 179°C. Reflectivity change at aluminium surface for aluminium thickness of 535Å.

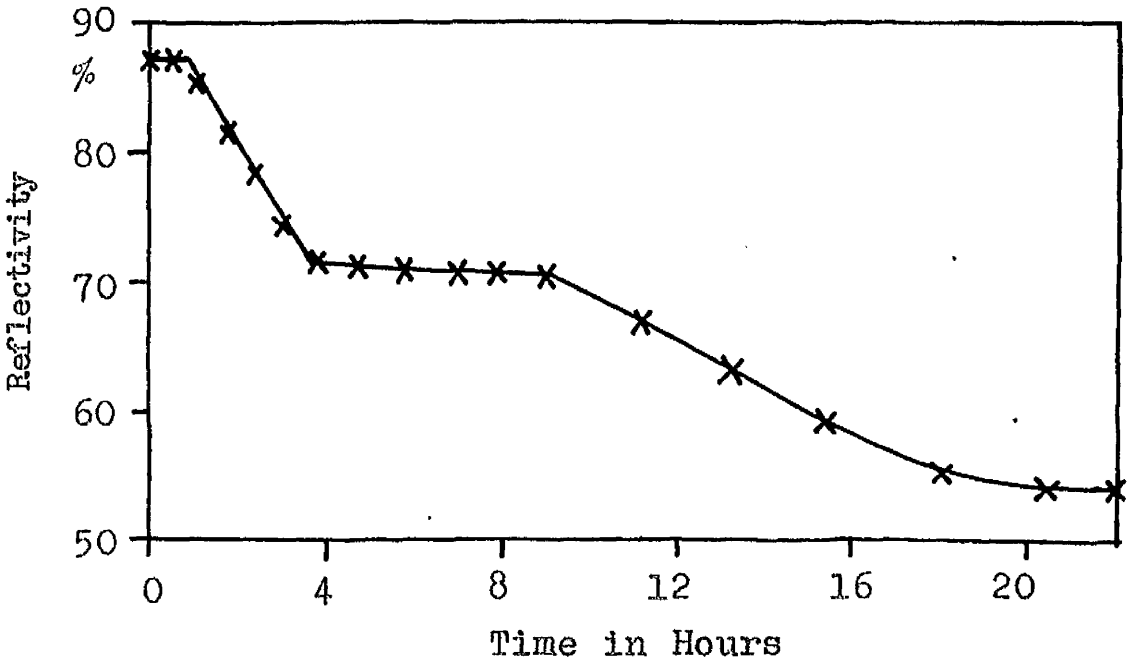

Fig. 8.7 Ageing of Copper-Aluminium Film at 179°C. Reflectivity change at aluminium surface for aluminium thickness of 1230Å

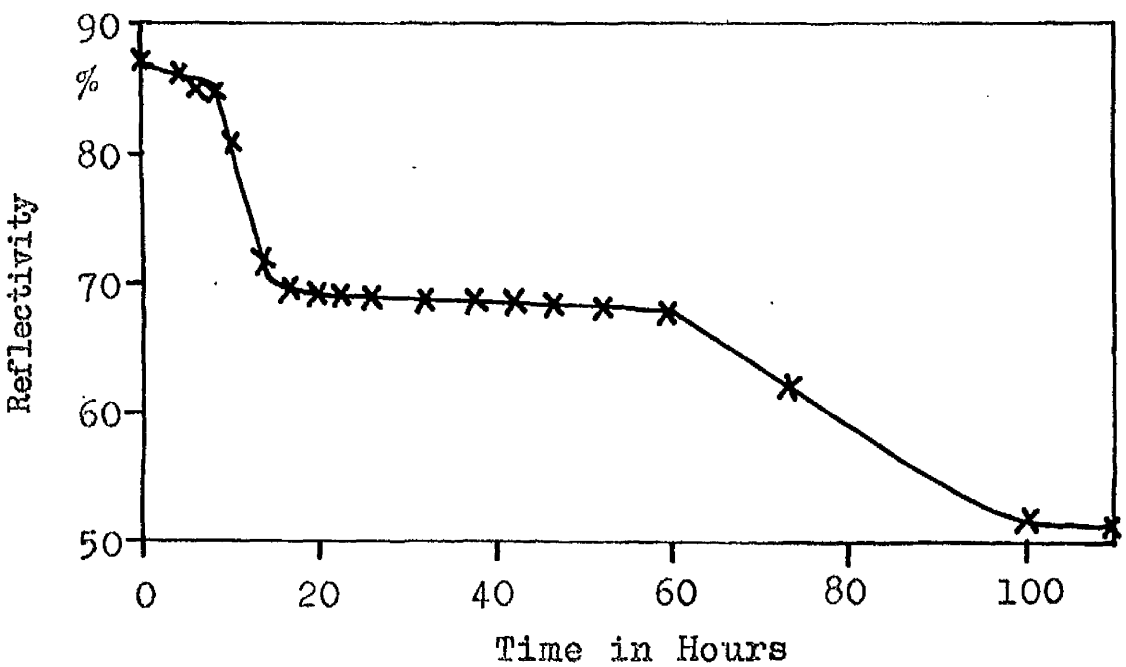

Fig. 8.8 Ageing of Copper-Aluminium Film at 179°C. Reflectivity change at aluminium surface for aluminium thickness of 2730Å.

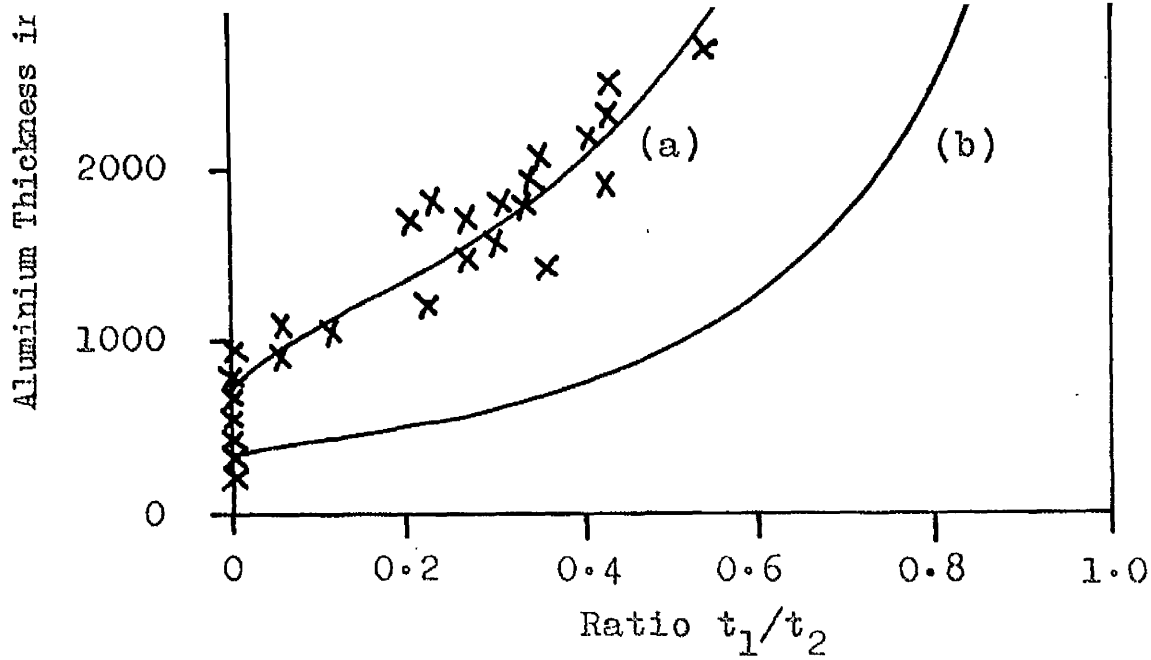

Fig. 8.9 Graph of Aluminium Thickness against the Ratio t_1/t_2 for the first part of the Ageing Curve. Theoretical curves are plotted for light penetrations of (a) 750Å (b) 300Å.

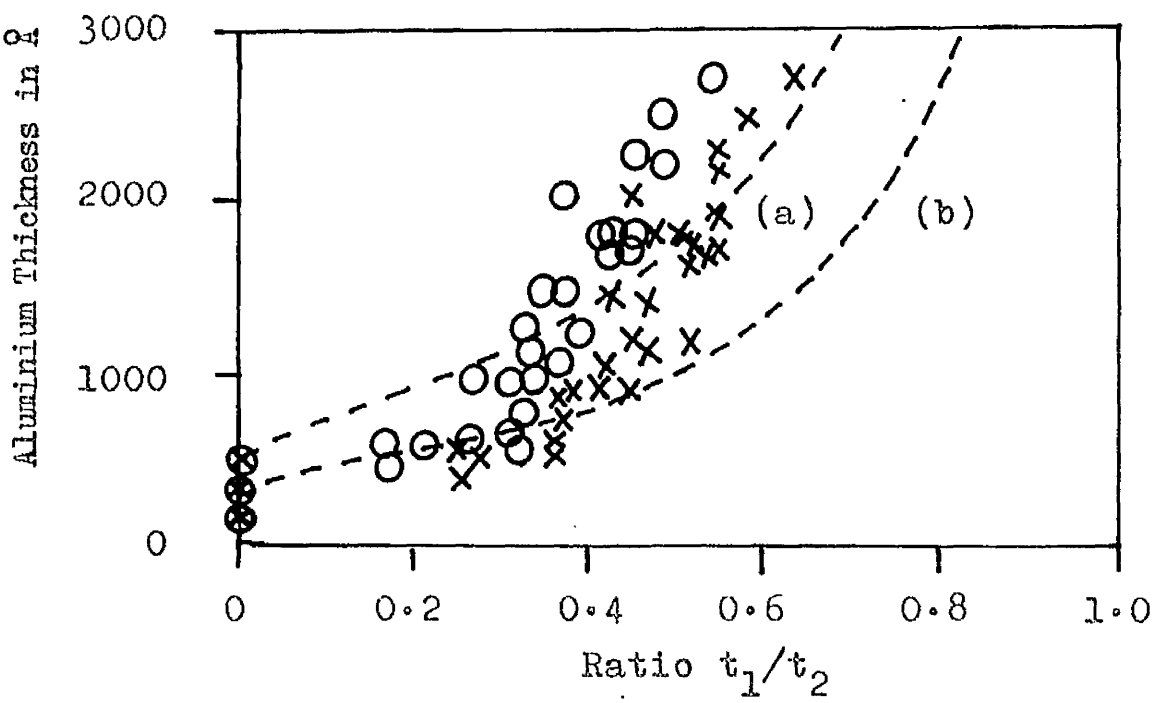

Fig. 8.10 Graph of Aluminium Thickness against the Ratio t_1/t_2 for the Second Part of the Ageing Curve. ✕ represent results calculated from the time origin, O represent results calculated from the end of the first part of the ageing curve. Curves are plotted for light penetrations of (a) 500Å (b) 300Å.

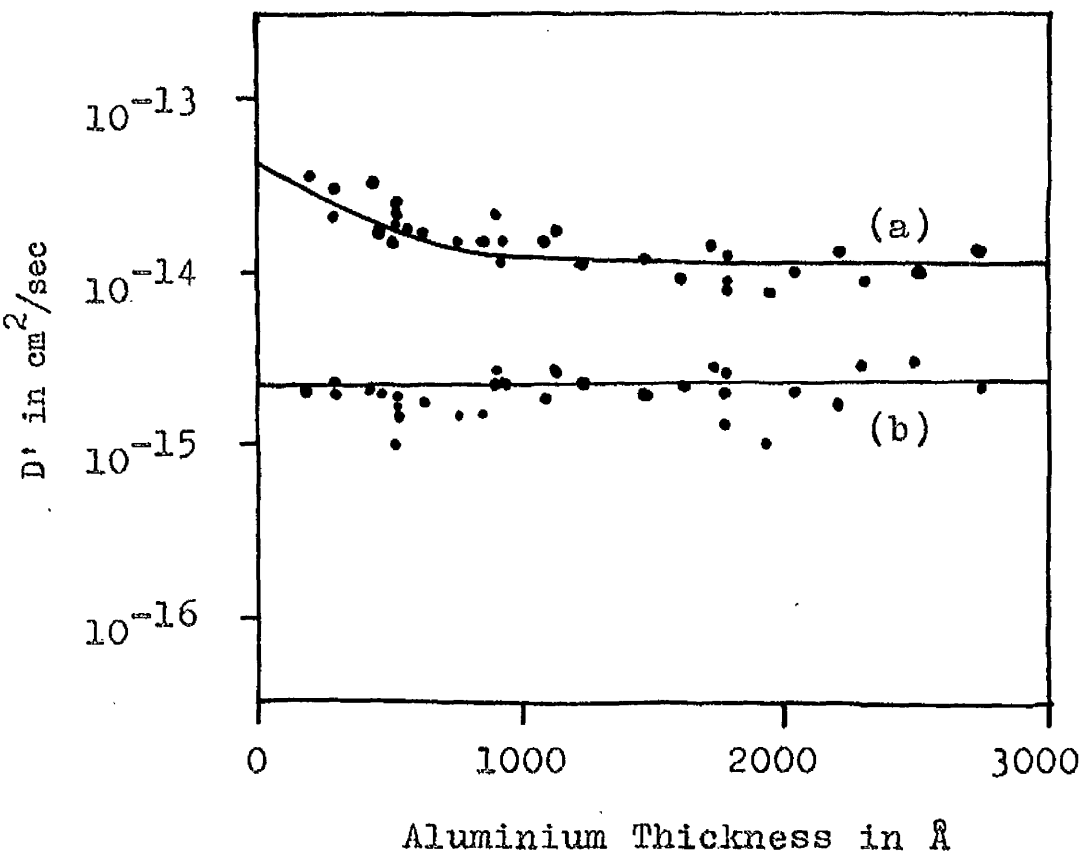

Fig. 8.11 Graph of Aluminium Thickness against Diffusion Coefficient, D', at 179°C. (a) is for the first part of the ageing curve, (b) is for the second part of the curve.

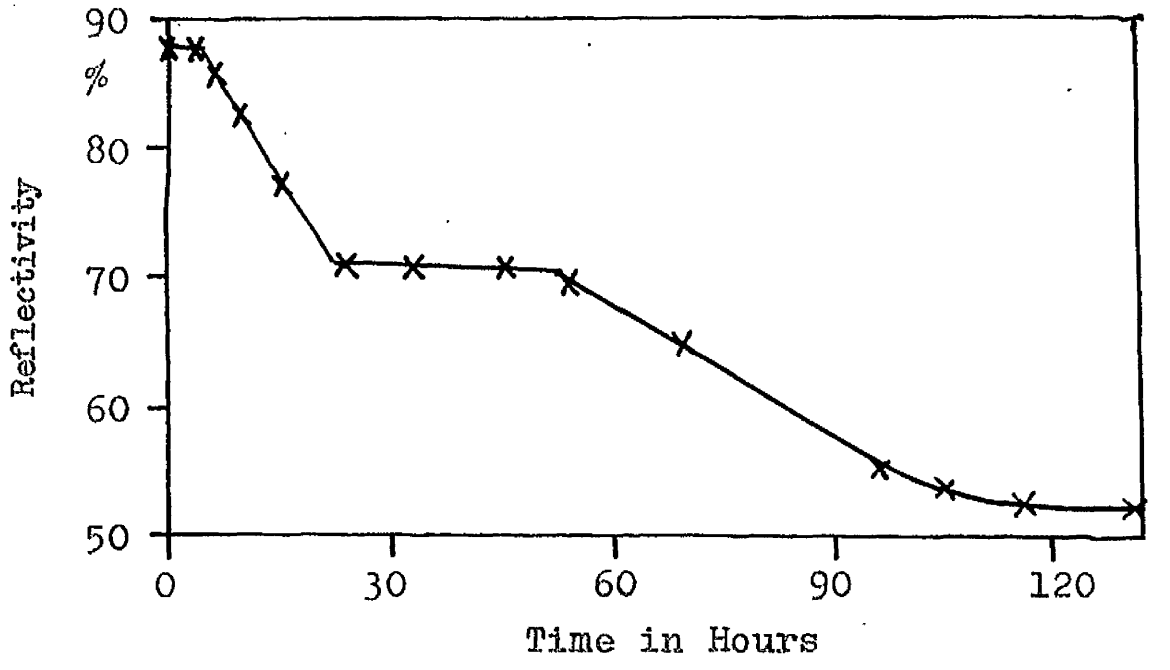

Fig. 8.12 Ageing of Copper-Aluminium Film at 158°C. Reflectivity change at aluminium surface for aluminium thickness of 1090Å.

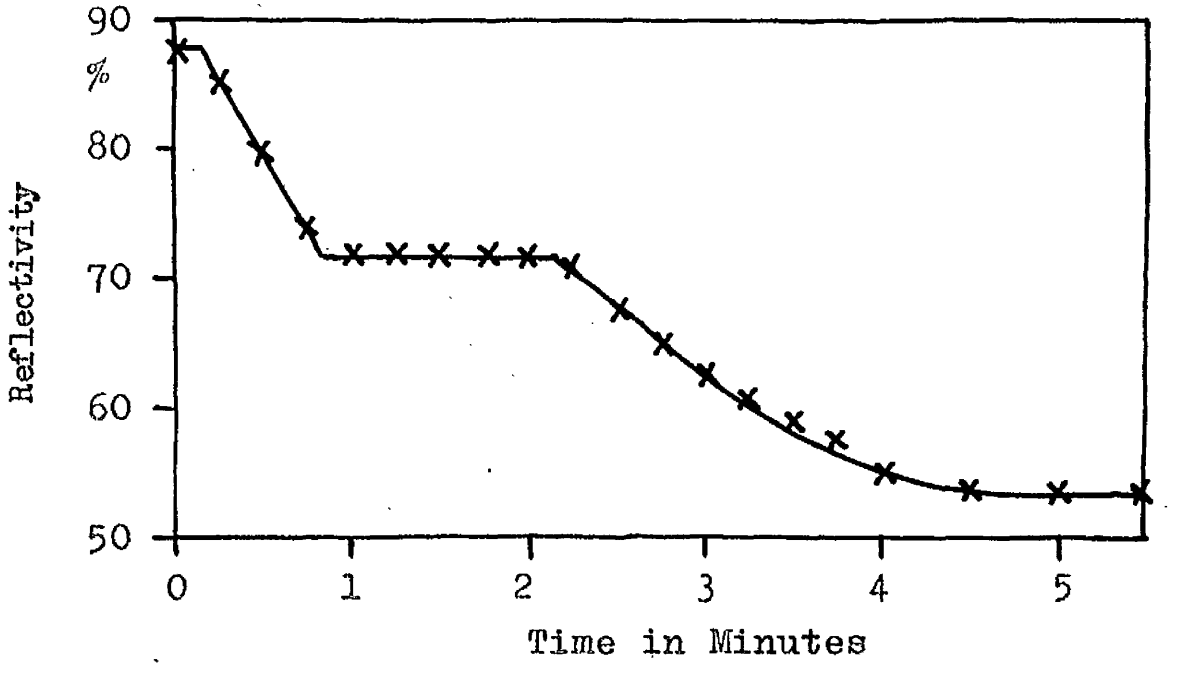

Fig. 8.13 Ageing of Copper-Aluminium Film at 266°C. Reflectivity change at aluminium surface for aluminium thickness of 1090Å.

aluminium lattice. This penetration must have taken place either during evaporation or in the very first stages of ageing.

Values of D' at 179°C for the first part of the ageing curve were calculated from the time taken for the reflectivity to stop changing (fig. 8.11). D' was constant at $1{\cdot}1 \times 10^{-14}$ cm^2/sec above a thickness of 700Å, but below this figure, D' increased steadily with decreasing film thickness, till with an aluminium thickness of only 180Å, D' was three times higher than its steady value.

In the second part of the ageing curve the reflectivity fell to 53%. This reflectivity value was rather variable and tended to decrease with increasing aluminium thickness because of ageing of the aluminium. In fig. 8.10 the ratio t_1/t_2 has been plotted against film thickness, the origin being taken either as the time origin or the end of the first part of the ageing curve. Neither of the two sets of experimental points lies on a curve for a fixed value of light penetration, and the penetration appears to increase from 300Å to 600Å with increasing aluminium thickness. This is not surprising, as the stage at which the phase starts to grow is not known, and may vary with thickness. None of the experimental points lie far away from the expected value

which might reasonably be taken to be 400Å, indicating that as far as this phase is concerned, any initial penetration has little effect.

Values of D' at 179°C were calculated for this part of the ageing curve from the time taken for the reflectivity to cease varying, calculating from the time origin. D' was found to be constant with increasing film thickness (fig. 8.11), and the mean value was 2.35×10^{-15} cm^2/sec. D' will be little different if calculated from the end of the first stage of diffusion, since the major part of the total ageing time (approx. 85%) is for the second stage of diffusion. This would make D' no more than 12% greater than the calculated value.

Different portions of the same slides were aged over a temperature range from 124°C to 266°C to find the activation energy. Typical results are shown in fig. 8.12 and 8.13 for an aluminium thickness of 1090Å. The relative positions along the time axis of the two parts of the ageing curve did not appear to vary at all. Hence the activation energy associated with the formation of the first compound was the same as that associated with the formation of the second compound. From a graph of $\log_{10} t_{60}$ against (1/T), this activation energy was found to be

31·5 kcal/mole. Values of D_o' were calculated from the diffusion coefficients (D') at 179°C. For the first part of the ageing curve D_o' was found to be 22 cm^2/sec, and for the second part 4·7 cm^2/sec.

8.4 The Reflectivity of Copper-Aluminium Alloys

The reflectivities of a series of evaporated copper-aluminium alloy films are plotted in fig. 8.14 as a function of the alloy concentration. The results obtained by Holland (1958) using a similar technique are also plotted on the same diagram. The agreement between the two sets of results is in general quite satisfactory.

Alloys of copper containing up to 20% aluminium in solid solution had a definite yellow tint, in agreement with Holland's observations. This yellow colour has never been observed in ageing observations at the copper surface, and indicates that only a very thin layer of this solid solution was formed. This is in agreement with observations on the systems given in chapter 7, in none of which solid solutions were observed.

Two compounds have been observed by ageing at the aluminium surface, the first with a reflectivity of 72% and the second with a reflectivity of 53%. There can be no no doubt that the first compound formed is the θ phase

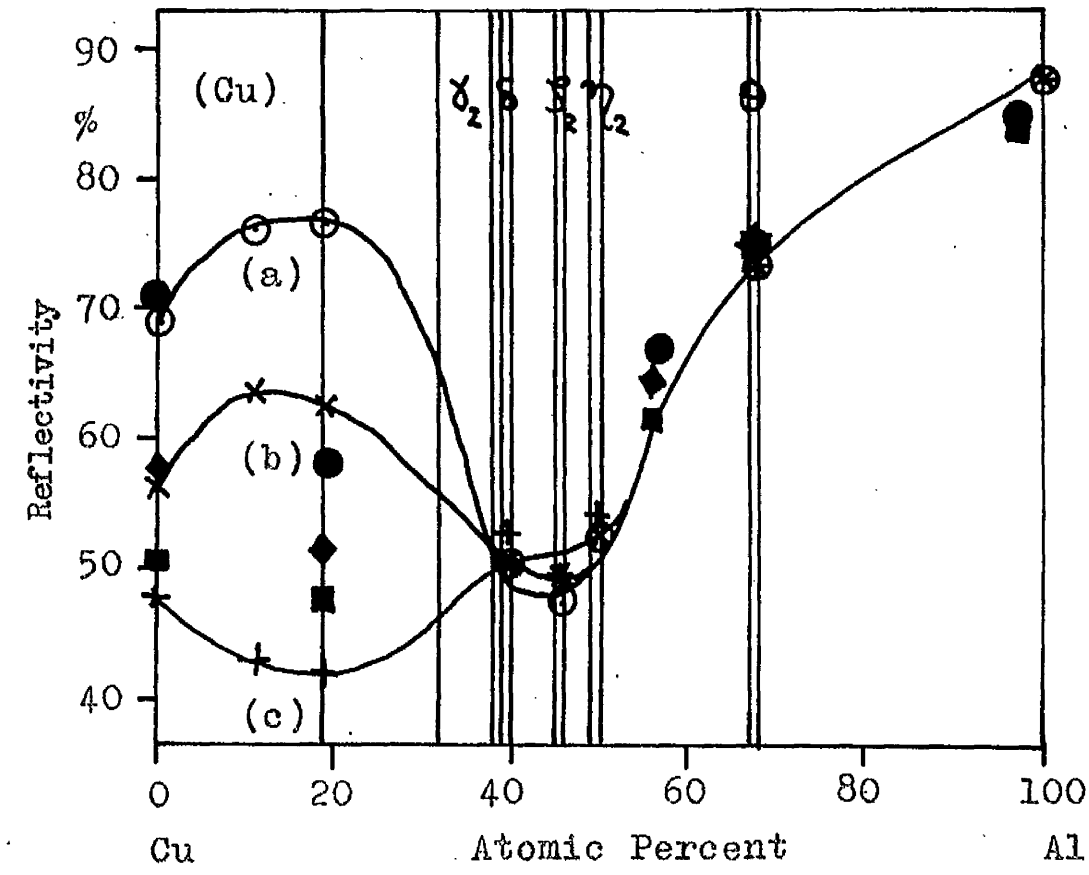

(a) Air Surface

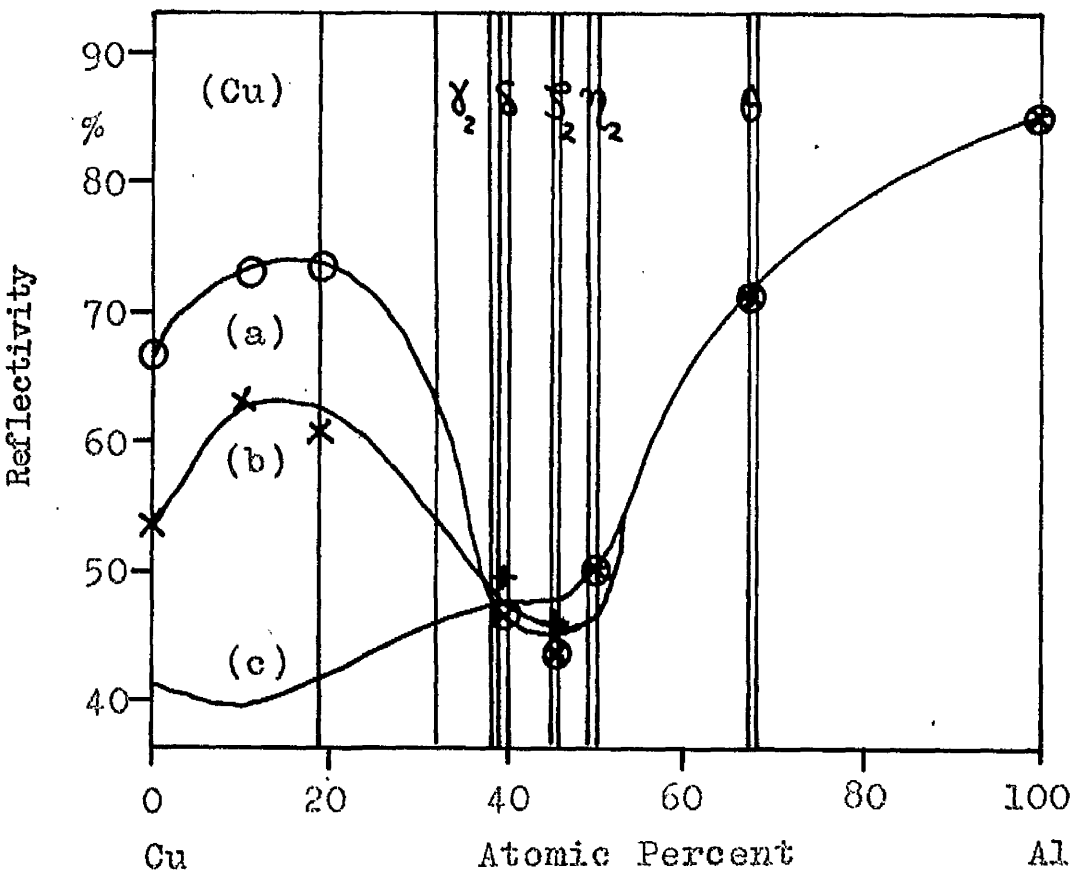

(b) Glass Surface

Fig. 8.14 Graph of Reflectivity against Concentration for Mercury Light of Wavelength (a) 5790Å (b) 5461Å (c) 4358Å. ● , ◆, and ■ represent the results of Holland (1958) for the same wavelengths.

($CuAl_2$), as the reflectivity of 74% found for an evaporated alloy film is in good agreement with 72%. There is rather more uncertainty about the second compound formed, and a reflectivity of 53% is in good agreement with the η_2 phase (54½%), the γ_2 phase (48½%) and the δ phase (50%), and the compound formed may be any one of these three.

The reflectivity of the compound formed by diffusion at the copper surface was 43%. This was presumably the same compound as was formed in the second stage of ageing at the aluminium surface. The difference of 10% between the two values of reflectivity can probably be explained by the glass surface which reduces the reflectivity readings. It is again difficult to say whether the phase formed is the δ phase (47%), the γ_2 phase (45%) or the η_2 phase (50½%), as they all have reflectivities which are in moderate agreement with the observed values.

8.5 Effect of Thickness Ratio

Several slides were prepared with a single layer of copper and four separate aluminium films of different thicknesses. The slides were aged at 179°C and reflectivity measurements were made at the copper surface (fig. 8.15). From the seven slides prepared the critical

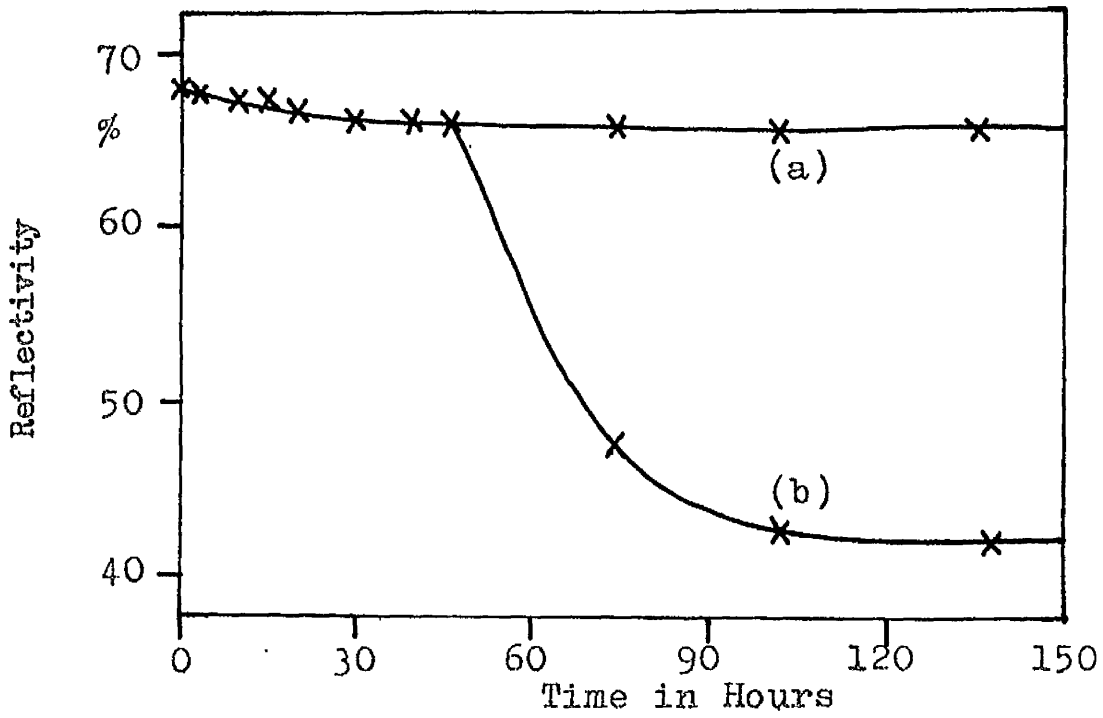

Fig. 8.15 Ageing of Copper Surface at 179°C for Copper Thickness of 1770Å. (a) aluminium thickness = 930Å (Al:Cu = 0·53:1), (b) aluminium thickness = 1800Å, 3100Å, and 5200Å (Al:Cu = 1·0, 1·8, and 2·9:1)

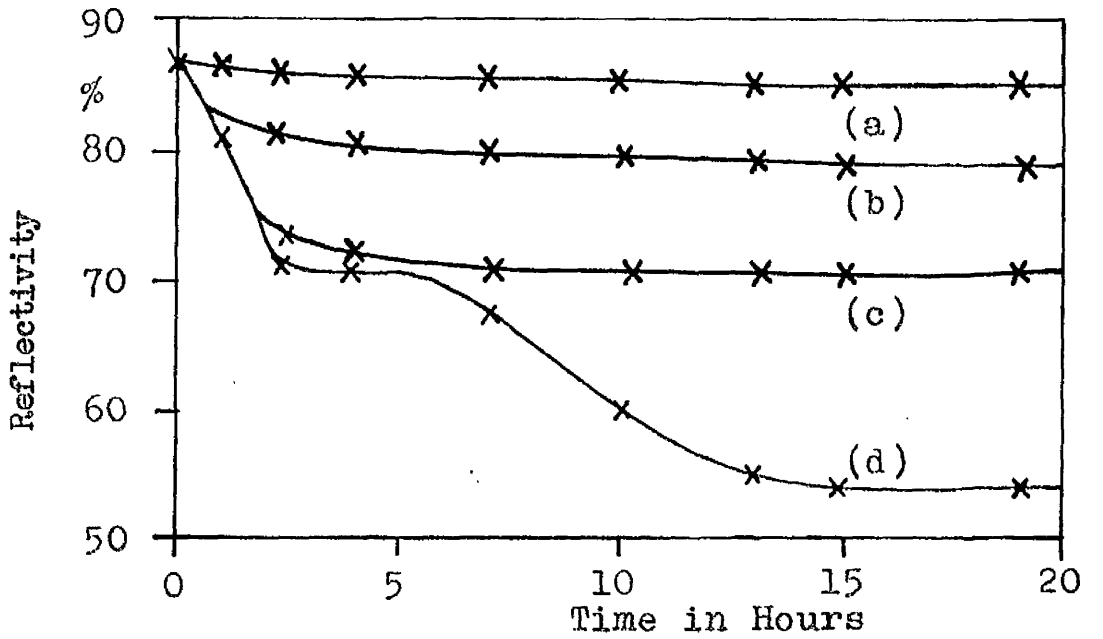

Fig. 8.16 Ageing of Aluminium Surface at 179°C for Aluminium Thickness of 1120Å.
(a) copper thickness = 200Å (Al:Cu = 5·6:1)
(b) copper thickness = 360Å (Al:Cu = 3·1:1)
(c) copper thickness = 710Å (Al:Cu = 1·6:1)
(d) copper thickness =1150Å (Al:Cu = 1·0:1)

critical thickness ratio of aluminium to copper was found to be 0·9, corresponding to an aluminium concentration of 22% by weight. Reference to fig. 8.1 shows that this is close to the compositions of the δ and γ_2 phases, indicating that one of these is probably the phase formed.

Reflectivity changes at the aluminium surface were studied with slides having a single aluminium layer and four separate thicknesses of copper substrate. A typical ageing curve at 179°C is shown in fig. 8.16. In this case two critical ratios require to be found, corresponding to the first and second parts of the ageing curve.

In fig. 8.16 it can be seen that for the first part of the ageing curve, the critical thickness ratio of aluminium to copper lies between 1·6 and 3·1. From the twelve slides prepared this was narrowed to a ratio of aluminium to copper of 2·6. We have shown in 8·4 that the first part of the ageing curve corresponds to formation of $CuAl_2$. The critical thickness ratio if this phase were formed alone throughout the diffusion couple would be 2·86. Hence we must conclude that the diffusion zone consists mainly of $CuAl_2$ with only a small amount of the copper-rich phase present.

For the second part of the ageing curve it can be seen in fig. 8.16 that the critical thickness ratio of

aluminium to copper lies between 0.98 and 1.6. From the twelve slides prepared the accurate value of the critical thickness ratio was found to be 1.2. This corresponds to an aluminium concentration of 26% by weight, and reference to fig. 8.1 shows that this is close to the compositions of the η_2 and ζ_2 phases. The phase formed at the copper surface has been found to be either δ or ζ_2. If the same phase is being formed at both metal surfaces, then this is most probably the ζ_2 phase.

Values of critical thickness ratio have been observed at 179°C. The values for activation energy in the two directions were almost equal (31.5 kcal/mole and 31.9 kcal/mole), and so the critical ratios will have the same values at all temperatures.

8.6 Discussion

Measurements of critical thickness ratio and measurements of the alloys formed indicate the presence of at least two phases in the diffusion zone (fig. 8.17). In the first stages of ageing the θ phase is much wider than the ζ_2 phase. Nevertheless the ζ_2 phase is always present in the diffusion zone (fig. 8.17(b)) even at the beginning of diffusion and it is this phase that is always seen at the copper surface. The ageing curve at the copper surface appears to be the same whether or not the θ phase has

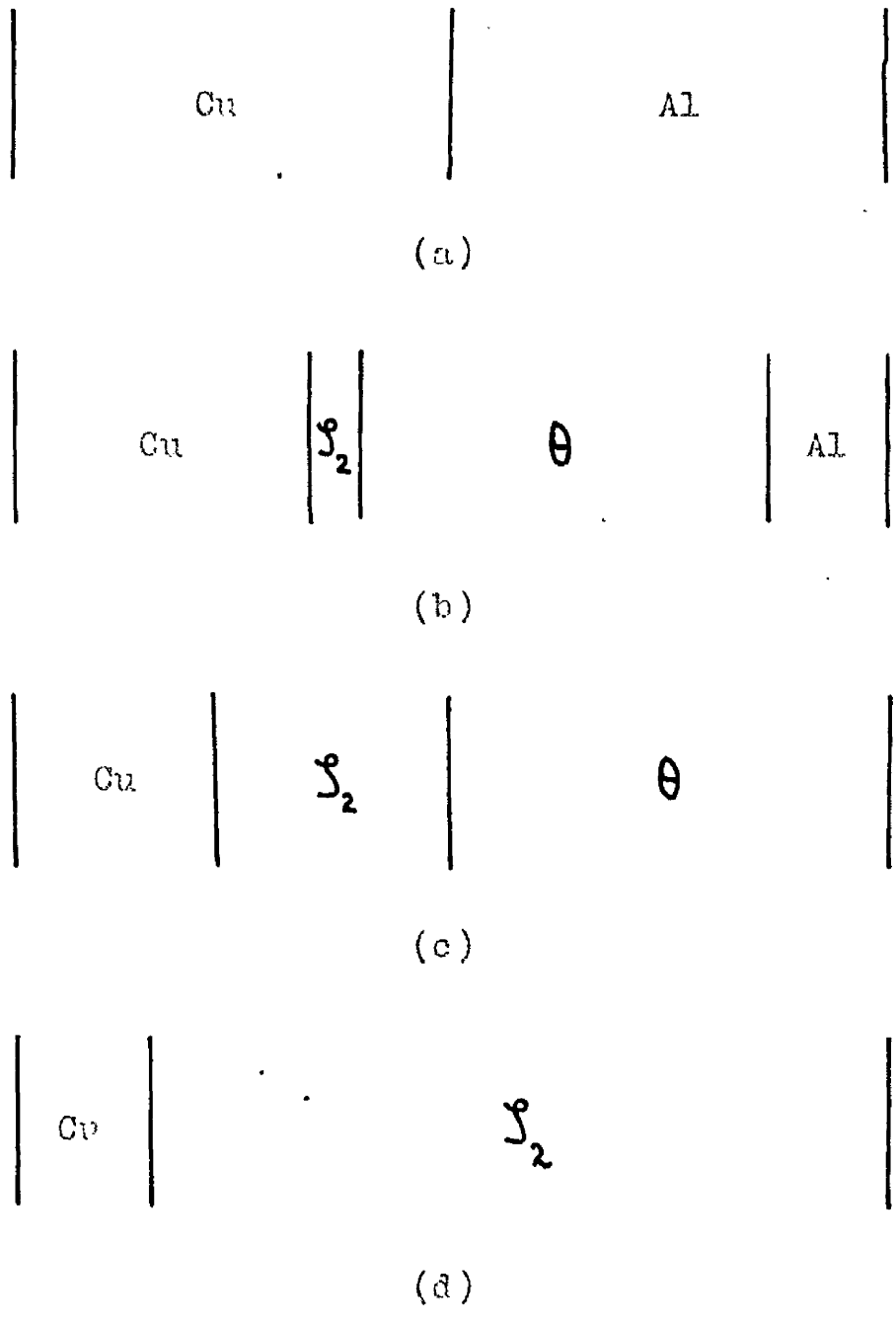

Fig. 8.17 Phases Observed in a Thin Film Diffusion Couple of Copper-Aluminium for Increasing Ageing Periods.

reached the aluminium surface. This indicates that the copper atoms are being used up at the same rate whether or not the θ phase is still growing. Hence in the first part of the ageing curve most of the copper atoms react to form the θ phase and only a few form the γ_2 phase. In the second part of the ageing curve all the copper atoms react with the θ phase to form γ_2 (fig. 8.17(c)), and so at this stage the γ_2 phase will appear to grow more quickly than in the first part of ageing.

D' at 179°C for diffusion into the copper has been found to be 1.25×10^{-15} cm^2/sec. In the first part of the ageing curve at the aluminium surface D' has been found to be equal to 1.1×10^{-14} cm^2/sec. Hence the penetration of the diffusion layer into the aluminium is 2.97 times that into the copper. This corresponds to a ratio of 2.6 found from observations of critical thickness ratio, the difference being due probably to errors in the determination of D'. This again indicates that in an infinite diffusion couple the θ phase would grow much faster than the γ_2 phase.

In the second part of the aluminium ageing curve D' at 179°C was found to be 2.35×10^{-15} cm^2/sec. Hence the penetration of the diffusion layer into the θ phase is 1.4 times the penetration into the copper. The

density of the θ phase is given as 4·34 gm/cc (Bradley and Jones 1934) and from this we can work out the concentration of the phase formed to be 23·4% of aluminium by weight. The γ_2 phase which has been postulated from thickness ratio measurements has an aluminium concentration of 25% by weight, in good agreement with the value given above.

A large value for apparent light penetration has been found for the first part of the ageing curve at the aluminium surface, far greater than can be explained by actual light penetration. The value of D' was also found to increase with decreasing film thickness, till with a thickness of 180Å, D' was three times higher than the steady value.

These observations are very similar to those found in silver-aluminium, and it appears that a similar explanation holds in both cases. As in silver-aluminium, aluminium can take up copper in solid solution at high temperatures, and it seems quite possible that aluminium can accept a considerable amount of copper in metastable solid solution at low temperatures. We must consider that the copper diffuses into the aluminium either during evaporation or during the first stages of annealing or both. This would give rise to a region of supersaturated solid

solution of copper in the aluminium. Precipitation of the the aluminium rich compound would then take place - the θ phase - and reflectivity changes would be observed. In the initial stages the θ phase would be precipitated readily, and so D' would be higher as observed experimentally.

As precipitation proceeds the effect of the initial fast diffusion will diminish, and the phase edge will tend to follow the motion of a normal phase boundary. Because of the initial fast diffusion, however, the phase boundary will be rather diffuse, and this will give an anomolous light penetration for all film thicknesses. The value of D' will tend to a constant value for thick films, and beyond a certain thickness (700Å) will show no change.

Only a slight anomolous effect was observed with the second phase formed (ζ_2), presumably since this phase grew much more slowly than the θ phase, and precipitation of the θ phase would remove the effect of the metastable solid solution. The light penetration at the copper surface was 550Å, slightly greater than the theoretical value of 400Å. This discrepancy may have been due to the formation of a metastable solid solution, or it may simply have been caused by penetration of the condensing aluminium into imperfections in the copper.

In discussing the observations on diffusion we have considered that copper atoms diffusing into the aluminium are responsible for the observed results. Buckle and Blin (1950) and da Silva and Mehl (1950) have investigated the Kirkendall effect in Cu - Cu + 12% Al diffusion couples. They found that inert markers moved towards the aluminium rich side, indicating that the aluminium atoms were more mobile than the copper atoms. A similar result might be expected in a copper-aluminium diffusion couple but no results are available for this.

It is not possible to explain the present results on the basis of movement of the aluminium atoms for the following reasons :

(a) Only one reflectivity change takes place at the copper surface and this suggests that there is no tendency for the γ_2 phase to transform into the θ phase even when excess aluminium is available.

(b) The yellow colour of the solid solution of aluminium in copper has never been observed - it should have been if aluminium diffused into the copper.

(c) An aluminium rich phase (the θ phase) has been observed to grow much faster than a copper rich phase (the γ_2 phase). If aluminium diffused into copper the matrix would be copper rich, and we would expect the copper rich phase to grow faster.

(d) Apparent initial penetration is greater for the θ phase than for the γ_2 phase, consistent with the penetration of aluminium by the copper atoms. No anomolous effects were detected at the copper surface, indicating that very few aluminium atoms penetrated into the copper.

We would expect diffusion in copper-aluminium to be a true volume diffusion, as in the other metal systems investigated. We would anticipate that the values of diffusion coefficient and activation energy would lie fairly close to the values for bulk specimens. In table 8.1 the corresponding results are compared. The agreement between thin film values and bulk values for the diffusion of copper into aluminium (i.e. the faster direction of diffusion) is good, with D_o very close and E around 10% less in thin films. The agreement between thin film values and bulk values for the diffusion of aluminium into copper is poor, with both D_o and E being considerably different. We must therefore conclude that diffusion of copper into the aluminium is the rate determining process, and that the reflectivity observations at the copper surface are due simply to the loss of copper in the formation of intermetallic compounds.

TABLE 8.1

VALUES FOR DIFFUSION COEFFICIENT IN COPPER-ALUMINIUM

System	D_o cm^2/sec	E kcal/mole
Aluminium into Copper (Thin Films)	4·0	31·9
Copper into Aluminium (Thin Films)	22 4·7	31·5
Aluminium into Copper (Bulk Specimens)	$7·1\times10^{-2}$	39·2*
Copper into Aluminium (Bulk Specimens)	2·3	34·9†

* Results of Brick and Philips (1937)

† Results of Matano (1934)

CHAPTER 9

REFLECTIVITY CHANGES IN GOLD-LEAD

9.1 Introduction

The reflectivity changes discussed in chapters 5 to 8 have been shown to be characteristic of the motion of a phase boundary. Schopper (1955) found that in gold-lead the reflectivity changes were caused by the gradual formation of intermetallic compound at the gold surface (chapter 1.2). As this appeared to be a different mechanism of diffusion from that normally observed, it was decided to repeat Schopper's results in more detail.

The phase diagram of gold-lead is shown in fig. 9.1. Two phases appear stable at low temperatures - $AuPb_2$ and Au_2Pb.

Gold was usually deposited before the lead to prevent aggregation effects in the lead affecting the gold films. Reflectivity changes took place at the gold surface, the reflectivity dropping to a value close to that of lead. No change was ever observed at the lead surface, even with very thin lead films and thick gold ones.

Gold-lead diffuses at room temperature, and this has been used as the standard ageing temperature.

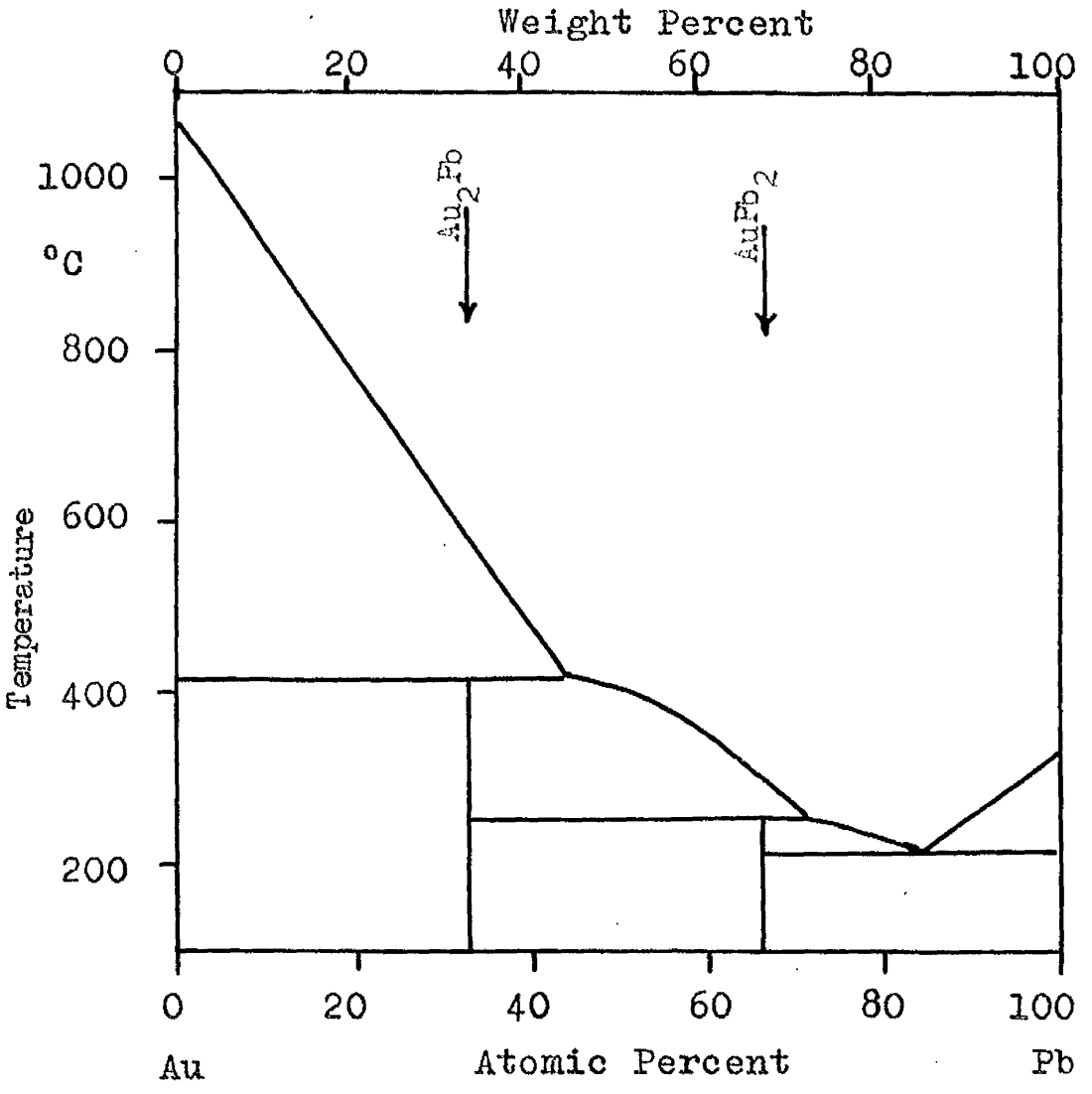

Fig. 9.1 Equilibrium Phase Diagram for Gold-Lead (Hansen 1958)

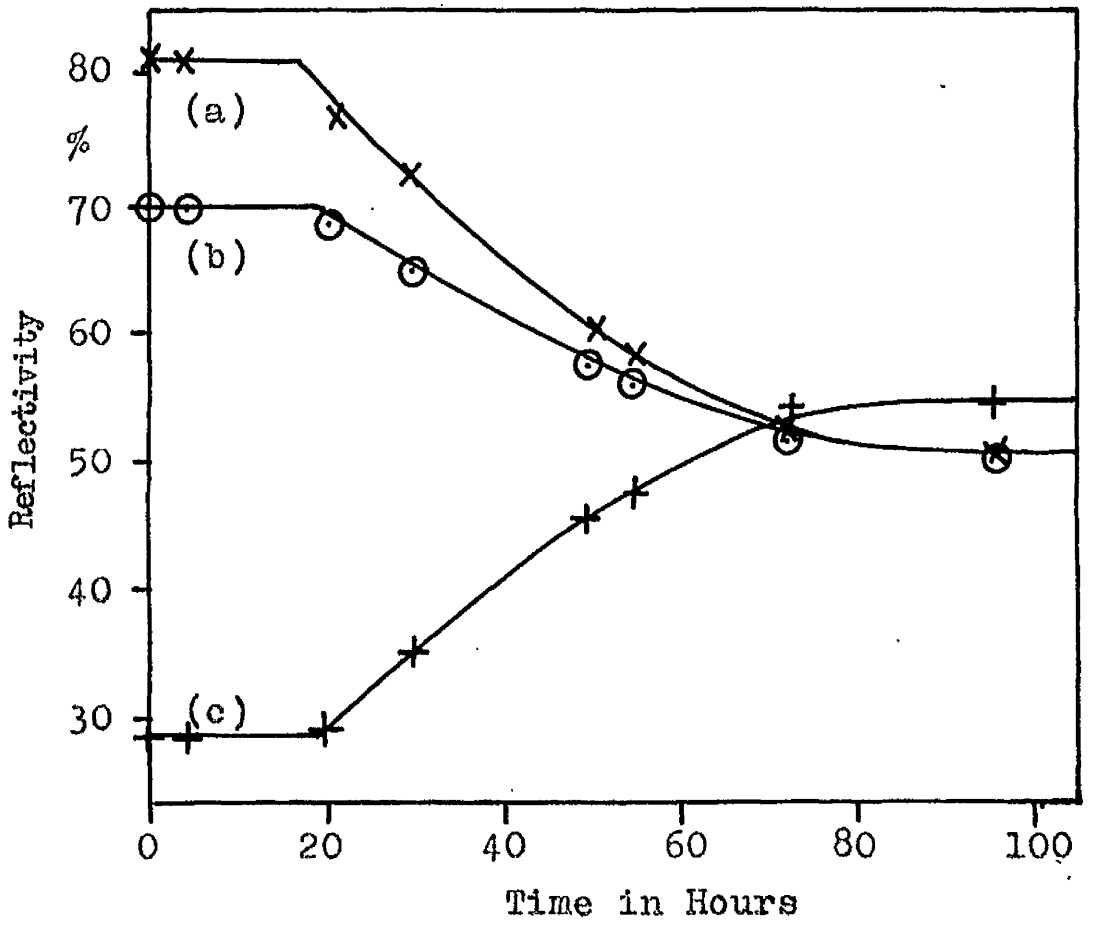

Fig. 9.2 Ageing of Gold-Lead Film at 21°C. Reflectivity change at gold surface for gold thickness of 1410Å. Reflectivity measured with mercury light of wavelength (a) 5790Å (b) 5461Å (c) 4358Å.

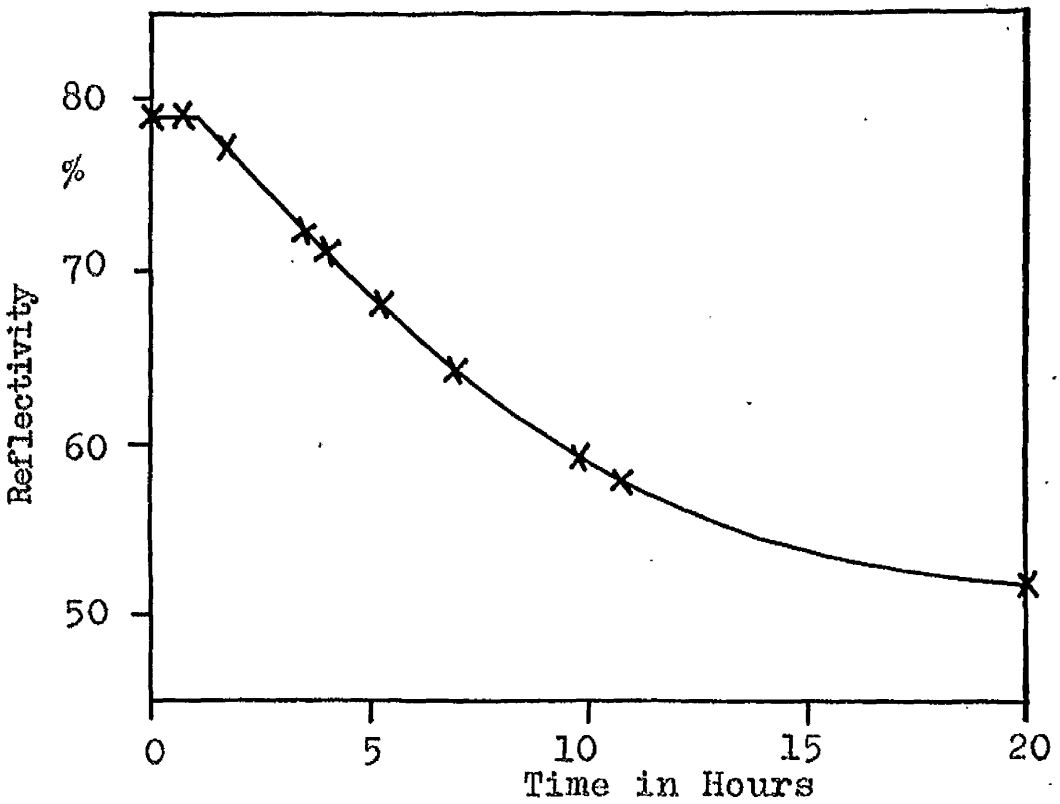

Fig. 9.3 Ageing of Gold-Lead Film at 21°C. Reflectivity change at gold surface for gold thickness of 600Å

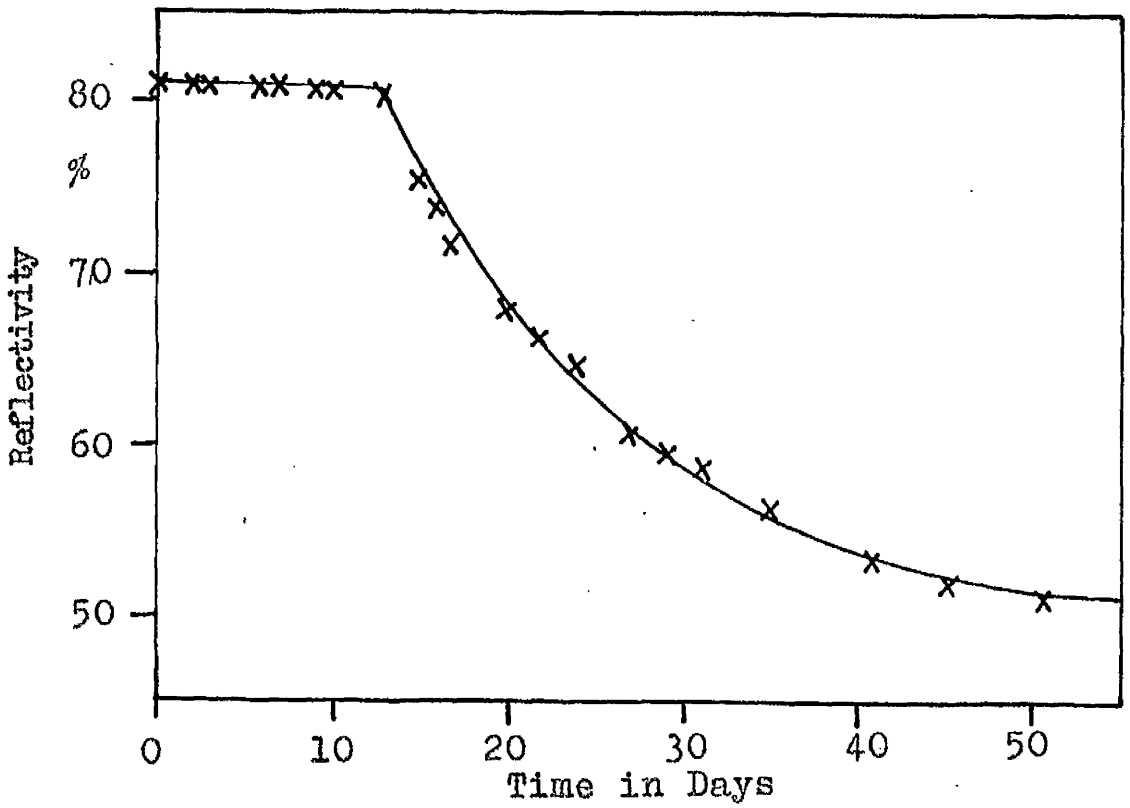

Fig. 9.4 Ageing of Gold-Lead Film at 21°C. Reflectivity change at gold surface for gold thickness of 5050Å.

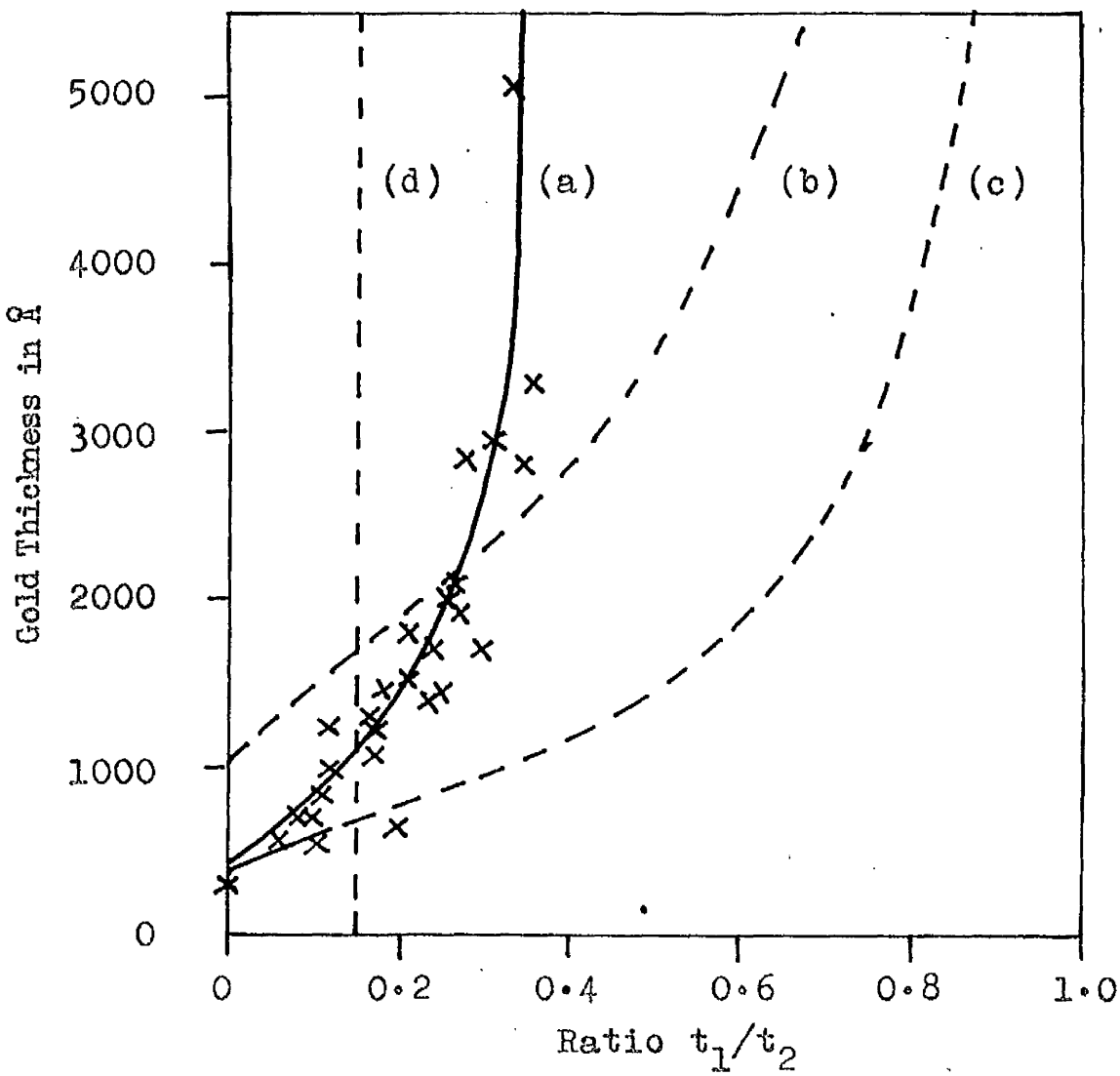

Fig. 9.5 Graph of Gold Thickness against Ratio t_1/t_2. (a) is the curve found experimentally. (b) and (c) are theoretical curves assuming a sharply defined phase boundary for light penetrations of 1000Å and 400Å. (d) is the theoretical line given by Schopper's theory.

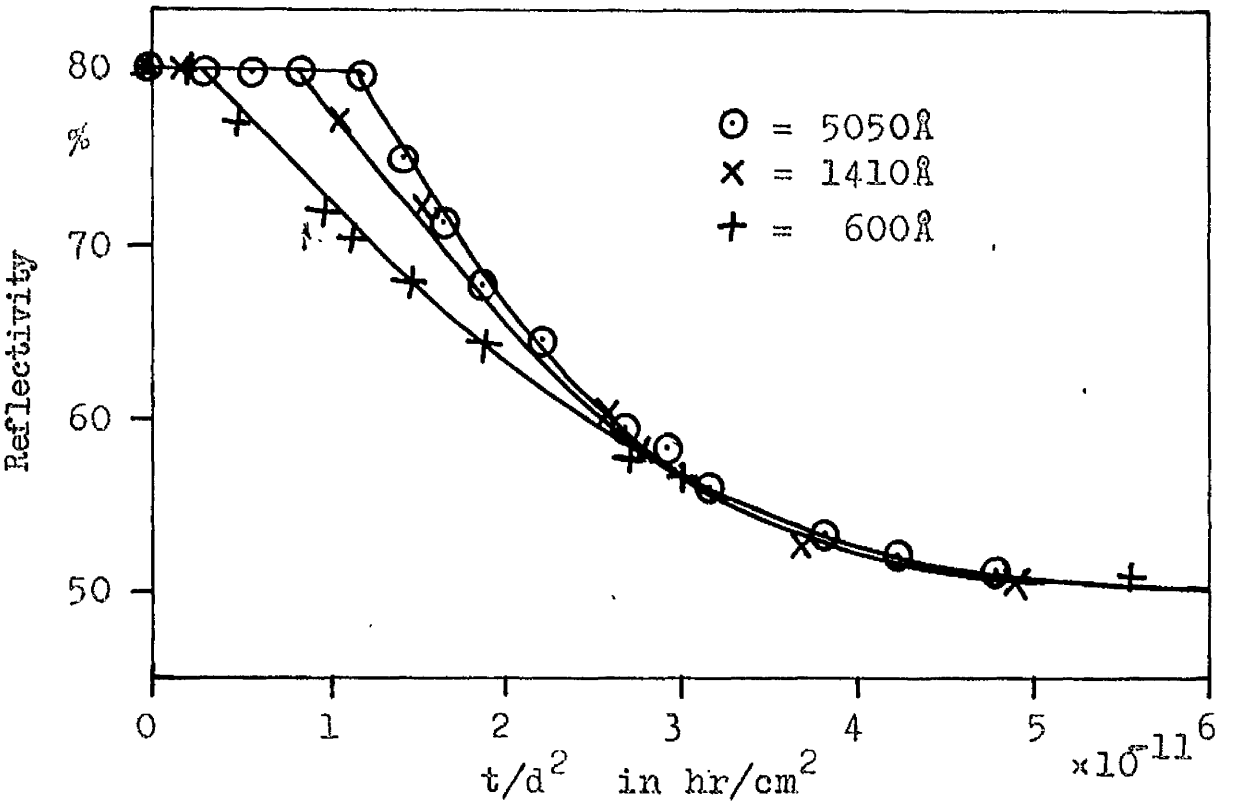

Fig. 9.6 Graph of Reflectivity against t/d^2 for Specimens given in fig. 9.2 to 9.4.

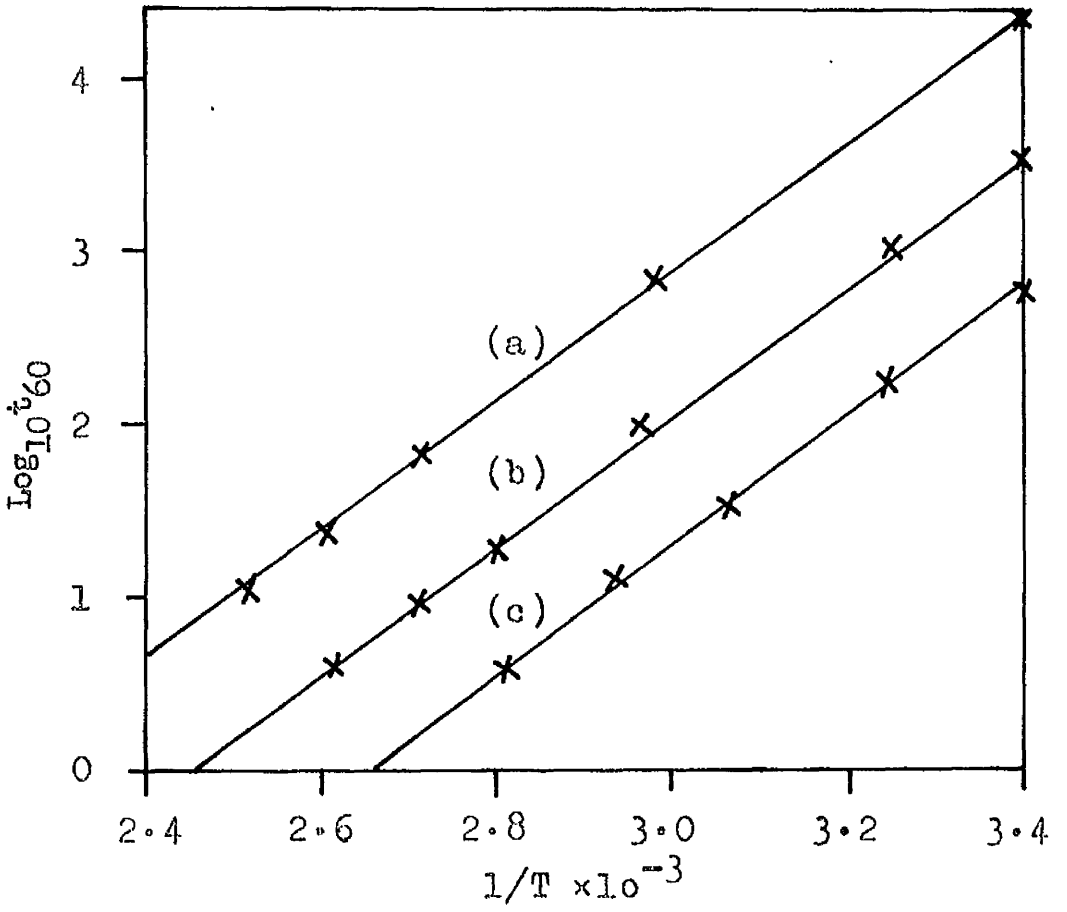

Fig. 9.7 Graph of $Log_{10} t_{60}$ against 1/T for Gold Thicknesses of (a) 3300Å, (b) 1410Å, and (c) 600Å.

9.2 Reflectivity Changes at the Gold Surface

The effect of light wavelength on a typical ageing curve is shown in fig. 9.2. The reflectivity change with mercury yellow light (30%) was greater than with mercury blue light (25%) or mercury green (18%), and has been used for all subsequent measurements.

Slides were prepared with gold films of different thicknesses in the range 300Å to 5050Å, overlaid with very thick films of lead to avoid thickness ratio difficulties. Typical ageing curves are shown in fig. 9.2 to 9.4.

Film thicknesses above 600Å had an initial plateau on the ageing curve, but the length of the plateau was much less than was found in systems with a sharply defined phase boundary. This is well illustrated in fig. 9.5, in which the gold thickness is plotted against the ratio t_1/t_2. The values obtained were consistent and lay on a smooth curve, but this curve was far away from that obtained for 400Å light penetration and did not coincide with any curve for a fixed value of light penetration.

Values of D' were calculated from the time taken for the reflectivity to cease changing, assuming the results to be characteristic of the motion of a phase boundary. The mean value of D' at 21°C was found to be

2.17×10^{-15} cm^2/sec. The values were consistent and did not increase significantly in thin gold films.

In view of the constancy of D' and the comparatively small variation of the ratio t_1/t_2 with thickness, we can make the curves practically coincide by plotting against t/d^2. This is illustrated in fig. 9.6 and confirms Schopper's results shown in fig. 1.2, although the fit is not as good as Schopper obtained.

Different portions of the same slides were aged over a range of temperature from 21°C to 110°C. From a plot of $\log_{10} t_{60}$ against (1/T) (fig. 9.7), the mean value found for the activation energy was 17.1 kcal/mole. This figure is in excellent agreement with Schopper's value of 17.0 kcal/mole.

It is interesting to compare fig. 1.3, showing the experimental points used by Schopper for finding the activation energy, with fig. 9.7. The results in the present investigation have been obtained with different portions of the one slide, and so errors in film thickness determination and spread in the values of diffusion coefficient do not affect the results. The points all lie almost exactly on straight lines, and different film thicknesses give lines with equal gradients, indicating that spread in D' values lies in D'_0 rather than in

activation energy. Schopper's results were obtained with a large number of separate films which accordingly showed considerable spread, and there must therefore be some uncertainty about the accuracy of the value obtained for the activation energy.

Taking the mean value of D' at 21°C, D'_0 can be calculated to be 0·014 cm^2/sec, again in excellent agreement with Schopper's value of 0·016 cm^2/sec, despite the use of two rather different theories.

Several slides were prepared with one gold film and four separate thicknesses of lead overlayer. The slides were aged in an oven at 36°C and a typical result is shown in fig. 9.8. From the eight specimens prepared the value of the critical thickness ratio of lead to gold was found to be 3·6. If the lead thickness was more than 3·6 times the gold thickness, the full reflectivity change took place. If the lead thickness was less than this, some reflectivity change took place because of the diffuseness of the phase boundary, but the full reflectivity drop to 52% was not obtained.

Schopper has claimed that a lead thickness twice the gold thickness gave the full reflectivity change, but this has not been found in the present investigation. In Fig. 9.8, we can see that a lead thickness of 1·9 times the

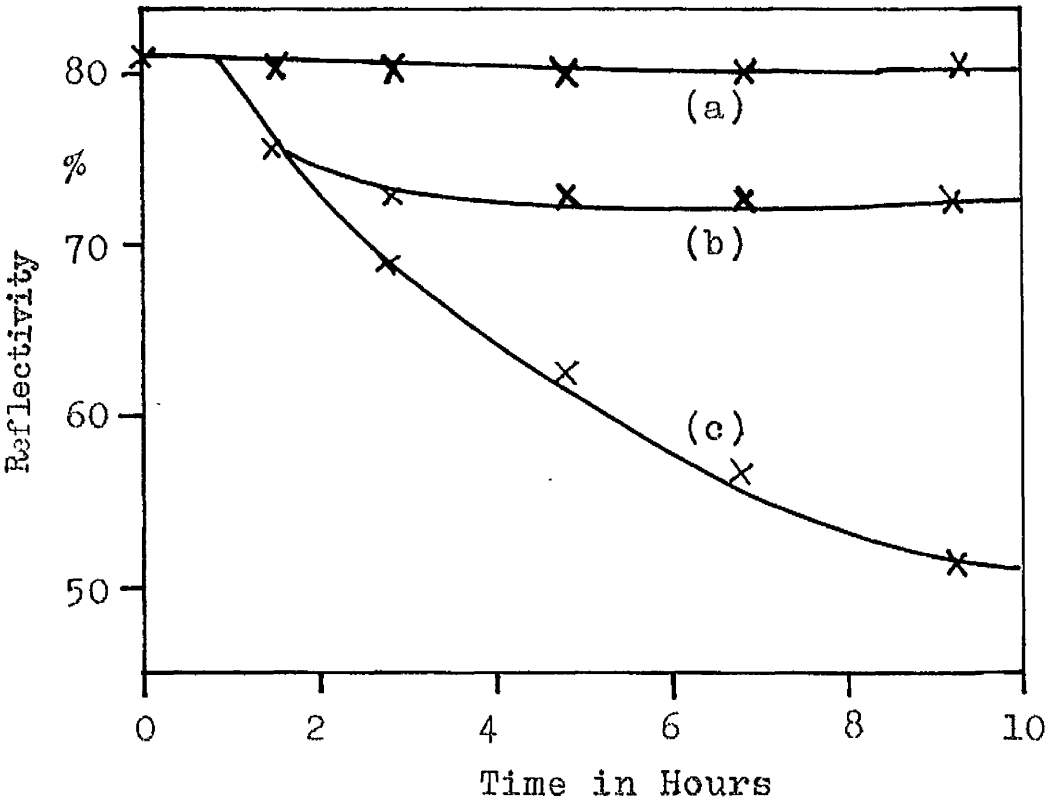

Fig. 9.8 Ageing of Gold Surface at 35°C for Gold Thickness of 735Å.

(a) lead thickness = 820Å (ratio Pb:Au = 1·1:1)

(b) lead thickness = 1390Å (ratio Pb:Au = 1·9:1)

(c) lead thickness = 3330Å and 4810Å (ratio Pb:Au = 4·5 and 6·6:1)

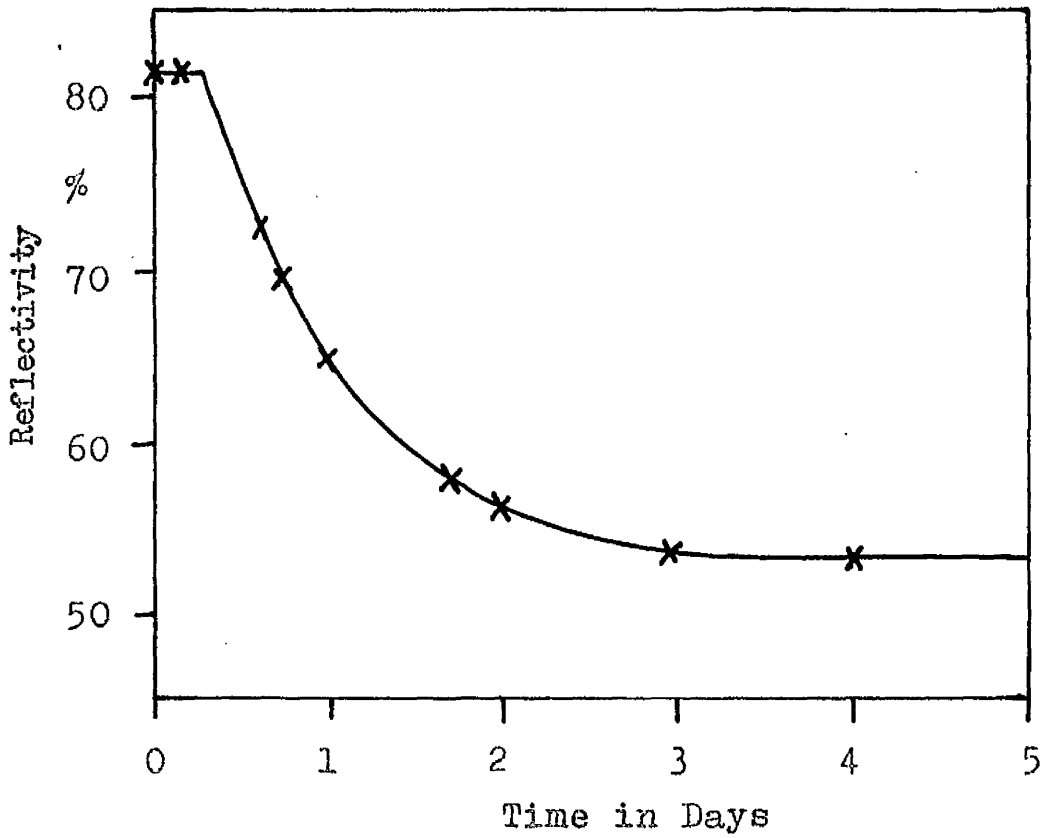

Fig. 9.9 Ageing of Gold-Lead Film at 21°C with Gold Overlayering the Lead. Gold thickness = 780Å

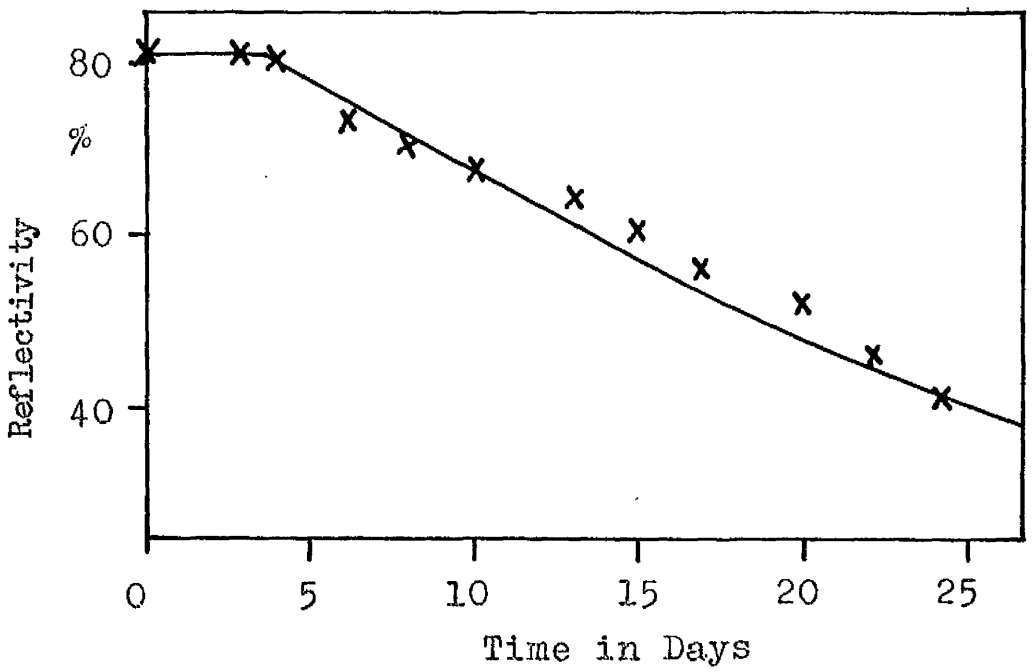

Fig. 9.10 Ageing of Gold-Lead Film at 21°C with Gold Overlayering the Lead. Gold thickness = 2450Å.

gold thickness gave some reflectivity change, but not by any means the full drop to 52%. In view of the large number of specimens studied in the present investigation, all of which were in agreement with a critical ratio of 3·6, it seems probable that this is the accurate value. A ratio of lead to gold of 3·6 corresponds to a lead concentration of 68·0% by weight. This is very close to the composition of the intermetallic compound $AuPb_2$, and it therefore seems likely that the reflectivity changes are due to the formation of this compound.

9.3 Reflectivity Changes with Lead Substrating the Gold

Several specimens were prepared with lead substrate films and gold overlayers. Precautions similar to those observed in gold-aluminium were taken to prevent any possible oxide formation on the lead between the evaporations.

Typical results are shown in fig. 9.9 and 9.10. Oxidation or aggregation appeared to take place as the $AuPb_2$ reached the air surface, and the reflectivity tended to drop to a figure much less than the 60% expected for the reflectivity of the compound. This effect was particularly noticeable in thick gold films, and in these the aggregation was so bad that the reflectivity fell below 20%. The ageing curves were definitely characteristic of the formation

of compound, but because of the aggregation it was not possible to determine the ratio t_1/t_2 in these films. This was most unfortunate, because measurements of this would have given valuable information on the mechanism of diffusion.

The diffusion coefficients were calculated approximately from the time taken for the reflectivity to drop to 60% (the reflectivity of $AuPb_2$). From the 10 specimens prepared the mean value of D' at 21°C was found to be $1{\cdot}05 \times 10^{-15}$ cm^2/sec.

Different portions of the specimen 2450Å thick, whose ageing curve at 21°C is shown in fig. 9.10, were aged over the temperature range 21°C to 133°C. All the ageing curves had the same form with an initial plateau followed by a reflectivity drop to a very low value. A graph of $\log_{10} t_{70}$ against (1/T) gave the activation energy to be 17·6 kcal/mole, in excellent agreement with the value of 17·1 kcal/mole found earlier. D_0' was found to be 0·016 cm^2/sec, again in good agreement with the value of 0·014 cm^2/sec found with lead overlayering the gold. These results indicate that the order of evaporating the metal films makes no difference to the value of diffusion coefficient obtained.

9.4 The Reflectivity of Gold-Lead Alloys

The reflectivities of a series of gold-lead alloys prepared by "flash" evaporation are shown in fig. 9.11. The two intermetallic compounds had fairly similar reflectivities, but with mercury blue light the reflectivity of Au_2Pb was definitely less than that of $AuPb_2$. The reflectivity of the phase formed by diffusion at the gold surface was 51½%, 51% and 53½% with mercury yellow, green and blue light respectively. These figures go in the same sequence as flash evaporated alloys of $AuPb_2$ which has reflectivities of 52%, 53% and 56%. The reflectivity of Au_2Pb goes in the different sequence 54%, 53% and 48½%, and so we can say that this is not the compound giving the reflectivity changes on ageing. These results indicate that the compound formed by diffusion in this system is $AuPb_2$.

$AuPb_2$ has almost the same reflectivity as pure lead. Diffusion of this compound up to the lead surface would therefore not give any reflectivity change. This would explain why it has proved impossible to obtain any diffusion observations at the lead surface.

Schopper attempted to measure the reflectivities of a number of gold-lead alloys by evaporating a wedge-shaped gold film onto a glass substrate, and depositing

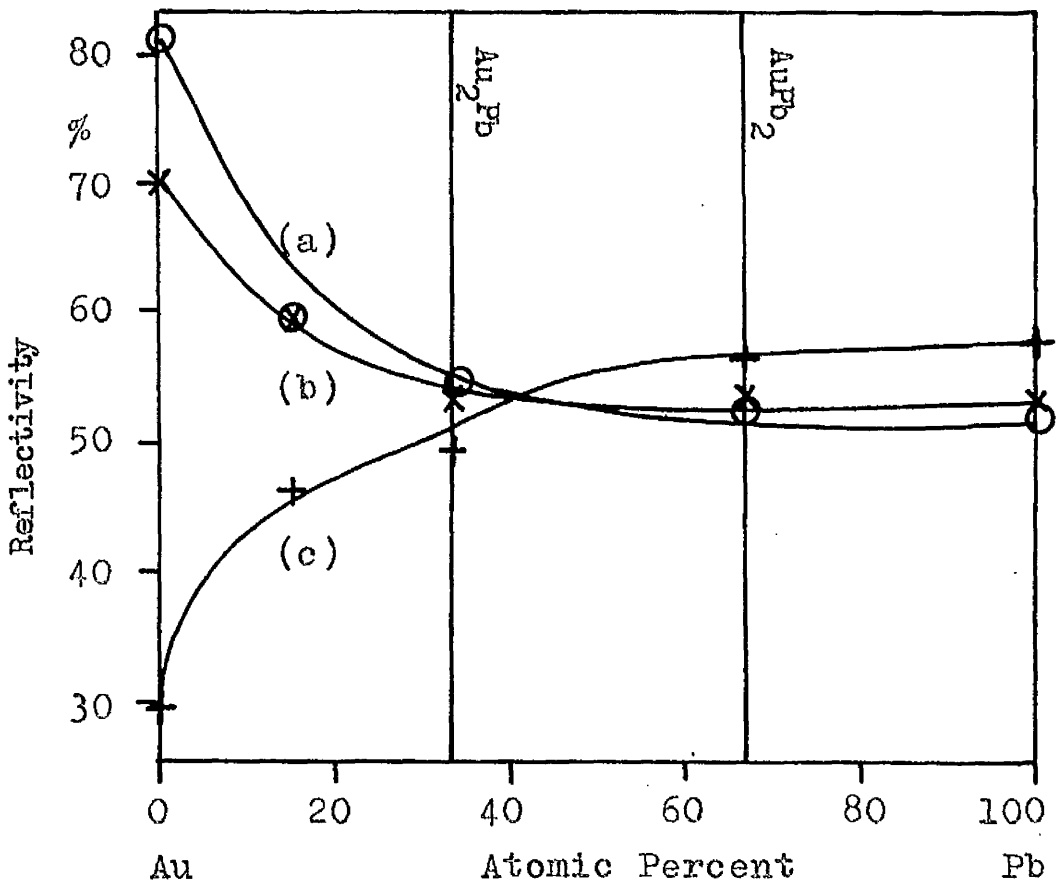

Fig. 9.11 Graph of Reflectivity against Concentration for "Flash" Evaporated Gold-Lead Alloys. Reflectivities measured at the glass surface with mercury light of wavelength (a) 5790Å, (b) 5461Å, and (c) 4358Å.

a uniform lead film on top to give a series of gold-lead concentrations. The film was then annealed at 70°C for ½ hr. to allow all the reflectivity changes to be completed. Schopper measured the reflectivity at various points along the glass surface, calculated the concentrations at these points, and took the reflectivity values as characteristic of these concentrations. This procedure is not permissible, however. Reflectivity changes certainly take place at the gold surface, and the value of the thickness ratio will determine the reflectivity. No reflectivity change takes place at the lead surface, however, under any circumstances. At one surface there is a reflectivity intermediate between gold and lead: at the other there is the reflectivity of pure lead. The system in this final state is certainly not a homogeneous alloy. A homogeneous alloy can never be obtained in a diffusion couple if the overall composition lies in a miscibility gap in the phase diagram. Such a diffusion couple will always consist of two separate phases with a phase boundary between them. The diffusion couple used by Schopper would therefore always consist of the two separate phases $AuPb_2$ and gold.

Schopper found that the addition of 12% lead to the gold caused its reflectivity to fall to that of pure lead. This is not in agreement with the results shown in in fig. 9.11, where a "flash" evaporated alloy with a

lead concentration of 14 at. % (15% by weight) had a reflectivity considerably different from pure lead.

9.5 Discussion

Observations of the value of the critical thickness ratio indicate that the reflectivity changes are due to the formation of the compound $AuPb_2$. Measurements of the reflectivity of $AuPb_2$ confirm this conclusion, and show that, since $AuPb_2$ has the same reflectivity as lead, no reflectivity changes would be visible at the lead surface even though diffusion into it took place. It is not surprising that $AuPb_2$ is the phase observed, for there is some doubt whether Au_2Pb is stable at low temperatures as indicated on the phase diagram. Kleppa and Clifton (1954) have found that Au_2Pb dissociated into $AuPb_2$ and gold on cold working. This indicates that Au_2Pb is unstable below some unknown temperature, the very low rate of decomposition being increased by cold work.

In view of the constancy of D', we can say that the growth of the the phase boundary obeys the parabolic law $x^2 = D't$. The experimental values for the ratio t_1/t_2 did not fit the curve for a light penetration of 400Å, thus showing that the phase boundary was diffuse. The experimental values did not lie on any curve for a fixed value of light penetration, and the apparent value appeared

to increase with gold thickness. This indicates that the boundary became more and more diffuse with increasing gold thickness.

Schopper's theory of a gradual change in concentration is an attractive one to apply in view of the similarity of the curves on plotting against t/d^2 (fig. 9.6), although according to this theory the initial plateau should only comprise 15% of the total ageing period, rather different from the 20% to 35% observed experimentally. This theory would not be expected to apply in a system which has a miscibility gap. In gold-lead there is no solubility from pure gold to pure lead except for the compound $AuPb_2$, and so Schopper's theory could not apply here.

Penetration into grain boundaries and dislocations in the gold by the condensing lead atoms does not seem possible. Lead has an evaporation temperature of only 718°C, much less than aluminium which did not penetrate into gold at all. In any case, lead has a large atomic size (3·50Å) and would find penetration into the gold more difficult than, say, aluminium with its smaller atomic size of 2·86Å.

Fujiki (1959) has made an electron diffraction study of successively evaporated gold-lead films, and has

claimed that diffusion into the upper film took place instantaneously on evaporation. This effect was observed with gold substrating and overlayering the lead, penetration occurring respectively into the lead and into the gold. He found that annealing the gold at 200°C for 1 hr. completely eliminated the penetration, and Fujiki attributed this to a change in structure of the gold. Fujiki's experiments are interesting although it seems unlikely that lead atoms have sufficiently high energies to remove large numbers of gold atoms from their lattice sites. A simple experiment was carried out to see whether Fujiki's explanation might be responsible for the results obtained in the present investigation. A gold film was evaporated onto a glass substrate, and lead was immediately deposited over half the area of the gold. The slide was removed from the vacuum chamber and divided into two halves. The single gold film was annealed at 200°C for 1 hr. 20 min. in a hot air oven. The film was returned to the vacuum chamber and lead was evaporated over the gold. According to Fujiki this annealing should certainly prevent any penetration of the gold into the lead. The ageing curves of the two halves of the slide were obtained on the hot stage reflectometer. No difference whatsoever was found between the two ageing curves, the diffusion coefficients and the ratio t_1/t_2 of both being the same.

Hence Fujiki's explanation does not help to account for the observed ageing curves.

The experimental ageing results which have been obtained are not characteristic of the motion of a sharply defined phase boundary, and to explain the results we must assume a fairly gradual increase in the amount of $AuPb_2$ present at the surface. It has been shown above that interpenetration cannot explain the results, and in any case the boundary becomes more and more diffuse with increasing film thickness (i.e. the apparent light penetration increases) which is not characteristic of the interpenetration found, for example, in silver-aluminium. The reflectivity changes have been shown to be due to the formation of the compound $AuPb_2$, and in view of the apparent gradual change in concentration, we must conclude that precipitation is taking place at a number of points distributed throughout a region of the film. This must be the region in which gold and lead are mixed together and must have been formed by diffusion of the pure metals at the beginning of ageing.

It is not surprising that initial fast diffusion takes place in gold-lead to give the apparently gradual increase in the concentration of the compound. $AuPb_2$ is the only thermally stable phase in the gold-lead system, and it is formed with low energy by a peritectic reaction.

In such a system ordering would be expected to occur fairly slowly and initial diffusion might be expected to have a considerable influence on the ageing curve obtained. Lead has a very large atomic size and diffusion will take place quickly in gold-lead because of the large difference in atomic sizes (Le Claire 1949). It is possible that gold will move into interstitial positions in the lead lattice, and this mechanism will occur very quickly in view of the low activation energy of diffusion. These explanations are not valid in the other systems with gold (gold-aluminium, gold-cadmium and gold-indium). These systems therefore show no initial diffusion and so form fairly sharply defined phase boundaries.

For diffusion ~~diffusion~~ at the gold surface, D'_o has been found to be 0·014 cm^2/sec and E to be 17·1 kcal/mole. These values are in excellent agreement with Schopper's figures of 0·016 cm^2/sec and 17·0 kcal/mole. Gold has a higher melting point than lead, and so diffusion of gold into lead will be the rate determining process, the concentration changes at the gold surface being due simply to the loss of gold in the formation of $AuPb_2$. In a given time the penetration into the lead will be 3·6 times greater than into the gold. The diffusion coefficient in the lead will therefore be 13·0 times greater than that observed at the gold surface. For

diffusion at the lead surface we therefore obtain the values 0·18 cm^2/sec and 17·1 kcal/mole. Measurements on bulk specimens for the diffusion of gold into lead are given in Jost (1952). D_o is given as 0·35 cm^2/sec, in good agreement with the thin film results, and E is given as 14·0 kcal/mole, in reasonable agreement with the 17·1 kcal/mole found in thin films. The two sets of results are in good agreement, confirming that diffusion in the faster direction does determine the rate of formation of compound.

Schopper took the value of activation energy in thin films to be characteristic of diffusion of lead into gold, and attributed the difference compared with bulk values to the large activation energies required for lattice changes in gold compared with lead. 17 kcal/mole does appear to be a very low value of activation energy for diffusion of lead into gold in view of the high melting point of gold, and particularly because of the large atomic size of lead. A figure higher than the 24·4 kcal/mole found for the diffusion of indium into silver (Jost 1952) would appear most likely for the diffusion of lead into gold. From this we must conclude that the activation energy observed at the gold surface is characteristic of diffusion into the lead rather than into the gold.

CHAPTER 10

REFLECTIVITY CHANGES IN SILVER-LEAD

10.1 Introduction

The eight metal pairs which have so far been investigated have been intermediate phase systems, and the reflectivity changes have been shown to be due to the formation of intermetallic compounds in the diffusion zone. As shown in chapter 4.4, silver-lead, although a non-miscible system, gave a definite reflectivity change on annealing, and this change did not appear to be caused by aggregation or similar effects.

The phase diagram for silver-lead is shown in fig. 10.1. The two metals appear almost completely non-miscible. At 150°C the solubility of silver in lead is 0·06 at. %, whilst the solubility of lead in silver has not been determined, but must be less than 0·1 at.%.

Silver was always evaporated before the lead, and ageing took place at the silver surface. No reflectivity changes were ever observed at the lead surface on annealing. Several specimens were prepared with the silver film overlayering the lead, but in no case was any ageing observed at either the silver or the lead surface.

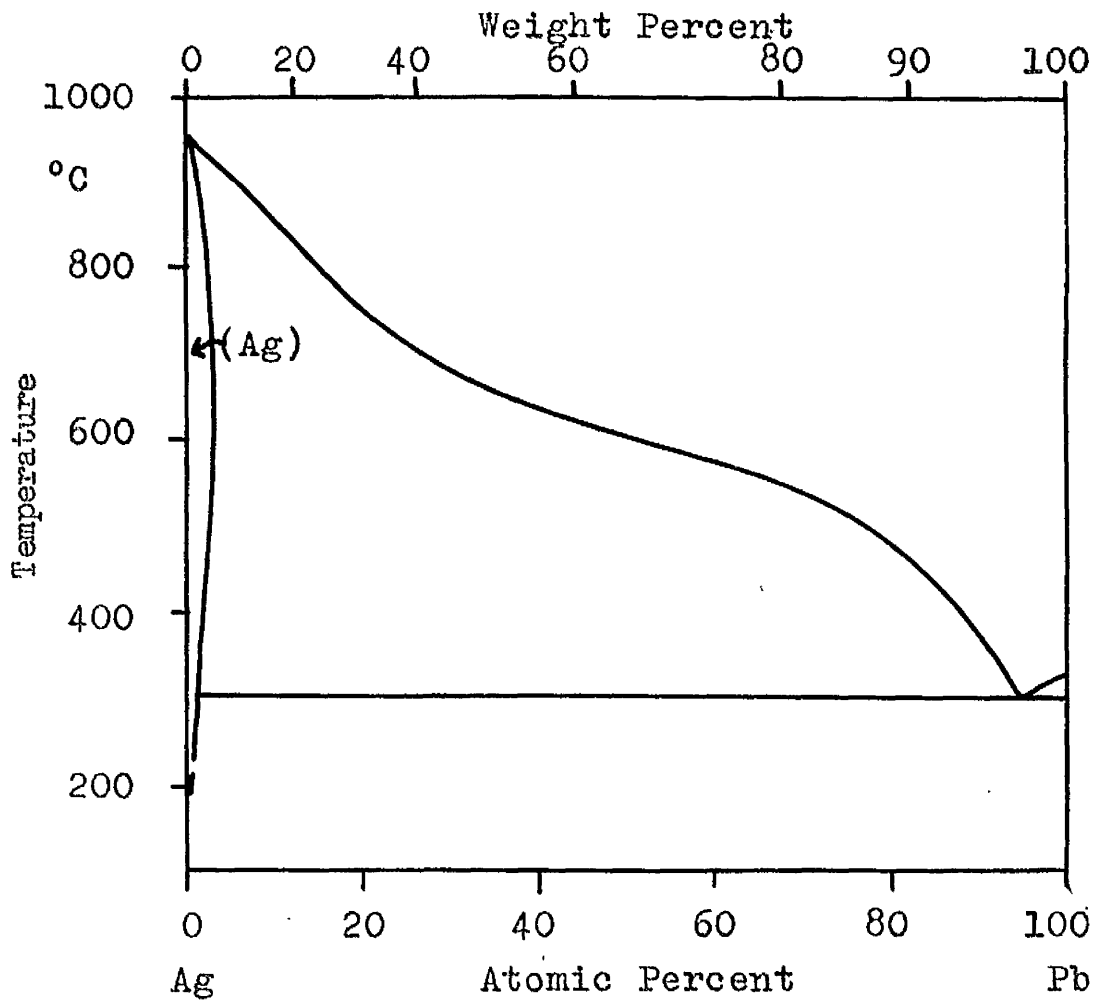

Fig. 10.1 Equilibrium Phase Diagram for Silver-Lead (Hansen 1958)

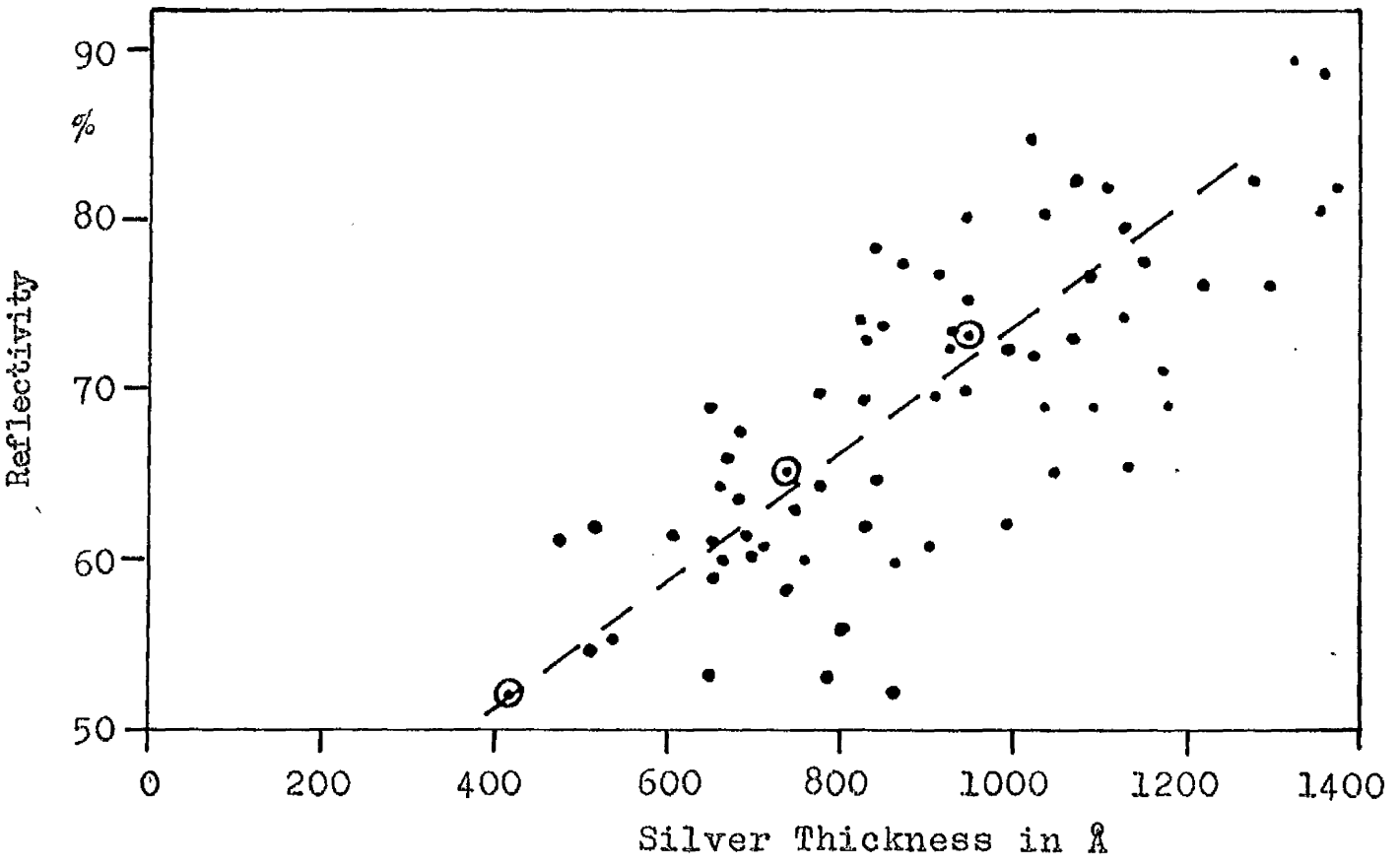

Fig. 10.2 Graph of Silver Thickness against Final Reflectivity Value at the Silver Surface in Silver-Lead Diffusion Couples. Circled Points indicate films whose ageing curves are given in fig. 10.3.

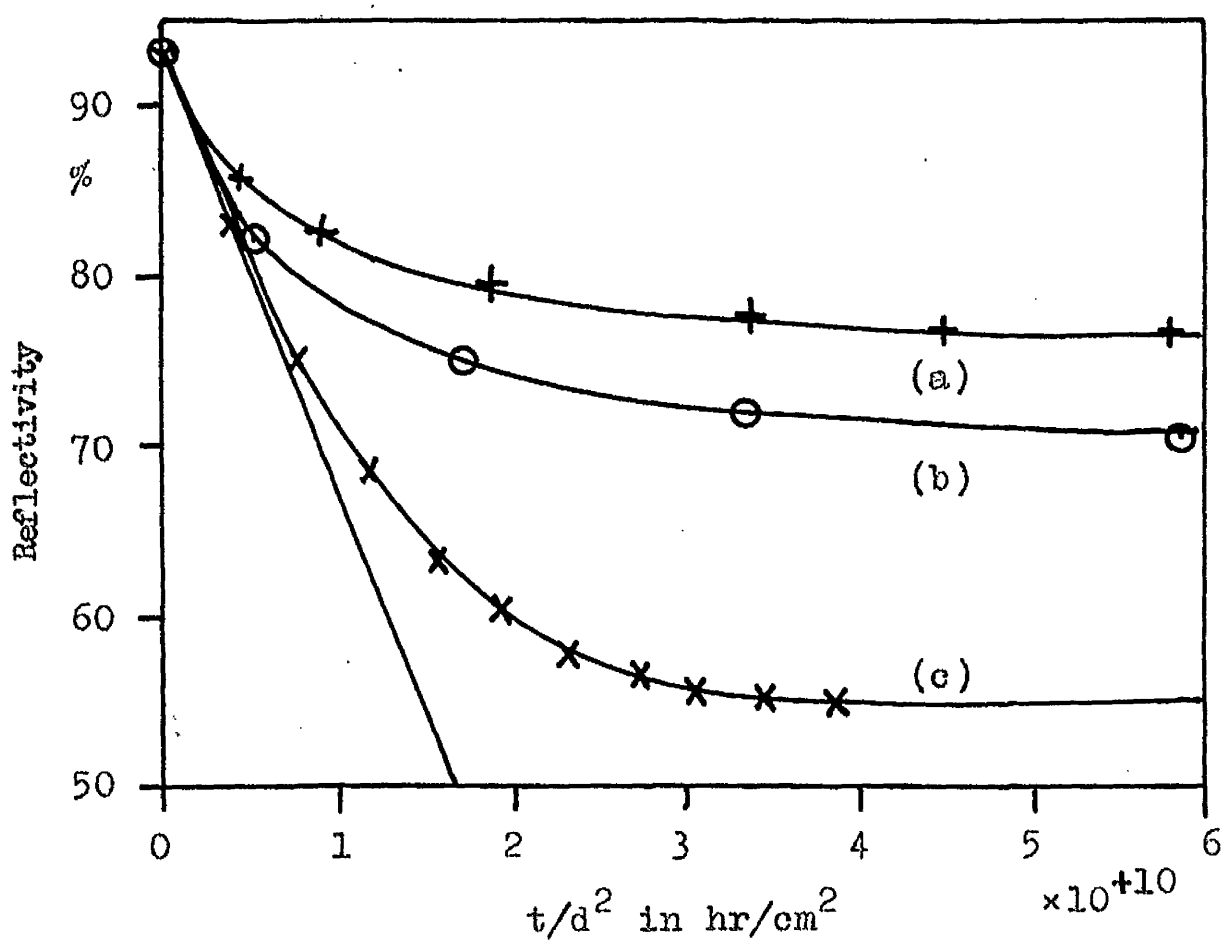

Fig. 10.3 Ageing of Silver-Lead Film at 146°C. Graph of reflectivity against t/d^2 for silver thicknesses of (a) 1020Å (b) 745Å (c) 415Å.

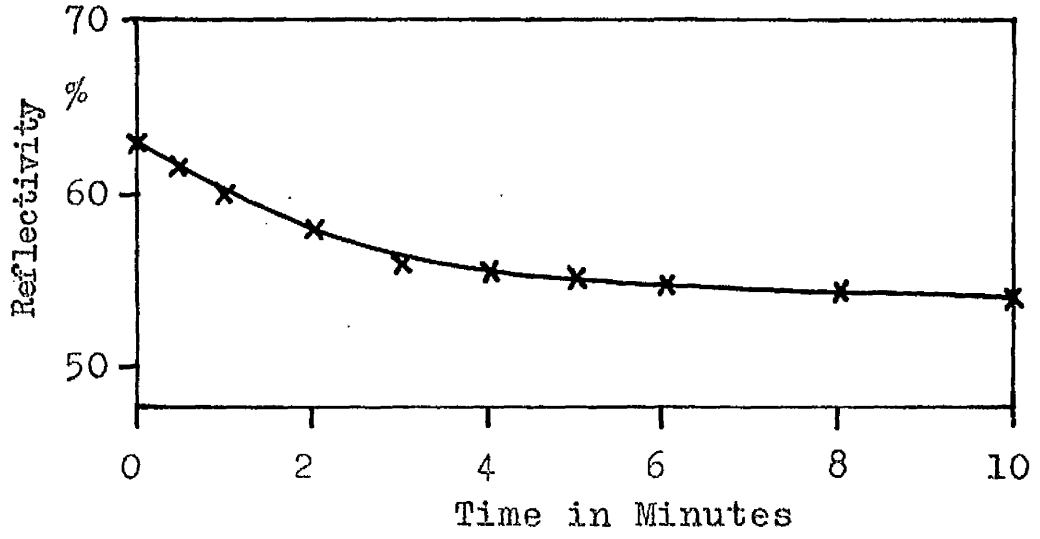

Fig. 10.4 Ageing of Silver-Lead Film at 94°C with very thin Silver Layer. Reflectivity change at silver surface for silver thickness of 60Å.

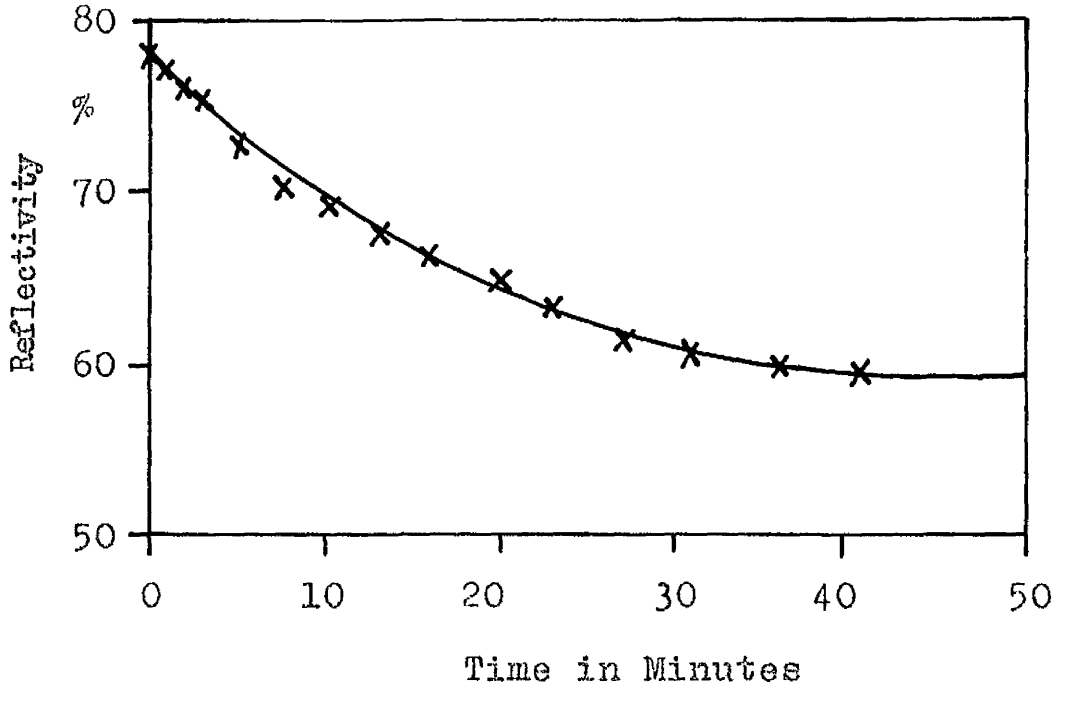

Fig. 10.5 Ageing of Silver-Lead Film at 96°C. Reflectivity change at silver surface for silver thickness of 180Å.

Mercury green light was used for all reflectivity measurements on this system, the silver having a colourless appearance before and after ageing.

10.2 Reflectivity Changes at the Silver Surface

146°C was selected as a standard ageing temperature as this allowed most of the films to be aged in the hot air oven. A large number of slides were prepared with the silver thickness varying in the range 400Å to 1400Å. Above this thickness limit no reflectivity changes were observed. The results showed a wide scatter, and in fig. 10.2 the final reflectivity obtained after ageing has been plotted against film thickness. Graphs of reflectivity against t/d^2 are plotted in fig. 10.3 for three specimens whose final reflectivities lay close to the mean line drawn in fig. 10.2. The reflectivity change decreased with increasing film thickness.

It can be seen in fig. 10.3 that the tangent drawn at the beginning of diffusion is practically the same for all three silver thicknesses. Hence values of diffusion coefficient (D) calculated from the intercept of the tangent on the t-axis at 51% reflectivity (the reflectivity of pure lead), using Schopper's formula (2.18), will be consistent. Strictly speaking, Schopper's theory will apply only in miscible systems, and the agreement of the

results for different thicknesses must be considered rather fortuitous. The mean value of the diffusion coefficient at 146°C was 1.4×10^{-14} cm^2/sec.

Different portions of the same slides were aged over a range of temperature from 102°C to 241°C. It was found that the shape of the curves did not vary with temperature and that the final reflectivity was always the same. The activation energy was calculated to be 21.1 kcal/mole, and this did not vary with different silver thickness. This gave D_o to be 1.8×10^{-3} cm^2/sec.

Several slides were prepared with very thin silver films in the range 60Å to 250Å and typical ageing curves are shown in fig. 10.4 and 10.5. Even with a silver thickness of only 60Å, the initial reflectivity was 63%, which is quite high if one takes into account the low reflectivity lead film behind the silver, some of which had doubtless penetrated to the glass surface because of the aggregated nature of a 60Å thick silver film. This indicates that no diffusion took place before annealing the films. The reflectivity of all the films fell to around 55%, just greater than the reflectivity of pure lead, and in agreement with the results found for rather thicker films. The activation energy for these thin films was found to be 20.7 kcal/mole, and D_o was calculated to be

5.2×10^{-3} cm^2/sec. These are in good agreement with the values found in thicker films, and indicates that grain boundary diffusion is not responsible for the observed results.

Several slides were prepared with one silver film and four different thicknesses of lead overlayer. In every case it was found that the lead thickness was sufficient to give the full reflectivity change at the silver surface, and that only 35 at.% lead or even less was necessary to give the full reflectivity change.

10.3 The Reflectivity of Silver-Lead Alloys

The reflectivity of a series of silver-lead alloys prepared by "flash" evaporation are shown in fig. 10.6. The reflectivity of the silver was fairly sensitive to small amounts of lead. The addition of 10% lead to the silver caused the reflectivity to drop fully 18%. Beyond approximately 40% lead, the reflectivity was fairly close to that of lead. It seems very likely that it is the sensitivity of silver to small amounts of lead that allows reflectivity changes to be seen at the silver surface on ageing.

10.4 Discussion

Values of diffusion coefficient have been calculated

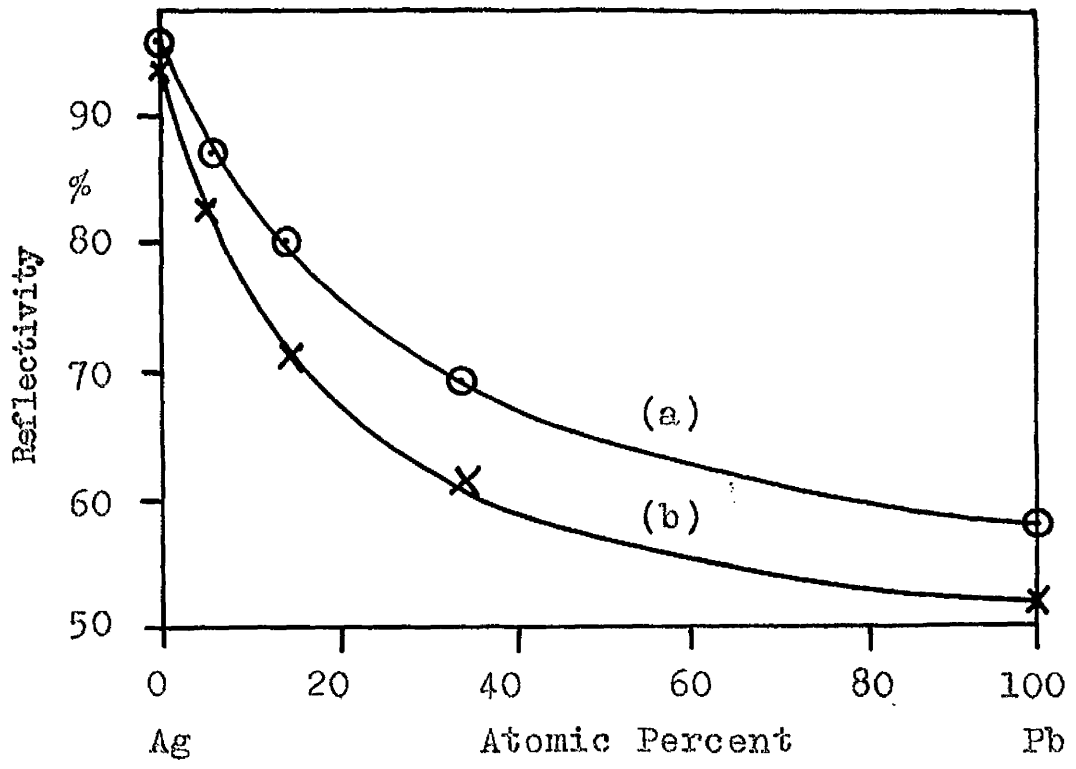

Fig. 10.6 Graph of Reflectivity against Concentration for "Flash" Evaporated Silver-Lead Films.
(a) Reflectivity measured at air surface
(b) Reflectivity measured at glass surface.

assuming that Schopper's theory for a miscible system can be applied. The diffusion coefficient has been found to be consistent, and for diffusion of lead into silver in thin films, D_o has been found to be 1.8×10^{-3} cm^2/sec and E to be 21.1 kcal/mole. Values of diffusion coefficient for diffusion of lead into silver are not given in the literature, but values of $D_o = 7.4 \times 10^{-2}$ cm^2/sec and E = 15.1 kcal/mole for silver diffusing into lead are quoted in Jost (1952). This is the faster direction of diffusion, and a considerably higher value of activation energy would be expected for diffusion of lead into silver. The value of D_o in thin films is in good agreement with bulk values for diffusion of silver into lead, but the activation energy is considerably higher. It would therefore appear that the results are characteristic of diffusion of lead into silver.

The experimental results suggest, therefore, a diffusion of lead into silver. This diffusion is not a result of penetration of lead into silver during evaporation, for the reflectivity of silver is sensitive to small amounts of lead, and any significant amount of it in the silver would affect the reflectivity. Even with thin silver films, however, the reflectivity of the silver appears unaffected by the evaporation of the lead overlayer. In any case, no trace of interpenetration has been observed

with a lead substrate and silver overlayer, although such a system would be expected to show a much greater effect, because of the high evaporation temperature of silver (1047°C) compared with lead (718°C), and the smaller atomic size of silver (2·89Å compared with 3·50Å) which would permit penetration of the substrate film more easily.

We must conclude that diffusion of lead into silver takes place during annealing. It is surprising that such a large amount of diffusion takes place in this system in view of the almost complete lack of solubility shown in the phase diagram. It has been shown by Raub and Engel (1943), however, that in electrodeposited alloys, silver can take up to 10% lead by weight in supersaturated solid solution, and it seems probable that a similar effect can take place in evaporated films of silver under certain circumstances. The amount of lead that can diffuse into the silver depends on the thickness of the silver, and is very much greater for thin films than for thick ones, probably because of the greater disorder in thin films. The amount of penetration will vary with thickness, but the actual value of diffusion coefficient and activation energy will remain constant since the basic mechanism of diffusion remains the same. This is in full agreement with the experimental results

in which the diffusion coefficient and activation energy are constant for film thicknesses of from 60Å to 1400Å. It is not surprising that the spread in final reflectivities in fig. 10.2 is so large, because the final reflectivity is a function of the structure of the film, which will depend to a large extent on the evaporation conditions.

We have shown that diffusion in thin films of silver-lead is a very unusual mechanism, depending on the ability of thin films films of silver to take up lead in supersaturated solid solution. Such diffusion will not generally occur in non-miscible systems, which would normally show no reflectivity changes on ageing.

CHAPTER 11

ELECTRON DIFFRACTION INVESTIGATION

11.1 Introduction

Electron diffraction is probably the simplest technique for observing diffusion in thin metallic films. Diffraction of electrons can take place either by transmission through a thin film or by reflection from its surface. The instrument available was an electron microscope with a subsidiary diffraction mechanism, and only transmission examination was possible. This meant that the maximum possible thickness of the metal films was approximately 300Å, since above this thickness the rings became blurred.

Care was taken throughout the investigation to keep the projector lens settings on the microscope constant, so that the magnification of all the photographs was the same. From the Bragg law

$$n\lambda = 2d \sin\theta \qquad (11.1)$$

where λ is the wavelength of the electron beam, d is the lattice spacing, θ is the angular deviation of the electron beam, and n is an integer. For any setting of the lens system

$$D = 2r$$
$$\propto \sin\theta \qquad (11.2)$$

where D is the diameter of the diffraction ring. From (11.1) and (11.2) we find

$$Dd = k \qquad (11.3)$$

where k is a constant for one setting of the lens system. If k can be found, ring diameters can be converted to values of d spacing.

11.2 Experimental

k was calculated from a diffraction photograph of a material with known lattice spacings. A gold film was used (fig. 11.1) and the results are shown in table 11.1. The ring diameters were measured by means of a low power travelling microscope, whilst the d spacings were calculated knowing the structure of gold to be f.c.c. with a lattice spacing of 4.08Å. The mean value of k obtained was 2·71 cm-Å, and over a period of months this varied by only $\pm$1%.

The specimens used in this investigation were prepared under exactly the same conditions as the films used for reflectivity observations. Films of the two metals were evaporated successively onto a glass microscope slide and formvar covered electron microscope grids placed side by side in the vacuum chamber. Formvar films were

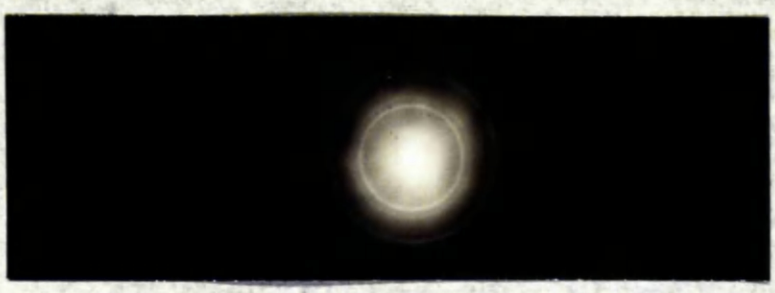

Fig. 11.1 Electron Diffraction Photograph of a Gold Film used for Calibrating the Electron Microscope.

TABLE 11.1

CALIBRATION OF MAGNIFICATION OF ELECTRON MICROSCOPE

No	D (cm)	Calculated d (Å)		k (cm-Å)
1	1·15	(111) 2·34	2·36	2·69
2	1·34	(200) 2·02	2·04	2·71
3	1·90	(220) 1·43	1·445	2·72
4	2·24	(311) 1·22	1·23	2·73
5	2·33	(222) 1·17	1·18	2·72
6	-	1·01		-
7	2·93	0·93		2·72
8	3·00	0·91		2·71

Mean value of k = 2·71 cm-Å

used as condensing surfaces as it has been suggested (van Itherbeck et al 1952) that the structure of films on formvar and on glass is similar. The grids were shielded from the glow discharge during the pumping cycle. Three specimens were prepared at each evaporation, one of each of the parent metals, and a composite film of the two.

Diffraction photographs of the three films were taken immediately after removal from the vacuum chamber. The composite film and the glass slide were both inserted in the hot air oven and aged for a suitable period. On removal, a second diffraction photograph was taken, and the reflectivity of the glass slide was found. This was repeated for further ageing periods, until no subsequent change in reflectivity was obtained. The reflectivity measurements enabled a graph of reflectivity against time to be drawn, and the diffraction photographs showed the composition of the film at different values of reflectivity.

11.3 Results

(a) Gold-Aluminium The composite film of gold-aluminium was aged at 58°C. The graph of reflectivity against time for the glass slide is shown in fig. 11.2. Diffraction photographs of pure gold and pure aluminium are shown in fig. 11.3(a) and (b). The ring diameters of aluminium

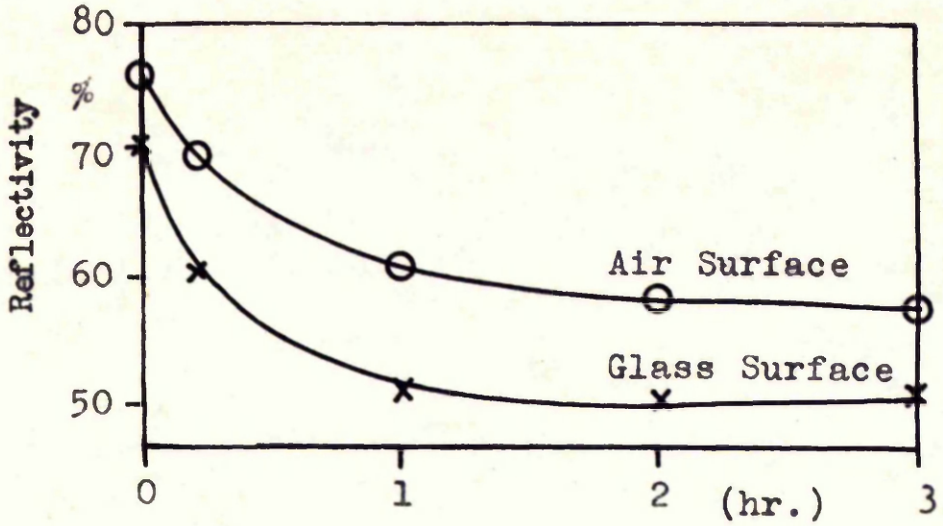

Fig. 11.2 Ageing of Gold-Aluminium Film used for Electron Diffraction Measurements at 58°C. Gold thickness = 100Å, aluminium thickness = 120Å.

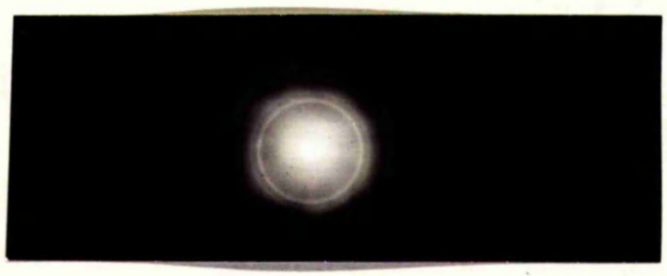

(a) Gold Film

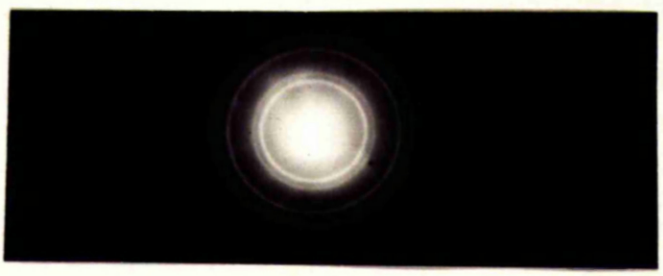

(b) Aluminium Film

Gold-Aluminium Composite Film

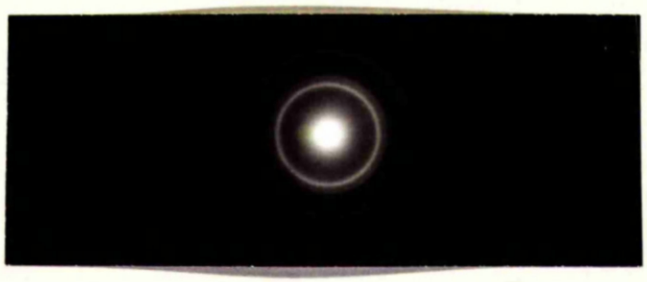

(c) Unaged

(d) Aged for 1 hr.

(e) Aged for 15½ hr.

Fig. 11.3 Electron Diffraction Photographs of Gold-Aluminium Films.

and gold are almost exactly equal as they have similar f.c.c. structures with lattice spacings of 4·05Å and 4·08Å respectively. Fig. 11.3(c) shows the composite film immediately after evaporation. The rings are characteristic of pure aluminium and pure gold, and no trace of intermetallic compounds is seen. Ageing for $\frac{1}{4}$ hr. also showed rings characteristic of the pure metals only. After ageing for 1 hr., however, extra rings became visible (fig. 11.3 (d)). Ageing for further periods up to 15½ hr. did not produce extra rings nor any change in the relative intensities of the rings (fig. 11.3(e)), and the reflectivity remained constant.

The results show that reflectivity changes are associated with diffusion and the formation of intermetallic compounds. Presumably a thin layer of compound had been formed after $\frac{1}{4}$ hr. ageing, but any diffraction effects of this layer were obscured by the patterns from the thicker aluminium and gold layers.

The ring diameters of the photograph for 1 hr. ageing were analysed in some detail to see whether particular intermetallic compounds could be identified. The results are shown in table 11.2. The probable presence of Au_2Al in the diffusion zone has been shown from measurements of the thickness ratio and relative rates

TABLE 11.2

STRUCTURE OF GOLD-ALUMINIUM FILM AGED FOR 1 HOUR AT 58°C

No	Int.	D (cm)	Observed dSSpacing (Å)	Calculated d Spacings Au_2Al (Å)	Au&Al (Å)	$AuAl_2$ (Å)
1	M	0·61	4·49			
2	vW	0·80	3·42			3·47
3	M	0·91	3·01			3·00
4	W	1·02	2·69	2·79		
5	M	1·16	2·36	2·36	2·34	
6	vS	1·26	2·17			2·17
7	vW	1·32	2·08	2·08		
8	M	1·72	1·59	1·61		
9	M	1·88	1·46	1·47	1·43	
10	S	2·09	1·31	1·33		1·34
11	M	2·22	1·24	1·25	1·22	1·22
12	W	2·33	1·18	1·18	1·17	1·15

of diffusion. Unfortunately the structure of this phase is complex and has not been determined (Coffinberry and Hultgren 1938). The d spacings of this phase were found experimentally, by taking an X-ray powder photograph of grains filed from a bulk specimen of the alloy. These results are shown in column 5 of table 11.2, and it can be seen that good agreement was obtained with the observed d spacings in the diffraction photograph. Diffraction rings were observed in the photograph which could not be explained by Au_2Al or the pure metals (column 6). It was found that d spacings for the compound $AuAl_2$ fitted these remaining rings satisfactorily (column 7). Rings at d spacings of 2·69Å, 2·08Å and 1·59Å could, however, be due only to Au_2Al.

From these results we must conclude that in thin films, Au_2Al and $AuAl_2$ are both formed in the diffusion zone. Presumably small quantities of other phases were present, but any effects were masked by the large quantities of the main phases.

(b) Silver-Aluminium The ageing curve of the silver-aluminium specimen at 85°C is shown in fig. 11.4. Diffraction photographs of the pure metals are shown in fig. 11.5(a) and (b), and it can be seen that the two photographs have similar ring diameters, since both metals

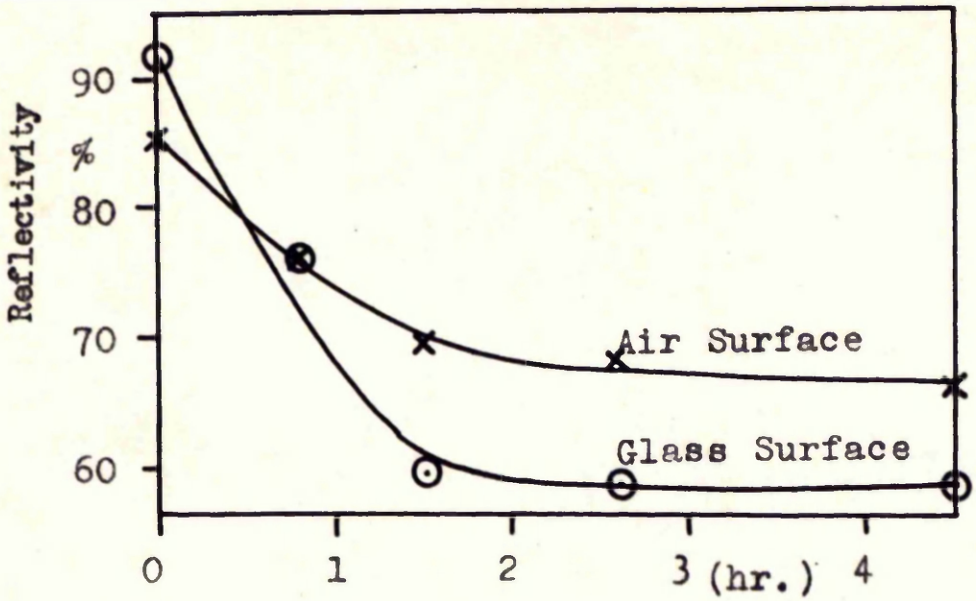

Fig. 11.4 Ageing of Silver-Aluminium Film used for Electron Diffraction Measurements at 85°C. Silver thickness = 100Å, aluminium thickness = 160Å.

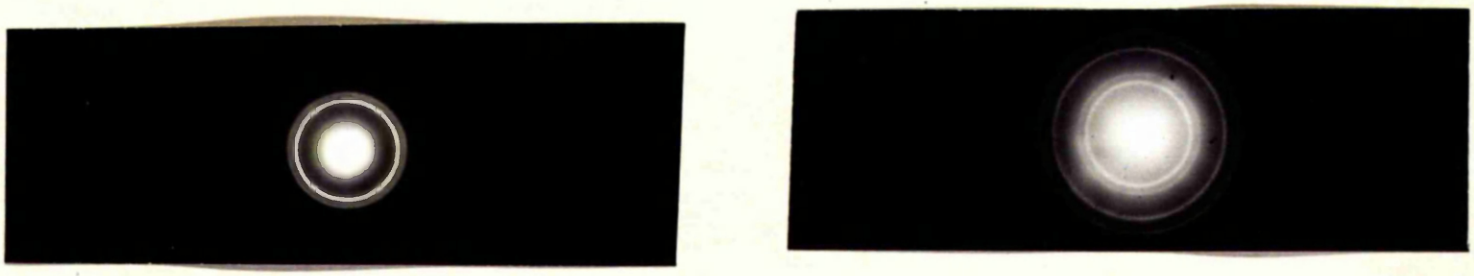

(a) Silver Film (b) Aluminium Film

Silver-Aluminium Composite Film

(c) Unaged (d) Aged for 1½ hr.

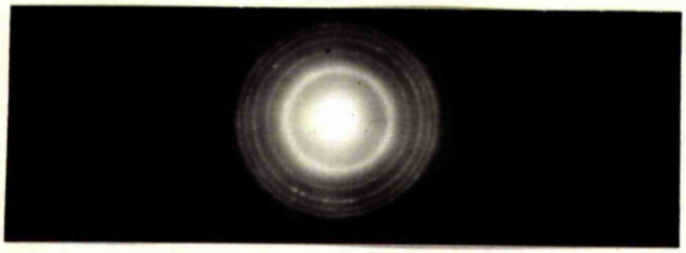

(e) Aged for 4½ hr.

Fig. 11.5 Electron Diffraction Photographs of Silver-Aluminium Films.

are f.c.c. with lattice spacings of 4·09Å for silver and 4·05Å for aluminium. The composite film immediately after evaporation showed no trace of intermetallic compounds (fig. 11.5(c)), whilst ageing for 40 min. gave a similar photograph showing only the pure metals. Ageing for 1½ hr. gave a considerable change in reflectivity whilst the diffraction photograph (fig. 11.5(d)) showed extra rings due to diffusion. Further ageing periods did not change the intensities of the rings (fig. 11.5(e)) and the reflectivity remained almost constant.

The results show that reflectivity changes are associated with diffusion and the formation of intermetallic compounds. Probably a thin layer of compound had been formed after 40 min. ageing, but any diffraction effects from this layer were obscured by the patterns from the pure metals.

The ring diameters of the photograph for 1½ hr. ageing were analysed to determine the intermetallic compounds formed by the diffusion. The d spacings are shown in table 11.3. Only two intermetallic compounds are formed in silver-aluminium - the μ phase and the ζ phase. No agreement was obtained with the d spacings of the μ phase (cubic, a= 6·92Å), but as can be seen in column 6 an excellent fit was found for the ζ phase (h.c.p., a= 2·88Å c= 4·62Å).

TABLE 11.3

STRUCTURE OF SILVER-ALUMINIUM FILM AGED FOR 1½ HOUR AT 85°C

No	Int	D (cm)	Observed d Spacing (Å)	Calculated d Spacings Ag&Al (Å)	Ag_2Al (Å)
1	vW	1·07	2·50		2·50
2	S	1·15	2·32	2·34	2·31
3	S	1·22	2·19		2·19
4	W	1·30	2·05	2·02	
5	M	1·60	1·67		1·69
6	M	1·88	1·42	1·43	1·44
7	M	2·08	1·28		1·31
8	M	2·20	1·21	1·22	1·22
9	M	2·24	1·19		1·20
10	W	2·61	1·02		1·05
11	vW	2·82	0·94		0·92
12	W	2·97	0·91	0·91	0·90

(c) Copper-Aluminium The ageing curve of the copper-aluminium specimen at 121°C is shown in fig. 11.6. This is not the complete ageing curve, and corresponds only to the first stage of ageing at the aluminium surface. The ageing could not be continued beyond this stage because of breaking up of the formvar film. Diffraction photographs of the pure metals are shown in fig. 11.7(a) and (b). The composite film immediately after evaporation showed rings characteristic of pure aluminium and pure copper with no trace of diffusion (fig. 11.7(c) and table 11.4), whilst ageing for 20 min. gave a similar photograph. Ageing for 45 min. gave a photograph (fig. 11.7(d)) showing rings of the pure metals but with two extra rings at d spacings of 1.90Å and 1.51Å, showing that some diffusion had taken place, but it was not possible to identify thecompound formed from these spacings. Ageing for 100 min. gave a completely new diffraction pattern (fig. 11.7 (e)) and none of the rings corresponded to copper or aluminium. The d spacings of this photograph are shown in table 11.5 and it can be seen that the d spacings of $CuAl_2$ (b.c. tet. a= 6.07Å c= 4.87Å) fit the observed values very well, and so we must conclude that in this part of the ageing curve $CuAl_2$ is the main phase present. It was not possible to take further diffraction photographs as the formvar film broke up with the heat.

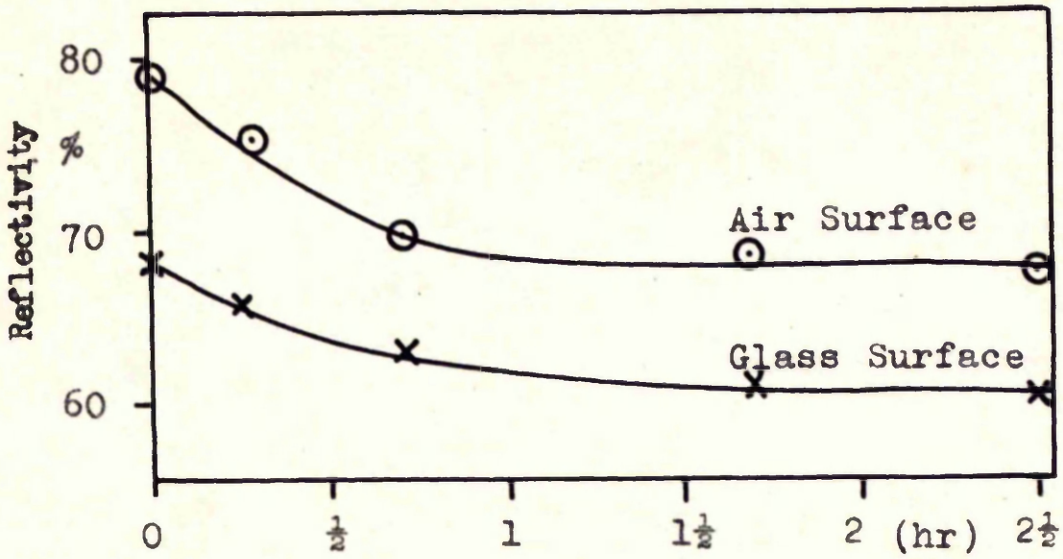

Fig. 11.6 Ageing of Copper-Aluminium Film used for Electron Diffraction Measurements at 121°C. Copper thickness = 100Å, aluminium thickness = 110Å.

(a) Copper Film

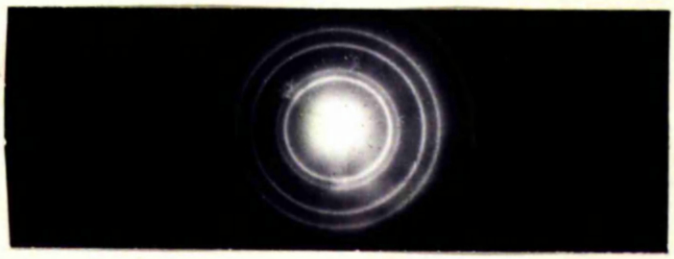

(b) Aluminium Film

Copper-Aluminium Composite Film

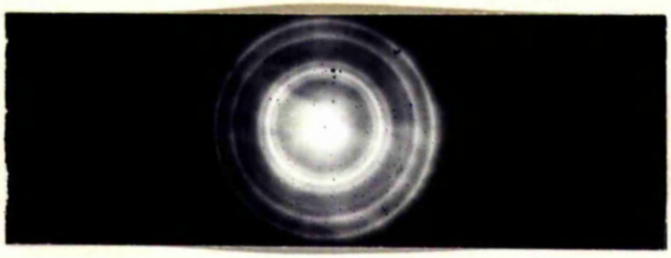

(c) Unaged

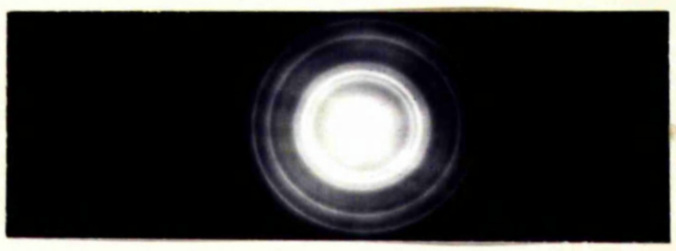

(d) Aged for 45 min.

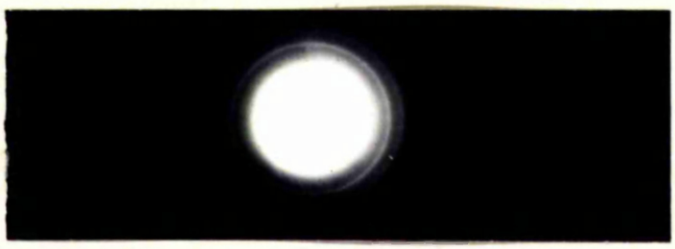

(e) Aged for 100 min.

Fig. 11.7 Electron Diffraction Photographs of Copper-Aluminium Films.

TABLE 11.4

STRUCTURE OF UNAGED COPPER-ALUMINIUM FILM

No	Int.	D (cm)	Observed d Spacing (Å)	Calculated d Spacings Al (Å)	Cu (Å)
1	M	1·16	2·33	2·34	
2	vS	1·31	2·06	2·03	2·09
3	S	1·51	1·79		1·81
4	W	1·90	1·42	1·43	
5	S	2·12	1·27	1·22	1·28
6	vW	2·28	1·18	1·17	
7	S	2·51	1·08		1·09
8	vW	2·63	1·02	1·01	
9	vW	3·10	0·87		0·90
10	M	3·25	0·83		0·83
11	M	3·40	0·79		0·80

TABLE 11.5

STRUCTURE OF COPPER-ALUMINIUM FILM AGED FOR 100 MIN. AT 121°C

No	Int	D (cm)	Observed d Spacings (Å)	Calculated d Spacings of $CuAl_2$ (Å)
1	W	0·89	3·04	3·03
2	vS	1·09	2·48	2·45
3	S	1·26	2·14	2·14
4	S	1·78	1·52	1·51
5	M	2·05	1·29	1·29

(d) Gold-Lead Diffraction photographs of the pure metals are shown in fig. 11.8(a) and (b). The composite film showed a completely different structure, however, which was not characteristic of the pure metals (fig. 11.8(c)). This photograph was taken 25 min. after evaporating the specimen, and shows that diffusion had occurred within this period. The gold colour at the glass side had disappeared within this time, giving a reflectivity of 60% at the former gold surface and 47% at the lead surface.

It has been shown in chapter 9 that reflectivity changes in this system take place at room temperature. The diffusion coefficient at the gold surface at 21°C was found to be $2{\cdot}17 \times 10^{-15}$ cm^2/sec, and this would give a penetration of 100Å (the thickness of the gold film) in 8 min.. We would therefore expect diffusion to be completed within 25 min.

The d spacings of the composite film are shown in table 11.6. Only two intermetallic compounds are formed in gold-lead - Au_2Pb and $AuPb_2$. No agreement was obtained with the d spacings of Au_2Pb (f.c.c., a= 7·94Å), but as can be seen in column 7 an excellent fit was found for $AuPb_2$ (b.c.tet., a= 7·32Å c= 5·65Å). We can therefore conclude that $AuPb_2$ is the main or only phase present in the diffusion zone. Schopper (1955) reached a similar

(a) Gold Film

(b) Lead Film

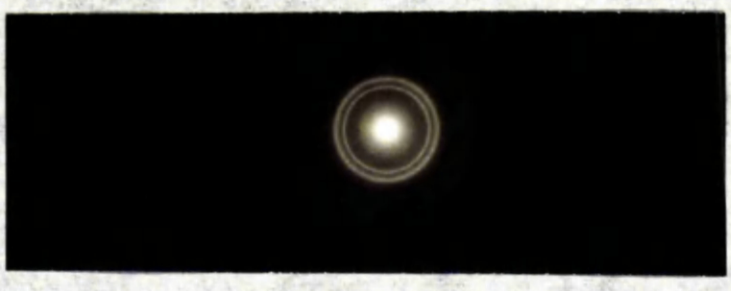

(c) Gold-Lead Composite Film

Fig. 11.8 Electron Diffraction Photographs of Gold-Lead Films. Gold thickness = 100Å, lead thickness = 100Å.

TABLE 11.6

STRUCTURE OF GOLD-LEAD FILM AGED FOR ½ HOUR AT ROOM TEMPERATURE

No	Int.	D (cm)	Observed d Spacing (Å)	Calculated d Spacings Au (Å)	Pb (Å)	$AuPb_2$ (Å)
1	W	0·53	5·17			5·12
2	W	0·60	4·57			4·45
3	vS	0·97	2·83		2·86	2·81
4	M	1·11	2·47		2·48	2·47
5	vS	1·17	2·34	2·34		
6	M	1·21	2·25			2·22
7	W	1·36	2·02	2·02		
8	vW	1·43	1·92			1·89
9	vW	1·52	1·80			1·81
10	vW	1·61	1·70			1·71
11	M	1·70	1·61			1·62
12	W	1·82	1·51		1·49	1·52
13	M	1·90	1·44	1·43	1·43	1·46

conclusion using X-ray analysis on a thin film diffusion couple.

11.4 Discussion

The electron diffraction investigations on gold-aluminium, silver-aluminium and copper-aluminium have shown conclusively that reflectivity changes on ageing are due to diffusion and the formation of intermetallic compounds. If there is no change in reflectivity on annealing, there is no change in the corresponding diffraction pattern.

In table 11.7 the compounds observed in the diffusion zone by electron diffraction and by reflectivity measurements are given. The phases found by electron diffraction were generally the same as those found from reflectivity observations.

Electron diffraction could be used to determine diffusion coefficients and activation energies in thin film couples. Michel (1956), indeed, has used this technique to show a correlation between the formation of intermetallic compounds in the diffusion zone and diffusion coefficients extrapolated from bulk values at high temperatures. It is, however, a very insensitive method of following the ageing process, since the patterns

TABLE 11.7

COMPARISON OF COMPOUNDS OBSERVED BY ELECTRON DIFFRACTION AND BY REFLECTIVITY MEASUREMENTS

System	Compounds Observed by e.d.	Compounds Observed by Reflectivity
Gold-Aluminium	$AuAl_2$ Au_2Al	Au_2Al
Silver-Aluminium	Ag_2Al	Ag_2Al
Copper-Aluminium	$CuAl_2$	$CuAl_2$
	-	S_2
Gold-Lead	$AuPb_2$	$AuPb_2$

of the pure metals tend to obscure the weaker lines of the alloy in the early stages, and there is usually a time lapse before these lines become sufficiently distinct for observation. These criticisms apply only to transmission electron diffraction and not to reflection electron diffraction, which should be a fairly sensitive technique.

CHAPTER 12

POLARISING SPECTROMETER OBSERVATIONS

12.1 Introduction

Measurements of diffusion have so far been made by studying changes in reflectivity. A second optical method which can be used is to study the phase change on reflection from the metal surface. This technique can only be used for observations at the metal-air interface which limits its scope considerably.

The phase shift and reflection coefficient of a plane polarized light wave reflected from a metal surface depends on whether the incident beam is polarised parallel or perpendicular to the plane of incidence. Drude (1890) considered the case of an incident light beam plane polarised at $\frac{\pi}{4}$ to the plane of incidence, and showed that, generally, the reflected beam would be elliptically polarised. Measurements of the degree of ellipticity enable two angles $-\Psi$ and Δ - to be found, where $\tan \Psi$ is the ratio of the reflection coefficients for parallel and perpendicular incidence, and where Δ is the relative phase shift introduced between the two components.

In the present investigation, measurements were

made of the change in Ψ and Δ on ageing thin film couples of gold-aluminium and silver-aluminium

12.2 Experimental

The experimental measurements were made on a polarising spectrometer based on the design of Tronstad and Feachem (1934). A compensator was placed in the light beam between the polariser and the specimen, giving an incident beam that was elliptically polarised. The degree of ellipticity of the beam could be adjusted so as to give plane polarised light after reflection at the metal surface. The compensator used was a mica quarter-wave plate with its principal axis at $\frac{\pi}{4}$ to the plane of incidence. The degree of ellipticity could be adjusted by varying the setting of the polariser. Plane polarised light was detected by obtaining an extinction position for the analyser. If P and A are the required angles of rotation of the polariser and analyser from the plane of incidence, Ψ and Δ can be found from the relationships

$$\tan\Psi \tan A = 1$$

$$\sin\Delta = \cos 2P$$

A diagram of the apparatus is shown in fig. 12.1. Lens L_1 focussed an image of the source, an 80 watt mercury discharge tube, onto a screen, in which a pin-hole (A_1) acted as a point source. Lens L_2 and filter F

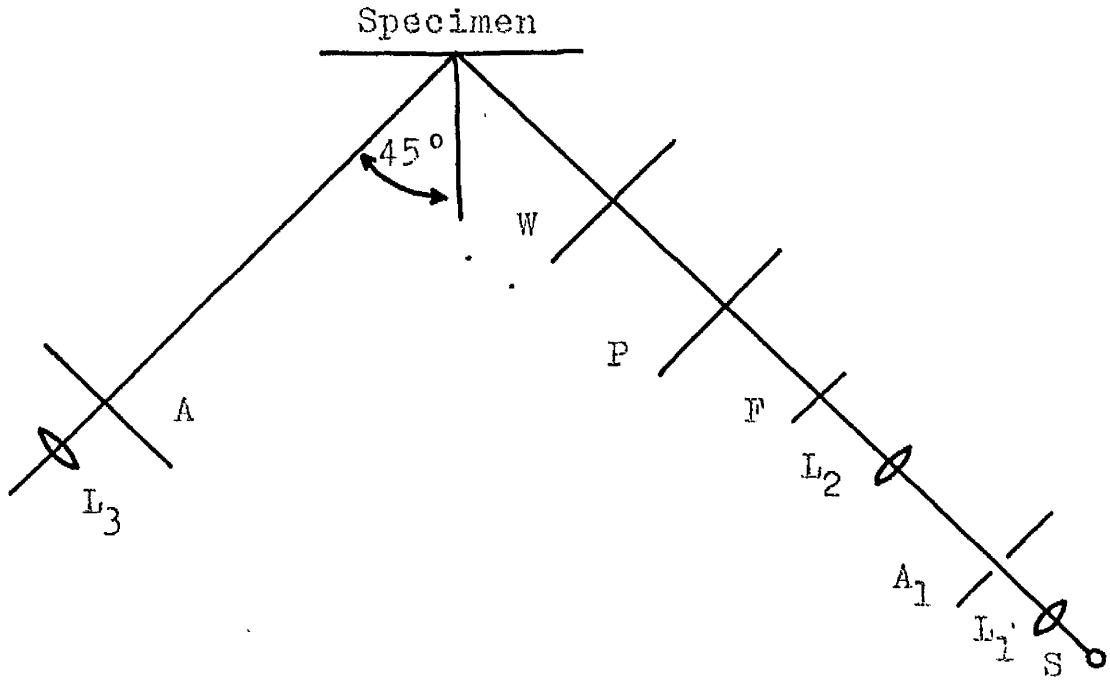

Fig. 12.1 Diagram of Polarising Spectrometer.

S_1 Source, $L_1 L_2 L_3$ Lenses, A_1 Aperture, F Filter, P Polariser, W Quarter Wave Plate, A Analyser.

gave a beam of parallel monochromatic light of wavelength 5461Å. The polariser and analyser were Nicol prisms mounted on 360° scales which could be read to ±0.1°. The error in setting the extinction positions, however, was fairly considerable, probably ± 0.2°, since no half-shade device was used. Lens L_3 acted as an eyepiece and focussed on the surface of the specimen.

12.3 Results

Measurements were first made at the aluminium surface of a gold-aluminium diffusion couple. Graphs of reflectivity, Ψ and Δ against time for the one specimen are shown in fig. 12.2. Reflectivity and polarisation measurements were made together to avoid errors due to variations in the ageing conditions. The variation in Ψ and Δ is very small, and consequently the experimental points are somewhat inaccurate. Taking into account the error in the readings, which is ±0.2° for Ψ and ±0.4° for Δ, we can see that the experimental points lie on smooth curves. These curves are of exactly the same form as the reflectivity against time curves, with an initial plateau at a constant value of Ψ and Δ followed by a sudden change.

Similar measurements were made at the aluminium surface of a silver-aluminium diffusion couple (fig. 12.3).

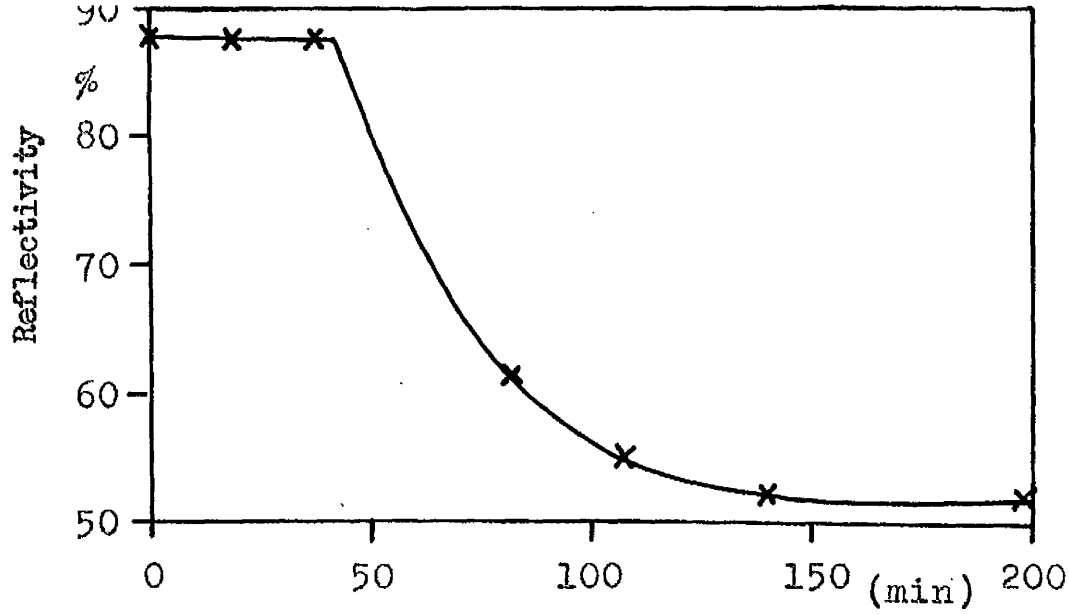

(a)

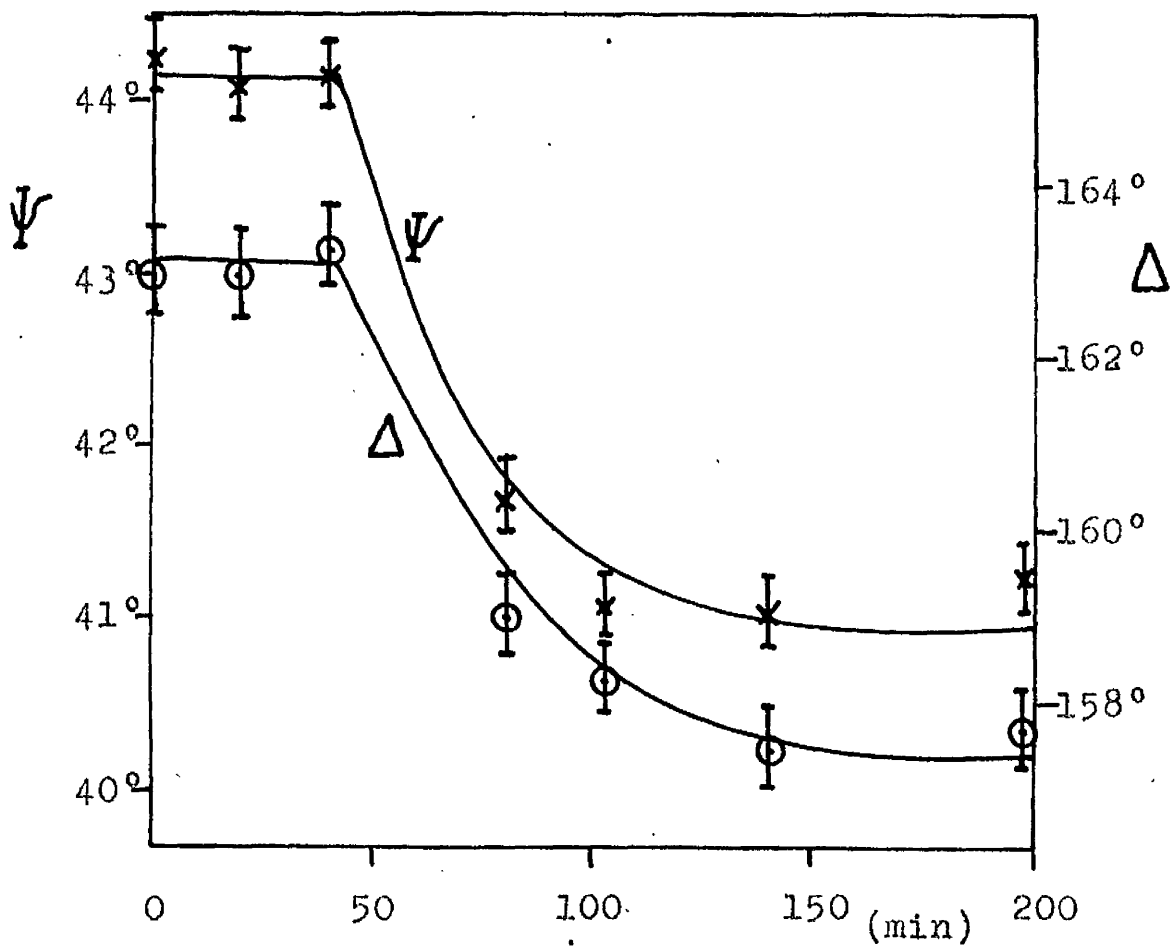

(b)

Fig. 12.2 Ageing of Gold-Aluminium Film at 105°C.

Variation of (a) reflectivity and (b) Ψ and Δ with time for an aluminium thickness of 820Å.

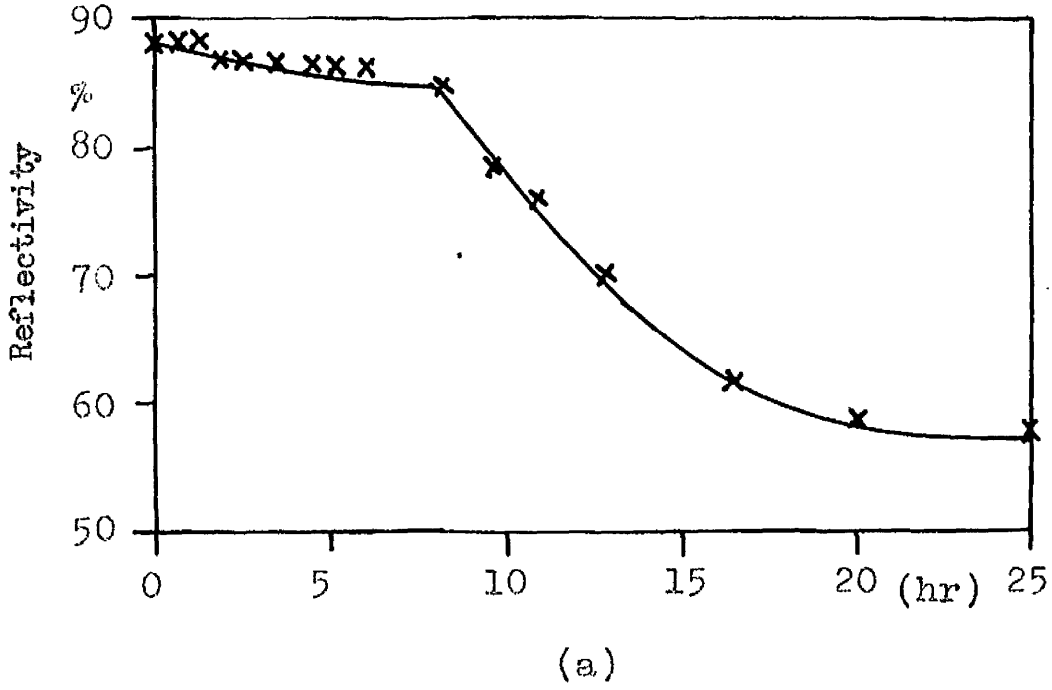

(a)

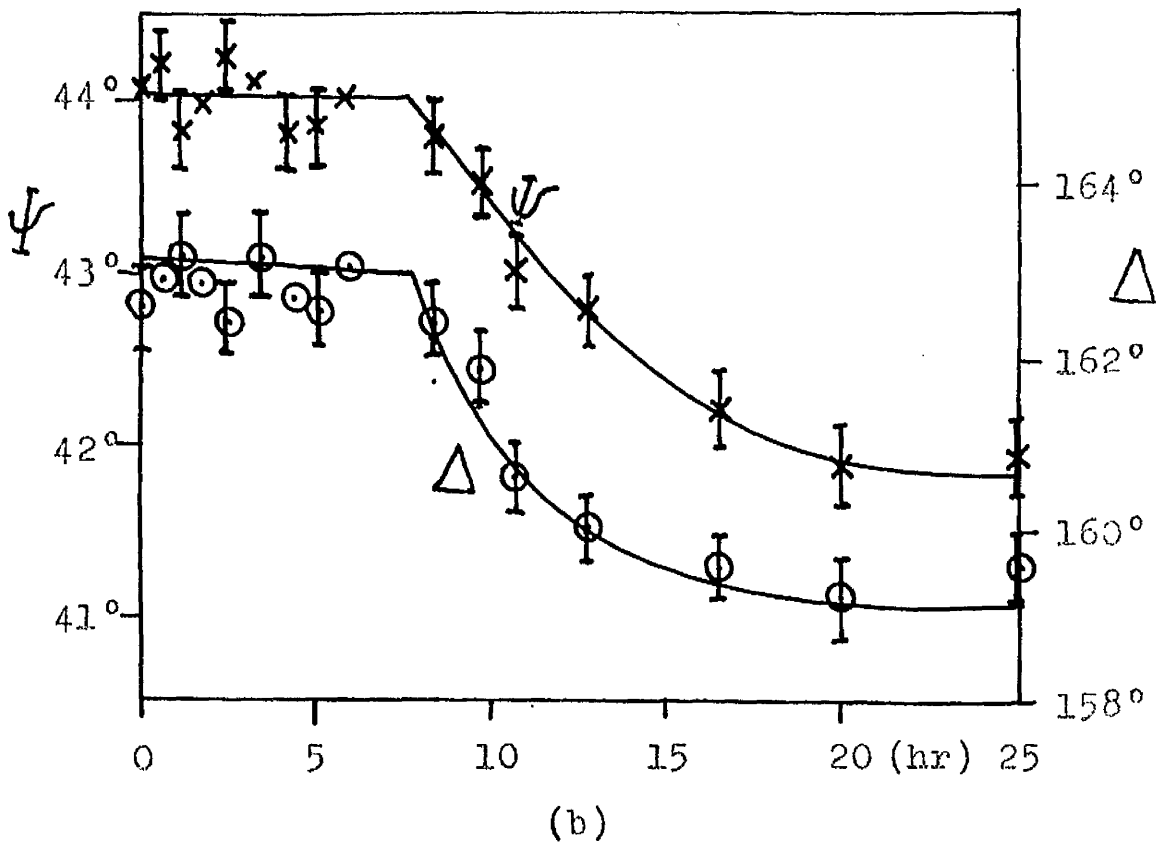

(b)

Fig. 12.3 Ageing of Silver-Aluminium Film at 141°C. Variation of (a) reflectivity and (b) Ψ and Δ with time for an aluminium thickness of 2400Å.

The graphs of and against time again had exactly the same form as the reflectivity against time graph. The variation in and being less than in gold-aluminium, there is more uncertainty as to the shape of the curves.

12.4 Discussion

Drude (1890) has derived equations for the refractive index of a metal surface in terms of Ψ, Δ and ϕ (the angle of incidence)

viz.

$$n = \frac{\sin\phi \tan\phi \cos 2\Psi}{1 + \cos\Delta \sin 2\Psi} \qquad (12.1)$$

$$k = n \sin\Delta \tan 2\Psi \qquad (12.2)$$

where the refractive index of the surface is given by

$$N = n - ik$$

In the case of aluminium, a layer of oxide approx. 50Å thick is present on the metal surface and equations (12.1) and (12.2) cannot be used. Expressions have been derived (Drude 1891) for the observed values of Ψ and Δ for a clean metal surface covered with a thin non-absorbing oxide film. The equations are, however, insoluble unless assumptions are made of the refractive index and thickness of the surface film. It is for this reason that the results have not been analysed in more detail to determine n and k and to work out the theoretical reflectivity values from them. Values of 44.0° and

162·9° for and of pure aluminium are in good agreement with the figures of 43·5° and 161·0° obtained by Winterbottom (1955) for the same experimental conditions.

Polarisation measurements gave ageing curves closely similar to those obtained by reflectivity measurements, and in particular the ratio t_1/t_2 seems to be the same for both. We must therefore conclude that light penetration into the metal has the same effect for both reflectivity and polarisation measurements. It might have been thought that polarisation measurements were more characteristic of the surface of the metal, as they are sensitive to the presence of surface oxide layers, but the experimental observations do not agree with this.

Reflectivity and polarisation observations give the same form of ageing curves, but reflectivity measurements are to be preferred because:

(a) reflectivity measurements are much more accurate

(b) reflectivity measurements can be made at both the glass and air surfaces

(c) reflectivity measurements are easy and quick.

CHAPTER 13

CONCLUSIONS

13.1 General Conclusions

It was shown in chapter 1 that the only method for finding diffusion coefficients in thin film diffusion couples was to measure the time required for one film to be completely penetrated by atoms of the other metal. Reflectivity measurements at the metal surface proved to be the simplest method for detecting the penetrating atoms, and the variation of reflectivity with time has been used to find diffusion coefficients and activation energies in nine metal systems.

The method gave repeatable results and proved to be very satisfactory. Reproducible ageing curves were generally obtained. The activation energies for diffusion were found using different portions of the one evaporated specimen. This gave most satisfactory graphs for finding the activation energy, since it did not involve measurements of film thickness with consequent errors.

The reflectivity changes in the systems investigated were characteristic of the motion of a phase boundary rather than of a gradual change in concentration. The

composition of the intermediate phase could usually be deduced from measurements of the value of the critical thickness ratio.

Most of the systems investigated gave reflectivity changes at both the glass and air surfaces. Measurements at the two surfaces always gave the same activation energies, indicating that the changes observed at both surfaces were due to the motion of only one of the constituent atoms. Measurements of the relative rates of diffusion at both surfaces gave a second check as to the phase or phases formed.

Evaporated alloy films were prepared either by "flash" evaporation or (in the case of copper-aluminium) by evaporation of the alloy. These enabled direct measurements of the reflectivity of the alloys to be made. Comparison with the refleotivity of the phase formed in the diffusion couple gave a third check as to the phase or phases formed.

Electron diffraction observations gave a direct indication of the phases formed in the diffusion zone. These results were generally in agreement with reflectivity observations.

The reflectivity changes were shown to be due, in

general, to the formation of a particular intermediate phase or phases. In some of the systems investigated, several phases appeared thermally stable at low temperatures, but the reflectivity changes appeared to be due to only one of the phases. There did not seem to be much correlation between the phases formed in different systems. In some systems (for example gold-lead) it seems probable that the published phase diagram is incorrect at low temperatures at which diffusion was studied, and that the compound formed was the only thermally stable phase. In the other systems it appears probable that all phases would be precipitated at the interface at the beginning of diffusion, but that one phase would grow faster than the others. According to Buckle's theory (chapter 2.9), the rate of growth of a phase depends on the diffusion coefficients and concentration limits involved. The phase that grows fastest may thus have any alloy concentration. Several of the phases formed appeared to exist over a zero concentration range. This was unexpected as it can be seen from equations (2·27) and (2·28) that these phases should not be formed. However, in terms of the atomic movements discussed in the next section, this is not surprising.

Diffusion coefficients and activation energies were found to be the same in very thin films (< 300Å) as in

thicker films, indicating that the diffusion observed was a true volume diffusion rather than grain boundary diffusion. This does not agree with the theory given in 2.10. For diffusion in gold-aluminium at 84°C, if the activation energy for grain boundary diffusion is taken to be 50% of that for volume diffusion, the ratio D'_{gb}/D'_{v} is found equal to 10^{7}. In 2.10 it was shown that if D'_{gb}/D'_{v} was 10^{5} or greater, then grain boundary diffusion should be the dominant method for transport of atoms. It is therefore surprising that grain boundary diffusion is not occurring, particularly since thin films are known to contain large numbers of grain boundaries. The diffusion observed is of rather a special kind, however, since it gives rise to intermediate phases. It would be very difficult to imagine this diffusion taking place along a grain boundary.

Observations on most of the metal films investigated have shown that values for diffusion coefficient and activation energy in thin films are similar to bulk values for diffusion in the faster direction (i.e. for diffusion into the lower melting point metal). The observed diffusion coefficients at the other metal surface were then due simply to the loss of metal in the formation of intermetallic compound.

Several of the systems examined had considerable solid solubility in the higher melting point component. In no case, however, was any trace of this solid solution visible on ageing, which shows that the amount formed was very small. This suggests again that diffusion into the low melting point metal is the rate determining process, and so only a very thin layer of alloy rich in the higher melting point metal will be formed. None of the systems investigated had any considerable solid solubility in the lower melting point metal, since this was the higher valency one (Hume - Rothery and Raynor 1956). Consequently solid solutions might be formed, but would not be detected.

The phase boundary was frequently sharply defined, but in certain metal pairs a diffuse boundary was observed. This was attributed either to penetration of the substrate metal during evaporation of the overlayer, or to the effects of an initial fast diffusion to form supersaturated solid solution before precipitation of the compound. This initial fast diffusion was apparently characteristic of the first stages of diffusion before equilibrium conditions were established across the phase boundary. Kirkaldy (1958) has discussed this effect, and considers that non-equilibrium conditions could exist in a diffusing system for experimentally significant times, the effect appearing as deviations from the parabolic law, $x^2 = D't$, near the

time origin. Such a deviation was observed in the present investigation. This effect could only be observed in thin film diffusion couples which measure the first stages of diffusion. Bulk diffusion couples would never show this effect, and all investigations on them have found the parabolic law to be obeyed.

13.2 Atomic Mechanism for Diffusion

The experimental observations discussed in the previous section enable a mechanism for the flow of atoms in a diffusion couple to be deduced. Consider a couple of two metals A and B with negligible terminal solid solution and one intermediate phase, γ, (fig. 13.1). We will assume that B has a higher melting point than A, i.e. that diffusion of B to A is the rate determining process. The mechanism of diffusion is the same as in bulk specimens and is a true volume diffusion. Interstitial diffusion is generally unlikely, since the atoms of, for example, silver and aluminium are almost identical in size. Furthermore, observations of the thickness of several diffusion couples showed that there was no change in thickness after diffusion, such as would occur if interstitial diffusion was taking place. Hence the diffusion is most probably a vacancy mechanism. Diffusion of metal from B to A implies a migration of vacancies from A to B.

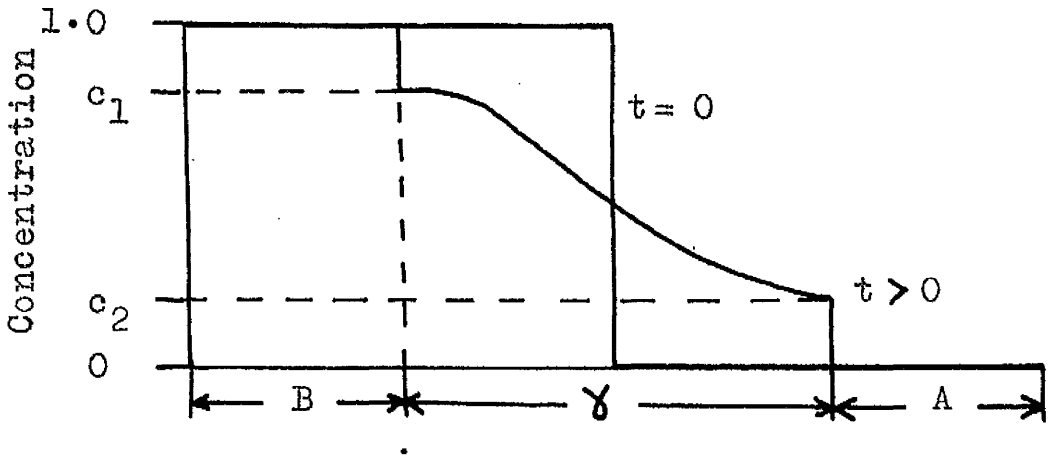

Fig. 13.1 A Diffusion Couple in an Intermediate Phase System with No Terminal Solubility.

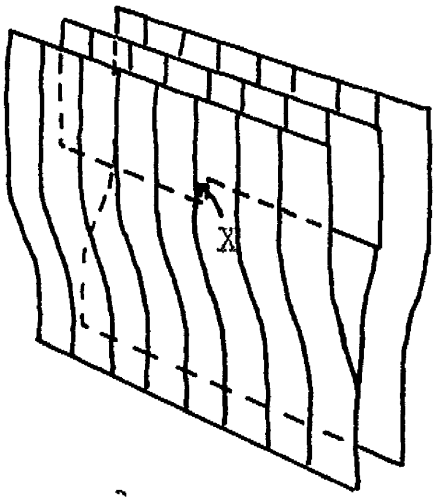

Fig. 13.2 Diagram of an Edge Dislocation with Jog at X.

Vacancies generated in metal A close to the γ surface tend to become occupied by atoms of B. Metals B and A react to form more γ phase, and vacancies move into the γ layer. Vacancies in the γ surface close to the interface with metal B would tend to become occupied by atoms of B from the pure metal, and the vacancies would move into the pure metal. If the mean vacancy concentration in the phase remains constant, there must be steady drift of vacancies from A to B causing the processes at the two interfaces to take place at the same rate, and giving rates of diffusion in agreement with the experimental observations. The γ phase would advance into A at one side, and would appear to advance into B at the other, the measured rates of diffusion differing because of the atomic ratio in the compound.

The source of the vacancies is of great interest. A certain number exist in thermal equilibrium in a metal at low temperatures (approximately 1 in 10^6 lattice sites), but this number is far too small to account for the observed mass flow. Thin films are known to contain large numbers of vacancies (Seitz 1946), and it might be thought that these gave the observed mass flow. In equation 2.11 it has been shown that the rate of diffusion depends on the vacancy concentration and on the height of the potential barrier, so that the overall activation energy is made up of

two terms, the activation energy to form vacancies and the activation energy for their motion. The two terms are generally found to be approximately equal. If the excess vacancies in thin films were responsible for diffusion, E would be around half the values observed in bulk specimens, and D' would be many orders of magnitude higher. This is not in agreement with the experimental values, and so we must conclude that large numbers of vacancies are generated in metal A near the interface with the γ phase, and that these are absorbed in metal B. According to Le Claire (1958), dislocations act as ideal sources and sinks for vacancies, and thin films are known to have large numbers of dislocations (Bassett Menter and Pashley 1958). A jogged edge dislocation is shown in fig. 13.2. If an atom at X moves one place to the right, a vacancy is left at X and this may then diffuse away by exchange with other atoms. If this is repeated for all the planes shown in the diagram, the dislocation will move across from one side of the crystal to the other, to form a new plane of atoms and to provide an equal number of vacancies. Accomodation is therefore provided for the net number of atoms of B diffusing into A (fig. 13.1) by the very process which produces vacancies for their transfer.

A jogged dislocation can similarly act as a sink for vacancies. Motion of the vacancy to X (fig. 13.2)

moves the jog one position to the left and results in the elimination of the vacancy. Adding one plane of vacancies to the dislocation removes one plane of atoms from the metal. Hence in fig. 13.1, metal B becomes thinner because of the absorption of large numbers of vacancies.

It can be shown (van Bueren 1960) that in a normal metal, dislocations can easily supply the necessary number of vacancies in this way.

Incoherent phase boundaries?

13.3 Future Work

It is considered that certain lines of investigation arising out of the present work could be tackled and might lead to interesting results.

Most of the interesting systems giving reflectivity changes in thin film diffusion couples have been investigated, and it seems unlikely that a more extended investigation would give much more useful information. Copper-zinc would, however, be an interesting system to study. Coleman and Yeagley (1943) have studied reflectivity changes at the zinc surface in this system and state that that the activation energy of diffusion was the same as in bulk specimens, but that K_o was several orders of magnitude higher. The formula (1.1) used by Coleman and Yeagley was purely empirical, but it can be shown that in

the practical case, where the copper thickness is much greater than the zinc thickness, the value of K_o is very close to the value of D_o' used in the present investigation. It would be interesting to check the results on this system to see whether agreement was obtained with Coleman and Yeagley. If D' is found to be four orders of magnitude higher than in bulk specimens, it will be totally different from the results found in the present investigation. A theoretical explanation for this discrepancy would be very difficult to find. The explanation given by Coleman and Yeagley (1944) in terms of preferred orientation in the precipitated layer seems most unlikely, since it involves assuming a (111) fibre orientation in a copper film on a glass substrate. Such an orientation has never been observed by other workers.

The whole question of the orientation of the precipitated layer is of great interest. Work on age-hardening indicates that there is a relation between the orientation of the phase precipitated and the bulk matrix (Barrett 1952). Woo Barrett and Mehl (1944) have found the same orientation relation in a diffusion layer of β -brass on copper as in age-hardening. No work has been carried out on this subject in thin films. In the present investigation the substrate metal was always randomly oriented and no effect would be visible by electron diffraction.

The problem could be studied very conveniently by preparing a single crystal gold film, using the method of Pashley (1959) of evaporating onto a silver film deposited on a mica surface held at 270°C. The silver could then be dissolved away in nitric acid to leave a single crystal gold film. Evaporating aluminium on top would give two metals with the same orientation. On ageing of this specimen, precipitation of the compound would take place, and by studying the extra spots in the diffraction photograph, it should be possible to determine the orientation of the precipitated layer, and check whether it is the same as in age-hardening.

Observing the variation of adhesion is one of the most sensitive methods for studying the first stages of diffusion in thin films (Weaver and Hill 1958, 1959). In this method the hardness of the intermediate zone is measured, and phenomena similar to those found in age-hardening in bulk metals are observed. It would be interesting to know how far diffusion had proceeded before precipitation of the new phase could be detected by adhesion measurements. By measuring the variation of adhesion with time in the systems studied by reflectivity observations, it should be possible to study this. This effect is at present being investigated (Parkinson 1961).

Reflection electron diffraction would be a useful technique for repeating the results obtained in the present investigation, and for studying systems in which reflectivity changes could not be observed. It was unfortunate that no such instrument was available in the present work.

In the course of the present work the author has been surprised at the lack of existing results in bulk diffusion couples with the pure metals. Very few observations have been made of the motion of phase boundaries in diffusion couples (Buckle 1946 1957 1958, Kirkaldy 1958, Philibert and Adda 1958). It is felt that these observations might well be extended.

REFERENCES

C.S. Barrett	(1952)	"Structure of Metals" 2nd Ed. (New York, McGraw-Hill). p. 538.
G.A. Bassett, J.W. Menter & D.W. Pashley	(1958)	Proc. Roy. Soc. A246, 345.
A. Beerwald	(1939)	Z. Elektrochem. 45, 789.
R.B. Belser	(1960)	J. Appl. Physics, 31, 562.
P. Benjamin & C. Weaver	(1961)	Proc. Roy. Soc. A261, 516.
A.J. Bradley & P. Jones	(1933)	J. Inst. Metals. 51, 131.
R.M. Brick & A. Philips	(1937)	Metals Technology. 4. Tech. Publ. No. 781.
H. Brooks	(1955)	"Impurities and Imperfections." (Cleveland, Ohio: Am. Soc. for Metals).
H. Buckle	(1946)	Metallforschung. 1, 175.
H. Buckle & J. Blin	(1950)	J. Inst. Metals. 80, 385.
H. Buckle	(1957)	Rev. de Metallurgie. 54, 16.
H. Buckle	(1958)	Colloquium on Solid State Diffusion: Saclay, France. (Amsterdam: North Holland Publ. Co.) p. 170.
H.G. van Bueren	(1960)	"Imperfections in Crystals." (Amsterdam: North Holland Publ. Co.) p. 422.

A.A. Burr, H.S. Coleman & W.P. Davey (1944) Trans. Am. Soc. Metals. 33, 73.

H.S. Carslaw & J.C. Jaeger (1959) "Conduction of Heat in Solids." (Oxford: Clarendon Press). p. 101

A.S. Coffinberry & R. Hultgren (1938) Trans. A.I.M.M.E. 128, 249.

H.S. Coleman & H.L. Yeagley (1943) Trans. Am. Soc. Metals. 31, 105.

H.S. Coleman & H.L. Yeagley (1944) Phys. Rev. 65, 56.

J. Crank (1956) "The Mathematics of Diffusion" (Oxford: Clarendon Press). p.8.

L.S. Darken (1948) Trans. A.I.M.M.E. 171, 184.

P. Drude (1890) Weid. Ann. 36, 481.

P. Drude (1891) Weid. Ann. 43, 126.

S. Dushman (1949) "Scientific Foundations of Vacuum Technique." (New York: John Wiley).

A. Fick (1855) Ann. Phys. 170, 59.

J.C. Fisher (1951) J. Appl. Physics. 22, 74.

R. Fleischmann & H. Schopper (1951) Z. Physik. 129, 285:
do. 130, 304.

Y. Fujiki (1959) J. Phys. Soc. Japan. 14, 913.

S. Glasstone, K.J. Laidler & H. Eyring (1941) "The Theory of Rate Processes." (New York: McGraw-Hill)

Handbook of Chemistry and Physics (1957) 39th Ed. (Cleveland, Ohio: Chem. Rubber Publ. Co.) p. 2731.

M. Hansen (1958) "Constitution of Binary Alloys." (New York: McGraw-Hill).

L. Harris & B.M. Siegel	(1948)	J. Appl. Phys. 19, 739.
L. Holland	(1954)	Vacuum. 2, 385.
L. Holland	(1958)	"Vacuum Deposition of Thin Films." (London: Chapman and Hall).
W. Hume-Rothery & G.V. Raynor	(1956)	"The Structure of Metals and Alloys" (London: Inst. of Metals). p. 108.
J.S. Kirkaldy	(1958)	Can. J. Phys. 36, 917.
H.B. Huntington & F. Seitz	(1949)	Phys. Rev. 76, 1728.
A. van Itherbeck, L. de Greve, G.F. van Veelen & C.A.F. Tugneem	(1952)	Nature. 170, 795.
W. Jost	(1952)	"Diffusion in Solids, Liquids and Gases" (New York: Academic Press).
O.J. Kleppa & D.F. Clifton	(1951)	Acta Cryst. 4, 74.
A. Kuper, H. Letaw, L. Slifkin, E. Sonder, C. Tomizuka	(1955)	Phys. Rev. 98, 1870.
D. Lazarus	(1960)	Solid State Physics. 10, 71.
A.D. Le Claire	(1949)	Progress in Metal Physics 1, 370.
A.D. Le Claire	(1953)	Progress in Metal Physics 4, 265.
H. Lowery & R.L. Moore	(1932)	Phil. Mag. (7). 13, 938.
C. Matano	(1934)	Japan J. Phys. 9, 41.
P. Michel	(1956)	Thesis, University of Strasbourg.

N.F. Mott & R.W. Gurney	(1940)	"Electronic Processes in Crystals." (Oxford: Clarendon Press).
D.T. Parkinson	(1961)	Private Communication.
D.W. Pashley	(1959)	Phil. Mag. (8). 4, 324.
J. Philibert & Y. Adda	(1958)	Colloquium on Solid State Diffusion: Saclay, France. (Amsterdam: North Holland Publ. Co.) p. 156.
E. Raub & M. Engel	(1943)	Z. Elektrochem. 49, 89.
P. Rouard, D. Malé & J. Trompette	(1953)	J. Phys. Radium. 14, 587.
H. Schopper	(1955)	Z. Physik. 143, 93.
F. Seitz	(1946)	Reviews of Modern Physics. 18, 384.
R.S. Sennett & G.D. Scott	(1950)	J. Opt. Soc. Am. 40, 203.
L.C.C. da Silva & R.F. Mehl	(1951)	Trans. A.I.M.M.E. 191, 155.
A.D. Smigelskas & E.O. Kirkendall	(1947)	Trans. A.I.M.M.E. 171, 130.
S. Tolansky	(1948)	"Multiple-Beam Interferometry." (Oxford: Clarendon Press). p147.
L. Tronstad & C.G.P. Feachem	(1934)	Proc. Roy. Soc. A145, 115.
C. Wagner	(1952)	Quoted in W. Jost (1952) "Diffusion in Solids, Liquids and Gases." (New York: Academic Press). p. 74.
W. Walkenhorst	(1941)	Z. Tech. Phys. 22, 14. (see O.S. Heavens (1955) "Optical Properties of Thin Solid Films." (Butterworths: London). p. 167.)

C. Weaver & R.M. Hill (1958) Phil. Mag. (8). 3, 1402.

C. Weaver & R.M. Hill (1959) Phil. Mag. Supplement. 8, 375.

W. Winterbottom (1955) "Optical Studies of Metal Surfaces." (D. Kgl. Norske V.S. Skrifter. No. 1) p. 122.

S. Woo, C.S. Barrett & R.F. Mehl (1944) Trans. A.I.M.M.E. 156, 100.

J. Wulff (1934) J. Opt. Soc. Am. 24, 223.

C. Zener (1950) Acta Cryst. 3, 346.

GENERAL REFERENCES AND BACKGROUND READING

C.S. Barrett — "Structure of Metals" (1952) (New York: McGraw-Hill) 2nd. Ed.

A.H. Cottrell — "Theoretical Structural Metallurgy" (1955) (London: Arnold & Co.) 2nd. Ed.

O.S. Heavens — "Optical Properties of Thin Solid Films" (1955) (London: Butterworths) 1st. Ed.

L. Holland — "Vacuum Deposition of Thin Films" (1956) (London: Chapman & Hall) 1st. Ed.

W. Jost — "Diffusion in Solids, Liquids and Gases" (1952) (New York: Academic Press) 1st. Ed.

A.D. Le Claire — "Progress in Metal Physics" (1949) 1, 370. (1953) 4, 265.

DIFFUSION IN EVAPORATED FILMS OF GOLD - ALUMINIUM

by

C. Weaver and L.C. Brown

Department of Natural Philosophy

The Royal College of Science and Technology, Glasgow

ABSTRACT

Diffusion coefficients and activation energies for diffusion in successively evaporated films of gold and aluminium have been determined by observing the changes in reflectivity at the gold and aluminium surfaces on annealing. The changes were characteristic of a sharply defined reaction boundary rather than of a gradual change in concentration. The variations with film thickness showed that this was a phase boundary caused by the formation of the intermetallic compound Au_2Al. The presence of this compound was confirmed by electron diffraction. Results indicated a vacancy diffusion mechanism rather than grain boundary diffusion.

1. INTRODUCTION

Metal films of uniform thickness can easily be produced by vacuum deposition. When two such films are deposited one on top of the other and the resultant bimetallic film is annealed, diffusion will generally occur (unless the metals are completely immiscible), giving rise to solid solutions or intermetallic compounds or both. In some cases compound formation has been confirmed by electron diffraction or deduced from other measurements such as electrical resistance or adhesion (Weaver and Hill 1959).

The information obtained from such measurements is, however, essentially qualitative in nature and more detailed knowledge of the diffusion mechanism is desirable. Diffusion coefficients are usually measured in bulk couples by annealing for a suitable period and then investigating the distribution by sectioning or other techniques. With thin metal films it is more convenient to measure the time required for one film to be penetrated completely by atoms of the other metal. The simplest way of detecting the penetrating atoms is to measure the variation of reflectivity at the surface with time, and this technique has been used by Schopper (1955) for

studying the diffusion of lead into gold. He found that the reflectivity remained constant for a time at the reflectivity of the pure solvent metal and then dropped to a figure close to that of lead. Varying the thickness of the gold did not vary the shape of the ageing curve but simply altered the time scale. The curves could be made to coincide by plotting the values of reflectivity against t/d^2, where d is the thickness of the gold. On the basis of a rigorous analysis of his results, Schopper concluded that the reflectivity changes were due to the formation of an intermetallic compound ($AuPb_2$), and that the concentration of this compound at the surface increased continuously with time.

This method of measuring changes in reflectivity has been used to study the interdiffusion of thin films of aluminium and gold. Changes occur at both metal surfaces, and measurements have been made for diffusion in both directions. The gold was always deposited before the aluminium to prevent the possible formation of an oxide layer on the aluminium which might hinder diffusion (Belser 1960).

2. EXPERIMENTAL

Films were evaporated onto glass microscope

slides which were carefully cleaned with Teepol and polished with lens tissue before insertion in the vacuum chamber. The slides were finally exposed to a glow discharge for 10 min during the pumping cycle. The evaporations were carried out in a glass bell-jar evacuated by an oil diffusion pump using Apiezon oil, which produced pressures of $2-5 \times 10^{-5}$ mm of mercury as measured by an ionization gauge. The slides were supported on a jig 20 cm above the evaporating heaters, and the jig could be rotated so that the slides lay directly above each heater in turn, thus ensuring that the film thickness did not vary significantly over the surface of the slide.

The gold was evaporated from a molybdenum boat at a rate of approximately 70 Å/sec over the whole area of the slide, a step being left clear at one edge for thickness measurements. Aluminium was then evaporated on top of the gold, there being a delay of around 1 min between the two evaporations. The aluminium was evaporated at a rate of approximately 90 Å/sec from a spiral of 1 mm stranded tungsten wire. A step was again left clear for thickness measurements. Finally an opaque silver film was deposited over the steps at the edge of the slide. The slide was removed from the chamber, and

the thicknesses of the gold and aluminium films were found by multiple-beam interferometry measurements at the steps on the edge of the slide, using Fizeau fringes as described by Tolansky (1948).

For reflectivity changes taking 3 hr or longer, the slides were annealed in a hot air oven thermostatically controlled at the appropriate ageing temperature, and were removed at regular intervals for reflectivity measurements. The reflectometer had a mercury discharge tube as the light source, and measurements were made by comparing the light intensity reflected by the slide under measurement with the ½ intensity of the undeviated light beam, the intensity being measured by a photomultiplier cell. Allowance had to be made for the time taken by the slide to regain the temperature of the oven. For periods under 3 hr this allowance led to considerable errors, and a reflectometer was designed for these measurements in which the reflectivity could be measured whilst the slide was being heated, this being based on the design of Coleman and Yeagley (1943). The "hot stage" reflectometer allowed ageing processes of duration as short as 2 min to be investigated, and in conjunction with the hot air oven, ageing periods of from 2 min to 40 hr or more could be covered.

3. RESULTS

At the beginning of annealing we would expect all thermally stable phases to be precipated at the gold-aluminium interface, since there is an initial gradient of concentration from pure gold to pure aluminium, and this would permit all compounds to be formed. According to the phase diagram of gold-aluminium (Hansen 1958), the compounds $AuAl_2$, AuAl, Au_2Al, Au_5Al_2 and Au_4Al should all be formed.

3.1 Reflectivity Changes at Gold Surface.

Slides were prepared with gold films of different thicknesses in the range 400Å to 3000Å. In each case the gold was overlaid with a thick film of aluminium, so that all reflectivity changes at the gold surface were complete before any change took place at the surface of the aluminium. The slides were aged at 84°C, and a typical ageing curve is shown in fig. 1. The reflectivity change with mercury yellow light (34%) was greater than for mercury green light (25%) or mercury blue light (20%), and has been used for all subsequent measurements. The effect of change in gold film thickness is shown in fig. 2, in which the reflectivity is plotted as a function of t/d^2, where d is the gold thickness.

According to Schopper's theory of a progressive change in surface composition, curves of different thicknesses should coincide when plotted against t/d^2. As shown in fig. 2, however, the curves coincide only at the beginning and end, and the position of the break in the curves varies with film thickness. It therefore appears that in this system, Schopper's theory is inapplicable.

It is well known that light waves can penetrate a small but finite distance into a metal, and it seems reasonable that the advancing atoms are detected before they reach the surface. The abruptness of the reflectivity change in fig. 2 suggests that the advancing front is fairly sharply defined. We should not expect a small concentration of aluminium atoms some distance from the surface to produce a marked change of reflectivity. Small proportions of silver in aluminium produce only small changes in reflectivity (Wulff 1934), and an analogous effect might be expected for small additions of aluminium to gold. These considerations, together with the low solubility of aluminium in gold, suggest that the reflectivity changes are produced by a sharply defined phase boundary.

It has been shown (Kirkaldy 1958) that the motion

of such a boundary should follow the law $x^2 = D't$, where x is the distance the boundary moves from the initial interface in a time t, and D' is the diffusion coefficient for the boundary. Assuming this relation in the case of a gold film 1000Å thick, the time required for the phase boundary to reach the glass surface, i.e. for the reflectivity to stop changing, is $t_2 = 10^{-10}/D'$ sec. Assuming that light can penetrate 400Å into a gold film, then the time for the reflectivity to start changing would be the time taken for the reaction boundary to penetrate (1000 - 400) Å, i.e. $t_1 = 3{\cdot}6\times10^{-11}/D'$ sec. Hence the ratio of the time taken for the reflectivity to begin changing to the time taken for the reflectivity to cease changing is given by

$$\frac{t_1}{t_2} = \frac{3{\cdot}6\times10^{-11}}{D'} \cdot \frac{D'}{10^{-10}} = 0{\cdot}36$$

This ratio was found for different values of film thickness, and in fig. 3 graphs gold thickness against ratio have been plotted for light penetrations of 300Å, 400Å and 500Å. The experimental ratios have also been plotted on this graph, and it can be seen that the points all lie close to the line for 400Å penetration. This is a reasonable value for the thickness of a near opaque gold film, and the close agreement of the experimental values with the theoretical curve suggests

that this theory is correct, and that the reflectivity changes are due to the motion of a sharply defined phase boundary rather than to a gradual change in concentration such as would occur if atoms in the gold lattice were progressively replaced by aluminium atoms.

Values of the diffusion coefficient, D', were calculated from the time taken for the reflectivity to stop changing. These results are plotted in fig. 4, which shows that although there is a slight spread in D' values, there is no tendency for D' to vary with gold thickness. The mean value of D' at 84°C was found to be 1.01×10^{-14} cm^2/sec.

Different portions of the same slides were aged over a range of temperature from 70°C to 164°C. The time of diffusion for a film 2620Å thick varied from 15 hr at 84°C to 4 min at 164°C, but the shape of the curve did not vary despite this vast change in time. The diffusion coefficient, D', will vary with temperature according to the Arrhenius equation

$$D' = D_0' \exp(-E/RT)$$

where E is the activation energy of diffusion in (cal/mole), R is the universal gas constant, and T is the absolute temperature.

Therefore

$$\log_{10}(1/D') = \log_{10}(1/D'_0) + E/2{\cdot}3\,RT$$

But $$D' = (d^2/t_2)$$

where d is the gold thickness. It is found experimentally that the shape of the ageing curve does not vary with temperature, and consequently,

$$t_2 = k\,t_{60}$$

where t_{60} is the time for the reflectivity to drop to, say, 60%, and k is a constant.

$$\therefore \log_{10}t_{60} = \log_{10}(d^2/D'_0\,k) + E/2{\cdot}3\,RT$$

$$\therefore \log_{10}t_{60} = K + E/2{\cdot}3\,RT$$

where K is a constant. Plotting $\log_{10}t_{60}$ against (1/T) should give a straight line with gradient (E/2·3 R). This has been carried out in fig. 5 for slides with different gold thicknesses. The gradients of the lines are all equal since this depends only on E, but the lines are shifted relative to each other. The activation energy was calculated to be 22·6 kcal/mole, and knowing D' at 84°C, D'_0 was calculated to be 0·65 cm^2/sec.

Several slides were prepared with very thin gold films in the thickness range 70Å to 350Å. These film thicknesses were determined by measuring the reflectivity and transmission of the films, and using the results of Rouard Malé and Trompette (1953) to obtain the thickness.

No initial plateau was found in any of the ageing curves as the gold was not opaque, and the moment any diffusion occurred at the interface with the aluminium, the reflectivity began to fall. The very thinnest film (70Å) gave only a very small reflectivity change (4%), as the diffusion zone in this case was very thin. Slides were aged over the temperature range 20°C to 95°C, and the activation energy of diffusion was found to be 23·3 kcal/mole, in excellent agreement with the values for thicker films (22·6 kcal/mole). Values of D' were calculated from the time taken for the reflectivit to stop varying. These values were converted to 84°C using the value for activation energy, and have been plotted with the previous results in fig. 4. We can see from this graph that there is no significant difference in D' for these very thin films compared with thicknesses greater than 400Å. Furthermore, the activation energy is the same, which suggests that the same diffusion mechanism holds in films from 70Å to 3000Å thick.

3.2 Reflectivity Changes at the Aluminium Surface

Reflectivity changes were measured at the aluminiu surface using very thick gold substrate films, so that all reflectivity changes at the aluminium surface were

complete before any change took place in the reflectivity of the gold. Results obtained at 102°C for aluminium thicknesses in the range 500Å to 1700Å are shown in fig. 6, plotted against t/d^2. The length of the initial plateau increased with aluminium thickness, and the results in general resembled those for diffusion in the opposite direction. It therefore seems likely that here also we have a sharply defined reaction boundary, and to check this, values of the ratio t_1/t_2 were calculated for all the specimens prepared. It was found that the points all lay close to the curve for a light penetration of 300Å. This is a reasonable figure for the thickness of a near opaque aluminium film. It is less than the corresponding light penetration into gold (400Å) which was found for diffusion of aluminium into gold, but this is not surprising, since the absorption coefficient (k) is greater for aluminium films (5·32) than for gold films (2·83) (Handbook of Chemistry and Physics 1957).

This tends to confirm that the reflectivity changes are again due to the motion of a phase boundary. This is to be expected, since the solid solubility of gold in aluminium is almost negligible, and so any gold atoms diffusing into aluminium would be closely followed

by a phase boundary.

Values of D' at 102°C were calculated for all the slides prepared from the time taken for the reflectivity to stop changing. The mean value of D' was found to be 8.2×10^{-15} cm^2/sec, and the results showed no tendency for D' to change with increasing aluminium thickness.

Different portions of the same slides were aged over a temperature range from 70°C to 152°C. From a graph of $\log_{10} t_{60}$ against (1/T), the activation energy was calculated to be 23·5 kcal/mole. From the known value of D' at 102°C, D'_0 was found to be 0·51 cm^2/sec.

3.3. Effect of Thickness Ratio

Several slides were prepared with a single layer of gold but with four separate aluminium films of different thicknesses. The complete slides were aged at 84°C, and a typical reflectivity curve at the gold surface is shown in fig. 7 for a gold thickness of 1450Å. An aluminium thickness of 0·61 or more times the gold thickness gave the full reflectivity change, but if the aluminium thickness was only 0·19 times the gold thickness, no reflectivity change took place. This suggested a critical thickness of aluminium between 0·61

and 0·19 of the gold thickness, such that the aluminium was just thick enough for the full reflectivity change to be obtained. From this and from the four other slides prepared, it was verified that the effect depends on the thickness ratio rather than on the absolute thicknesses of the films, and the critical thickness ratio of aluminium to gold was found to be 0·5. If the aluminium was greater than half the gold thickness, the full reflectivity change took place. If the aluminium was less than half the gold thickness, no reflectivity change occurred at the gold surface, and it would appear that the diffusing boundary did not reach the gold surface. Since the lattice spacings of gold and aluminium are nearly identical, this seems to imply that behind the boundary there must be at least one aluminium atom for every two gold atoms.

Reflectivity changes at the aluminium surface were similarly studied with slides having a single aluminium layer, but with three separate gold films of different thicknesses, the ageing being studied at 84°C. It was again found that there was a critical ratio of gold to aluminium below which the full reflectivity change at the aluminium surface was not obtained. From the six slides prepared it was verified that the effect depends

on the thickness ratio of the slides and the critical thickness ratio was found to be 2·0.

This result seems to indicate that behind the phase boundary there must be at least two gold atoms for every one aluminium atom. From measurements at the gold surface, we have already concluded that there must be at least one aluminium atom for every two gold atoms. This seems to suggest that there is preferential formation of a compound with one aluminium atom associated with two gold atoms i.e. with composition Au_2Al.

Values of critical ratio have been observed at 84°C. The value will vary with temperature, however, unless the activation energy in both directions is identical. The activation energy at the gold surface was found to be 22·6 kcal/mole, whilst that for diffusion into the aluminium was found to be 23·5 kcal/mole. The figures are close to one another, and it seemed likely that the difference between them was due to experimental error in their determination. This was checked by preparing a specimen with gold thickness twice the thickness of the aluminium, so that reflectivity measurements could be made at both surfaces. By ageing at two widely separate temperatures it was found that the curves at both surfaces remained the same

relative to each other at the two temperatures, indicating that the activation energies are equal in the two directions. Hence the value of the critical ratio must be the same for all temperatures.

3.4. Structural Investigation

An electron diffraction investigation was carried out on thin gold-aluminium films to see whether this would give any information on the compounds formed during diffusion.

Thin films of gold (100Å) and aluminium (120Å) were evaporated onto a glass slide and formvar covered copper grids placed side by side in the vacuum chamber. Three grids were prepared, one with pure aluminium, one with pure gold, and one with a composite film of aluminium and gold. Immediately after evaporation, transmission diffraction patterns of the three films were obtained using an electron microscope. Care was taken throughout the investigation to use the same lens settings on the microscope so that the magnification of all the photographs was the same. The aluminium and gold grid and the glass slide were both inserted in a hot air oven at 58°C and were aged for $\frac{1}{4}$ hr. On removal a second diffraction photograph was taken and the reflectivity

of the glass slide was found. This was repeated for net ageing periods of 1 hr, 2 hr, 4 hr, and 15½ hr, and it was found that reflectivity changes occurred only during the first hour of ageing.

Diffraction photographs of pure gold and pure aluminium are shown in fig. 8 (a) and (b). The ring diameters of aluminium and gold are almost exactly equal, since they have similar f.c.c. structures with a lattice spacing of 4·08Å for gold and 4·05Å for aluminium. The ring diameters on these plates were measured using a low power travelling microscope. The corresponding d spacings could be calculated, and hence the magnification produced by the projector lens of the microscope was obtained. It was then possible to calculate the d spacing for any diffraction ring in other photographs since the magnification was kept constant. Fig. 8 (c) shows the composite film immediately after evaporation. The rings are characteristic of pure aluminium and pure gold and no trace of intermetallic compounds is seen. Ageing for $\frac{1}{4}$ hr also gave a photograph showing rings of the pure metals only. After ageing for 1 hr, however, extra rings became visible (fig. 8 (d)). Ageing for further periods up to 15½ hr did not produce extra rings, nor any change in the relative intensities of the rings

(fig 8 (e)), and the reflectivity remained constant. This shows that the reflectivity changes are associated with diffusion and the formation of intermetallic compounds. Presumably a thin layer of compound had been formed after $\frac{1}{4}$ hr, but any diffraction effects of this layer would be obscured by the patterns from the thicker aluminium and gold layers.

The ring diameters of the photograph after 1 hr ageing were analysed in some detail to see whether particular intermetallic compounds could be identified. The results are shown in table 1. The probable presence of Au_2Al in the diffusion zone has been shown from measurements of the effect of the thickness ratio. Unfortunately, the structure of this phase is complex and has not been determined (Goffinberry and Hultgren 1938). The d spacings of this phase were found experimentally by taking a powder photograph of grains filed from a bulk specimen of the alloy. These results are shown in column 5 of table 1, and it can be seen that good agreement was obtained with the observed d spacings in the diffraction photograph. Rings were observed in the photograph which could not be explained by Au_2Al or by the pure metals (column 6). It was found that d spacings for the compound AuAl (f.c.c., a = 6·00Å) fitted these

remaining rings satisfactorily (column 7). Rings at d spacings of 2·69Å, 2·08Å and 1·59Å could, however, be due only to Au_2Al.

From these results we must conclude that for these thin films, Au_2Al and $AuAl_2$ are both formed in the diffusion zone. Presumably small quantities of other phases were present, but but any diffraction effects were masked by the large quantities of the main phases.

4. CONCLUSIONS

Previous work indicates that all thermally stable phases should be precipitated at the interface of the two metals (Burr Coleman and Davey 1944), and electron diffraction measurements tend to confirm this. Reflectivity measurements at both the gold and the aluminium surfaces seem to indicate the motion of a particular phase boundary, and in view of the critical thickness ratios which have been found, it would appear that this corresponds to formation of a layer of Au_2Al. The reflectivity of the phase formed at the glass surface is 47½% with mercury yellow light, whilst the reflectivity of the phase formed at the metal surface is 51%. Taking into account the refractive index of

the glass which would normally tend to reduce the reflectivity somewhat, we can say that the values are closely similar and tend to confirm the formation of a similar compound at both surfaces.

For diffusion into the aluminium, D_o' has been found to equal 0·51 cm^2/sec and E to be 23·5 kcal/mole. D' at 84°C can be calculated from these and is found to be $2·0 \times 10^{-15}$ cm^2/sec. D' at 84°C for diffusion into the gold has already been found to be $10·1 \times 10^{-15}$ cm^2/sec. In a given time, the penetration of the reaction layer is proportional to $\sqrt{(D')}$. Hence the penetration of the diffusion layer into the gold is 2·3 times greater than its penetration into the aluminium. If the diffusion layer is homogeneous in nature, then we would expect 2·3 gold atoms to be associated with every aluminium atom. This is close to the composition of the compound Au_2Al, the difference being due probably to errors in the determination of D'.

The values of critical thickness ratio and the relative rates of diffusion are both in agreement with the formation of the compound Au_2Al, and the structural investigation appears to confirm the presence of this compound. It is difficult to see why preferential formation of this phase should occur, since we would

expect all thermally stable phases to be formed. It would appear that there are only two reasonable explanations for the observed results, either that the light measurements are peculiarly sensitive to this phase and not to other phases, or that the layers of the other compounds formed are extremely thin and have little effect upon the measurements. The first explanation seems unlikely, as $AuAl_2$ has a pronounced purple colouration and any significant amount of it should have affected the reflectivity measurements. A specimen with gold and aluminium layers in the ratio of approximately 1 to 2 was aged in a furnace at 300°C for 6 hr. On removal the film had a definite red colour, but, unfortunately, was badly aggregated and its reflectivity could not be measured. The second of the two explanations implies that the diffusion rate into the Au_2Al is higher than for the other compounds, and consequently the width of the zone is high compared with the other zones formed.

Due to aggregation, very thin films (< 400Å) usually contain many grain boundaries (Sennett and Scott 1950), and any grain boundary diffusion should have a greater effect, so that we would expect E to be less and D' to be higher than in thick films. It has been shown in fig. 4, however, that D' for very thin gold films is the same as for thicker specimens, and the activation

energy of diffusion has been found to be the same for both. This means that the mechanism of diffusion in very thin films is exactly the same as in thicker ones. With the extreme aggregation in films below 150Å, some penetration of the gold by the aluminium might be expected to occur, but this would only affect the beginning of the ageing, and the time taken for reflectivity changes to be complete would still depend upon the time for complete penetration to occur. There is no evidence for grain boundary diffusion, and we can say that the diffusion observed is a true volume diffusion, most probably being a vacancy mechanism. It would be expected that the values of diffusion coefficient and activation energy lie fairly close to values for bulk specimens, but, unfortunately, these figures are not available for this system. However, where measurements have been obtained on other metallic pairs, values found by thin film methods are of the same order as the published values for bulk metals.

We have been able to show the formation of Au_2Al by measuring the relative rates of diffusion of the compound into the gold and into the aluminium. This implies that either diffusion of gold or of aluminium into the compound is the rate determining process, since if

both gold and aluminium diffused independently into the compound, the rates of diffusion would bear no relation to one another, and in particular, the two activation energies would be different. As diffusion generally occurs more rapidly into the lower melting point component (Jost 1952), it seems possible that diffusion of gold into aluminium is the rate determining process. Interstitial diffusion is most unlikely, since the atoms of the two elements are identical in size; consequently, diffusion of the gold atoms implies a migration of vacancies from the aluminium towards the gold. Vacancies in the aluminium close to the Au_2Al surface would tend to be occupied by gold atoms, and the gold and aluminium would react to form more Au_2Al, the vacancies moving into the layer of Au_2Al. Vacancies in the Au_2Al close to the gold surface would tend to become occupied by gold atoms from the pure metal and the vacancies would move into the gold. If the mean vacancy concentration in the Au_2Al remains constant, there must be a steady drift of vacancies into and out of the Au_2Al, causing the processes at the two interfaces to take place at the same rate and giving rates of diffusion in agreement with the experimental observations. The Au_2Al would advance into the aluminium at one side and would appear to advance into the gold at the other, the measured rates of diffusion differing

because of the atomic ratio in the compound. This explanation neglects the formation of other phases, but the experimental evidence suggests that other phases can be present only as very thin layers.

The source of the vacancies is of great interest. A certain number can exist in thermal equilibrium in a metal at low temperatures (approximately 1 in 10^6 lattice sites) but this number is far too small to account for the observed mass flow. Thin films are generally considered to have large numbers of vacancies (1 - 2 %), similar to the vacancies quenched into a bulk metal when it is rapidly cooled (van Bueren 1960), and it might be thought that that these gave the observed mass flow. In vacancy diffusion the activation energy is made up of two terms corresponding to the vacancy concentration and to the potential barrier between atomic sites. If diffusion were due to the excess vacancies quenched in the lattice, then the activation energy would be approximately half the values obtained in bulk specimens, and D' would be several orders of magnitude higher. This is not in agreement with the experimental observations, and so we must conclude that large numbers of vacancies are generated in the aluminium near the interface with the Au_2Al, and that these are absorbed in in the gold. According to Le Claire (1953), dislocations

act as ideal sources and sinks for vacancies, and thin films are known to have large numbers of dislocations (Dassett Menter and Pashley 1958). Movements of jogged dislocations in the aluminium could supply the necessary number of vacancies for the observed mass flow. Movements of the dislocations would also form new atomic planes in the aluminium to provide accomodation for the gold atoms diffusing in and reacting to form Au_2Al. Accomodation is therefore provided for the number of atoms of gold diffusing into aluminium by the very process which produces vacancies for their transfer.

Dislocations can similarly act as sinks for vacancies. Motion of vacancies to a jog results in the annihilation of the vacancy and movement of the jog. Adding one plane of vacancies to the dislocation removes one plane of atoms from the metal. Hence the gold becomes thinner because of the absorption of large numbers of vacancies.

It can be shown (van Bueren 1960) that in a normal metal, dislocations can easily supply the necessary number of vacancies, and there should be no trouble in thin films with their large numbers of dislocations.

TABLE 1

STRUCTURE OF GOLD-ALUMINIUM FILM AGED FOR 1 HOUR AT 58°C.

No	Intensity	Ring Diameter (cm)	Observed d Spacing (Å)	Calculated d Spacings Au_2Al (Å)	Au & Al (Å)	AuAl (Å)
1	M	0·61	4·49			
2	vW	0·80	3·42			3·47
3	M	0·91	3·01			3·00
4	W	1·02	2·69	2·79		
5	M	1·16	2·36	2·36	2·34	
6	vS	1·26	2·17			2·17
7	vW	1·32	2·08	2·08		
8	M	1·72	1·59	1·61		
9	M	1·88	1·46	1·47	1·43	
10	S	2·09	1·31	1·33		1·34
11	M	2·22	1·24	1·25	1·22	1·22
12	W	2·33	1·18	1·18	1·17	1·15

ACKNOWLEDGEMENTS

One of us (L.C.B.) wishes to thank the Department of Scientific and Industrial Research for the provision of a post graduate maintenance grant.

REFERENCES

Bassett, G.A., Menter, J.W., and Pashley, D.W., 1958, Proc. Roy. Soc. A, 246, 345.

Belser, R.B., 1960, J. Appl. Phys., 31, 562.

van Bueren, H.G., 1960, Imperfections in Crystals (Amsterdam: North Holland Publishing Co.).

Burr, A.A., Coleman, H.S., and Davey, W.P., 1944, Trans. Amer. Soc. Metals, 33, 73.

Coffinberry, A.S. and Multgren, R., 1938, Trans. Amer. Inst. min. (metall.) Engrs., 128, 249.

Hansen, M., 1958, Constitution of Binary Alloys (New York: McGraw-Hill), p. 69

Jost, W., 1952, Diffusion in Solids, Liquids and Gases (New York: Academic Press), p. 238.

Kirkaldy, J.S., 1958, Canadian J. Phys., 36, 917.

Le Claire, A.D., 1953, Progress in Metal Physics, 4, 265.

Rouard, P., Malé, D., and Trompette, J., 1953, J. Phys. Radium, 14, 587.

Sennett, R.S., and Scott, G.D., 1950, J. Opt. Soc. Amer., 40, 203.

Schopper, H., 1955, Z. Phys., 143, 93.

Tolansky, S., 1948, Multiple Beam Interferometry (Oxford: Clarendon Press), p. 147.

Weaver, C., and Hill, R.M., 1959, Phil. Mag. Supplement, 8, 375.

Wulff, J., 1934, J. Opt. Soc. Amer., 24, 223.

CAPTIONS

Fig. 1 — Ageing of gold-aluminium film at 84°C. Reflecti changes at gold surface for a gold thickness of 790Å. Reflectivity measurements made with mercury light of wavelength (a) 5790Å (b) 5461Å (c) 4358Å.

Fig. 2 — Ageing of gold-aluminium films at 84°C. Graph of reflectivity against t/d^2 for gold thicknesse of (a) 790Å (b) 1530Å (c) 3120Å.

Fig. 3 — Graph of gold thickness against the ratio t_1/t_2. Theoretical curves are plotted for light penetrations of (a) 500Å (b) 400Å (c) 300Å.

Fig. 4 — Graph of diffusion coefficient, D', at 84°C against gold thickness.

Fig. 5 — Graph of $\log_{10} t_{60}$ against $1/T$, where t_{60} is the time in minutes for the reflectivity to fall to 60%, and T is the temperature in °K. Lines are plotted for gold thicknesses of (a) 2620Å (b) 1630Å (c) 790Å.

Fig. 6 — Ageing of gold-aluminium films at 102°C. Graph of reflectivity against t/d^2 for aluminium

thicknesses of (a) 620Å (b) 1050Å (c) 1730Å.

Fig. 7 Ageing of gold surface at 84°C for a gold thickness of 1450Å
(a) aluminium thickness = 275Å (ratio of aluminiu to gold = 0·19)
(b) aluminium thickness = 880Å, 1300Å and 5300Å (ratio of aluminium to gold = 0·61, 0·90 and 3·7)

Fig. 8 Transmission electron diffraction patterns obtain from a gold-aluminium film.
(a) gold film 100Å thick, (b) aluminium film 120Å thick, (c) gold + aluminium film unaged, (d) gold + aluminium film aged for 1 hr. (e) gold + aluminium film aged for 15½ hr.